CHEMNITZ UNIVERSITY
OF TECHNOLOGY

Numerical Methods for Model Reduction of Time-Varying Descriptor Systems

Dissertation

submitted to **Faculty of Mathematics**
at **Chemnitz University of Technology**
in accordance with the requirements for the degree
Dr. rer. nat.

Submitted by: MS. Mohammad-Sahadet Hossain

Advisor: Prof. Dr. Peter Benner
Reviewer: Prof. Dr. Daniel Kressner

Chemnitz, May 12, 2011

dedicated to my parents
Abdul Hamid Bepary and **Mrs. Sahana Akther**
who did all impossibilities possible for me

ABSTRACT

Science and technology have profoundly influenced the course of human civilization on earth and opened a new horizon of enormous possibilities in various fields of application. Almost all technological applications require a solid understanding of processes, components, and the physical and dynamical features of the concerned systems. Mathematical models are the key towards representing our knowledge and understanding of dynamical systems. In most of those applications, such models become extremely huge and complex and sometime impossible to handle for the purpose of simulation, analysis or control system design. A solution to simplify the preceding task in both fields of simulation and system analysis is to find a low order approximation of the original high order complex model that still preserves the input-output behavior of the original complex model as good as possible. This is the basic concept of model reduction.

This dissertation concerns the model reduction of linear periodic descriptor systems both in continuous and discrete-time case. Linear periodic descriptor systems represent a broad class of time evolutionary processes in micro-electronics and circuit simulation. They are suitable models for several natural as well as man-made phenomena, and have applications in modeling of periodic time-varying filters and networks, multirate sampled-data systems, circuit simulation, micro-electronics, aerospace realm, control of industrial processes and communication systems.

In this dissertation, mainly the projection based approaches are considered for model order reduction of linear periodic time varying descriptor systems. Krylov based projection method is used for large continuous-time periodic descriptor systems and balancing based projection technique is applied to large sparse discrete-time periodic descriptor systems to generate the reduce systems.

For very large dimensional state space systems, both the techniques produce large dimensional solutions. Hence, a recycling technique is used in Krylov based projection methods which helps to compute low rank solutions of the state space systems and also accelerate the computational convergence. The outline of the proposed model order reduction procedure is given with more details. The accuracy and suitability of the proposed method is demonstrated through different examples of different orders and

the results are compared and discussed.

Model reduction techniques based on balance truncation require to solve matrix equations. For periodic time-varying descriptor systems, these matrix equations are projected generalized periodic Lyapunov equations and the solutions are also time-varying. Solving these periodic Lyapunov equations requires the computation the the kronecker-like canonical forms of the periodic matrix pairs associated with the periodic systems and then to solve the resulting periodic Sylvester equations. Rather than this approach, the cyclic lifted representation of the periodic time-varying descriptor systems is considered in this dissertation and the resulting lifted projected Lyapunov equations are solved to achieve the periodic reachability and observability Gramians of the original periodic systems. The main advantage of this solution technique is that the cyclic structures of projected Lyapunov equations can handle the time-varying dimensions as well as the singularity of the period matrix pairs very easily. Another nice feature about the use of this lifting isomorphism is that one can exploit the theory of time-invariant systems for the control of periodic ones, provided that the results achieved can be easily reinterpreted in the periodic framework.

Since the dimension of cyclic lifted system becomes very high for large dimensional periodic systems, one needs to solve the very large scale periodic Lyapunov equations which also generate very large dimensional solutions. Hence iterative techniques, which are the generalization and modification of alternating directions implicit method and generalized Smith method, are implemented to obtain low rank Cholesky factors of the solutions of the periodic Lyapunov equations. Also the application of the solvers in balancing-based model reduction of discrete-time periodic descriptor systems is discussed. Numerical results are given to illustrate the efficiency and accuracy of the proposed methods.

ACKNOWLEDGEMENTS

First of all, I would like to thank the sponsors which made this work possible by providing the required financial support: the research group Mathematics in Industry and Technology (MIIT) of Chemnitz University of Technology, and the German Federal Ministry of Education and Science (BMBF).

I would like to express my gratitude to my supervisor, Professor Peter Benner for his contribution, patience, friendly manner and guidance in all steps of the thesis work. I am grateful to him for his intellectual insights and skills that have proven the quality of the current work.

I am also grateful to Prof. Dr. Tatjana Stykel of Berlin University of Technology (TU Berlin) for her valuable discussions, advices and guidance at the time of my project work there in July-November, 2008 and also for several discussions during this thesis work. I also acknowledge Dr. Michael Striebel (former research scientist, NXP Semiconductors, Eindhoven, Netherlands) for providing me the mathematical models from discretization of nonlinear circuit problems and for several discussions.

I would also like to thank all my colleagues from the research group Mathematics in Industry and Technology (MIIT) from Chemnitz University of Technology, especially to Dr. Jens Saak for his great help and nice interesting discussions to the problem of low rank Lyapunov solvers using ADI iteration. I would like to mention the name of Dr. René Schneider for his remarkable friendly cooperations to this thesis work and also in several administrative cases during my stay at Chemnitz.

Further, many thanks to my parents who did all the impossibilities possible for me and always inspired me to reach to my goal even in the most crucial moments of my life.

Finally, and most of all, I would like to thank my beloved Tanzina. I thank her for bearing with me when I was too deep in thought regarding this work and could not manage even a short little time for her.

CONTENTS

LIST OF FIGURES

LIST OF TABLES

LIST OF ALGORITHMS

LIST OF ABBREVIATIONS

ACS	attitude control system (of satellite)
ADI	alternating directions implicit (iterative parametric solver)
(C)ARE	(continuous time) algebraic Riccati equation
BT	balanced truncation
CPU	central precessing unit (of a computer)
DAEs	differential algebraic equations
DRE	differential Riccati equation
EVP	eigenvalue problem
FD	finite difference (method)
HB	harmonic balance
GUPTRI	generalized upper triangular form (of matrix pencil)
GPRSF	generalized periodic real Schur form
HSV	Hankel singular values
LRCF	low-rank Cholesky factor
LRCF-ADI	versions of ADI computation using LRCFs of the solution
LTI	linear time-invariant (system)
LTV	linear time-varying (system)
LPTV	linear periodic time-varying (system)
MEMS	micro-electric-mechanical systems
MIMO	multiple input multiple output (system)
MNA	modified nodal analysis
MOR	model order reduction
ODE	ordinary differential equation
PCALE	projected continuous-time Lyapunov equation
PDE	partial differential equation
PPDALE	projected periodic discrete-time algebraic Lyapunov equation
PLDALE	projected lifted discrete-time algebraic Lyapunov equation
POD	proper orthogonal decomposition
PSS	periodic steady state (solution)
RF	radio frequency
RRQR	rank-revealing QR factorization
SISO	single input single output (system)
spd	symmetric positive definite
SRBT	square-root balanced truncation

SVD	singular value decomposition
TBR	truncated balanced realization
TFM	transfer function matrix
TVS	time-varying system (function)

LIST OF SYMBOLS

Sets and Spaces

$\mathbb{C}$	field of complex numbers
$\mathbb{N}_0$	set of natural numbers, $\mathbb{N}_0 = \{0, 1, \dots\}$
$\mathbb{C}^-$	the open left half-plane
$\mathbb{C}^+$	the open right half-plane
$\mathbb{R}$	field of real numbers
$\mathbb{R}^n$	vector space of real n-tuples
$\mathbb{C}^n$	vector space of complex n-tuples
$\mathbb{R}^{m\times n}$	real $m \times n$ matrices
$\mathbb{C}^{m\times n}$	complex $m \times n$ matrices
$\mathbb{F}^{m\times n}$	the space of real ($\mathbb{F} = \mathbb{R}$) or complex ($\mathbb{F} = \mathbb{C}$) matrices of size $m \times n$
$Re(z)$	the real part of $z \in \mathbb{C}$
$\mathcal{K}_m$	the order m Krylov subspace
colspan(A)	the column span of A
Ω	computational domain or subset of eigenspectrum (depending on the context)
Im(A)	Image of A
Ker(A)	Kernel of A

Matrices and Matrix Pencils

a_{ij}	the i, j-th entry of matrix A
A^T	the transpose of A
A^H	$:= (\bar{a}_{ij})^T$, the conjugate transpose (Hermitian) of A
A^*	either of the above depending on the context
diag($A_1, \dots, A_k$)	a block diagonal matrix with matrices A_j, $j = 1, \dots, k$

$\Lambda(A)$	spectrum of A
$\lambda_j(A)$	j-th eigenvalue of A
(E, A)	short form of the matrix pencil $\lambda E - A$
$\Lambda(\lambda E - A)$	spectrum of the pencil $\lambda E - A$
$\lambda_j(E, A)$	j-th eigenvalue of the pencil $\lambda E - A$
$\mathrm{Sp}(E, A)$	the set of eigenvalues of $\lambda E - A$
$\mathrm{Sp}_s(E, A)$	the set of stable eigenvalues of $\lambda E - A$
$\rho(A)$	spectral radius of A
$\sigma_{\max}(A)$	largest singular value of A
$\sigma_{\min}(A)$	smallest singular value of A
$\mathrm{trace}(A)$	$:= \sum_{i=1}^{n} a_{ii}$ trace of A
$\exp(A)$	$:= e^A$ the exponential of A
$\det(A)$	the determinant of A
$\mathrm{rank}(A)$	the rank of A
$\kappa(A)$	$:= \|A\|_2 \|A^{-1}\|_2$ the spectral condition number for A
$A \succ 0; A \succeq 0$	short form for A is selfadjoint positive definite or positive semi-definite, respectively
$A \prec 0; A \preceq 0$	short form for A is selfadjoint negative definite or negative semi-definite, respectively
$A \otimes B$	the Kronecker product of A and B
$A \oplus B$	the direct sum of A and B
$\{(E_k, A_k)\}_{k=0}^{K-1}$	the periodic matrix pairs for $k = 0, \ldots, K-1$
$(\mathbb{E}, \mathbb{A})$	the set of $\{(E_k, A_k)\}_{k=0}^{K-1}$
$(\mathbb{E}_f, \mathbb{A}_f)$	the set containing all finite eigenvalues of $\{(E_k, A_k)\}_{k=0}^{K-1}$
$(\mathbb{E}_\infty, \mathbb{A}_\infty)$	the set containing all infinite eigenvalues of $\{(E_k, A_k)\}_{k=0}^{K-1}$
$\mathbf{\Sigma}(E, A, B, C)$	realization of a system
$\lambda\mathcal{E} - \mathcal{A}$	cyclic lifted pencil
$(\mathcal{E}, \mathcal{A})$	short form of the cyclic lifted pencil $\lambda\mathcal{E} - \mathcal{A}$.

Norms

$\|u\|_p$	$:= \sqrt[p]{\sum_{i=1}^{n} \|u_i\|}$ for n-tuples u and $1 \leq p < \infty$
$\|u\|_\infty$	the maximum norm, i.e., the maximum absolute value of components (u an n-tuple) or function values (u a continuous function)
$\|A\|_2$	$:= \sup \frac{\|Ax\|}{\|x\|} = \sigma_{\max}(A)$ the spectral matrix norm of A

$\|A\|_p$	$:= \sup\left\{\|Au\|_p : \|u\|_p = 1\right\}$ for operators A (including matrices) and $1 \leq p \leq \infty$
$\|A\|_F$	$:= \sqrt{\sum_{i,j} a_{ij}^2} = \sqrt{\mathrm{tr}\,(A^*A)}$ the Frobenius-norm of $A \in \mathbb{R}^{m\times n}$
$\|G(i\omega)\|_{\mathbb{H}_\infty}$	$\mathbb{H}_\infty$ norm of $G(i\omega)$

CHAPTER

ONE

INTRODUCTION

Motivation. Various complicated systems which arise in many engineering applications (microelectronics, micro-electro-mechanical systems (MEMS), aerospace realm, computer control of industrial processes, chemical processes, communication systems, etc.) are composed of large numbers of separate devices and they are described by very large mathematical models consisting of more and more mathematical systems with very large dimensions. Simulations of such systems can be unacceptably expensive and time-consuming due to limited computer memory and CPU consumption. Model reduction is concerned with replacing a large complex model by a much smaller one which can be fast and efficiently simulated and which has nearly the same response characteristics compare to the original large model.

As the mathematical model of a device gets more detailed and the model is composed of a large system of ordinary differential equations (ODEs), or a set of partial differential equations (PDEs), it is quite common that the concerned mathematical model may consist a vast amount of redundant information that have very little importance in the input-output characterization of the device. Model reduction is an efficient tool to eliminate those redundant parts from the original model so that the size of the reduced model becomes smaller compare to the original one and it is then amenable for simulation and analysis.

Linear systems, in continuous or discrete-time, in very simple language, are systems of linear differential or difference equations. A systems is called *time-varying* when the behavior and characteristics of that system varies over time. Almost every natural or technical process, however, is more or less nonlinear in nature, and therefore is actually time-variant (see Subsection 2.1.1 in Chapter 2 for detail). In recent years, scientists and engineers have put a lot of attention on the analysis and control of linear periodic time-varying (LPTV) systems as they explain several man made and natural

phenomena [36, 63, 66, 68, 73, 94, 115].

In this thesis, efficient implementations for model order reduction of certain large-scale, LPTV descriptor systems, both for continuous and discrete-time case, have been studied. A continuous-time LPTV descriptor system in general has the form

$$\begin{aligned} E(t)\dot{x}(t) &= A(t)x(t) + B(t)u(t), \\ y(t) &= C(t)x(t) + D(t)u(t), \end{aligned} \tag{1.1}$$

where $x(t) \in \mathbb{R}^n$, called the descriptor vector, $u(t)$ is the system input, $y(t)$ is the system output, and n is the system order at any given time t. All the system matrices are time-varying, periodic with period $K \geq 1$ and the matrices $E(t)$ and $A(t)$ can be singular at any given time t.

Analogous to the continuous-time case, a discrete-time LPTV descriptor system defined on the time interval $[0, K]$ has the form

$$\begin{aligned} E_k x_{k+1} &= A_k x_k + B_k u_k, \\ y_k &= C_k x_k + D_k u_k, \end{aligned} \tag{1.2}$$

where $k = 0, 1, \ldots,$ and $k \in \mathbb{N}_0$. For each k, x_k is an n_k-dimensional vector of descriptor variables, u_k is an p_k-dimensional vector of input variables, and $\sum_{k=0}^{K-1} n_k = n$. The system matrices are time-varying, periodic with period $K \geq 1$ and the matrices E_k and A_k can be singular at any sampling time point k. For both type descriptor systems the matrices $D(t)$ or D_k do not have any affect on the dynamics of the corresponding systems. Hence they are considered zero in most references and we will omit them in the description of LPTV descriptor systems in the consequent chapters.

Formally speaking, a reduced-order system of order r for system (1.1) (omitting $D(t)$) would be a system of the form

$$\begin{aligned} \tilde{E}(t)\dot{\tilde{x}}(t) &= \tilde{A}(t)\tilde{x}(t) + \tilde{B}(t)u(t), \\ \tilde{y}(t) &= \tilde{C}(t)\tilde{x}(t). \end{aligned} \tag{1.3}$$

The system is of potentially smaller dimension, i.e., $r << n$, and thus lower computational cost, than the original system (1.1), but it is now in a form suitable for use in higher level simulation. Analogous to the continuous-time case, a reduced-order system of dimension r for system (1.2) (omitting D_k) would be a system of the form

$$\begin{aligned} \tilde{E}_k \tilde{x}_{k+1} &= \tilde{A}_k \tilde{x}_k + \tilde{B}_k u_k, \\ \tilde{y}_k &= \tilde{C}_k \tilde{x}_k, \qquad k \in \mathbb{Z}, \end{aligned} \tag{1.4}$$

where for each k, $\tilde{x}_k$ is an r_k-dimensional vector, $\sum_{k=0}^{K-1} r_k = r$ and $r \ll n$. Apart from having much smaller state-space dimension, the reduced-order system preserves some essential and important characteristics of the original system.

The system is called single input single output (SISO) if it has only one input and one output, otherwise it is called multiple input and multiple output (MIMO). It is easier

to analysis the system dynamics and behavior for systems not containing any singular pencil (E_k, A_k). For a singular system, the overall process becomes more complicated. In that case, usual model order reduction techniques can not be used directly to generate a reduced-order model. This dissertation is concerned with the model order reduction techniques of such singular descriptor systems which arise both in continuous-time and discrete-time case.

In this thesis, mainly the projection based approaches are considered for model order reduction of LPTV descriptor systems. Krylov based projection method is used for large continuous-time LPTV descriptor system and balancing based projection technique is applied to large sparse discrete-time LPTV descriptor system to generate the reduce systems.

For very large dimensional state space systems, both the techniques produce large dimensional solutions. Hence, a recycling technique is used in Krylov based projection methods which helps to compute low rank solutions of the state space system and also accelerate the computational convergence.

Model reduction techniques based on balance truncation require to solve matrix equations. We need to solve the very large scale periodic Lyapunov equation which also generates very large dimensional solution. Hence an iterative technique, which is a generalization and modification of alternating directions implicit (ADI) method, is implemented to obtain low rank Cholesky factors of the solutions of the periodic Lyapunov equations.

Chapter Outline. The thesis is organized in the following way:

Chapter 2 introduces some test examples and model problems which describe the physical phenomena and system structures from where the LPTV descriptor systems can arise. The models are mainly sketched and more detailed descriptions are referenced. The modeling of nonlinear circuit models is described very detailed where we linearize the nonlinear model around some equilibrium trajectory and use discretization in the time domain.

In Chapter 3 we review some basic concepts of system and control theory for linear time-invariant (LTI) descriptor systems, both for continuous- and discrete-time systems, which will be needed later in the period settings by the subsequent chapters of this thesis. The main idea behind this is that the description in the LTI structures will help more precisely to understand their corresponding periodic structures. We summarize some necessary definitions and introduce functions of generalized matrix pencils and their decompositions. We also introduce the projected generalized periodic Lyapunov equations and their roles in applications of model order reduction.

Chapter 4 is devoted to LPTV discrete-time descriptor systems. In this chapter we review the concept of stability with the help of periodic matrix pencils and discuss the

decomposition of the periodic matrix pencils regarding their finite and infinite eigenvalues. We study the concepts of periodic reachability and observability Gramians of LPTV discrete-time descriptor systems in a different way. Also the structures and characteristics of periodic projected Lyapunov equations and the periodic transfer functions are discussed in this chapter.

Chapter 5 introduces the time-invariant reformulation of the LPTV discrete-time descriptor systems which is known as *lifted system*. In this thesis, we consider only the *cyclic lifted representation* of the LPTV discrete-time descriptor systems, which is introduced by Park and Verriest [79] in 1989 and Flamm [38] in 1991, known as *Cyclic lifting representation* of discrete-time LPTV systems. We reconstruct the concepts of stability as well as the reachability and observability Gramians of LPTV descriptor system regarding its cyclic lifted LTI model. Lifted representation of periodic Lyapunov equations and the transfer function are also discussed. A short discussions is given at the end of this chapter to clarify the relationship of LPTV descriptor system and its lifting isomorphism.

In Chapter 6 we consider the introductory idea of model reduction for the LTI case and generalizes this idea to our LPTV descriptor system. First, we describe the system theoretical background of model reduction approach via projection onto a rational Krylov subspace, and then the Balanced Truncation (BT) method, which requires exact system Gramians. We focus on descriptor systems and recall some basic information about the transfer functions and system norms.

Chapter 7 provides one of the main important contributions of this thesis. We develop efficient implementations of Krylov subspace based projection methods for model order reduction. The algorithmic realization of the method employes recycling techniques for shifted Krylov subspaces and their invariance properties. The efficiency and accuracy of the developed algorithm is illustrated by numerical examples and compared to other Krylov based projection methods used for model reduction.

Chapter 8 then provides another main contribution of this thesis. In this chapter we develop efficient implementations of balancing-related methods for model order reduction of discrete-time linear periodic descriptor systems. Efficient algorithms for solving projected periodic discrete-time algebraic Lyapunov equations via their lifted LTI representations are discussed here. We discuss the modified concepts of the periodic Gramians and the resulting concepts of Hankel singular values. We illustrate the behavior of the suggested model reduction technique using numerical examples.

Chapter 9 motivates the low rank approximation of the solution to large scale projected periodic discrete-time algebraic Lyapunov equations in lifted form. We start with short review of the ADI method and give detail derivation of the generalized ADI method to the projected lifted discrete-time algebraic Lyapunov equations with large sparse matrix coefficients. The generalized Cayley transformation is introduced which copes up with the singularity of the matrix equations. The column compression technique for the optimal memory requirements and computational effort are discussed. The chapter

includes numerical results on how well the low rank ADI approximation captures the original solution of the projected periodic discrete-time algebraic Lyapunov equations and implementations in model reduction technique.

Chapter 10 offers some conclusions and briefly discusses possibilities for improvements and future research.

CHAPTER

TWO

MODEL PROBLEMS AND TEST EXAMPLES

Contents

This chapter introduces the different model problems and test examples, where periodic descriptor systems have specific applications and demands. We describe model problems of three different areas that have set the stage for renewed interest in the study of periodic descriptor systems, both in continuous and discrete-time [36, 63, 66, 68, 73, 94, 115], in the last twenty years. The main goal is to familiarize the real life problems where the mathematical model demands periodic descriptor settings.

2.1. Nonlinear Circuit Models

The most common components for model reduction of linear time-varying (LTV) systems are the radio frequency (RF) communication circuits, where the systems are designed to have nearly linear responses, but may exhibit strongly nonlinear behaviors

for the strong local oscillator signals. The nonlinear responses present there are considered as redundant terms in the modeling of RF communication circuits, and hence they need to be removed. An usual approach to get ride of these redundant terms is the linearization of a nonlinear circuit model around the time-varying large signal, and hence, the resulting model is an LTV model. In the second half of last century and also in recent years, RF communication circuits such as mixer, switched-capacitor filters [73, 78, 84, 86, 128] have taken a lot attention as prime components of LTV model order reduction. In the following subsection we briefly discuss the linearization of nonlinear circuit systems.

2.1.1. Linearization of Nonlinear Circuit Systems

Let us consider a nonlinear system that describes a circuit equation whose input is the sum of two periodic signals, $u_L(t) + u_s(t)$, where $u_L(t)$ is an arbitrary periodic waveform with period T_L and $u_s(t)$ is a small signal of frequency f_s. Using modified nodal analysis (MNA) [53], the differential equations for the circuit can be written as,

$$f(v(t)) + \frac{d}{dt}q(v(t)) = u_L(t) + u_s(t), \tag{2.1}$$

where $u_L(t), u_s(t)$ are the vectors of large and small signal input sources, $v(t)$ describes the node voltages, $f()$ and $q()$ are nonlinear functions describing the charge/flux and resistive terms, respectively.

If $u_s(t)$ is assumed to be zero, then the periodic steady state (PSS) solution $v_L(t)$ is the solution of (2.1) which also satisfies the periodic property

$$v(T_L) = v(0). \tag{2.2}$$

Now, assume that $u_s(t)$ is not zero, but is small. We consider that the new perturbed solution $v_L(t) + v_s(t)$ also satisfies (2.1), i.e.,

$$f(v_L(t) + v_s(t)) + \frac{d}{dt}q(v_L(t) + v_s(t)) = u_L(t) + u_s(t), \tag{2.3}$$

where $v_s(t)$ is the difference between the exact solution to (2.1) and the solution computed assuming $u_s(t) = 0$.

Linearizing around the steady state solution $v_L(t)$, which is accurate only if $u_s(t)$ is small, yields a time-varying linear system of the form

$$\frac{df(v_L(t))}{dv_L}v_s(t) + \frac{d}{dt}(\frac{dq(v_L(t))}{dv_L}v_s(t)) = u_s(t) \tag{2.4}$$

for $v_s(t)$. Here, $v_s(t)$ can be interpreted as the small signal response to $u_s(t)$.

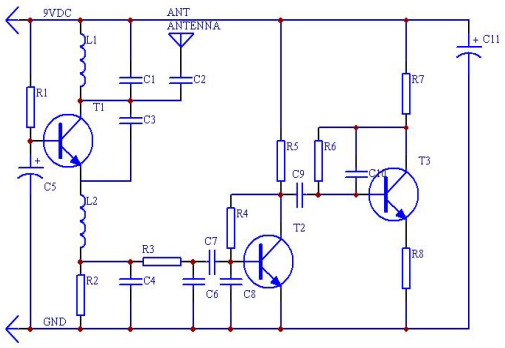

Figure 2.1. Schematic view of a simple RF receiver.
image source: http://jap.hu/electronic/sregrcvr.html

Defining the time-varying conductance and capacitance matrices, as

$$\bar{G}(t) = \frac{df(v_L(t))}{dv_L} \quad \text{and} \quad \bar{C}(t) = \frac{dq(v_L(t))}{dv_L}, \tag{2.5}$$

respectively, the linearized LTV system takes the familiar form

$$\bar{G}(t)v + \frac{d}{dt}(\bar{C}(t)v) = u(t), \tag{2.6}$$

where the notations $v_s(t) = v$ and $u_s(t) = u$ are used for simplicity. To relate to the standard notations analogous to (1.1), we may make the identification $E(t) = \bar{C}(t)$, $A(t) = -(\bar{G}(t) + \dot{\bar{C}}(t))$.

Figure 2.1 shows a schematic view of a simple RF receiver which is composed of several capacitors, conductors and many other micro-machined devices. This simple RF receiver is mainly used for low-distance digital radio receiver application. A model TDA1572T/V3 integrated AM receiver in shown in Fig. 2.2, which was released by NXP Semiconductors in May 1992, and designed for use in mains-fed home receivers and car radios.

2.1.2. Model Example of RF Circuit Systems

We consider here a simple example where the data are obtained from small RF circuit simulator. The circuit system consist of $n = 5$ nodes, and is excited by a local oscillator at 2 KHz driving the mixer, while the RF input is fed into the I-channel buffer. The time-varying system is obtained around a steady state of the circuit at the oscillatory frequency; a total of $N = 129$ harmonics are considered for the time-variation.

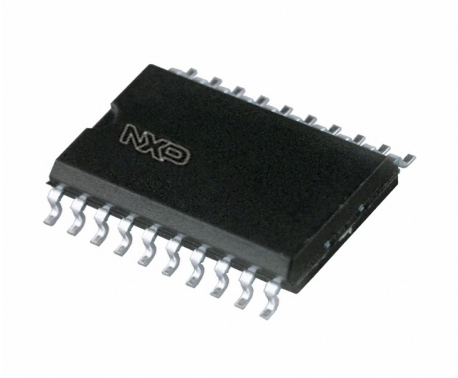

Figure 2.2. TDA1572T/V3 AM Radio Receiver, manufactured by NXP Semiconductors.
image source: http://parts.digikey.com

"The TDA1572T/V3 integrated AM Receiver, manufactured by NXP Semiconductors, performs all the active function and part of the filtering required of an AM radio receiver. It is intended for use in mains-fed home receivers and car radios. The circuit can be used for oscillator frequencies upto 50MHz and can handle RF signals up to 500mV." -source: http://www.nxp.com/documents/data_sheet/TDA1572T_CNV.pdf.

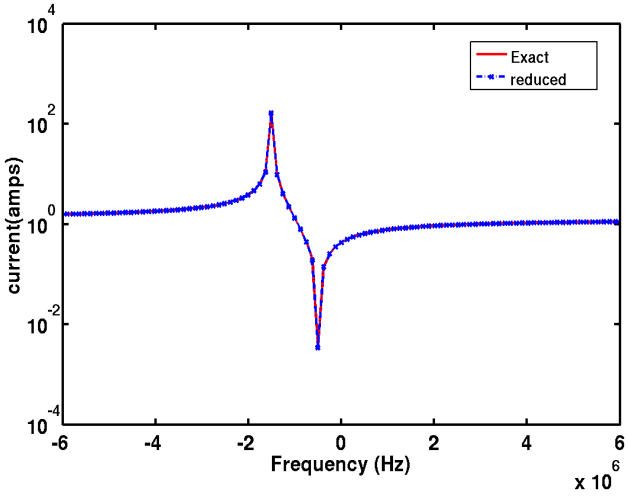

Figure 2.3. Transfer functions: full versus reduced system.

To specify an output function, the sample function is taken over a 1-ms period. Essentially the final model is a real LTI system [84], which has the size, $nN = 645$.

A Krylov based projection technique [84, 113, 87, 88] has been used to find a reduced-order model. The reduced model is generated by machining four moments on the imaginary axis. The reduced system has order, $r = 3$. Fig. 2.3 shows the transfer functions of full- and reduced order systems. The relative error is bounded by the

Figure 2.4. $M-$ fold Decimator (downsampler).

magnitude 10^{-10}. We discuss more details of this calculation in Chapter 7.

2.2. Multirate Data Sampling Models

One of the major motivations for theoretical study of LPTV systems is multirate data sampling. The process of converting or sampling of the given rate of data or a signal into a different rate is called *sampling rate conversion*. Systems that employ multiple sampling rates in the processing of data or digital signals are called *multirate sampled-data control systems*, or *multirate digital control systems*, respectively.

In the signal processing area, multirate digital filters and filter banks have applications in communications, speech processing, image compression, and in the digital audio industry they have vast applications and great demand [4, 73, 115]. In control theory, multirate data sampling is largely used in multirate feedback systems, also named as sampled-data control systems in the literature.

2.2.1. Components in Multirate Sampling

The fundamental components in multirate data sampling are decimators and interpolators [39, 115]. Decimetors are used to reduce the sampling rate which is called *sampling rate decimation*, or simply *decimation*.

Let us consider the sampling rate of a discrete signal $x(n)$ reduced by a factor M by taking only every M-th value of the signal. The relationship between the resulting signal $y(m)$ and the original signal $x(n)$ is as follows:

$$y(m) = x(mM). \tag{2.7}$$

Fig. 2.4 shows a signal flow representation of this process. The quadratic symbol in Fig. 2.4, with the arrow pointing downwards, is called a *downsampler*. The output signal $y(m)$ is a *downsampled* signal with respect to the input signal $x(n)$. For many problems, it is possible to decrease the bandwidth of a signal with a low-pass filter before downsampling it. Fig. 2.5 shows a decimator which uses a filter with an impulse response $h(n)$ and a downsampler with a factor M. An input signal $u(n)$ is converted into a decimated signal $y(m)$.

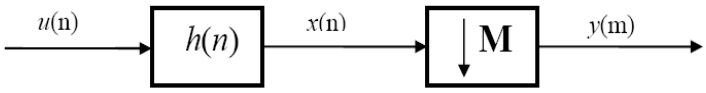

Figure 2.5. Decimator consisting of anti-aliasing filter $h(n)$ and downsampler M.

It is natural that an input signal $u(n)$ with an unacceptably large bandwidth can have redundant components, known as *aliasing*, that can change the signal irreversibly. After filtering with a low-pass filter, these unwanted components can be reduced to an acceptable level. We can then treat the signals as if they were really band-limited [39]. The signal thus obtained after filtering,

$$x(n) = u(n) * h(n) = \sum_{k=-\infty}^{\infty} u(k)h(n-k),$$

can be downsampled as given by (2.7). The entire decimation process is thus

$$y(m) = \sum_{k=-\infty}^{\infty} u(k)\, h(mM-k).$$

The downsampler shown in Fig. 2.5 is a linear system, but it is not time-invariant. By choosing the input as a series

$$x(n) = \delta(n) = \begin{cases} 1 & \text{for } n = 0, \\ 0 & \text{for } n \neq 0, \end{cases}$$

we obtain the output as

$$y(m) = x(mM) = \begin{cases} 1 & \text{for } m = 0\,, \\ 0 & \text{for } m \neq 0. \end{cases}$$

Hence the impulse response is the impulse series $y(m)$. Now assume that in the impulse series there is a delay and it is n_0. Upon excitation from this delay, the resulting input series

$$x(n) = \delta(n-n_0) = \begin{cases} 1 & \text{for } n = n_0, \\ 0 & \text{for } n \neq n_0, \end{cases}$$

gives the output of the sampler as

$$y(m) = \begin{cases} 1 & \text{for } m = m_0 \text{ with } m_0 = n_0/M, \\ 0 & \text{otherwise.} \end{cases}$$

Here m_0 is an integer, and the response clearly depends on the delay n_0. The downsampler is thus a time-dependent system. However, it is a *periodically time-invariant* system. With time delay which are multiples of M, we obtain a delayed output, which is a downsampled version of the input signal.

The sampling rate also needs to be increased if a narrow-band signal is to be observed with a finer resolution in the time-domain. This is useful, for instance, for detecting zero-crossings of the signals. Interpolators are used to increase the sampling rate of a signal, which is called *interpolation*, and consists of *upsampling*, followed by *anti-imaging filtering*.

Suppose that the sampling rate of a discrete signal $y(m)$ is increased by a factor L by placing $L-1$ equally spaced zeroes between each pair of samples. The resulting signal $u(n)$ is then given by

$$u(n) = \begin{cases} y(n/L) & \text{for } n = mL, \, m \text{ integer}, \\ 0 & \text{otherwise.} \end{cases}$$

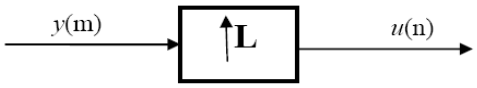

Figure 2.6. L-fold Interpolator (upsampler).

Fig. 2.6 shows a signal flow representation of this process. The upsampling signal generally contains redundant spectra, called *image spectra*. Therefore, this upsampled signal is then passed through a low-pass filter with a cutoff frequency to generate an ideally interpolated signal.

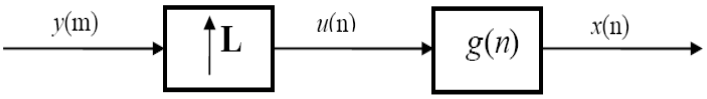

Figure 2.7. Interpolation using an upsampler L and anti-imaging filter $g(n)$

It can be easily figured out that both decimators and interpolators are simple time-varying systems and they are not periodic in general. However, when a decimator and interpolator with the same sampling rate appear in cascade, even separated by other samplers or filters, they form a LPTV system as a whole.

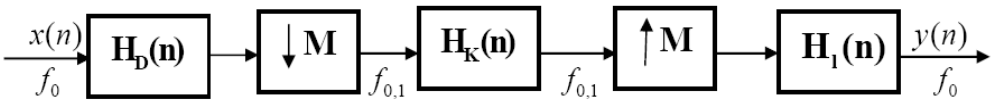

Figure 2.8. Cascade filters: a decimator with filter $H_D(n)$, a kernel filter $H_K(n)$ and an interpolator with filter $H_I(n)$

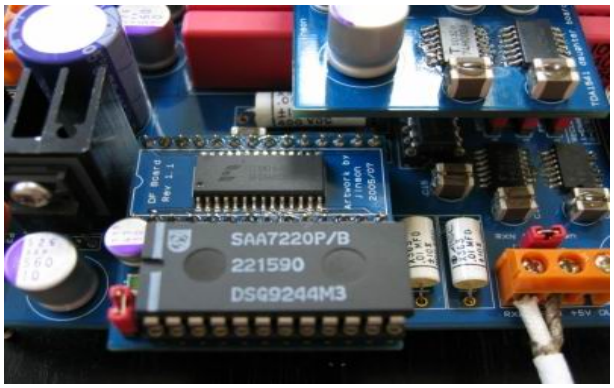

Figure 2.9. Philips SAA7220P/B digital filter, used in superb sound Marantz CD Player.
image source: http://www.marantzphilips.nl

"The SAA7220P/B digital filter, was slightly improved released of its previous version SAA7220P/A by Philips. These new digital filters conformed to the 28kHz DAT sampling rate, and plans were implemented to improve the precision of DACs. It was incorporated into the Marantz CD-94 after its initial release and also used in the Marantz CD94ltd and Marantz CDA-94". source: http://www.marantzphilips.nl

2.2.2. Model Example of Digital Audio Systems

This example is taken from [115]. Changing the sampling rates of band-limited sequences is a very common demand in audio industry. For example, assume that the significant information of a certain music waveform $x_a(t)$ is in the band $0 \le |\Omega|/2\pi \le 22$kHz. For the better quality and performance a minimum sampling rate of 44kHz is suggested (Fig. 2.10(a)). Hence one needs to perform analog filtering before sampling to eliminate aliasing of out-of-band noise.

Hence, an analog filter $H_a(j\Omega)$ (Fig. 2.10(b)) is used. It has a fairly flat passband and a narrow transition band and hence $x_a(j\Omega)$ is not distorted and only a small amount of unwanted energy can pass through. A suitable choice in such a case can be optimal filters (see [115] and references therein). But they have very high nonlinear phase response around the bandedge (i.e., around 22kHz). In high quality music this is not

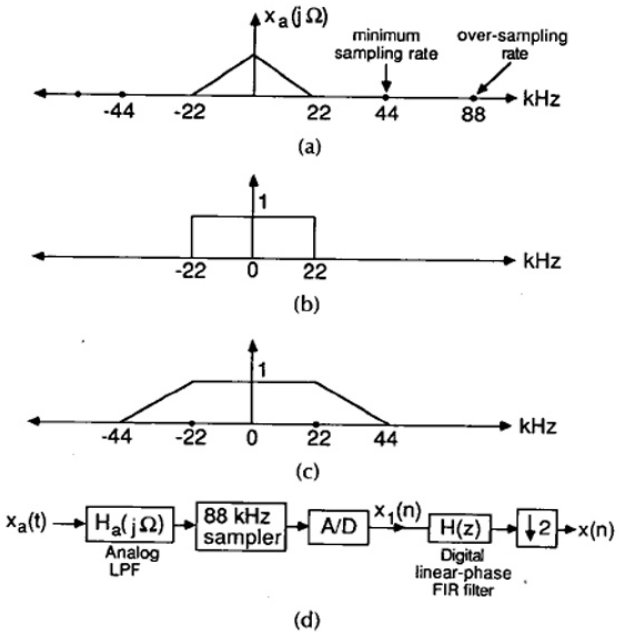

Figure 2.10. (a) Spectrum of $x_a(t)$. (b) Antialiasing filter response for sampling at 44 kHz. (c) Antialiasing filter response for sampling at 88 kHz. (d) improved scheme for A/D stage of digital audio system. image source: [115]

acceptable and considered as objectionable.

A usual method to overcome this problem is to oversample $x_a(t)$ by a factor of two (and often four). Then the filter $H_a(j\Omega)$ have much wider transition band (Fig. 2.10(c)), so that the nonlinearity in the phase-response is very low. Now a simple analog linear filter (i.e., Bessel filter) can be used to recover the signal from the unwanted nonlinearity (which is acceptably low) still present in it. The sequence $x_1(n)$ so generated is then passed through a digital filter $H(z)$. Hence the signal is lowpass filtered (Fig. 2.10(d)) by $H(z)$ and after that it is decimated (downsampled) by the same factor of two to obtain the final digital signal $x(n)$ (see [115] for details).

The reason of using a digital filter $H(z)$ at the last part of the above process is that, since $H(z)$ is digital, it can be designed to remove all the nonlinear phase-response of the signal for its linear phase, while at the same time providing the desired degree of sharpness and quality. The resulting is superb sound quality from digital audio systems.

2.3. Orbital Motion Modelling of Spacecraft

In order to track satellites through space, it is important to know their orientations in space to carryout mission planning and design. The path a rocket or guided missile takes during powered flight is directly influenced by its attitude, that is its orientation in space. During the atmospheric portion of flight, fins may deflect to steer a missile. Outside the atmosphere, changing the direction of thrust by articulating exhaust nozzles or changing the rocket's attitude influences its flight path. Therefore, the spacecraft's attitude must be stabilized and controlled not only for the survival of a satellite, but also for a satisfactory achievement of mission goals.

Several possible approaches have been developed the recent years in the field of control system engineering of spacecrafts and it has become a most interesting topics for several research now-a-days. Among all these possible approaches, a particularly effective and reliable one is constituted by use of electromagnetic actuators. The reason is that it turn out to be specially suitable for tracking and controlling the low Earth orbit (LEO) satellites. Such actuators are time-varying and their control is periodic. The feasibility of periodic techniques has opened a door of vast possibilities of applications and research in the field of attitude control system (ACS) of small satellites [17, 68, 69, 94].

2.3.1. Spacecraft Attitude Control Dynamics

The attitude dynamics of a rigid spacecraft is nonlinear, and generally described by well-known Euler's equations, as follows [130, 94]:

$$\mathbf{I}\dot{\omega} = -\omega \times \mathbf{I}\omega + T_{contr} + T_{dist}, \tag{2.8}$$

where $\omega \in \mathbb{R}^3$ is the vector of spacecraft angular rate (expressed in the body frame), $\mathbf{I} \in \mathbb{R}^{3\times3}$ is the inertia matrix, $T_{dist} \in \mathbb{R}^3$ is the vector of external disturbing torques, and $T_{contr} \in \mathbb{R}^3$ is the vector of magnetic control torques.

The attitude kinematics of the spacecraft can be described by means of possible parameterisations [68]. The most common parametrization is given by four Euler parameters, which gives the following representation for the attitude kinematics

$$\dot{q} = \tfrac{1}{2}W(\omega)q, \tag{2.9}$$

where $q = [q_1\ q_2\ q_3\ q_4]^T$ is the vector of Euler parameters with unit norm ($q^Tq = 1$), and

$$W(\omega) = \begin{bmatrix} 0 & \omega_z & -\omega_y & \omega_x \\ -\omega_z & 0 & \omega_x & \omega_y \\ \omega_y & -\omega_x & 0 & \omega_z \\ -\omega_x & -\omega_y & -\omega_z & 0 \end{bmatrix}. \tag{2.10}$$

For the ACS of an earth pointing spacecraft in a circular orbit the following reference frames are considered: the orbital axes (X_e, Y_e, Z_e), and the satellite body axes (X, Y, Z). The satellite's center of mass is the origin for both axes systems. The ACS of the satellite in space is determined by considering both the reference frames [94].

The magnetic attitude control torques generated by the set of three magnetic coils aligned with the spacecraft principal axes can be represented as [130, 69]

$$T_{mag} = m \times b = B(b)m, \tag{2.11}$$

where $m \in \mathbb{R}^3$ is the vector of magnetic dipoles of the coils , $b \in \mathbb{R}^3$ is the vector formed with the components of the Earth's magnetic field in the body frame of reference and

$$B(b) = \begin{bmatrix} 0 & b_z & -b_y \\ -b_z & 0 & b_x \\ b_y & -b_x & 0 \end{bmatrix}. \tag{2.12}$$

We assume for the spacecraft a momentum bias configuration (i.e., one momentum wheel, aligned with the body z-axis, with moment of inertia $J \in \mathbb{R}^3$ and angular velocity v). Hence, the modified system's dynamics takes the form

$$\mathbf{I}\dot{\omega} = -\omega \times [\mathbf{I}\omega + Jv] + T_{contr} + T_{dist}. \tag{2.13}$$

It is also natural that external disturbance torque will occur which may deflect the ACS. These disturbance torque can come through different sources, such as gravity gradient, aerodynamics, solar radiation and residual magnetic dipoles. Hence the question rises how to store the accurate momentum. Among inertial torques, it is possible to distinguish those that occur as disturbances and those that provide controllable torques to store momentum. The external disturbance torques that come from disturbing resources (i.e., gravity gradient, aerodynamics, solar radiation), can be separated into a secular component (i.e., a part with nonzero mean around each orbit) and a cyclic component (i.e., with zero mean, periodic part).

Introducing now the state vector $x = [q', \omega']'$ and considering small displacements from the nominal values of the vector part of the attitude quaternion $q_1 = q_2 = q_3 = 0$, $q_4 = 1$, and small deviations of the body rates from the nominal ones $\omega_x = \omega_y = 0$, $\omega_z = -\Omega$, (Ω being the angular frequency associated with the orbit period), we can linearize the attitude dynamics for the system as [94]

$$\dot{\delta}x = A\delta(x) + \begin{bmatrix} 0 \\ \mathbf{I}^{-1} \end{bmatrix} (T_{contr} + T_{dist}), \tag{2.14}$$

where

$$A = \frac{\partial f(x,t)}{\partial x}|_{x=x_{norm}} = \begin{bmatrix} \frac{\partial \dot{q}}{\partial q} & \frac{\partial \dot{q}}{\partial \omega} \\ \frac{\partial \dot{\omega}}{\partial q} & \frac{\partial \dot{\omega}}{\partial \omega} \end{bmatrix}|_{x=x_{norm}}. \tag{2.15}$$

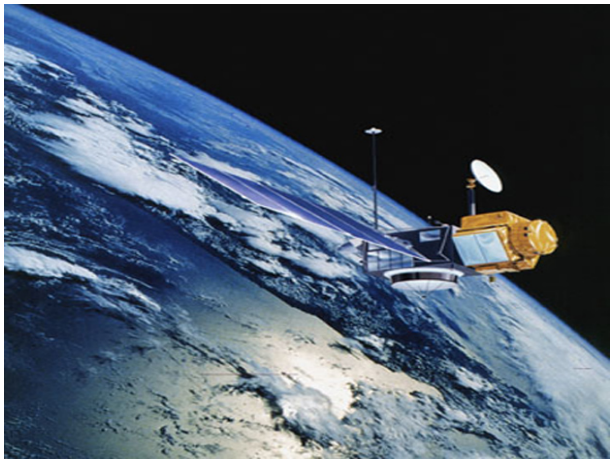

Figure 2.11. TOPEX/Poseidon, made for precise measurements of the ocean surface.
image source: http://topex-www.jpl.nasa.gov/mission/topex.html

Considering the control torques generated by the magnetic coils as in (2.11), the overall linearized model take the form

$$\dot{\delta x} = A\delta(x) + \begin{bmatrix} 0 \\ \mathbf{I}^{-1} \end{bmatrix} (B(b)m + T_{dist}). \tag{2.16}$$

If the time variation of the magnetic field is periodic, then this model can be considered as a linear-periodic model.

2.3.2. Periodic Attitude Control of Topex/Poseidon Satellite

TOPEX/Poseidon (launched in 1992) was a joint satellite mission between NASA, the U.S. space agency, and CNES, the French space agency, to map ocean surface topography. It was the first major oceanographic research vessel into space which helped revolutionize oceanography by proving the value of satellite ocean observations [51].

From orbit 1,336 kilometers above Earth, TOPEX/Poseidon provided measurements of the surface height of 95 percent of the ice-free ocean to an accuracy of 3.3 centimeters. TOPEX/Poseidon made it possible for the first time to determine the patterns of ocean circulation by observing how heat stored in the ocean moves from one place to another. Comparing the satellite based computer models of ocean circulation with actual global observations, TOPEX/Poseidon opened the door of vast possibilities to improve climate predictions.

The onboard ACS controls the orientation of the TOPEX/Poseidon satellite in space (see Figure 2.12). First of all, the orientation of the satellite is observed by the ACS. This orientation is determined from star trackers, the digital fine sun sensor, gyros, magnetometers, and the Earth Sensor Assembly Module. Then, the observed information is

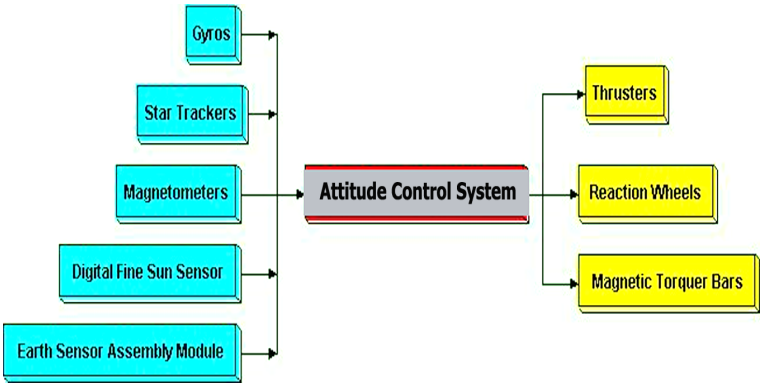

Figure 2.12. Block diagram of ACS for TOPEX/Poseidon .
image source: http://www.tsgc.utexas.edu/spacecraft/topex/atti.html

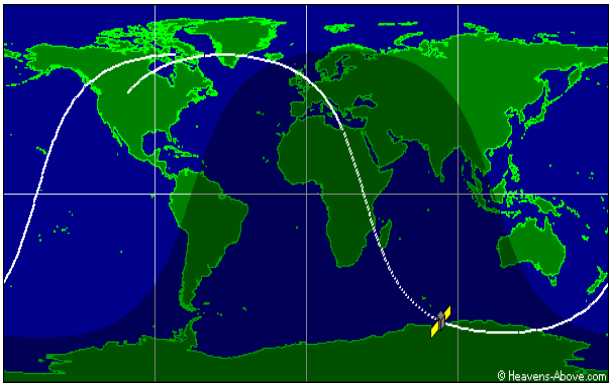

Figure 2.13. TOPEX/Poseidon: periodic orbital motion (Ground track view).
image source: http://topex-www.jpl.nasa.gov/mission/mission.html

carried to the Propulsion Module of the satellite where it uses reaction wheels, magnetic torquer bars, and the thrusters to control the attitudes of the satellite. This ensures the satellite to place the altimeter antenna accurately at the desired point (place) on the surface of the Earth right underneath the satellite for the data acquisition with efficient accuracy at all times.

Fig. 2.13 shows the controlled orbital periodic motion of TOPEX/Poseidon satellite in space. The dashed part of the orbit path shows where the satellite is in the earth's shadow, and the full part is where it is sunlit.

CHAPTER

THREE

BASIC CONCEPTS

Contents

In this chapter we introduce some basic concepts of system and control theory for LTI descriptor systems, both for continuous and discrete-time systems, which will be needed later in the period settings by the subsequent chapters of this thesis. The periodic reformulations of these basic contents will be discussed in Chapter 4. The main idea behind this is that the description in the LTI structures will help more precisely to understand their corresponding periodic structures in the subsequent chapters.

We start with some important definitions of LTI descriptor systems and discuss some of their basic properties. We then discuss the generalized matrix pencils and some of their decomposition techniques that we will use in the periodic case. The canonical form and the deflating subspaces corresponding to the generalized matrix pencil are discussed in this chapter.

The Lyapunov equations, which are projected Lyapunov equations in our case, are discussed later. Important theorems that guarantee the existence and uniqueness of these projected Lyapunov equations are also presented. We put some important notes and remarks at the end of this chapter.

3.1. Linear Descriptor Systems

Descriptor systems present a general mathematical framework for the modelling, simulation and control of complex dynamical systems arising in many areas of mechanical, electrical and chemical engineering. They have received a lot of importance and attention in last several decades.

A linear time-invariant continuous-time system is characterized by the equation

$$\begin{aligned} E\dot{x}(t) &= Ax(t) + Bu(t), \quad x(0) = x_0, \\ y(t) &= Cx(t), \end{aligned} \tag{3.1}$$

and a linear time-invariant discrete-time system is characterized by the equation

$$\begin{aligned} Ex_{k+1} &= Ax_k + Bu_k, \quad x(0) = x_0, \\ y_k &= Cx_k, \end{aligned} \tag{3.2}$$

where $x(t), x_k \in \mathbb{R}^n$ are descriptor variables, $u(t), u_k \in \mathbb{R}^p$ $(p \leq n)$ are system inputs, $y(t), y_k \in \mathbb{R}^q$ are system outputs, n is the system order, and p and q are the numbers of system inputs and outputs, respectively. The matrices $E, A \in \mathbb{R}^{n\times n}$, $B \in \mathbb{R}^{n\times p}$, $C \in \mathbb{R}^{q\times n}$ are the time-invariant system matrices. Both the systems are shortly referred to as $\mathbf{\Sigma}(E, A, B, C)$. For SISO systems, p, q=1, the matrices B and C change to vectors b and c^T, respectively.

Linear dynamical systems, where the input-to-state equation is written with a leading matrix E, are called *generalized state space systems* or *singular systems*. For E being singular (3.1) and (3.2) are called *descriptor systems*. If $E = I_n$, then systems (3.1) and (3.2) are called *standard state space systems*.

Assume that the matrices E, A present is systems (3.1) and (3.2) are nonsingular. The output function for u to y for system (3.1) can be defined as $\bar{y}(s) = H(s)\bar{u}(s)$, where $\bar{u}(s)$ and $\bar{y}(s)$ are the Laplace transforms of u(t) and y(t) with $x(0) = 0$, and

$$H(s) = C(sE - A)^{-1}B$$

is called the *transfer function* of the system. The transfer function matrix for a discrete-time system (3.2) can be expressed as

$$H(z) = C(zE - A)^{-1}B.$$

It is obtained by taking the z-transformation of the system.

Clearly, the Laplace transform maps the continuous-time system into frequency domain representation, whereas the z-transform maps the discrete-time system into frequency domain representation and the transfer functions relate inputs to outputs via $y(.) =$

$H(.)u(.)$ in the frequency domain. Here $y(.)$ and $u(.)$ are the corresponding Laplace transformation/z-transformation for u and y in (3.1) and (3.2), respectively.

Two systems $\mathbf{\Sigma}(E, A, B, C)$ and $\bar{\mathbf{\Sigma}}(\bar{E}, \bar{A}, \bar{B}, \bar{C})$ are called *restricted system equivalence* if there exist nonsingular matrices $W, T \in \mathbb{R}^{n\times n}$ such that

$$\bar{E} = WET,\ \bar{A} = WAT,\ \bar{B} = WB,\ \bar{C} = CT. \tag{3.3}$$

The pair (W, T) is called *system equivalence transformation*. A characteristic quantity of (3.1) and (3.2) is *system invariant* if it is preserved under a system equivalence transformation. The transfer function $H(s)$ is system invariant, since

$$\begin{aligned} H(s) = C(sE - A)^{-1}B &= \bar{C}T^{-1}(sW^{-1}\bar{E}T^{-1} - W^{-1}\bar{A}T^{-1})^{-1}W^{-1}\bar{B} \\ &= \bar{C}T^{-1}T(s\bar{E} - \bar{A})^{-1})^{-1}WW^{-1}\bar{B} \\ &= \bar{C}(s\bar{E} - \bar{A})^{-1}\bar{B}. \end{aligned}$$

Similar expression can be obtained also for $H(z)$. All representations of the same system (that can be transformed into each other) are called *realizations* of the system. A realization $\mathbf{\Sigma}(E, A, B, C)$ of order $\bar{n}$ is called *minimal* if $\bar{n}$ is the smallest possible dimension under all possible realizations. This minimal number of states is called the *McMillan degree* of the realization.

An LTV system consequently is a system where the system matrices may depend on time as well.

3.2. Generalized Matrix Pencils

A matrix pencil $\alpha E - \beta A$, denoted by (E, A), associated with the descriptor systems (3.1) and (3.2) is called *regular* if E and A are square, and $\det(\alpha E - \beta A) \neq 0$ for some $(\alpha, \beta) \in \mathbb{C}^2$, otherwise, (E, A) is called *singular*. A pair $(\alpha, \beta) \in \mathbb{C}^2 \setminus (0, 0)$ is said to be a *generalized eigenvalue* of (E, A) if $\det(\alpha E - \beta A) = 0$, and a *finite eigenvalue* λ of (E, A) is given by $\lambda = \alpha/\beta$, for $\beta \neq 0$. If $\beta = 0$, then the pair $(\alpha, 0)$ represents an *infinite eigenvalue* of $\lambda E - A$. Singularity of the matrix E leads to infinite eigenvalue(s) of the pencil $\lambda E - A$. The set of all generalized eigenvalues (finite and infinite) of the pencil $\lambda E - A$ is called the *spectrum* of $\lambda E - A$ and denoted by $\Lambda(E, A)$.

Definition 3.2.1:

A matrix pencil (E, A) associated with the system (3.1) is called *c-stable* if it is regular and all its finite eigenvalues lie in the open left half-plane. ◊

Example 3.2.1:

Consider

$$E = \begin{bmatrix} 1 & 1 \\ 0 & -1 \end{bmatrix} \quad \text{and} \quad A = \begin{bmatrix} -2 & 0 \\ 0 & 1 \end{bmatrix} \tag{3.4}$$

The matrix pencil (E, A) is regular and its eigenvalues are $-2, -1$. Since all eigenvalues of (E, A) have negative real part, the pencil is c-stable. ◊

Example 3.2.2:
Consider

$$E = \begin{bmatrix} 1 & 1 \\ 0 & 0 \end{bmatrix} \quad \text{and} \quad A = \begin{bmatrix} -2 & 1 \\ 0 & 1 \end{bmatrix} \tag{3.5}$$

The matrix pencil (E, A) is regular, and it has two eigenvalues, -2 and ∞. The pencil is c-stable since its only finite eigenvalue has negative real part. ◊

Definition 3.2.2:
The continuous-time descriptor system (3.1) is called *asymptotically stable* if $\lim_{t\to\infty} x(t) = 0$ for all solutions $x(t)$ of the system $E\dot{x}(t) = Ax(t)$. ◊

The trivial solution $x(t) \equiv 0$ of system (3.1) is *asymptotically stable* if and only if the corresponding matrix pencil (E, A) is c-stable.

Definition 3.2.3:
A matrix pencil (E, A) associated with the system (3.2) is called *d-stable* if it is regular and all its finite eigenvalues lie inside the unit circle. ◊

Example 3.2.3:
Let

$$E = \begin{bmatrix} 1 & 1 \\ 0 & -1 \end{bmatrix} \quad \text{and} \quad A = \begin{bmatrix} 0.4854 & 0.1419 \\ 0.8003 & 0.4218 \end{bmatrix}. \tag{3.6}$$

The matrix pencil (E, A) is regular and it has eigenvalues 0.9590 and -0.0951. All eigenvalues have magnitude less then 1. Hence, the pencil is d-stable. ◊

Example 3.2.4:
Consider

$$E = \begin{bmatrix} 0.5 & 1 \\ 0 & 0 \end{bmatrix} \quad \text{and} \quad A = \begin{bmatrix} 0.9157 & 0.9595 \\ 0.7922 & 0.6557 \end{bmatrix} \tag{3.7}$$

The regular matrix pair (E, A) has eigenvalues 0.3439 and ∞. The pencil is d-stable since its finite eigenvalue has magnitude less than 1. ◊

Definition 3.2.4:
The discrete-time descriptor system (3.2) is called *asymptotically stable* if $\lim_{k\to\infty} x_k = 0$ for all solutions x_k of the system $Ex_{k+1} = Ax_k$. ◊

The trivial solution $x_k \equiv 0$ of system (3.2) is *asymptotically stable* if and only if the corresponding matrix pencil (E, A) is d-stable.

3.2.1. Matrix Decompositions

Generalized Schur Decomposition. Given square matrices A and E in $\mathbb{C}^{n\times n}$, the *generalized Schur decomposition* factorizes both matrices as

$$A = QSZ^T \quad \text{and} \quad E = QTZ^T, \tag{3.8}$$

where Q and Z are orthogonal matrices, and S is quasi-upper triangular with 1-by-1 and 2-by-2 blocks on the diagonal, and T is upper triangular with non-negative diagonal entries. The generalized Schur decomposition is also sometimes called the QZ *decomposition* [43]. The 1-by-1 diagonal blocks of (S, T) contain real eigenvalues of (E, A) and the 2-by-2 diagonal blocks of (S, T) contain conjugate pairs of complex eigenvalues of (E, A).

If A and E are complex, then Q and Z are unitary matrices in (3.8), and S and T are upper triangular. In that case the generalized eigenvalue λ that solves the generalized eigenvalue problem $Ax = \lambda Ex$ (where x is unknown nonzero vector) can be computed from the ratio of the diagonal elements of S and T. That is, using subscripts to denote matrix elements, the i-th generalized eigenvalue λ_i satisfies

$$\lambda_i = S_{ii}/T_{ii}.$$

In the periodic setting, we define the *periodic Schur decomposition* and it has a very wide application is periodic control systems, especially for pole placement of periodic systems [98, 19], multirate sampling and in optimal control of periodic systems [4, 63, 73, 115].

Generalized Singular Value Decomposition. One of the most useful matrix decompositions used in linear control systems and in model reduction techniques is the *singular value decomposition* (SVD). The *generalized singular value decomposition* (GSVD) is the generalization and extension of SVD.

The generalized (or quotient) singular value decomposition of an $m \times n$ real matrix A and a $p \times n$ real matrix E is given by the pair of factorizations

$$A = U\begin{bmatrix}\Sigma_1 & 0\\ 0 & 0\end{bmatrix}Q^T \quad \text{and} \quad E = V\begin{bmatrix}\Sigma_2 & 0\\ 0 & 0\end{bmatrix}Q^T,$$

where $U \in \mathbb{R}^{m\times m}, V \in \mathbb{R}^{p\times p}$, $Q \in \mathbb{R}^{n\times n}$ are orthogonal matrices, and Σ_1 and Σ_2 are diagonal matrices of dimension r with positive, decreasing diagonal elements. Here $r \le n$ is the rank of $[A^T, E^T]$.

If $\Sigma_1 = \text{diag}(\alpha_1 \ge \alpha_2 \ge \cdots \ge \alpha_r) > 0$ and $\Sigma_2 = \text{diag}(\beta_1 \ge \beta_2 \ge \cdots \ge \beta_r) > 0$, then the ratios $\sigma_i = \alpha_i/\beta_i$ are called *generalized singular values* of the pencil (E, A).

If A and E are complex, matrices U, V, Q are unitary instead of orthogonal, and Q^T should be replaced by Q^H in the pair of factorizations. In linear control system theory,

the singular value decomposition is an important factorization of a rectangular real or complex matrix, with many applications in signal processing and system approximation as well as determining rank, range and null space of a matrix.

Generalized QR Decomposition. Let A be a $n \times m$ matrix, E be a $n \times p$ matrix. Then there exist orthogonal matrices Q ($n \times n$) and Z ($p \times p$) such that

$$A = QR, \quad \text{and} \quad E = QTZ,$$

where R has the form

$$R = \begin{array}{c} \\ m \\ n-m \end{array} \begin{array}{c} \begin{array}{c} m \end{array} \\ \begin{bmatrix} R_{11} \\ 0 \end{bmatrix} \end{array}, \quad \text{if n} \geq \text{m},$$

or

$$R = \begin{array}{c} \\ n \end{array} \begin{array}{c} \begin{array}{cc} n & m-n \end{array} \\ \begin{bmatrix} R_{11} & R_{12} \end{bmatrix} \end{array}, \quad \text{if n} < \text{m},$$

where R_{11} is upper triangular matrix. T has the form

$$T = \begin{array}{c} \\ n \end{array} \begin{array}{c} \begin{array}{cc} p-n & n \end{array} \\ \begin{bmatrix} 0 & T_{12} \end{bmatrix} \end{array}, \quad \text{if n} \leq \text{p},$$

or

$$T = \begin{array}{c} \\ n-p \\ p \end{array} \begin{array}{c} \begin{array}{c} p \end{array} \\ \begin{bmatrix} T_{11} \\ T_{21} \end{bmatrix} \end{array}, \quad \text{if n} > \text{p},$$

where T_{12} or T_{21} is an upper triangular matrix.

3.2.2. Deflating Subspaces

A k-dimensional subspace $S \subseteq \mathbb{R}^n$ is called *deflating subspace* for the pencil $\lambda E - A$ if the subspace $\{Ax + Ey : x, y \in S\}$ has dimension k or less ($k \leq n$). Deflating subspaces are a generalization of invariant subspaces.

Suppose that E, A are complex matrices and $S \in \mathbb{C}^n$ is a deflating subspace of $\lambda E - A$ of dimension k. Then there exist unitary matrices V and W such that the first k columns of W span S, and

$$V^*AW = \begin{bmatrix} A_{11} & A_{12} \\ 0 & A_{22} \end{bmatrix}, \quad V^*EW = \begin{bmatrix} E_{11} & E_{12} \\ 0 & E_{22} \end{bmatrix}, \tag{3.10}$$

where A_{11} and E_{11} are of order k [102]. Note that if λ is an eigenvalue of $\lambda E_{11} - A_{11}$, then it is not an eigenvalue of $\lambda E_{22} - A_{22}$. That means the deflating subspace S of $\lambda E - A$

has deflated it into two smaller pencils (have no common eigenvalues) by unitary equivalences. A special case of the representation (3.10) is that the eigenvalue of the pencil $\lambda E_{11} - A_{11}$ are finite, while the pencil $\lambda E_{22} - A_{22}$ contains only infinite eigenvalues. This can happen when the matrix E is singular. We will discuss this special case in the next subsection.

3.3. Canonical Form of Matrix Pencils

The Kronecker canonical form (KCF) describes the generalized eigenvalues and generalized eigenspace of the pencil $\lambda E - A$ in detail. A regular pencil $\lambda E - A$ can be represented by a canonical decomposition,

$$P(\lambda E - A)Q = \lambda \begin{bmatrix} I_{n_f} & 0 \\ 0 & N \end{bmatrix} - \begin{bmatrix} J & 0 \\ 0 & I_{n_\infty} \end{bmatrix}, \tag{3.11}$$

where P and Q are nonsingular, J corresponds to the finite eigenvalues of $\lambda E - A$ (including zero eigenvalues) and the nilpotent N corresponds to the infinite eigenvalues of $\lambda E - A$. The index ν of the pencil $\lambda E - A$ is defined as $N^{\nu-1} \neq 0$ and $N^{\nu} = 0$. If E is nonsingular, then $\lambda E - A$ has index zero.

The canonical representation (3.11) of the matrix pencil $\lambda E - A$ can be used to define the decomposition of $\mathbb{F}^n$ into two complementary deflating subspaces corresponding to the finite and infinite eigenvalues of the matrix pencil $\lambda E - A$. The matrices

$$P_l = P \begin{bmatrix} I_{n_f} & 0 \\ 0 & 0 \end{bmatrix} P^{-1}, \quad P_r = Q^{-1} \begin{bmatrix} I_{n_f} & 0 \\ 0 & 0 \end{bmatrix} Q, \tag{3.12}$$

are the *spectral projectors* onto the left and right deflating subspaces of $\lambda E - A$ corresponding to the finite eigenvalues.

In many applications, it is also required that the deflated pencils $\lambda E_{11} - A_{11}$, and $\lambda E_{22} - A_{22}$ in (3.10) should have some specific block structures. If the pencil $\lambda E - A$ is regular, we can always have the more suitable form of the deflated pencils, which is known as *Generalized upper triangular form* (GUPTRI) [34, 35] of generalized matrix pencil, and defined as,

$$V^* E W = \begin{bmatrix} E_f & E_u \\ 0 & E_\infty \end{bmatrix}, \quad V^* A W = \begin{bmatrix} A_f & A_u \\ 0 & A_\infty \end{bmatrix}, \tag{3.13}$$

where V and W are unitary matrices, the pencil $\lambda E_f - A_f$ is quasi-triangular and has only finite eigenvalues, while the pencil $\lambda E_\infty - A_\infty$ is triangular and has infinite eigenvalues. The GUPTRI form is a special case of the generalized Schur form for a regular pencil.

3.4. Projected Generalized Matrix Equations

Lyapunov equations play an important role in the context of stability of linear systems, as well as for descriptor systems. The generalized continuous-time- and discrete-time algebraic Lyapunov equations associated with the descriptor systems (3.1) and (3.2) can be expressed as

$$E^*XA + A^*XE = -G, \tag{3.14}$$

and

$$A^*XA - E^*XE = -G, \tag{3.15}$$

respectively, where X is an unknown solution matrix. The continuous-time algebraic Lyapunov equation (3.14) has a unique solution for every G if the matrix E is nonsingular and all the eigenvalues of the pencil $\lambda E - A$ have negative real part. For (3.15), the unique solution exists for every G if the matrix E is nonsingular and all the eigenvalues of the pencil $\lambda E - A$ have modulus smaller than one.

The situation differs when E is singular. In that case (3.14) may have no solutions even if all the finite eigenvalues of $\lambda E - A$ have negative real part and a solution, if it exists, is not unique. For the discrete-time case analogous problems arise when both E and A are singular. Equation (3.15) may have no solutions even if all the eigenvalues of the pencil $\lambda E - A$ lie inside the unit circle and a solution, if it exists, is not unique.

To overcome these difficulties, we consider the following *projected generalized continuous-time algebraic Lyapunov equation*

$$\begin{aligned} E^*XA + A^*XE &= -P_r^*GP_r, \\ X &= XP_l \end{aligned} \tag{3.16}$$

and the *projected generalized discrete-time algebraic Lyapunov equation*

$$\begin{aligned} A^*XA - E^*XE &= -P_r^*GP_r + \xi(I - P_r)^*G(I - P_r), \\ P_l^*X &= XP_l \end{aligned} \tag{3.17}$$

with $\xi = -1, 0, 1$. Here P_l and P_r are the spectral projectors onto the left and right deflating subspace of the matrix pencil $\lambda E - A$ corresponding to its finite eigenvalues. The projector on the right-hand sides of equations (3.16) and (3.17) ensure that they are solvable and the unique solutions exists. Also existence and uniqueness of solutions are independent of the index of the pencil $\lambda E - A$. The following theorems give the necessary and sufficient conditions for the existence and uniqueness and of the solutions of (3.16) and (3.17).

Theorem 3.4.1:

[103] *Let $\lambda E - A$ be a regular pencil with finite eigenvalues $\lambda_1, \ldots, \lambda_{n_f}$ counted according to their multiplicities and let P_l and P_r be the spectral projections as in (3.12). The projected generalized continuous-time algebraic Lyapunov equation (3.16) has a solution for every G if and only if $\lambda_j + \bar{\lambda}_k \neq 0$ for all $j, k = 1, \ldots, n_f$. Moreover, if the solution X of (3.16) satisfies $X = XP_l$, then it is unique.* ◊

Proof. See [103]. □

The condition $\lambda_j + \bar{\lambda}_k \neq 0$ in (3.16) implies that the pencil $\lambda E - A$ has no eigenvalues on the imaginary axis. If the pencil $\lambda E - A$ is c-stable and the matrix G in (3.16) is Hermitian, positive (semi)definite, then the solution X is also Hermitian, positive (semi)definite.

Theorem 3.4.2:

[103] *Let $\lambda E - A$ be a regular pencil with finite eigenvalues $\lambda_1, \ldots, \lambda_{n_f}$ counted according to their multiplicities and let P_l and P_r be the spectral projections as in (3.12). The projected generalized discrete-time algebraic Lyapunov equation (3.17) has a solution for every G if and only if $\lambda_j \bar{\lambda}_k \neq 1$ for all $j, k = 1, \ldots, n_f$. Moreover, if the solution X of (3.16) satisfies $P_l^* X = XP_l$, then it is unique.* ◊

Proof. See [103]. □

The condition $\lambda_j \bar{\lambda}_k \neq 1$ in (3.17) implies that the pencil $\lambda E - A$ has no eigenvalues on the unit circle. If the pencil $\lambda E - A$ is d-stable and the matrix G in (3.17) is Hermitian, positive (semi)definite, then the solution X is also Hermitian, positive (semi)definite on Im P_l.

3.5. Remarks and Notes

Note that we will only consider the case $\xi = 1$ in (3.17) in the subsequent chapters and also in the periodic setting of (3.17). The other two cases $\xi = -1$, and $\xi = 0$ will be neglected. The reason is that if $\lambda E - A$ is d-stable and G is positive definite, then the solution X of (3.17) with $\xi = -1$ is positive definite on Im P_l and negative definite on Ker P_l. For $\xi = 0$, the solution of (3.17) is positive definite on Im P_l and positive semidefinite on $\mathbb{F}^n$. The solution of (3.17) is positive definite on $\mathbb{F}^n$ when $\xi = 1$ [103].

CHAPTER

FOUR

LPTV SYSTEM ANALYSIS

Contents

We now discuss the most theoretical part of this thesis. In this chapter we generalize the context of Chapter 3 for periodic time-varying setting, both for continuous-time and discrete-time systems. We start with an introduction of Floquet theory for LPTV systems of ODEs and describe the stability of LPTV systems of ODEs with Floquet decomposition. After that we discuss the extension of Floquet theory for LPTV continuous-time systems of differential algebraic equations (DAEs). Here we show that the Floquet theory can transform the LPTV continuous-time systems of DAEs (index-1) into a system with constant coefficients. We also deduce that the whole behaviour of the solutions of the LPTV continuous-time systems of DAEs (index-1) can be described with the corresponding constant coefficient of DAE system.

We then discuss the system dynamics of the LTV discrete-time descriptor systems in the next section. We start by reviewing some basic concepts of LTV discrete-time descriptor

systems and then discuss the spectral decomposition technique to decompose an LTV discrete-time descriptor system into two subsystems: causal subsystem and noncausal subsystem.

We then discuss the periodic reachability and observability Gramians of LTV discrete-time descriptor systems exploiting the structures of their periodic decomposed subsystems. The periodic projected Lyapunov equations are presented with more details in the last section.

4.1. LPTV Continuous-Time Descriptor Systems

A time-varying continuous-time periodic descriptor system is the generalized state-space model

$$\begin{aligned} E(t)\dot{x}(t) &= A(t)x(t) + B(t)u(t), \\ y(t) &= C(t)x(t), \end{aligned} \tag{4.1}$$

where $E(t)$, $A(t)$, $B(t)$, $C(t)$ are matrices of order compatible with $x(t)$, $u(t)$, and $y(t)$ and are assumed to be continuous functions of time. All the above matrices are periodic with a period $T > 0$ and the matrices $E(t)$ are allowed to be singular.

In the context of integrated circuits, $E(t)$ and $A(t)$ describe the conductive and capacitive lumped elements [78, 114] in the circuit, and system (4.1) is represented as more usual form :

$$\begin{aligned} \frac{d}{dt}(\bar{C}(t)x(t)) &= -\bar{G}(t)x(t) + B(t)u(t), \\ z(t) &= L^T x(t), \end{aligned} \tag{4.2}$$

where $u(t)$ is the vector of signal input sources, $x(t)$ describes the internal states, and $\bar{C}(t)$, $\bar{G}(t)$ are the time-varying capacitance and conductance matrices, respectively. The output z of the system can be any arbitrary node voltage and L is a selected vector that maps the set of variables to the output node.

Usually these circuit models come from the linearization of nonlinear circuit systems on its unperturbed orbit (see, e.g., Chapter 2 and also in [78, 84, 114]), or from harmonic balance analysis (HB) [42, 58] of nonlinear circuits.

The general theory of time-varying linear differential equation is an amazing task which is still a leading issue to investigate the behaviors and natures of periodic systems. In the 19th century, two mathematicians Gaston Floquet [1]

[1] Achille Marie Gaston Floquet (December 15, 1847 - October 7, 1920) was a French mathematician, best known for his work in mathematical analysis, especially in theory of differential equations. source: http://en.wikipedia.org.

and Aleksandr Mikhailovic Lyapunov [2] established their celebrated theorem on the structure of solutions of periodic differential equations, now named after them *Floquet-Lyapunov Theory* [31]. Although this theory was first introduced for linear ODEs with periodic coefficient matrices, an equivalent representation can be established for periodic time-varying systems of linear DAEs [62, 33].

In the next section we first discuss the Floquet theory and some related results for periodically time-varying systems of linear ODEs and later we establish an equivalent representation of Floquet theory (and some related results) for periodic-time varying systems of linear DAEs.

4.1.1. Floquet Theory for LPTV Systems of ODEs

Consider the n-dimensional inhomogeneous linear system of ODEs

$$\dot{x} = A(t)x + b(t), \quad x(t_0) = x_0, \tag{4.3}$$

where $A(t) \in \mathbb{R}^{n\times n}$ and $b(t) \in \mathbb{R}^n$ are continuous. The homogeneous system corresponding to Equation (4.3) is given by

$$\dot{x} = A(t)x, \tag{4.4}$$

The initial value problems (4.3) and (4.4) satisfy the Picard-Lindelöf existence and uniqueness theorem [25, 22]. Hence, they have unique solutions with initial condition $x(0) = x_0 \in \mathbb{R}^n$.

Let $x_1(t), \ldots, x_n(t)$ be n linearly independent solutions of (4.4). Then, $X(t) = [x_1(t), \ldots, x_n(t)]$ is called a *fundamental matrix*. We say $X(t)$ is the *state transition matrix* for (4.4) when $X(0) = I_n$. The state transition matrix is denoted by $\Phi(t, 0)$. The solution ϕ of (4.3) satisfying the initial condition $x(0) = x_0$ can be represented by $\Phi(t, 0)$, and it is given by

$$x(t) = \phi(t, x_0) = \Phi(t, 0)x_0 + \int_0^t \Phi(t, \tau)b(\tau)d\tau \tag{4.5}$$

Now consider (4.4) is periodic with period $T > 0$, i.e. $A(t + T) = A(t)$ for $t \in \mathbb{R}$. The state transition matrix $\Phi(t, \tau)$ then satisfies

$$\dot{\Phi}(t, \tau) = A(t)\,\Phi(t, \tau), \quad \Phi(\tau, \tau) = I. \tag{4.6}$$

Here $X(t, \tau) := \Phi(t + T, \tau)$ is the fundamental matrix, which satisfies $X(t, \tau) := \Phi(t, \tau) \cdot C$. Here $C = \Phi(T, 0)$ is a nonsingular matrix, called *monodromy* matrix. Moreover it satisfies

[2] Aleksandr Mikhailovich Lyapunov (June 6, 1857 - November 3, 1918) was a Russian mathematician, mechanician and physicist. His surname is sometimes romanized as Ljapunov, Liapunov or Ljapunow. Lyapunov is known for his development of the stability theory of a dynamical system, as well as for his many contributions to mathematical physics and probability theory. source: http://en.wikipedia.org.

the following conditions [22]:

$$\begin{aligned}
\Phi(t+T,0) &= \Phi(t,0)\cdot\Phi(T,0) && (4.7)\\
\Phi(t_2,t_0) &= \Phi(t_2,t_1)\cdot\Phi(t_1,t_0) && (4.8)\\
\Phi(t_0,t_1) &= \Phi^{-1}(t_1,t_0) && (4.9)\\
\Phi(t_1,t_0) &= \Phi(t_1,0)\cdot\Phi(0,t_0) = \Phi(t_1,0)\cdot\Phi^{-1}(t_0,0) && (4.10)\\
\Phi(t+T,T) &= \Phi(t,0) && (4.11)
\end{aligned}$$

Floquet in 1883 derived the decomposition technique of the state transition matrix for periodically time-varying ODEs. Floquet theory for continuous-time linear periodic systems can be summarized in the following theorem and discussions.

Theorem 4.1.1:

[31, 33] (**The unified Floquet Decomposition**)
Given the linear periodic system

$$\dot{x} = A(t)x, \quad A(t+T) = A(t). \tag{4.12}$$

Then the state transition matrix $\Phi(t,\tau)$ *of (4.12) can be written as*

$$\begin{aligned}
\Phi(t,\tau) &= U(t)\, exp\,(D\cdot(t-\tau))\, V(\tau),\\
V(t) &= U^{-1}(t),
\end{aligned} \tag{4.13}$$

where $U(t)$ *is a* T*-periodic matrix and* D *is a constant matrix.*

Proof. The proof proceeds by finding a (constant) matrix D such that the state transition matrix over one period, i.e., the monodromy matrix $\Phi(T,0) =: \exp(D\cdot T)$. To justify the existence of such a matrix D we refer to [31] (see Theorem 3.5 therein). We write $\Phi(t,0)$ as $\Phi(t,0) =: \Phi(t,0)\exp(-D\cdot t)\exp(D\cdot t)$ and define the matrix $U(t)$ by

$$U(t) = \Phi(t,0)\exp(-D.t).$$

Since the exponential functions $\exp(-D\cdot T)$ and $\exp(-D\cdot t)$ are commutative, the periodicity of $U(t)$ can be shown easily as

$$\begin{aligned}
U(t+T) &= \Phi(t+T,0)\exp(-D\cdot(t+T))\\
&= \Phi(t,0)\,\Phi(T,0)\exp(-D\cdot T)\exp(-D\cdot t)\\
&= \Phi(t,0)\exp(-D\cdot t) = U(t)
\end{aligned}$$

Hence, the state transition matrix $\Phi(t,0)$ can be written as: $\Phi(t,0) = U(t)\exp(D\cdot t)$. From (4.10), it finally follows that

$$\begin{aligned}
\Phi(t,\tau) &= \Phi(t,0)\cdot\Phi^{-1}(\tau,0),\\
&= U(t)\exp(D\cdot t)\exp(-D\cdot\tau)U^{-1}(t),\\
&= U(t)\exp(D\cdot(t-\tau))\,V(\tau),
\end{aligned}$$

which completes the proof. □

Corollary 4.1.1:
We define the adjoint system corresponding to (4.4) given by

$$\dot{\hat{x}} \;=\; -A^T(t)\hat{x}. \tag{4.14}$$

The state transition matrix $\hat{\Phi}(\tau, t)$ of the adjoint system (4.14) in terms of the state transition matrix $\Phi(t, \tau)$ of Equation (4.4) can be written as

$$\hat{\Phi}(\tau, t) = V^T(t)\, exp(D^T \cdot (\tau - t))\, U^T(\tau), \tag{4.15}$$

where U, V are defined in Equation (4.13). ◊

Remark 4.1:
The eigenvalues μ_i of D are called the *characteristic (Floquet) exponents* of (4.12) and the eigenvalues of $\exp(D \cdot T)$: $\lambda_i = \exp(\mu_i T)$ are called the *characteristic (Floquet) multipliers*. ◊

With the Floquet theorem, it can be shown that any homogeneous LPTV systems of ODEs can be transformed into a system of constant coefficients [33]. The following theorem shows the summarized result of the Floquet theory in LPTV continuous-time systems of ODEs.

Theorem 4.1.2:
(**Lyapunov, 1982**) *The periodic matrix $U(t) := \Phi(t, 0)\, exp(-D.t)$ with the coordinate transformation $x = U(t)\hat{x}$ transforms the homogeneous periodic system (4.12) into a homogeneous system with constant coefficient.*

Proof. We sketch the proof from [22]. The proof proceeds with the substitution of $x = U(t)\hat{x}$ in $\dot{x} = A(t)x$, which gives the following differential equation:

$$\dot{\hat{x}} = U^{-1}(A\,U - \dot{U})\hat{x} \tag{4.16}$$

We simply observe that

$$\begin{aligned} U^{-1}(A\,U - \dot{U}) &= \exp(D \cdot t)\,\Phi^{-1}\,(A\,\Phi \exp(-D \cdot t) - \dot{\Phi} \exp(-D \cdot t) + \Phi\, D \exp(-D \cdot t)) \\ &= \exp(D \cdot t)\,\Phi^{-1}\,\Phi\, D\, \exp(-D \cdot t) = D. \end{aligned} \tag{4.17}$$

Here we used the commutative argument of $\exp(D \cdot t)$ and D, and this finally completes the proof. □

Hence, the homogeneous periodic system (4.12) is transformed into a homogeneous system with constant coefficient $\dot{\hat{x}} = D\hat{x}$. Indeed, we see that through that coordinate transformation $x = U(t)\hat{x}$, the solution $x(t)$ of (4.12) passing through x_0 at $t = 0$ is given by

$$\begin{aligned} x(t) = \phi(t, x_0) &= \Phi(t, 0)x_0 \\ &= U(t)\exp(D \cdot t)\, x_0 \\ &= U(t)\,\hat{\phi}(t, x_0) = U(t)\hat{x}(t) \end{aligned}$$

Thus $\hat{x}(t) = \exp(D \cdot t)\, x_0$.

Remark 4.2:
From Theorems 4.1.1- 4.1.2 and from discussions therein, we can conclude that the behaviour of the solutions of the linear system with periodic coefficients such as (4.12) can be characterized by the eigenvalues of the constant matrix D. These eigenvalues have the form $\frac{1}{T}\ln\lambda_j$, where λ_j are the eigenvalues of the monodromy matrix $\Phi(T, 0)$. Note that T is considered as the period in (4.12). ◊

Remark 4.3:
If $\exp(D.(t-\tau))$ is diagonalisable through similarity transformation, i.e.,

$$\exp(D.(t-\tau)) = X\, \Lambda(t-\tau)\, X^{-1},$$

then the state transition matrix $\Phi(t, \tau)$ with the substitutions $U(t)\ X \mapsto U(t)$ and $X^{-1}\ V(\tau) \mapsto V(\tau)$ can be written as

$$\Phi(t, \tau) = U(t)\, \Lambda(t-\tau)\, V(\tau),\ \Lambda(t-\tau) = \text{diag}\,[\exp(\mu_1(t-\tau)), \ldots, \exp(\mu_n(t-\tau))]. \tag{4.18}$$

◊

Now consider that $u_i(t)$ be the columns of $U(t)$ and $v_i^T(t)$ be the rows of $V(t)$:

$$U(t) = [u_1(t), u_2(t), \ldots, u_n(t)], \tag{4.19}$$
$$V^T(t) = [v_1(t), v_2(t), \ldots, v_n(t)]. \tag{4.20}$$

Then $\{u_1(t), u_2(t), \ldots, u_n(t)\}$ forms a basis for $U(t)$ and $\{v_1(t), v_2(t), \ldots, v_n(t)\}$ forms a basis for $V^T(t)$ and they together form a basis for $\mathbb{R}^n$. Moreover, they satisfy the following orthogonality conditions [32]:

$$v_i^T(t)u_j(t) = \delta_{ij}, \quad i = 1, \ldots, n,\ j = 1, \ldots, n,$$

for every t. Then the state transition matrix $\Phi(t, \tau)$ in (4.18) can be rewritten in terms of the basis vectors as

$$\Phi(t, \tau) = \sum_{i=1}^{n} \exp(\mu_i(t-\tau))\, u_i(t)\, v_i^T(\tau), \tag{4.21}$$

The monodromy matrix $\Phi(T, 0)$ for (4.12), which is nothing but the state transition matrix evaluated at $t = T$, is given by

$$\Phi(T, 0) = \sum_{i=1}^{n} \exp(\mu_i T)\, u_i(T)\, v_i^T(0) = \sum_{i=1}^{n} \exp(\mu_i T)\, u_i(0)\, v_i^T(0). \tag{4.22}$$

Similarly, we can define the state transition matrix $\hat{\phi}(\tau, t)$ of the adjoint system (4.14) which is simply given by $\phi^T(\tau, t)$, where $\phi(t, \tau)$ is the state transition matrix in (4.21) for

the linear periodic system (4.12). The monodromy matrix for the adjoint system (4.14) is given by

$$\Phi^T(0,T) = \sum_{i=1}^{n} \exp(-\mu_i T)\, v_i(T)\, u_i^T(T) = \sum_{i=1}^{n} \exp(-\mu_i T)\, v_i(0)\, u_i^T(0). \tag{4.23}$$

The monodromy matrix is the basic tool in the stability analysis of the periodic systems. Indeed, the stability of the LPTV system (4.12) can be defined with the characteristic of the eigenvalues λ_i, $i = 1, \ldots, n$, of the monodromy matrix $\Phi(T, 0)$.

Stability of LPTV Systems of ODEs:

Let us consider the LPTV system (4.12) and its Floquet decomposition as in (4.13). Consider the eigenvalues λ_i as in Remark 4.1. The sufficient condition for the *stability* of the LPTV system (4.12) is then given by

$$|\lambda_i| < 1 \Leftrightarrow Re\{\mu_i\} < 0, \forall i = 1, 2, \ldots, n.$$

There is a relation between the product of the characteristic multipliers and the trace of the coefficient matrix $A(t)$ [22]:

$$\prod_{i=1}^{n} \lambda_i = \exp(\int_0^T \text{trace}(A(\tau))d\tau). \tag{4.24}$$

Hence, a necessary condition of the stability of the system (4.12) is given by,

$$Re\,\{\int_0^T \text{trace}(A(\tau))d\tau\} \leq 0. \tag{4.25}$$

4.1.2. Floquet Theory for LPTV DAEs of Index-1

We now consider the n-dimensional inhomogeneous linear system of DAEs

$$\frac{d}{dt}(\bar{C}(t)x) + \bar{G}(t)x = b(t), \tag{4.26}$$

where $\bar{C}(t) \in \mathbb{R}^{n\times n}$ is not necessarily full rank. We assume that its rank is a constant, $m \leq n$, as a function of t. $\bar{C}(t)$ and $\bar{G}(t)$ are T-periodic matrices. We assume that the DAEs we are dealing with are index-1 [62]. The homogeneous system corresponding to (4.26) is given by

$$\frac{d}{dt}(\bar{C}(t)x) + \bar{G}(t)x = 0. \tag{4.27}$$

When $\bar{C}(t)$ is rank deficient, i.e., rank of $\bar{C}(t)$ is m and $m \leq n$, Equation (4.27) does not have solutions for all initial conditions $x(0) = x_0 \in \mathbb{R}^n$. Then, the solutions of the homogeneous system (4.27) lie in an m-dimensional subspace defined by [62, 22]

$$R(t) = \{z \in \mathbb{R}^n : \Big(\frac{d}{dt}\bar{C}(t) + \bar{G}(t)\Big)z \in \text{Im } \bar{C}(t)\}. \tag{4.28}$$

Also, every $x(t) \in R(t)$ is a solution of (4.27). The the null space of $\bar{C}(t)$, denoted ny $N(t)$, can be defined as

$$N(t) = \text{Ker } \bar{C}(t), \tag{4.29}$$

which is an $n - m = k$-dimensional subspace. For index-1 DAEs, we have the following relations, [72] and

$$R(t) \cap N(t) = \{0\}, \quad R(t) \oplus N(t) = \mathbb{R}^n, \tag{4.30}$$

where $\oplus$ denotes the direct sum decomposition.

If $L(t) = \{l_1(t), l_2(t), \ldots, l_m(t)\}$ forms a basis for $R(t)$ and $W(t) = \{w_1(t), w_2(t), \ldots, w_k(t)\}$ is a basis for $N(t)$, then it follows from (4.30) that $L(t) \cup W(t)$ forms a basis for $\mathbb{R}^n$.

The adjoint system corresponding to (4.27) is given by

$$\bar{C}^T(t)\frac{d}{dt}\hat{x} - \bar{G}^T(t)\hat{x} = 0 \Leftrightarrow \Big(\frac{d}{dt}\hat{x}^T\Big)\,\bar{C}(t) - \hat{x}^T\,\bar{G}(t) = 0 \tag{4.31}$$

If $\hat{x}(t)$ is a solution of (4.31) and $x(t)$ is a solution of (4.27), then we have

$$\begin{aligned} \frac{d}{dt}\,(\hat{x}^T(t)\bar{C}(t)x(t)) &= \Big(\frac{d}{dt}\hat{x}^T(t)\Big)\,\bar{C}(t)x(t) + \hat{x}^T(t)\frac{d}{dt}(\bar{C}(t)x(t)) \\ &= \hat{x}^T(t)\bar{G}(t)x(t) - \hat{x}^T(t)\bar{G}(t)x(t) = 0. \end{aligned}$$

Thus $\hat{x}^T(t)\bar{C}(t)x(t) = \hat{x}^T(0)\bar{C}(0)x(0)$ for all $t \geq 0$.

Let

$$R^T(t) = \{z \in \mathbb{R}^n : \bar{G}^T(t)z \in \text{Im } \bar{C}^T(t)\},$$

and

$$N^T(t) = \text{Ker } C^T(t).$$

Then $R^T(t) \cap N^T(t) = \{0\}$ and $R^T(t) \oplus N^T(t) = \mathbb{R}^n$.

The adjoint system plays an important role when computing the eigenvectors of special Floquet multipliers. Consider two time-varying coordinate transformation matrices, $P(t)$ and $Q(t)$. Then

$$\frac{d}{dt}(P\,\bar{C}\,Q\,\hat{x}) + \Big(P\,\bar{G}\,Q - \frac{d}{dt}P\,\bar{C}\,Q\Big)\,\hat{x} = P\,b, \tag{4.32}$$

is called the *analytically equivalent* system of (4.26).

Definition 4.1.1:
The system (4.26) is said to be in *canonical form*, if it can be written in the following form:

$$\frac{d}{dt}\left(\begin{pmatrix} I & 0 \\ 0 & N(t) \end{pmatrix} x\right) + \begin{pmatrix} \bar{G}(t) & 0 \\ 0 & I \end{pmatrix} x = f(t), \tag{4.33}$$

where N is a strictly triangular nilpotent matrix.

Remark 4.4:
For our index-1 problem, $N(t) = 0$ in Definition 4.1.1. ◊

Theorem 4.1.3:
[23] *Let us assume $\bar{C}$, $\bar{G}$ to be analytically real. Then the DAE (4.26) is solvable, if and only if it is analytically equivalent to a system (4.32) in canonical form, under a real analytical coordinate transformation.* ◊

Theorem 4.1.4:
[22] *Let $\bar{C}$, $\bar{G}$ be T-periodic real analytic matrices. The solution ϕ of the homogeneous system (4.27) satisfying the initial condition $x(0) = x_0 \in S(0)$ is given by*

$$\phi(t, x_0) = \Phi(t, 0)x_0, \tag{4.34}$$

where the state transition matrix $\Phi(t, \tau)$ is given by

$$\Phi(t, \tau) = U(t)\, \Sigma(t - \tau)\, V(\tau)\, \bar{C}(\tau), \tag{4.35}$$

with

$$\Sigma(t - \tau) = \begin{pmatrix} \exp(D(t - \tau)) & 0 \\ 0 & 0 \end{pmatrix}, \tag{4.36}$$

$\exp(D(t-\tau)) = diag\,[\exp(\mu_1(t-\tau)), \ldots, \exp(\mu_m(t-\tau))]$, *and $U(t) : n \times n$ and $V(t) : n \times n$ are T-periodic nonsingular matrices (for all t), and satisfy*

$$V(t)\bar{C}(t)U(t) = \begin{bmatrix} I_m & 0 \\ 0 & 0 \end{bmatrix}. \qquad \text{◊}$$

Proof. We sketch the proof from [22] with more detail. Let us consider the DAE (4.27). Using the analytical equivalence transformation as in (4.32) we will find a canonical representation of (4.27). There exists T-periodic analytical real matrices $P(t)$ and $Q(t)$ such that the system (4.27) can be transformed to the following canonical form through an analytical equivalence transformation [22]:

$$\begin{pmatrix} I_m & 0 \\ 0 & 0 \end{pmatrix} \dot{\hat{x}}(t) + \begin{pmatrix} \bar{G}_f(t) & 0 \\ 0 & I \end{pmatrix} \hat{x}(t) = 0$$

For the above system, the state transition matrix for the ODE-part can be written (using Theorem 4.1.1) as

$$\hat{\Phi}_f(t,\tau) = \hat{U}_f(t)\exp\left(D.(t-\tau)\right)\hat{U}_f^{-1}(\tau),$$

where $\hat{U}_f(t)$ is a T-periodic regular matrix . Therefore the state transition matrix for the DAE can be written as

$$\begin{aligned}\Phi(t,\tau) &= Q(t)\begin{pmatrix}\hat{U}_f(t) & \\ & I\end{pmatrix}\begin{pmatrix}\exp(D(t-\tau)) & \\ & 0\end{pmatrix}\begin{pmatrix}\hat{U}_f^{-1}(\tau) & \\ & I\end{pmatrix}Q^{-1}(\tau)\\ &= Q(t)\begin{pmatrix}\hat{U}_f(t) & \\ & I\end{pmatrix}\begin{pmatrix}\exp(D(t-\tau)) & \\ & \hat{D}_f(t,\tau)\end{pmatrix}\begin{pmatrix}\hat{U}_f^{-1}(\tau) & \\ & I\end{pmatrix}\begin{pmatrix}I_m & \\ & 0\end{pmatrix}Q^{-1}(\tau)\end{aligned}$$

Here $\hat{D}_f(t,\tau)$ is an arbitrary matrix and therefore without loss of generality we take $\hat{D}_f(t,\tau) \equiv 0\ \forall t,\tau$. This corresponds to an interpretation of the index-1 DAE as the limit value of an ODE with infinite stiffness.

Now defining

$$U(t) := Q(t)\begin{pmatrix}\hat{U}_f(t) & \\ & I\end{pmatrix}, \quad V(t) := \begin{pmatrix}\hat{U}_f^{-1}(t) & \\ & I\end{pmatrix}P(t),$$

and with the identity

$$\bar{C}(t) = P^{-1}(t)\begin{pmatrix}I_m & \\ & 0\end{pmatrix}Q^{-1}(t),$$

finally follows the statement. This completes the proof. □

Remark 4.5:

The μ's in Theorem 4.1.4 are called the characteristic (Floquet) exponents of (4.27), and the eigenvalues $\lambda_i = \exp(\mu_i T)$ are called the characteristic (Floquet) multipliers. Note that (4.27) has $k = n - m$ Floquet multipliers that are zero. ◊

Let $u_i(t)$ be the columns of $U(t)$ and $v_i^T(t)$ be the rows of $V(t)$:

$$U(t) = [u_1(t),\ldots,u_m(t),u_{m+1}(t),\ldots,u_n(t)], \tag{4.37}$$
$$V^T(t) = [v_1(t),\ldots,v_m(t),v_{m+1}(t),\ldots,v_n(t)]. \tag{4.38}$$

Then $\{u_1(t),\ldots,u_m(t)\}$ forms a basis for $R(t)$ and $\{u_{m+1}(t),\ldots,u_n(t)\}$ forms a basis for $N(t)$. Then $x(t) = u_i(t)\exp(\mu_i t)$ is a solution of (4.27) with the initial condition $x(0) = u_i(0)$ for $1 \le i \le m$. Similarly, $\{v_1(t),\ldots,v_m(t)\}$ is a basis for $R^T(t)$ and $\{v_{m+1}(t),\ldots,v_n(t)\}$ is a basis for $N^T(t)$. Then, for $1 \le i \le m$, $\hat{x}(t) = v_i(t)\exp(-\mu_i t)$ is a solution of (4.31) with the initial

condition $\hat{x}(0) = v_i(0)$. Moreover, we have the following orthogonality/biorthogonality conditions [32]:

$$v_j^T(t)\bar{C}(t)u_i(t) = \delta_{ij}, \quad i = 1,\dots,m,\ j = 1,\dots,m, \tag{4.39}$$

$$v_j^T(t)\bar{C}(t)u_i(t) = 0, \quad i = 1,\dots,m,\ j = m+1,\dots,n, \tag{4.40}$$

$$v_j^T(t)\bar{G}(t)u_i(t) = 0, \quad i = m+1,\dots,n,\ j = 1,\dots,m, \tag{4.41}$$

Now the state transition matrix $\Phi(t,\tau)$ in (4.35) can be written in a different form as

$$\Phi(t,\tau) = \sum_{i=1}^{m} \exp(\mu_i(t-\tau))\ u_i(t)\ v_i^T(\tau)\bar{C}(\tau). \tag{4.42}$$

Similarly, we can define the state transition matrix $\hat{\phi}(t,\tau)$ of the adjoint system (4.31). For the DAEs (4.27), this is not simply given by $\Phi^T(\tau,t)$ in terms of the state transition matrix $\Phi(t,\tau) = U(t)\ \Sigma(t-\tau)\ V(\tau)\ \bar{C}(\tau)$ as it was in the ODEs case. Instead, it is given by given by

$$\varphi(t,\tau) = V^T(t)\ \Sigma^T(\tau - t))\ U^T(\tau)\ \bar{C}^T(\tau) = \sum_{i=1}^{m} \exp(-\mu_i(t-\tau))v_i(t)u_i^T(\tau)\bar{C}^T(\tau). \tag{4.43}$$

Theorem 4.1.5:

[32] *The solution ϕ of (4.26) satisfying the initial condition $x(0) = x_0 \in R(0)$ (for $b(0) = 0$) is given by*

$$\phi(t,x_0) = \Phi(t,0)x_0 + \int_0^t \Psi(t,\tau)\ b(\tau)\ d\tau + \Gamma(t)b(t), \tag{4.44}$$

where

$$\Psi(t,\tau) = U(t)\Sigma(t-\tau)V(\tau) \tag{4.45}$$

and $\Gamma(t) \in \mathbb{R}^{n\times n}$ is a T-periodic matrix of rank k which satisfies

$$\Gamma(t)\bar{C}(t)[u_1(t),\dots,u_m(t)] = 0,$$

i.e. the null space of $\Gamma(t)$ is spanned by $\{\bar{C}(t)u_1(t),\dots,\bar{C}(t)u_m(t)\}$.

Monodromy matrix. The monodromy matrix for system (4.27) is defined as $\Phi(T,0)$, and it is given by

$$\Phi(T,0) = \sum_{i=1}^{m} \exp(\mu_i T)\ u_i(T)v_i^T(0)\bar{C}(0) = \sum_{i=1}^{m} \exp(\mu_i T)\ u_i(0)v_i^T(0)\bar{C}(0). \tag{4.46}$$

Similarly, the monodromy matrix for the adjoint system (4.31) is defined as $\hat{\Phi}(T,0)$, and it is given by

$$\hat{\Phi}(T,0) = \sum_{i=1}^{m} \exp(-\mu_i T)\, v_i(0) u_i^T(0) \bar{C}^T(0). \tag{4.47}$$

The eigenvalues of the monodromy matrix determine the stability of (4.27) and this stability is very much important when the concerned DAEs describe the dynamics of an electronic system or a mechanical system. In RF communication systems, for perturbation analysis and phase noise characterization of RF component (i.e., an oscillator), one needs to compute the steady-state periodic solutions of the DAEs associated with the systems. We discuss more details of LTPV continuous-time DAEs and model reduction approaches associated with those DAEs in Chapter 7.

4.2. LPTV Discrete-Time Descriptor Systems

Linear periodic systems, both continuous and discrete time, have a very long and successful history in physics and mathematics going back to the contribution in the second-half of the present century by several mathematicians and engineers. During this time the vast and versatile development of systems and control theory, together with the achievements of digital control and signal processing, have set renewed interest in the study and analysis of periodic systems for their specific application demands, specially in aerospace realm [68, 69, 94], control of industrial processes and communication systems [4, 86], modeling of periodic time-varying filters and networks [78, 93, 115], circuit simulation [17, 66, 132], micro-electronics [87, 86], and multirate sampled-data systems [4, 39, 73].

A linear discrete-time periodic descriptor system with time-varying dimensions has the form

$$\begin{aligned} E_k x_{k+1} &= A_k x_k + B_k u_k, \\ y_k &= C_k x_k, \qquad k \in \mathbb{Z}, \end{aligned} \tag{4.48}$$

where $E_k \in \mathbb{R}^{\mu_{k+1} \times n_{k+1}}$, $A_k \in \mathbb{R}^{\mu_{k+1} \times n_k}$, $B_k \in \mathbb{R}^{\mu_{k+1} \times p_k}$, $C_k \in \mathbb{R}^{q_k \times n_k}$ are time-varying, and periodic with a period $K \geq 1$. Clearly, $\sum_{k=0}^{K-1} \mu_k = \sum_{k=0}^{K-1} n_k = n$. The matrices E_k are allowed to be singular for all k.

The dynamics of the discrete-time periodic descriptor system (4.48) are often addressed by the regularity and the eigenstructure of the set of periodic matrix pairs $\{(E_k, A_k)\}_{k=0}^{K-1}$. If all E_k are nonsingular, the eigenvalues (also called *characteristic multipliers*) of system (4.48) are given by the eigenvalues of the matrix product (generally known as *monodromy*

matrix)

$$E_{K-1}^{-1}A_{K-1}E_{K-2}^{-1}A_{K-2}\cdots E_0^{-1}A_0 \tag{4.49}$$

associated with the periodic matrix pairs $\{(E_k, A_k)\}_{k=0}^{K-1}$. This product only yields a well-defined matrix if all E_k are nonsingular. Even if they are, the formulation of that matrix should be avoided for reasons of numerical stability. Note that even for some E_k being singular, we use (4.49) in a formal way to denote a generalization of matrix pencils to this periodic case (see [14] for details of this formal matrix product calculus). We compute the eigenvalues of (4.49) via the generalized periodic Schur decomposition [19, 45, 56].

There exist unitary matrices $P_k \in \mathbb{C}^{\mu_{k+1}\times\mu_{k+1}}$ and $Q_k \in \mathbb{C}^{n_k\times n_k}$, with $Q_{k+K} = Q_k$ such that the transformed matrices

$$S_k = P_k^* A_k Q_k, \quad T_k = P_k^* E_k Q_{k+1}, \quad k = 0, \ldots, K-1, \tag{4.50}$$

are all upper triangular [19, 99], where for the ease of notation we allow complex arithmetic (in practice, however, computations can be performed in real arithmetic leading to quasi-triangular structure of one of the S_k). Then the formal matrix product

$$T_{K-1}^{-1}S_{K-1}T_{K-2}^{-1}S_{K-2}\cdots T_0^{-1}S_0 \tag{4.51}$$

is also block upper triangular, has the same eigenvalues as (4.49) and the sequence $\{(S_k, T_k)\}_{k=0}^{K-1}$ is said to be in *generalized periodic real Schur form* (GPRSF) of $\{(E_k, A_k)\}_{k=0}^{K-1}$. The 1×1 and 2×2 blocks on the diagonals of the transformed matrices S_k and T_k are used to define the real eigenvalues and complex eigenvalues of the periodic matrix pairs $\{(E_k, A_k)\}_{k=0}^{K-1}$, respectively.

A real *finite eigenvalue* is given by

$$\lambda_l = \prod_{k=0}^{K-1} \frac{s_{ll}^{(k)}}{t_{ll}^{(k)}}, \tag{4.52}$$

provided $t_{ll}^{(k)} \neq 0$ for $k = 0, \ldots, K-1$. Here $s_{ll}^{(k)}, t_{ll}^{(k)}$ are the diagonal entries of the periodic matrices S_k and T_k for $k = 0, \ldots, K-1$, respectively. An eigenvalue is called *infinite* if $\prod_{k=0}^{K-1} t_{ll}^{(k)} = 0$, but $\prod_{k=0}^{K-1} s_{ll}^{(k)} \neq 0$.

For a pair of complex conjugate eigenvalues $\lambda_l, \bar{\lambda}_l$, $t_{ll}^{(k)}$ and $s_{ll}^{(k)}$ in (4.52) are 2×2 blocks, and

$$\lambda_l, \bar{\lambda}_l \in \Lambda\Big(\prod_{k=0}^{K-1} t_{ll}^{(k)^{-1}} s_{ll}^{(k)}\Big),$$

provided $t_{ll}^{(k)} \neq 0$, where Λ denotes the eigenspectrum of the corresponding matrix. In finite precision arithmetic, it requires to avoid the underflow and overflow problems when handling these 2×2 blocks to compute their eigenvalues explicitly [45].

4.2.1. Preliminaries

The regularity of the periodic matrix pairs is defined by the regularity of the monodromy matrix (4.49), i.e., the regularity of the whole set of periodic matrix pairs associated with the periodic system. A set of periodic matrix pairs $\{(E_k, A_k)\}_{k=0}^{K-1}$, denoted by $(\mathbb{E}, \mathbb{A})$, is called *singular* if there are 1×1 blocks on the diagonals of the transformed matrices S_k and T_k in (4.50) for which both $\prod_{k=0}^{K-1} s_{ll}^{(k)} = 0$ and $\prod_{k=0}^{K-1} t_{ll}^{(k)} = 0$, otherwise the set of matrix pairs is called *regular*. In the degenerate singular case, the eigenvalues become ill-defined and we find the *Kronecker canonical* representation of the periodic matrix pairs [123] to study the eigenvalue problem.

Definition 4.2.1:
Let $(\mathbb{E}, \mathbb{A})$ be the regular set of periodic matrix pairs $\{(E_k, A_k)\}_{k=0}^{K-1}$. The periodic matrix pairs $\{(E_k, A_k)\}_{k=0}^{K-1}$ are called *periodic stable* (shortly, *pd-stable*) if $(\mathbb{E}, \mathbb{A})$ is regular and all their finite eigenvalues lie inside the unit circle. ◊

Note that we are considering the regularity of the set of periodic matrix pairs, rather then the regularity of individual matrix pairs (E_k, A_k). It is also to be noted that the pd-stability of a periodic system depends on the spectrum of the whole set of periodic matrix pairs $\{(E_k, A_k)\}_{k=0}^{K-1}$, not that of individual matrix pairs.

Example 4.2.1:
Consider the period $K = 2$ and

$$E_0 = \begin{bmatrix} 2 & 0 \\ 0 & 1 \end{bmatrix}, \quad E_1 = \begin{bmatrix} 4 & 0 \\ 0 & 16 \end{bmatrix},$$

and

$$A_0 = \begin{bmatrix} 1 & 0 \\ 0 & 3 \end{bmatrix}, \quad A_1 = \begin{bmatrix} 6 & 0 \\ 0 & 1/4 \end{bmatrix}.$$

The set of matrix pairs, i.e., the monodormy matrix $E_1^{-1}A_1E_0^{-1}A_0$ has eigenvalues 0.0469 and 0.7500, both lie inside the unit circle. Hence, the periodic system is stable. But the individual matrix pairs are not stable, because (E_0, A_0) has eigenvalues 0.5 and 3.0, and (E_1, A_1) has eigenvalues 0.0156 and 1.5. ◊

Definition 4.2.2:
Let the set $(\mathbb{E}, \mathbb{A})$ of periodic matrix pairs $\{(E_k, A_k)\}_{k=0}^{K-1}$ be regular. The periodic descriptor system (4.48) is *asymptotically stable* if and only if all finite eigenvalues of the periodic matrix pairs $\{(E_k, A_k)\}_{k=0}^{K-1}$ lie inside the unit circle. ◊

In many applications, it is desirable to have the eigenvalues along the diagonal of the GPRSF in a certain order. If the generalized periodic Schur form has its eigenvalues ordered in a certain way as in (4.53), it is called an *ordered GPRSF* [45]. For example, if we have

$$\{(S_k, T_k)\}_{k=0}^{K-1} = \left\{ \begin{bmatrix} S_{11}^{(k)} & S_{12}^{(k)} \\ 0 & S_{22}^{(k)} \end{bmatrix}, \begin{bmatrix} T_{11}^{(k)} & T_{12}^{(k)} \\ 0 & T_{22}^{(k)} \end{bmatrix} \right\}_{k=0}^{K-1}, \tag{4.53}$$

such that the upper left part $\{(S_{11}^{(k)}, T_{11}^{(k)})\}_{k=0}^{K-1}$ contains all the eigenvalues in the open unit disk, then $\{(S^{(k)}, T^{(k)})\}_{k=0}^{K-1}$ is an ordered GPRSF.

One important application of this ordered GPRSF is the *stable-unstable spectral separation* of a periodic discrete-time system for computing the numerical solution of discrete-time periodic Lyapunov equations [103] in linear control theory.

4.2.2. Decomposition of Discrete-Time Descriptor Systems: Causal- and Noncausal Subsystems

The spectral decomposition theorem we state here extends a well known result for time invariant pencils to the periodic case.

Lemma 4.2.1:
[30] Let the set of periodic matrix pairs $\{(E_k, A_k)\}_{k=0}^{K-1}$ be regular. Then for $k = 0, 1, \ldots, K-1$, there exist nonsingular matrices $W_k \in \mathbb{R}^{\mu_{k+1} \times \mu_{k+1}}$ and $Z_k \in \mathbb{R}^{n_k \times n_k}$ such that

$$W_k E_k Z_{k+1} = \begin{bmatrix} I_{n_{k+1}^f} & 0 \\ 0 & E_k^b \end{bmatrix}, \quad W_k A_k Z_k = \begin{bmatrix} A_k^f & 0 \\ 0 & I_{n_k^\infty} \end{bmatrix}, \tag{4.54}$$

where $Z_K = Z_0$, $A_{k+K-1}^f A_{k+K-2}^f \cdots A_k^f = J_k$ is an $n_k^f \times n_k^f$ Jordan matrix corresponding to the finite eigenvalues, $E_k^b E_{k+1}^b \cdots E_{k+K-1}^b = N_k$ is an $n_k^\infty \times n_k^\infty$ nilpotent Jordan matrix corresponding to an eigenvalue at infinity, $n_k = n_k^f + n_k^\infty$ and $\mu_{k+1} = n_{k+1}^f + n_k^\infty$. ◊

Proof. The proof is sketched from [30] with some more detail. For the *pd-stable* matrix pairs, we can always obtain their upper triangular form using the periodic Schur algorithm [19] which always exits. There exist orthogonal periodic matrices $V_k \in \mathbb{R}^{\mu_{k+1} \times \mu_{k+1}}$ and $U_k \in \mathbb{R}^{n_k \times n_k}$, with $U_K = U_0$, $V_K = V_0$ and for $k = 0, 1, \ldots, K-1$, such that

$$V_k^T E_k U_{k+1} = \begin{bmatrix} E_{11,\,k} & E_{12,\,k} \\ 0 & E_{22,\,k} \end{bmatrix}, \quad V_k A_k U_k = \begin{bmatrix} A_{11,\,k} & A_{12,\,k} \\ 0 & A_{22,\,k} \end{bmatrix}, \tag{4.55}$$

where the matrices $E_{11,\,k} \in \mathbb{R}^{n^f_{k+1} \times n^f_{k+1}}$ and $A_{22,\,k} \in \mathbb{R}^{n^\infty_k \times n^\infty_k}$ are nonsingular and

$$(A_{22,\,k})^{-1}\, E_{22,\,k}\, (A_{22,\,k+1})^{-1}\, E_{22,\,k+1} \cdots (A_{22,\,k+K-1})^{-1}\, E_{22,\,k+K-1}$$

are nilpotent for $k = 0, 1, \ldots, K-1$. The spectrum $\Lambda(\mathbb{E}_f, \mathbb{A}_f)$ contains all the finite eigenvalues of the periodic matrix pairs $\{(E_k, A_k)\}_{k=0}^{K-1}$ that lie inside the unit circle and the spectrum $\Lambda(\mathbb{E}_\infty, \mathbb{A}_\infty)$ contains only infinite eigenvalues of the periodic matrix pairs $\{(E_k, A_k)\}_{k=0}^{K-1}$. Clearly, $\Lambda(\mathbb{E}_f, \mathbb{A}_f) \cap \Lambda(\mathbb{E}_\infty, \mathbb{A}_\infty) = \emptyset$. We then construct the following matrices:

$$\begin{bmatrix} E^{-1}_{11,\,k} & 0 \\ 0 & A^{-1}_{22,\,k} \end{bmatrix} \begin{bmatrix} E_{11,\,k} & E_{12,\,k} \\ 0 & E_{22,\,k} \end{bmatrix} = \begin{bmatrix} I_{n^f_{k+1}} & \hat{E}_{12,\,k} \\ 0 & \hat{E}^\infty_k \end{bmatrix}$$

and

$$\begin{bmatrix} E^{-1}_{11,\,k} & 0 \\ 0 & A^{-1}_{22,\,k} \end{bmatrix} \begin{bmatrix} A_{11,\,k} & A_{12,\,k} \\ 0 & A_{22,\,k} \end{bmatrix} = \begin{bmatrix} \hat{A}^f_k & \hat{A}_{12,\,k} \\ 0 & I_{n^\infty_k} \end{bmatrix},$$

where $\hat{E}_{12,\,k} \in \mathbb{R}^{n^f_{k+1} \times n^\infty_{k+1}}$, $\hat{E}^\infty_k \in \mathbb{R}^{n^\infty_k \times n^\infty_{k+1}}$, $\hat{A}^f_k \in \mathbb{R}^{n^f_{k+1} \times n^f_k}$, and $\hat{A}_{12,\,k} \in \mathbb{R}^{n^f_{k+1} \times n^\infty_k}$.

We will prove that there exist periodic matrices $P_k \in \mathbb{R}^{n^f_{k+1} \times n^\infty_k}$ and $Q_k \in \mathbb{R}^{n^f_k \times n^\infty_k}$ such that

$$\begin{bmatrix} I_{n^f_{k+1}} & P_k \\ 0 & I_{n^\infty_k} \end{bmatrix} \begin{bmatrix} I_{n^f_{k+1}} & \hat{E}_{12,\,k} \\ 0 & \hat{E}^\infty_k \end{bmatrix} \begin{bmatrix} I_{n^f_{k+1}} & Q_{k+1} \\ 0 & I_{n^\infty_{k+1}} \end{bmatrix} = \begin{bmatrix} I_{n^f_{k+1}} & 0 \\ 0 & \hat{E}^\infty_k \end{bmatrix}, \tag{4.56}$$

and

$$\begin{bmatrix} I_{n^f_{k+1}} & P_k \\ 0 & I_{n^\infty_k} \end{bmatrix} \begin{bmatrix} \hat{A}^f_k & \hat{A}_{12,\,k} \\ 0 & I_{n^\infty_k} \end{bmatrix} \begin{bmatrix} I_{n^f_k} & Q_k \\ 0 & I_{n^\infty_k} \end{bmatrix} = \begin{bmatrix} \hat{A}^f_k & 0 \\ 0 & I_{n^\infty_k} \end{bmatrix}. \tag{4.57}$$

Comparing both sides of (4.56) and (4.57), we obtain

$$Q_{k+1} + P_k \hat{E}^\infty_k + \hat{E}_{12,\,k} = 0 \tag{4.58}$$

and

$$\hat{A}^f_k Q_k + P_k + \hat{A}_{12,\,k} = 0, \tag{4.59}$$

for all k. From (4.59), we have $P_k = -\hat{A}^f_k Q_k - \hat{A}_{12,\,k}$ and substituting P_k in (4.58), we obtain,

$$Q_{k+1} = \hat{A}^f_k Q_k \hat{E}^\infty_k + \hat{A}_{12,\,k} \hat{E}^\infty_k - \hat{E}_{12,\,k} = 0 \tag{4.60}$$

Hence, recursive computation of (4.60), with $Q_K = Q_0$, gives

$$Q_1 = (\hat{A}^f_{K-1}\hat{A}^f_{K-2}\cdots\hat{A}^f_0)\, Q_0\, (\hat{E}^\infty_0\hat{E}^\infty_1\cdots\hat{E}^\infty_{K-1}) + G, \tag{4.61}$$

where G is independent of any Q_k. Since $\hat{E}^\infty_k$ corresponds to the nilpotent part and obviously $\Lambda(\hat{E}^\infty_0\hat{E}^\infty_1\cdots\hat{E}^\infty_{K-1}) = \{0\}$, we can uniquely determine Q_0 from (4.61), and the other Q_k from (4.60), and all the P_k from (4.59).

Using the Jordan decomposition with nonsingular K-periodic matrices $X_k \in \mathbb{R}^{n^f_k \times n^f_k}$ and $Y_k \in \mathbb{R}^{n^\infty_k \times n^\infty_k}$, we have the following Jordan forms

$$J_k = X_k^{-1}(\hat{A}^f_{k+K-1}\hat{A}^f_{k+K-2}\cdots\hat{A}^f_k)X_k\,, \tag{4.62}$$

and

$$N_k = Y_k^{-1}(\hat{E}^\infty_k\hat{E}^\infty_{k+1}\cdots\hat{E}^\infty_{k+K-1})Y_k\,. \tag{4.63}$$

Finally, defining

$$\begin{aligned} W_k &= \begin{bmatrix} X_{k+1}^{-1} & 0 \\ 0 & Y_k^{-1} \end{bmatrix}\begin{bmatrix} I_{n^f_{k+1}} & P_k \\ 0 & I_{n^\infty_k} \end{bmatrix}\begin{bmatrix} E^{-1}_{11,\,k} & 0 \\ 0 & A^{-1}_{22,\,k} \end{bmatrix} V_k^T\,, \\ Z_k &= U_k \begin{bmatrix} I_{n^f_k} & Q_k \\ 0 & I_{n^\infty_k} \end{bmatrix}\begin{bmatrix} X_k & 0 \\ 0 & Y_k \end{bmatrix}, \end{aligned}$$

and

$$E^b_k = Y_k^{-1}\hat{E}^\infty_k Y_{k+1}, \quad A^f_k = X_{k+1}^{-1}\hat{A}^f_k X_k\,;$$

we obtain the structure as in (4.54) and that completes the proof. □

Remark 4.6:

Note that if ν_k is the nilpotency of the matrix N_k for $k = 0, 1, \ldots, K-1$, then $(\nu_0, \nu_1, \ldots, \nu_{K-1})$ are called the indices of a regular set of periodic matrix pairs $\{(E_k, A_k)\}_{k=0}^{K-1}$. Hence the index ν of system (4.48) is defined as $\nu = \max(\nu_0, \nu_1, \ldots, \nu_{K-1})$. The periodic descriptor system (4.48) is of index at most 1 if $\nu \le 1$, i.e., E_k are all nonsingular or $N_k = 0$ for all k. ◊

For $k = 0, 1, \ldots, K-1$, the matrices

$$P_r(k) = Z_k\begin{bmatrix} I_{n^f_k} & 0 \\ 0 & 0 \end{bmatrix} Z_k^{-1} \in \mathbb{R}^{n_k \times n_k}, \quad P_l(k) = W_k^{-1}\begin{bmatrix} I_{n^f_{k+1}} & 0 \\ 0 & 0 \end{bmatrix} W_k \in \mathbb{R}^{\mu_{k+1}\times\mu_{k+1}}, \tag{4.64}$$

are the *spectral projectors* onto the k-th right and left deflating subspaces of the periodic matrix pairs $\{(E_k, A_k)\}_{k=0}^{K-1}$ corresponding to the finite eigenvalues, and $Q_r(k) = I - P_r(k)$ and $Q_l(k) = I - P_l(k)$ are the complementary projectors.

For every $k = 0, 1, \ldots, K-1$, define the vector $Z_k^{-1} x_k = [\,(x_k^f)^T,\ (x_k^b)^T\,]^T$ and let the matrices

$$W_k B_k = \begin{bmatrix} B_k^f \\ B_k^b \end{bmatrix}, \qquad C_k Z_k = \begin{bmatrix} C_k^f, & C_k^b \end{bmatrix}, \tag{4.65}$$

be partitioned in blocks conformally to the periodic matrix pairs $\{(E_k, A_k)\}_{k=0}^{K-1}$ in (4.54). Under this transformation, system (4.48) can be decoupled into *forward* and *backward periodic subsystems*

$$x_{k+1}^f = A_k^f x_k^f + B_k^f u_k, \quad y_k^f = C_k^f x_k^f, \tag{4.66}$$

$$E_k^b x_{k+1}^b = x_k^b + B_k^b u_k, \quad y_k^b = C_k^b x_k^b, \tag{4.67}$$

respectively, with $y_k = y_k^f + y_k^b$, $k = 0, 1, \ldots, K-1$. The state transition matrix for the forward subsystem (4.66) is given by $\Phi_f(i, j) = A_{i-1}^f A_{i-2}^f \cdots A_j^f$ for $i > j$ and $\Phi_f(i, i) = I_{n_i^f}$. For the backward subsystem (4.67), the state transition matrix is defined as $\Phi_b(i, j) = E_i^b E_{i+1}^b \cdots E_{j-1}^b$ for $i < j$ and $\Phi_b(i, i) = I_{n_i^\infty}$. Using these matrices we can now define the *forward and backward fundamental matrices* of the periodic descriptor system (4.48) as

$$\Psi_{i,j} = \begin{cases} Z_i \begin{bmatrix} \Phi_f(i, j+1) & 0 \\ 0 & 0 \end{bmatrix} W_j, & i > j, \\ Z_i \begin{bmatrix} 0 & 0 \\ 0 & -\Phi_b(i, j) \end{bmatrix} W_j, & i \le j. \end{cases} \tag{4.68}$$

These fundamental matrices play an important role in the definition of the reachability and observability Gramians of the periodic descriptor system (4.48) that we will consider in the next section.

4.3. Gramians and Matrix Equations for LPTV Discrete-Time Descriptor Systems

It is clear from the context above that the Gramians of the periodic discrete-time descriptor system (4.48) are defined separately for its forward and backward subsystems [30, 100]. Complete reachability and complete observability of the periodic descriptor system (4.48) are also defined via the complete reachability and complete observability of its forward and backward subsystems.

4.3.1. Reachability and Observability

Definition 4.3.1:

(i) The periodic descriptor system (4.48) is said to be *reachable* at time t if starting from any initial state $x_s = 0$, the system can be driven to any final state $x_t = \bar{x} \in \mathbb{R}^{n_t}$,

choosing a set of control inputs $\{u_i\}_{i=s}^{l}$ and two integers s, l with $s < t < l$ appropriately. The periodic descriptor system (4.48) is called *completely reachable* if it is reachable at all times t.

(ii) The forward subsystem (4.66) is said to be *reachable* at time t if starting from any initial state $x_s^f = 0$, the system can be driven to any final state $x_t^f = \bar{x}_f \in \mathbb{R}^{n_t^f}$, choosing a set of control inputs $\{u_i\}_{i=s}^{t-1}$ and an integer s with $s < t$ appropriately. The forward subsystem (4.66) is called *completely reachable* if it is reachable at all times t.

(iii) The backward subsystem (4.67) is said to be *reachable* at time t if any state $\bar{x}_b \in \mathbb{R}^{n_t^\infty}$ can be reached at a finite time t, i.e., $x_t^b = \bar{x}_b$, by choosing a set of control inputs $\{u_i\}_{i=t}^{l}$, and an integer l with $l > t$. The backward subsystem (4.67) is called *completely reachable* if it is reachable at all times t. ◊

Remark 4.7:
The periodic discrete-time descriptor system (4.48) is *completely reachable* if and only if both its forward and backward subsystems are completely reachable. ◊

Theorem 4.3.1:
[30] *Consider the forward subsystem (4.66). The following statements are equivalent.*

(1) The forward subsystem (4.66) is completely reachable.
(2) For $t = 0, 1, \ldots, K-1$, the matrices

$$\mathfrak{C}_f(t) = \left[B_{t-1}^f,\ A_{t-1}^f B_{t-2}^f, \ldots,\ \Phi_f(t, t - n_t^f K + 1) B_{t-n_t^f K}^f\right]$$

have full row rank.
(3) For $t = 0, 1, \ldots, K-1$ and

$$\mathfrak{B}_t^f = \left[B_{t-1}^f,\ A_{t-1}^f B_{t-2}^f,\ A_{t-1}^f A_{t-1}^f B_{t-3}^f, \ldots,\ \Phi_f(t, t-K+1) B_{t-K}^f\right],$$

the matrices

$$\left[\mathfrak{B}_t^f,\ \Phi_f(t, t-K)\mathfrak{B}_t^f,\ (\Phi_f(t, t-K))^2 \mathfrak{B}_t^f, \ldots,\ (\Phi_f(t, t-K))^{n_t^f - 1} \mathfrak{B}_t^f\right]$$

have full row rank. ◊

Proof. For the proof, see [29]. □

Remark 4.8:
For discrete-time descriptor system with period $K = 1$, statement (2) implies

$$\text{rank}\,([B^f, A^f B^f, \cdots, (A^f)^{n_f - 1} B^f]) = n_f,$$

and statement (3) implies rank $([\lambda I - A^f]) = n_f$ for any $\lambda \in \Lambda(A^f)$. Both the statements ensure the complete reachability for the forward subsystem for $K = 1$ and they coincide with the results for complete reachability of discrete-time descriptor systems (see [65, 8, 107], and references therein). ◊

Theorem 4.3.2:

[30] *Consider the backward subsystem (4.67). The following statements are equivalent.*

(1) The backward subsystem (4.67) is completely reachable.
(2) For $t = 0, 1, \ldots, K-1$, the matrices

$$\mathfrak{C}_b(t) = \left[B_t^b,\ E_t^b B_{t+1}^b, \ldots,\ \Phi_b(t, t+\nu K-1) B_{t+\nu K-1}^b\right]$$

have full row rank.
(3) For $t = 0, 1, \ldots, K-1$ and

$$\mathfrak{B}_t^b = \left[B_t^b,\ E_t^b B_{t+1}^b, \ldots,\ \Phi_b(t, t+K-1) B_{t+K-1}^b\right],$$

the matrices

$$\left[\mathfrak{B}_t^b,\ \Phi_b(t, t+K)\mathfrak{B}_t^b,\ (\Phi_b(t, t+K))^2 \mathfrak{B}_t^b, \ldots,\ (\Phi_b(t, t+K))^{\nu-1} \mathfrak{B}_t^b\right]$$

have full row rank. Note that $\Phi_b(t, t+K) = E_t^b E_{t+1}^b \cdots E_{t+K-1}^b$ and ν is the index of nilpotency of system (4.48). ◊

Proof. For the proof, see [29]. □

Remark 4.9:

For $K = 1$, statement (2) implies

$$\text{rank}\,([B^b, E^b B^b, \cdots, (E^b)^{\nu-1} B^b]) = n_\infty,$$

where ν is the index of the periodic descriptor system, and statement (3) implies rank $([\lambda I - N, B^b]) = n_\infty$ for any $\lambda \in \Lambda(N)$. Both the results coincide with those for the noncausal reachability of discrete-time descriptor systems [65, 8, 107]. ◊

Definition 4.3.2:

(i) The periodic descriptor system (4.48) is said to be *observable* at time t if the state x_t defined at time t, can be completely determined from the knowledge of the input sequence, $\{u_i\}_{i=s}^{l}$ and the output sequence, $\{y_i\}_{i=s}^{l}$, choosing two integers s, l with $s < t < l$ appropriately. The periodic descriptor system (4.48) is called *completely observable* if it is observable at all times t.

(ii) The forward subsystem (4.66) is said to be *observable* at time t if the state x_t defined at time t, can be completely determined from the knowledge of the input

sequence, $\{u_i\}_{i=t}^{l}$ and the output sequence, $\{y_i\}_{i=t}^{l}$, choosing an integer l with $l > t$ appropriately. The forward subsystem (4.66) is called *completely observable* if it is observable at all times t.

(iii) The backward subsystem (4.67) is said to be *observable* at time t if the state x_t defined at time t, can be completely determined from the knowledge of the input sequence, $\{u_i\}_{i=s}^{t}$ and the output sequence, $\{y_i\}_{i=s}^{l}$, choosing an integer s with $s < t$ appropriately. The backward subsystem (4.67) is called *completely observable* if it is observable at all times t. ◊

Remark 4.10:
The periodic discrete-time descriptor system (4.48) is *completely observable* if and only if both its forward and backward subsystems are completely observable. ◊

Theorem 4.3.3:
[30] *Consider the forward subsystem (4.66). The following statements are equivalent.*

(1) The forward subsystem (4.66) is completely observable.

(2) For $t = 0, 1, \ldots, K-1$, the matrices

$$\mathfrak{O}_f(t) = \begin{bmatrix} C_t^f \\ C_{t+1}^f A_t^f \\ C_{t+2}^f A_{t+1}^f A_t^f \\ \vdots \\ C_{t+n_t^f K-1}^f \Phi_f(t + n_t^f K - 1, t) \end{bmatrix}$$

have full column rank.

(3) For $t = 0, 1, \ldots, K-1$ and

$$\mathfrak{C}_t^f = \begin{bmatrix} C_t^f \\ C_{t+1}^f A_t^f \\ C_{t+2}^f A_{t+1}^f A_t^f \\ \vdots \\ C_{t+K-1}^f \Phi_f(t + K - 1, t) \end{bmatrix},$$

the matrices

$$\begin{bmatrix} \mathfrak{C}_t^f \\ \mathfrak{C}_t^f\ \Phi_f(t+K,t) \\ \mathfrak{C}_t^f\ (\Phi_f(t+K,t))^2 \\ \vdots \\ \mathfrak{C}_t^f\ (\Phi_f(t+K,t))^{n_i^f-1} \end{bmatrix}$$

have full column rank.

Remark 4.11:

For $K = 1$, statement (2) implies

$$\operatorname{rank}\left(\begin{bmatrix} C^f \\ C^f A^f \\ C^f (A^f)^2 \\ \vdots \\ C^f\ (A^f)^{n_f-1} \end{bmatrix}\right) = n_f,$$

and statement (3) implies rank $\left(\begin{bmatrix} \lambda I - A^f \\ C^f \end{bmatrix}\right) = n_f$, for any $\lambda \in \Lambda(A^f)$. Both the statements ensure the complete observability for the forward subsystem for $K = 1$ [65, 8, 108].

Theorem 4.3.4:

[30] *Consider the backward subsystem (4.67). The following statements are equivalent.*

(1) The backward subsystem (4.67) is completely observable.

(2) For $t = 0, 1, \ldots, K-1$, the matrices

$$\mathfrak{O}_b(t) = \begin{bmatrix} C_t^b \\ C_{t-1}^b E_{t-1}^b \\ C_{t-2}^b E_{t-2}^b E_{t-1}^b \\ \vdots \\ C_{t-\nu K+1}^b\ \Phi_b(t-\nu K+1,t) \end{bmatrix}$$

have full column rank.

(3) For $t = 0, 1, \ldots, K-1$ and

$$\mathfrak{C}_t^b = \begin{bmatrix} C_t^b \\ C_{t-1}^b E_{t-1}^b \\ C_{t-2}^b E_{t-2}^b E_{t-1}^b \\ \vdots \\ C_{t-K+1}^b\ \Phi_b(t-K+1,t) \end{bmatrix},$$

the matrices

$$\begin{bmatrix} \mathfrak{C}_t^b \\ \mathfrak{C}_t^b\, \Phi_b(t, t+K) \\ \mathfrak{C}_t^b\, (\Phi_b(t, t+K))^2 \\ \vdots \\ \mathfrak{C}_t^b\, (\Phi_b(t, t+K))^{\nu-1} \end{bmatrix}$$

have full column rank.

Remark 4.12:

For $K = 1$, statement (2) implies

$$\operatorname{rank}\left(\begin{bmatrix} C^b \\ C^bE^b \\ C^b(E^b)^2 \\ \vdots \\ C^b\,(E^b)^{\nu-1} \end{bmatrix}\right) = n_\infty,$$

and statement (3) implies rank $\left(\begin{bmatrix} \lambda I - N \\ C^b \end{bmatrix}\right)$=$n_\infty$ for any $\lambda \in \Lambda(N)$. Both the statements ensure the complete observability for the forward subsystem for $K = 1$ [65, 8, 108].

4.3.2. Periodic Reachability and Observability Gramians

In control theory and in balanced truncation model reduction, Gramians play a fundamental role [76, 108, 116, 121]. For the periodic descriptor system (4.48), the reachability and observability Gramians have been first introduced in [30]. In this subsection, we discuss the periodic reachability and observability Gramians for the periodic discrete-time descriptor system (4.48) regarding their corresponding forward and backward subsystems as in (4.66) and (4.67), respectively. For forward subsystem, the periodic Gramians are called *causal* Gramians and for backward subsystem, the periodic Gramians are called *noncausal* Gramians.

Definition 4.3.3:

Suppose that the periodic matrix pairs $\{(E_k, A_k)\}_{k=0}^{K-1}$ are pd-stable.

(i) For $k = 0, 1, \ldots, K-1$, the *causal reachability Gramians* of the periodic descriptor system (4.48) are defined by

$$G_k^{cr} = \sum_{j=-\infty}^{k-1} \Psi_{k,j} B_j B_j^T \Psi_{k,j}^T \in \mathbb{R}^{n_k \times n_k}.$$

(ii) For $k = 0, 1, \ldots, K-1$, the *noncausal reachability Gramians* of the periodic descriptor

system (4.48) are defined by

$$G_k^{ncr} = \sum_{j=k}^{k+\nu K-1} \Psi_{k,j} B_j B_j^T \Psi_{k,j}^T \in \mathbb{R}^{n_k \times n_k}.$$

(iii) The *complete reachability Gramians* G_k^c are the sum of the causal and noncausal Gramians, i.e.,

$$G_k^c = G_k^{cr} + G_k^{ncr}$$

for $k = 0, 1, \ldots, K-1$.

Definition 4.3.4:
Suppose that the periodic matrix pairs $\{(E_k, A_k)\}_{k=0}^{K-1}$ are pd-stable.

(i) For $k = 0, 1, \ldots, K-1$, the *causal observability Gramians* of the periodic descriptor system (4.48) are defined by

$$G_k^{co} = \sum_{j=k}^{\infty} \Psi_{j,k-1}^T C_j^T C_j \Psi_{j,k-1} \in \mathbb{R}^{\mu_k \times \mu_k}.$$

(ii) For $k = 0, 1, \ldots, K-1$, the *noncausal observability Gramians* of the periodic descriptor system (4.48) are defined by

$$G_k^{nco} = \sum_{j=k-\nu K}^{k-1} \Psi_{j,k-1}^T C_j^T C_j \Psi_{j,k-1} \in \mathbb{R}^{\mu_k \times \mu_k}.$$

(iii) The *complete observability Gramians* G_k^o are the sum of the causal and noncausal Gramians, i.e.,

$$G_k^o = G_k^{co} + G_k^{nco}$$

for $k = 0, 1, \ldots, K-1$.

The pd-stability of periodic matrix pairs $\{(E_k, A_k)\}_{k=0}^{K-1}$ ensures that the infinite series that appear in the definition of Gramians G_k^{cr} and G_k^{co} converge [121, 120]. The Gramians are symmetric positive semi-definite matrices for all k. These Gramians are used to define the *Hankel singular values* of the periodic discrete-time descriptor system (4.48), which we will use in the next consecutive chapters for balanced transformations and model order reduction.

Remark 4.13:
For period $K = 1$ and a regular matrix pair (E, A), Definitions 4.3.3 and 4.3.4 are equal to the Gramians defined for generalized discrete-time descriptor system in [107]. ◊

4.3.3. Periodic Matrix Equations

It is well established that the Gramians of discrete-time descriptor systems satisfy some projected generalized discrete-time Lyapunov equations with special right-hand sides [103]. A similar result also holds for periodic descriptor systems. The following theorem shows that the Gramians G_k^{cr}, G_k^{ncr}, G_k^{co} and G_k^{nco} of the periodic descriptor system (4.48) satisfy some projected generalized discrete-time periodic Lyapunov equations with special right-hand sides.

Theorem 4.3.5 (Thm. 4.1 in [30]):
Consider the periodic discrete-time descriptor system (4.48), where the periodic matrix pairs $\{E_k, A_k\}_{k=0}^{K-1}$ are pd-stable.

(1) For $k = 0, 1, \ldots, K-1$, the causal and noncausal reachability Gramians $\{G_k^{cr}\}_{k=0}^{K-1}$ and $\{G_k^{ncr}\}_{k=0}^{K-1}$ are the unique symmetric, positive semidefinite solutions of the generalized projected periodic discrete-time algebraic Lyapunov equations (PPDALEs)

$$\begin{aligned} A_k G_k^{cr} A_k^T - E_k G_{k+1}^{cr} E_k^T &= -P_l(k) B_k B_k^T P_l(k)^T, \\ G_k^{cr} &= P_r(k) G_k^{cr} P_r(k)^T, \end{aligned} \tag{4.69}$$

and

$$\begin{aligned} A_k G_k^{ncr} A_k^T - E_k G_{k+1}^{ncr} E_k^T &= Q_l(k) B_k B_k^T Q_l(k)^T, \\ G_k^{ncr} &= Q_r(k) G_k^{ncr} Q_r(k)^T, \end{aligned} \tag{4.70}$$

respectively, where $G_K^{cr} = G_0^{cr}$, $G_K^{ncr} = G_0^{ncr}$, $Q_l(k) = (I_{\mu_{k+1}} - P_l(k))$, and $Q_r(k) = (I_{n_k} - P_r(k))$.

(2) For $k = 0, 1, \ldots, K-1$, the causal and noncausal observability Gramians $\{G_k^{co}\}_{k=0}^{K-1}$ and $\{G_k^{nco}\}_{k=0}^{K-1}$ are the unique symmetric, positive semidefinite solutions of the generalized PPDALEs

$$\begin{aligned} A_k^T G_{k+1}^{co} A_k - E_{k-1}^T G_k^{co} E_{k-1} &= -P_r(k)^T C_k^T C_k P_r(k), \\ G_k^{co} &= P_l(k-1)^T G_k^{co} P_l(k-1), \end{aligned} \tag{4.71}$$

and

$$\begin{aligned} A_k^T G_{k+1}^{nco} A_k - E_{k-1}^T G_k^{nco} E_{k-1} &= Q_r(k)^T C_k^T C_k Q_r(k), \\ G_k^{nco} &= Q_l(k-1)^T G_k^{nco} Q_l(k-1), \end{aligned} \tag{4.72}$$

respectively, where $G_K^{co} = G_0^{co}$, $G_K^{nco} = G_0^{nco}$, $E_{-1} = E_{K-1}$, $P_l(-1) = P_l(K-1)$ and $Q_l(-1) = Q_l(K-1)$.

(3) For $k = 0, 1, \ldots, K-1$, the reachability and observability Gramians $\{G_k^c\}_{k=0}^{K-1}$ and $\{G_k^o\}_{k=0}^{K-1}$ are the unique symmetric, positive semidefinite solutions of the generalized PPDALEs

$$\begin{aligned} A_k G_k^c A_k^T - E_k G_{k+1}^c E_k^T &= -P_l(k) B_k B_k^T P_l(k)^T + Q_l(k) B_k B_k^T Q_l(k)^T, \\ G_k^c &= Q_r(k) G_k^c Q_r(k)^T, \end{aligned} \tag{4.73}$$

and

$$\begin{aligned} A_k^T G_{k+1}^o A_k - E_{k-1}^T G_k^o E_{k-1} &= -P_r(k)^T C_k^T C_k P_r(k) + Q_r(k)^T C_k^T C_k Q_r(k), \\ G_k^o &= Q_l(k-1)^T G_k^o Q_l(k-1), \end{aligned} \tag{4.74}$$

respectively. ◊

Proof. We only give the proof of (4.69). The other proofs are analogous. The proof is sketched from [30] with more details.

Let the pd-stable matrix pairs $\{E_k, A_k\}_{k=0}^{K-1}$ be in Weierstrass canonical from (4.54), where the eigenvalues of $J_k = A_{k+K-1}^f A_{k+K-2}^f \cdots A_k^f$ lie inside the unit circle and $N_k = E_k^b E_{k+1}^b \cdots E_{k+K-1}^b$ is nilpotent and contains only zero eigenvalues. Let the matrices

$$Z_k^{-1} G_k^{cr} Z_k^{-T} = \begin{bmatrix} G_{11,\,k} & G_{12,\,k} \\ G_{21,\,k} & G_{22,\,k} \end{bmatrix} \tag{4.75}$$

be partitioned in blocks such that $G_{11,\,k} \in \mathbb{R}^{n_k^f \times n_k^f}$ and $G_{22,\,k} \in \mathbb{R}^{n_k^\infty \times n_k^\infty}$. Then using (4.54) and (4.64), we can rewrite (4.69) into the following matrix equations:

$$G_{11,k+1} - A_k^f G_{11,k} (A_k^f)^T = B_k^f (B_k^f)^T, \tag{4.76}$$

$$G_{12,k+1} (E_k^b)^T - A_k^f G_{12,k} = 0, \tag{4.77}$$

$$E_k^b G_{21,k+1} - G_{21,k} (A_k^f)^T = 0, \tag{4.78}$$

$$E_k^b G_{22,k+1} (E_k^b)^T - G_{22,k} = 0. \tag{4.79}$$

Since all eigenvalues of J_k lie inside the unit circle and N_k contains all zero eigenvalues, the Lyapunov equations (4.76) and (4.79) have unique solutions $G_{11,k}$ and $G_{22,k}$, respectively. Taking into account that J_k and N_k have disjoint spectra, equations (4.77) and (4.78) are solvable and have trivial solutions.

Now from $G_k^{cr} = P_r(k) G_k^{cr} P_r(k)^T$, it follows that

$$\begin{aligned} G_k^{cr} &= Z_k \begin{bmatrix} G_{11,\,k} & G_{12,\,k} \\ G_{21,\,k} & G_{22,\,k} \end{bmatrix} Z_k^T = P_r(k) G_k^{cr} P_r(k)^T, \\ &= Z_k \begin{bmatrix} I_{n_k^f} & 0 \\ 0 & 0 \end{bmatrix} Z_k^{-1} Z_k \begin{bmatrix} G_{11,\,k} & G_{12,\,k} \\ G_{21,\,k} & G_{22,\,k} \end{bmatrix} Z_k^T Z_k^{-T} \begin{bmatrix} I_{n_k^f} & 0 \\ 0 & 0 \end{bmatrix} Z_k^T, \\ &= Z_k \begin{bmatrix} G_{11,k} & 0 \\ 0 & 0 \end{bmatrix} Z_k^T; \end{aligned}$$

i.e., $G_{12,k} = G_{21,k} = G_{22,k} = 0$.

Thus, the matrices

$$G_k^{cr} = Z_k \begin{bmatrix} G_{11,\,k} & 0 \\ 0 & 0 \end{bmatrix} Z_k^T$$

are the unique symmetric solutions of the generalized PPDALEs (4.76) with $G_k^{cr} = P_r(k) G_k^{cr} P_r(k)^T$.

To show that the causal reachability Gramians G_k^{cr} satisfy the generalized PPDALEs (4.76), we can use the direct substitution of (4.54) and (4.68) into the left hand-side of the first equation of (4.76), which gives

$$\begin{aligned}
& A_k G_k^{cr} A_k^T - E_k G_{k+1}^{cr} E_k^T \\
&= A_k \left(\sum_{i=-\infty}^{k-1} \Psi_{k,i} B_i B_i^T \Psi_{k,i}^T \right) A_k^T - E_k \left(\sum_{i=-\infty}^{k} \Psi_{k+1,i} B_i B_i^T \Psi_{k+1,i}^T \right) E_k^T \\
&= A_k Z_k \left(\sum_{i=-\infty}^{k-1} \begin{bmatrix} \Phi_f(k, i+1) & 0 \\ 0 & 0 \end{bmatrix} W_i B_i B_i^T W_i^T \begin{bmatrix} \Phi_f(k, i+1)^T & 0 \\ 0 & 0 \end{bmatrix} \right) Z_k^T A_k^T \\
&\quad - E_k Z_{k+1} \left(\sum_{i=-\infty}^{k} \begin{bmatrix} \Phi_f(k+1, i+1) & 0 \\ 0 & 0 \end{bmatrix} W_i B_i B_i^T W_i^T \begin{bmatrix} \Phi_f(k+1, i+1)^T & 0 \\ 0 & 0 \end{bmatrix} \right) Z_{k+1}^T E_k^T \\
&= W_k^{-1} \begin{bmatrix} A_k^f & 0 \\ 0 & I_{n_k^\infty} \end{bmatrix} \left(\sum_{i=-\infty}^{k-1} \begin{bmatrix} \Phi_f(k, i+1) & 0 \\ 0 & 0 \end{bmatrix} \begin{bmatrix} B_i^f \\ B_i^b \end{bmatrix} \begin{bmatrix} B_i^f \\ B_i^b \end{bmatrix}^T \begin{bmatrix} \Phi_f(k, i+1)^T & 0 \\ 0 & 0 \end{bmatrix} \right) \begin{bmatrix} (A_k^f)^T & 0 \\ 0 & I_{n_k^\infty} \end{bmatrix} W_k^{-T} \\
&\quad - W_k^{-1} \begin{bmatrix} I_{n_{k+1}^f} & 0 \\ 0 & E_k^b \end{bmatrix} \left(\sum_{i=-\infty}^{k} \begin{bmatrix} \Phi_f(k+1, i+1) & 0 \\ 0 & 0 \end{bmatrix} \begin{bmatrix} B_i^f \\ B_i^b \end{bmatrix} \begin{bmatrix} B_i^f \\ B_i^b \end{bmatrix}^T \begin{bmatrix} \Phi_f(k+1, i+1)^T & 0 \\ 0 & 0 \end{bmatrix} \right) \\
&\quad \begin{bmatrix} I_{n_{k+1}^f} & 0 \\ 0 & (E_k^b)^T \end{bmatrix} W_k^{-T} \\
&= W_k^{-1} \begin{bmatrix} \sum_{i=-\infty}^{k-1} \Phi_f(k+1, i+1) B_i^f (B_i^f)^T \Phi_f(k+1, i+1)^T & 0 \\ 0 & 0 \end{bmatrix} W_k^{-T} \\
&\quad - W_k^{-1} \begin{bmatrix} \sum_{i=-\infty}^{k} \Phi_f(k+1, i+1) B_i^f (B_i^f)^T \Phi_f(k+1, i+1)^T & 0 \\ 0 & 0 \end{bmatrix} W_k^{-T} \\
&= -W_k^{-1} \begin{bmatrix} B_i^f (B_i^f)^T & 0 \\ 0 & 0 \end{bmatrix} W_k^{-T}, \quad \text{since, } \Phi_f(k+1, k+1) = I_{n_{k+1}^f} \\
&= -P_l(k) B_k B_k^T P_l(k)^T,
\end{aligned}$$

and similar substitutions into the second equation of (4.76) gives

$$\begin{aligned} & P_r(k)G_k^{cr}P_r(k)^T \\ = \; & Z_k\begin{bmatrix} I_{n_k^f} & 0 \\ 0 & 0 \end{bmatrix}Z_k^{-1}\left(\sum_{i=-\infty}^{k-1}\Psi_{k,i}B_iB_i^T\Psi_{k,i}^T\right)Z_k^{-T}\begin{bmatrix} I_{n_k^f} & 0 \\ 0 & 0 \end{bmatrix}Z_k^T \\ = \; & Z_k\begin{bmatrix} \sum_{i=-\infty}^{k-1}\Phi_f(k,i+1)B_i^f(B_i^f)^T\Phi_f(k,i+1)^T & 0 \\ 0 & 0 \end{bmatrix}Z_k^T \\ = \; & G_k^{cr}, \end{aligned}$$

for all k, where $k = 0, 1, \ldots, K-1$. Hence the proof is complete. □

The complete reachability and observability of the periodic descriptor system (4.48) can be described via the corresponding Gramians. The following theorem establishes the statement.

Theorem 4.3.6 (Thm. 4.2 in [30]):

Let us consider the periodic matrix pairs $\{(E_k, A_k)\}_{k=0}^{K-1}$ of the periodic descriptor system (4.48) and assume that they are pd-stable.

(i) The periodic descriptor system (4.48) is completely reachable if and only if the reachability Gramians G_k^c are positive definite for $k = 0, 1, \ldots, K-1$.

(ii) The periodic descriptor system (4.48) is completely observable if and only if the observability Gramians G_k^o are positive definite for $k = 0, 1, \ldots, K-1$. ◊

Proof. [30] We sketch here the proof of statement (i). The proof of statement (ii) is analogous to the proof of statement (i).

Consider the generalized PPDALEs in (4.73). Premultiplying (4.73) by W_k and postmultiplying again by W_k^T, we obtain

$$W_kA_kG_k^cA_k^TW_k^T - W_kE_kG_{k+1}^cE_k^TW_k^T = -W_kP_l(k)B_kB_k^TP_l(k)^TW_k^T + W_kQ_l(k)B_kB_k^TQ_l(k)^TW_k^T. \tag{4.80}$$

It follows that

$$W_kA_kZ_k\bar{G}_k^cZ_k^TA_k^TW_k^T - W_kE_kZ_{k+1}\bar{G}_{k+1}^cZ_{k+1}^TE_k^TW_k^T = \begin{bmatrix} -B_k^f(B_k^f)^T & 0 \\ 0 & 0 \end{bmatrix} + \begin{bmatrix} 0 & 0 \\ 0 & B_k^b(B_k^b)^T \end{bmatrix}, \tag{4.81}$$

where $\bar{G}_k^c = Z_k^{-1}G_k^cZ_k^{-T}$. Now from the definition of causal reachability Gramians as in Definition 4.3.3, we can see

$$\bar{G}_k^c = Z_k^{-1}G_k^cZ_k^{-T} = \begin{bmatrix} \bar{G}_{1,k}^{cr} & 0 \\ 0 & \bar{G}_{2,k}^{ncr} \end{bmatrix}, \tag{4.82}$$

with

$$\begin{aligned}\bar{G}_{1,k}^{cr} &= \sum_{i=-\infty}^{k-1} \Phi_f(k,i+1)B_i^f(B_i^f)^T\Phi_f(k,i+1)^T,\\ \bar{G}_{2,k}^{ncr} &= \sum_{i=k}^{k+\nu K-1} \Phi_b(k,i)B_i^b(B_i^b)^T\Phi_b(k,i)^T.\end{aligned}$$

Following (4.54) and (4.82), we can decompose (4.81) into two periodic Lyapunov equations,

$$A_k^f\bar{G}_{1,k}^{cr}(A_k^f)^T - \bar{G}_{1,k+1}^{cr} = -B_k^f(B_k^f)^T, \tag{4.83}$$

$$\bar{G}_{2,k}^{ncr} - E_k^b\bar{G}_{2,k+1}^{cr}(E_k^b)^T = B_k^b(B_k^b)^T, \tag{4.84}$$

for $k = 0, 1, \ldots, K-1$.

Since the matrix pairs $\{E_k, A_k\}_{k=0}^{K-1}$ are pd-stable, the matrices $J_k = A_{k+K-1}^f A_{k+K-2}^f \cdots A_k^f$, $(k = 0, 1, \ldots, K-1)$, contain only eigenvalues lying inside the unit circle and $N_k = E_k^b E_{k+1}^b \cdots E_{k+K-1}^b$, for $k = 0, 1, \ldots, K-1$, contains only zero eigenvalues. Therefore, $\bar{G}_{1,k}^{cr}$ and $\bar{G}_{2,k}^{ncr}$ are the symmetric positive definite solutions of (4.83) and (4.84), respectively.

Equivalently, following (4.82), we can easily show that the reachability Gramians G_k^c are symmetric positive definite for all values of k ($k = 0, 1, \ldots, K-1$). Followed by Theorem 4.3.3- 4.3.4, we conclude that the forward and backward subsystems define by (4.83) and (4.84) respectively, are completely reachable. Hence the periodic descriptor system (4.48) is completely reachable. This completes the proof. □

The projected periodic discrete-time algebraic Lyapunov equations in (4.73) and (4.74) play an important role in the balanced truncation model order reduction approach. We will discuss more details in Chapter 8.

CHAPTER

FIVE

LTI REPRESENTATION OF LPTV DESCRIPTOR SYSTEMS

Contents

This chapter introduces the time-invariant reformulation of LPTV discrete-time descriptor systems and establishes some properties that link the two system representations. This time-invariant reformulation, often called *lifted system*.

We first discuss the available LTI reformulation techniques [124, 122] for LPTV discrete-time systems. In this thesis, we consider only the *cyclic lifted representation* of LPTV discrete-time descriptor systems, and hence, we analyse the system dynamics of the periodic descriptor system using its cyclic lifted representation.

In Section 5.2 we first study the concepts of solvability and conditionability of LPTV discrete-time descriptor systems in terms of the corresponding cyclic matrix pencil. We then give a characterization of stability for LPTV discrete-time descriptor systems in cyclic lifted structure in Subsection 5.2.2. We also discuss the links of solvability, conditionability and stability of LPTV discrete-time descriptor systems to those of the corresponding cyclic lifted system. Subsection 5.2.4 then represents the periodic Gramians and the matrix equations using cyclic lifted structure. We discuss the forward-backward reachability and observability Gramians of the cyclic lifted system and then represent

the cyclic lifted representations of the period matrix equations that we have already discussed in Chapter 4 in the period setting. In this subsection we establish the relationships of periodic Gramians and matrix equations of LPTV descriptor system with those of cyclic lifted system representations. The transfer function for lifted periodic system is discussed in Subsection 5.2.5. A short discussion about the index of periodic matrix pairs and the relationship of transfer functions of different lifted systems is presented in Section 5.3.

5.1. Lifted Representations of LPTV Descriptor Systems

In the last few decades, increasing attention and interest have been devoted for the development of numerical algorithms for analysis and control of linear periodic discrete-time systems [20, 46, 101]. Various possible computational approaches and algorithms have been developed, but among them the most prominent and useful technique is the *lifting isomorphism*, which reformulate a time-varying discrete-time periodic system as an equivalent time-invariant discrete-time system of increased dimensions [73, 46, 79]. Using the lifting isomorphism one can exploit the theory of time-invariant systems for the analysis and control of periodic systems, provided that the results achieved can be easily re-interpreted in a periodic framework.

The lifted representation of discrete-time periodic descriptor systems plays an important role in extending many theoretical results for descriptor systems to the periodic setting [117, 18, 125]. They are also used to define concepts which correspond to those for period discrete-time descriptor systems. There are several lifted representations available in the literature on LPTV descriptor systems [18, 124, 122].

Standard Lifted Representation: Let us recall the original discrete-time periodic descriptor system

$$\begin{aligned} E_k x_{k+1} &= A_k x_k + B_k u_k, \\ y_k &= C_k x_k, \qquad k \in \mathbb{Z}, \end{aligned} \tag{5.1}$$

where $E_k \in \mathbb{R}^{\mu_{k+1} \times n_{k+1}}$, $A_k \in \mathbb{R}^{\mu_{k+1} \times n_k}$, $B_k \in \mathbb{R}^{\mu_{k+1} \times p_k}$, $C_k \in \mathbb{R}^{q_k \times n_k}$ are time-varying, and periodic with a period $K \geq 1$. Clearly, $\sum_{k=0}^{K-1} \mu_k = \sum_{k=0}^{K-1} n_k = n$. The matrices E_k are allowed to be singular for all k.

For the *standard lifted representation*, the matrices E_k are required to be nonsingular. This lifted system was first introduced in [73] and corresponds to the time-lifted system discussed in [18]. The input-output vectors in this lifting approach are defined over time intervals of length K. For a given sampling time k, the corresponding $\sum_{k=0}^{K-1} p_k$-dimensional input vector and $\sum_{k=0}^{K-1} q_k$-dimensional output vector, and n_k-dimensional

state vector are

$$\begin{aligned} \mathcal{U}_k^L(h) &= [u^T(k+hK), u^T(k+hK+1), \ldots, u^T(k+hK+K-1)]^T, \\ \mathcal{Y}_k^L(h) &= [y^T(k+hK), y^T(k+hK+1), \ldots, y^T(k+hK+K-1)]^T, \\ \mathcal{X}_k^L(h) &= x(k+hK), \end{aligned}$$

where k, h are two integers. To define the lifted system we denote the state transition matrix of system (5.1) as

$$\phi(j,i) = E_{j-1}^{-1}A_{j-1}E_{j-2}^{-1}A_{j-2}\cdots E_i^{-1}A_i,$$

where $\phi(i,i) = I_{n_i}$. Then the *standard lifted system* at a sampling time k is defined as

$$\Sigma_k^L : \left\{ \begin{array}{rcl} \mathcal{X}_k^L(h+1) &=& \mathcal{A}_k^L\mathcal{X}_k^L(h) + \mathcal{B}_k^L\mathcal{U}_k^L(h), \\ \mathcal{Y}_k^L(h) &=& \mathcal{C}_k^L\mathcal{X}_k^L(h), \end{array} \right. \tag{5.2}$$

where

$$\begin{aligned} \mathcal{A}_k^L &= \phi(k+K,k), \\ \mathcal{B}_k^L &= [\phi(k+K,k+1)E_k^{-1}B_k,\ \phi(k+K,k+2)E_{k+1}^{-1}B_{k+1}, \ldots, E_{k+K-1}^{-1}B_{k+K-1}], \end{aligned}$$

$$\mathcal{C}_k^L = \begin{bmatrix} C_k \\ C_{k+1}\,\Phi(k+1,k) \\ \vdots \\ C_{k+K-1}\,\Phi(k+K-1,k) \end{bmatrix},$$

The *transfer function matrix* (TFM) of the periodic system (5.1) at sampling time k is defined as the TFM of the lifted system (5.2),

$$\mathcal{H}_k^L(z) = \mathcal{C}_k^L(zI_{n_k} - \mathcal{A}_k^L)^{-1}\mathcal{B}_k^L, \tag{5.3}$$

which depends on the sampling time k. The associated system pencil is defined as

$$\mathcal{W}_k^L(z) = \begin{bmatrix} \mathcal{A}_k^L - zI_{n_k} & \mathcal{B}_k^L \\ \mathcal{C}_k^L & 0 \end{bmatrix}, \tag{5.4}$$

which also depends on the sampling time k. The zeros and poles as well as reachability and observability of the period system (5.1) can be defined regarding its standard lifted representation [122, 125]. If the system (5.1) is minimal, then the lifted system (5.2) is also minimal and the converse is also true [18, 17].

Stacked Lifted Representation: The *stacked lifted representation* of the LPTV discrete-time descriptor system (5.1) is a time-invariant descriptor system representation of the form

$$\Sigma_k^S : \left\{ \begin{array}{rcl} \mathcal{E}_k^S\mathcal{X}_k^S(h+1) &=& \mathcal{A}_k^S\mathcal{X}_k^S(h) + \mathcal{B}_k^S\mathcal{U}_k^S(h), \\ \mathcal{Y}_k^S(h) &=& \mathcal{C}_k^S\mathcal{X}_k^S(h), \end{array} \right. \tag{5.5}$$

where

$$\begin{aligned} \mathcal{B}_k^S &= \operatorname{diag}(B_k, B_{k+1}, \ldots, B_{k+K-1}), \\ \mathcal{C}_k^S &= \operatorname{diag}(C_k, C_{k+1}, \ldots, C_{k+K-1}), \end{aligned}$$

and

$$\mathcal{E}_k^S = \begin{bmatrix} 0 & 0 & & \\ \vdots & & 0 & \\ \vdots & & & \ddots \\ & & & 0 \\ E_{k+K-1} & & & \end{bmatrix}, \quad \mathcal{A}_k^S = \begin{bmatrix} A_k & -E_k & & 0 \\ & \ddots & \ddots & \\ & & A_{k+K-2} & -E_{k+K-2} \\ & & & A_{k+K-1} \end{bmatrix}. \tag{5.6}$$

The subscript k in the calligraphic notations of the matrices (vectors) does not mean the time-variance of the corresponding matrix (vector), but it denotes the starting time of the lifted formulation. The stacked lifted representation was first introduced in [46] in the context of standard state space systems ($E_k = I_{n_{k+1}}$). This lifting uses again the input-output behavior of the system over time intervals of length K. For a given sampling time k, the corresponding $\sum_{k=0}^{K-1} p_k$-dimensional input vector and $\sum_{k=0}^{K-1} q_k$-dimensional output vector are the same as for the standard lifted system but an $\sum_{k=0}^{K-1} n_k$-dimensional state vector is defined as

$$\mathcal{X}_k^S(h) = [x^T(k+hK), x^T(k+hK+1), \ldots, x^T(k+hK+K-1)]^T.$$

Assume the square pencil $\mathcal{A}_k^S - z\mathcal{E}_k^S$ is regular, i.e., $\det(\mathcal{A}_k^S - z\mathcal{E}_k^S) \neq 0$, then the TFM of the stacked lifted system is defined as

$$\mathcal{H}_k^S(z) = \mathcal{C}_k^S(z\mathcal{E}_k^S - \mathcal{A}_k^S)^{-1}\mathcal{B}_k^S, \tag{5.7}$$

and the associated system pencil is defined as

$$\mathcal{W}_k^S(z) = \begin{bmatrix} \mathcal{A}_k^S - z\mathcal{E}_k^S & \mathcal{B}_k^S \\ \mathcal{C}_k^S & 0 \end{bmatrix}, \tag{5.8}$$

which both depend on the sampling time k.

Cyclic Lifted Representation: We now introduce another LTI representation of the LPTV discrete-time descriptor systems, using the method first introduced in [79].

For notational convenience, we introduce the following script notation

$$\mathbf{X}_k := \operatorname{diag}(X_k, X_{k+1}, \ldots, X_{k+K-1}),$$

which associates the block-diagonal matrix $\mathbf{X}_k$ to the cyclic matrix sequence X_i, $i = k, k+1, \ldots, k+K-1$ starting at time moment k, and a concatenated vector $\mathbf{r}_k$:

$$\mathbf{r}_k := [r_k^T, r_{k+1}^T, \cdots, r_{k-K+1}^T]^T.$$

Then the LPTV discrete-time descriptor system (5.1) can be written as

$$\begin{aligned} \mathbf{E}_k \mathbf{x}_{k+1} &= \mathbf{A}_k \mathbf{x}_k + \mathbf{B}_k \mathbf{u}_k, && (5.9)\\ \mathbf{y}_k &= \mathbf{C}_k \mathbf{x}_k, && (5.10) \end{aligned}$$

$k \in \mathbb{Z}$, and is merely K copies of (5.1) running in parallel, successively offset in time-index by one. Next, we introduce two cyclic shift matrices $\mathcal{M}_{\mu_k}$ and $\mathcal{N}_{n_k}$, which are the generators of a cyclic group of order K:

$$\mathcal{M}_{\mu_k} = \begin{bmatrix} 0 & & & I_{\mu_k} \\ I_{\mu_{k+1}} & & & \\ \vdots & \ddots & & \vdots \\ 0 & & I_{\mu_{k+K-1}} & 0 \end{bmatrix}, \quad \mathcal{N}_{n_k} = \begin{bmatrix} 0 & I_{n_{k+1}} & & 0 \\ \vdots & \ddots & & \\ & & & I_{n_{k+K-1}} \\ I_{n_k} & & & 0 \end{bmatrix}, \tag{5.11}$$

and perform the following transformation (similar as done in [101] for constant dimensions):

- $\mathbf{x}_k = \mathcal{N}_{n_k}^{k-1} \bar{\mathbf{x}}_k$,
- premultiply (5.9) by $\mathcal{M}_{\mu_k}^k$,
- $\mathbf{u}_k = \mathcal{N}_{p_k}^{k-1} \bar{\mathbf{u}}_k$, and
- premultiply (5.12) by $\mathcal{N}_{q_k}^k$.

Due to the identities

$$\begin{aligned} \mathcal{M}_{\mu_k} \mathbf{E}_k \mathcal{N}_{n_k} &= \mathbf{E}_{k+K-1}, \quad \mathcal{M}_{\mu_k} \mathbf{A}_k \mathcal{N}_{n_k} = \mathbf{A}_{k+K-1},\\ \mathcal{M}_{\mu_k} \mathbf{B}_k \mathcal{N}_{p_k} &= \mathbf{B}_{k+K-1}, \quad \mathcal{M}_{q_k} \mathbf{C}_k \mathcal{N}_{n_k} = \mathbf{C}_{k+K-1}, \end{aligned}$$

Equations (5.9) and (5.10) yield, rather pleasantly, an LTI system of the form

$$\Sigma_k^C : \begin{cases} \mathcal{E}_k^C \, \bar{\mathbf{x}}_{k+1} &= \mathcal{A}_k^C \, \bar{\mathbf{x}}_k + \mathcal{B}_k^C \, \bar{\mathbf{u}}_k, \\ \bar{\mathbf{y}}_k &= \mathcal{C}_k^C \, \bar{\mathbf{x}}_k, \end{cases} \tag{5.12}$$

where

$$\begin{aligned} \mathcal{E}_k^C : &= \mathcal{M}_{\mu_k}^k \mathbf{E}_k \mathcal{N}_{n_k}^k, \quad \mathcal{A}_k^C := \mathcal{M}_{\mu_k}^k \mathbf{A}_k \mathcal{N}_{n_k}^{k-1} \\ \mathcal{B}_k^C : &= \mathcal{M}_{\mu_k}^k \mathbf{B}_k \mathcal{N}_{p_k}^k, \quad \mathcal{C}_k^C := \mathcal{M}_{q_k}^k \mathbf{C}_k \mathcal{N}_{n_k}^{k-1}. \end{aligned} \tag{5.13}$$

Equation (5.12) represents the *cyclic lifted representation* of the LPTV discrete-time descriptor system (5.1) at time k, with $\sum_{k=0}^{K-1} p_k$ inputs and $\sum_{k=0}^{K-1} q_k$ outputs. The state dimension of the system is $\sum_{k=0}^{K-1} \mu_k = \sum_{k=0}^{K-1} n_k = n$ and its TFM is

$$\mathcal{H}_k^C(z) = \mathcal{C}_k^C (z\mathcal{E}_k^C - \mathcal{A}_k^C)^{-1} \mathcal{B}_k^C.$$

The cyclic lifted system can take different forms depending on its starting time k. For example, the cyclic lifted system starting at $k = 1$ have the following form:

$$\Sigma_1^C : \begin{cases} \mathcal{E}_1^C \, \bar{\mathbf{x}}_{k+1} &= \mathcal{A}_1^C \, \bar{\mathbf{x}}_k + \mathcal{B}_1^C \, \bar{\mathbf{u}}_k, \\ \bar{\mathbf{y}}_k &= \mathcal{C}_1^C \, \bar{\mathbf{x}}_k, \end{cases} \tag{5.14}$$

where

$$\begin{aligned} \mathcal{E}_1^C : &= \mathcal{M}_{\mu_k}^k \mathbf{E}_k \mathcal{N}_{n_k}^k = \mathcal{M}_{\mu_1} \mathbf{E}_1 \mathcal{N}_{n_1} = \mathbf{E}_0, \\ \mathcal{A}_1^C : &= \mathcal{M}_{\mu_k}^k \mathbf{A}_k \mathcal{N}_{n_k}^{k-1} = \mathcal{M}_{\mu_1} \mathbf{A}_1, \\ \mathcal{B}_1^C : &= \mathcal{M}_{\mu_k}^k \mathbf{B}_k \mathcal{N}_{p_k}^k = \mathcal{M}_{\mu_1} \mathbf{B}_1 \mathcal{N}_{p_1} = \mathbf{B}_0, \\ \mathcal{C}_1^C : &= \mathcal{M}_{q_k}^k \mathbf{C}_k \mathcal{N}_{n_k}^{k-1} = \mathcal{M}_{q_1} \mathbf{C}_1. \end{aligned} \tag{5.15}$$

The essence of the cyclic lifted system is putting inputs, states and outputs of the original LPTV descriptor system at cyclic places (depending on the starting time k) of those of the lifted LTI system. In any cyclic reformulation starting at time k, the matrix $\mathcal{E}_k^C$ has to block diagonal and $\mathcal{A}_k^C$ is a block cyclic matrix, while $\mathcal{B}_k^C$, and $\mathcal{C}_k^C$ can be either block diagonal or block cyclic, which depends on the relative places of input, state and output of the original LPTV system in those of the cyclic lifted system.

Remark 5.1:

The construction of the cyclic lifted system avoids matrix multiplication and only one LTI representation is needed for representing the system dynamics of the original LPTV system. But for the cyclic lifted LTI model, the number of states is much larger than that of the original LPTV system. ◊

In this thesis we consider only the cyclic lifted system for the LTI representation of LPTV discrete-time descriptor systems (5.1). Hence, we reserve the script notations (i.e., without superscripts) for the cyclic lifted representation Σ_1^C . We write Equation (5.14) in more usual form [12] as follows:

$$\begin{aligned} \mathcal{E} \mathcal{X}_{k+1} &= \mathcal{A} \mathcal{X}_k + \mathcal{B} \, \mathcal{U}_k, \\ \mathcal{Y}_k &= \mathcal{C} \mathcal{X}_k, \end{aligned} \tag{5.16}$$

where

$$\mathcal{E} = \operatorname{diag}(E_0, E_1, \ldots, E_{K-1}), \quad \mathcal{B} = \operatorname{diag}(B_0, B_1, \ldots, B_{K-1}),$$

$$\mathcal{A} = \begin{bmatrix} 0 & & \cdots & 0 & A_0 \\ A_1 & & & & 0 \\ & \ddots & & & \vdots \\ 0 & & & A_{K-1} & 0 \end{bmatrix}, \quad \mathcal{C} = \begin{bmatrix} 0 & & \cdots & 0 & C_0 \\ C_1 & & & & 0 \\ & \ddots & & & \vdots \\ 0 & & & C_{K-1} & 0 \end{bmatrix}. \tag{5.17}$$

The descriptor vector, system input and output of (5.16) are related to those of (5.1) via

$$\mathcal{X}_k = [x_1^T, \ldots, x_{K-1}^T, x_0^T]^T, \tag{5.18}$$
$$\mathcal{U}_k = [u_0^T, u_1^T, \ldots, u_{K-1}^T]^T, \tag{5.19}$$
$$\mathcal{Y}_k = [y_0^T, y_1^T, \ldots, y_{K-1}^T]^T, \tag{5.20}$$

respectively. The transfer function of the lifted system (5.16) can be rewritten as

$$\mathcal{H}(z) = \mathcal{C}(z\mathcal{E} - \mathcal{A})^{-1}\mathcal{B}. \tag{5.21}$$

5.2. Cyclic Lifted System Analysis

The cyclic lifted system (5.16) describes the eigenstructure and system dynamics of the LPTV discrete-time descriptor system (5.1). In this content, regularity of the set of periodic matrix pairs $\{(E_k, A_k)\}_{k=0}^{K-1}$, i.e., $(\mathbb{E}, \mathbb{A})$, can be described by the cyclic matrix pencil. The set $(\mathbb{E}, \mathbb{A})$ is said to be *regular* when $\det(\mathbb{M}(\alpha, \beta)) \not\equiv 0$, where

$$\mathbb{M}(\alpha, \beta) := \begin{bmatrix} \alpha_0 E_0 & 0 & \ldots & 0 & -\beta_0 A_0 \\ -\beta_1 A_1 & \alpha_1 E_1 & & & 0 \\ & \ddots & \ddots & & \\ & & & & \\ 0 & & 0 & -\beta_{K-1} A_{K-1} & \alpha_{K-1} E_{K-1} \end{bmatrix} \tag{5.22}$$

with $\alpha = (\alpha_0, \alpha_1, \ldots, \alpha_{K-1})$, $\beta = (\beta_0, \beta_1, \ldots, \beta_{K-1})$, and α_k, β_k are complex variables for $k = 0, 1, \ldots, K-1$.

Definition 5.2.1:

Let $(\mathbb{E}, \mathbb{A})$ be a regular set of matrix pairs. If there exist $\alpha = (\alpha_0, \alpha_1, \ldots, \alpha_{K-1})$, $\beta = (\beta_0, \beta_1, \ldots, \beta_{K-1})$, where α_k, β_k are complex variables for $k = 0, 1, \ldots, K-1$, which satisfy

$$\det(\mathbb{M}(\alpha, \beta)) = 0,$$

then the pair $(\pi_\alpha, \pi_\beta) = \left(\prod_{k=0}^{K-1} \alpha_k, \ \prod_{k=0}^{K-1} \beta_k \right) \neq (0, 0)$, is an *eigenvalue pair* of $\{(E_k, A_k)\}_{k=0}^{K-1}$.◊

Note that if $\pi_\beta \neq 0$, then $z = \pi_\alpha / \pi_\beta$ is a finite eigenvalue, otherwise $(\pi_\alpha, 0)$ represents an infinite eigenvalue of $\{(E_k, A_k)\}_{k=0}^{K-1}$ (see [30] for details). The set of periodic matrix pairs $(\mathbb{E}, \mathbb{A})$ is said to be *pd-stable* if it is regular and all its finite eigenvalues lie inside the unit circle. System (5.1) is *asymptotically stable* if the corresponding set of periodic matrix pairs $\{(E_k, A_k)\}_{k=0}^{K-1}$ is pd-stable.

5.2.1. Solvability and Conditionability

Two most important concepts associated with original periodic system (5.1), which characterize their well behaviors are solvability and conditionability. Both the concepts can be described by the corresponding cyclic lifted structure of (5.1). For LPTV discrete-time descriptor systems of constant dimensions, both the concepts have been briefly discussed in [71, 97].

It is clear that the original system (5.1) with period K can be re-interpreted by the system represented by K equations, and these can be written out in block matrix form as

$$\begin{bmatrix} -A_0 & E_0 & & & & \\ & -A_1 & E_1 & & & \\ & & \ddots & \ddots & & \\ & & & -A_{K-2} & E_{K-2} & \\ & & & & -A_{K-1} & E_{K-1} \end{bmatrix} \cdot \begin{bmatrix} x_0 \\ x_1 \\ \vdots \\ x_{K-1} \\ x_K \end{bmatrix} = \begin{bmatrix} B_0 & & & \\ & B_1 & & \\ & & \ddots & \\ & & & B_{K-1} \end{bmatrix} \begin{bmatrix} u_0 \\ u_1 \\ \vdots \\ u_{K-1} \end{bmatrix}. \tag{5.23}$$

Analogous to the work of [71, 97], we can also define the solvability and conditionability of system (5.1). The solvability matrix of (5.1), denoted by $S(0, K)$, is the coefficient matrix of (5.23). System (5.1) is said to be *solvable* if $S(0, K)$ is of full rank for every $K > 0$.

Similarly, the conditionability matrix of (5.1), denoted by $C(0, K)$, is the submatrix of $S(0, K)$ obtained by deleting the first and last block columns. System (5.1) is said to be *conditionable* if $C(0, K)$ is of full rank for every $K > 0$.

Solvability and conditionability of system (5.1) depend only on its homogeneous system

$$E_k x_{k+1} = A_k x_k, \quad k = 0, \ldots, K-1, \tag{5.24}$$

and they are dual concepts. This in turns implies that the LPTV system (5.24) is solvable if and only if it is conditionable [71, 97]. The solvability and conditionability of the LPTV discrete-time descriptor system (5.1) can be directly linked to the corresponding properties of the cyclic lifted system.

Definition 5.2.2:

The LPTV discrete-time descriptor system (5.1) is said to be solvable (conditionable) if the pencil

$$\alpha\mathcal{E} - \beta\mathcal{A} := \begin{bmatrix} \alpha E_0 & 0 & \ldots & 0 & -\beta A_0 \\ -\beta A_1 & \alpha E_1 & & & 0 \\ & \ddots & \ddots & & \\ & & & & \\ 0 & & 0 & -\beta A_{K-1} & \alpha E_{K-1} \end{bmatrix} \tag{5.25}$$

is regular, where α, β are complex variables, i.e., $\exists\, \alpha, \beta \in \mathbb{C}$ so that $\det(\alpha\mathcal{E} - \beta\mathcal{A}) \neq 0$.$\Diamond$

The following theorem establishes the relationship of the concepts of solvability and conditionability between the LPTV discrete-time descriptor system (5.1) and its corresponding cyclic lifted system (5.16).

Theorem 5.2.1:

The following statements are equivalent:

1. *The LPTV descriptor system (5.1) is solvable (conditionable).*
2. *The cyclic lifted system (5.16) is solvable (conditionable).* ◊

Proof. (1 ⇔ 2) We sketch the proof for system (5.1) of time-varying dimensions which is analogous to the proof of Theorem 2. in [97] given for constant dimensions. Let us consider the homogeneous form of the cyclic lifted system (5.16), i.e.,

$$\begin{aligned} \mathcal{E}\mathcal{X}_{k+1} &= \mathcal{A}\mathcal{X}_k, \\ \mathcal{Y}_k &= \mathcal{C}\mathcal{X}_k, \quad k = 0, \ldots, K-1. \end{aligned} \tag{5.26}$$

The solvability matrix of system (5.26), over an interval of length l, can be written as

$$\left.\begin{bmatrix} -\mathcal{A} & \mathcal{E} & & & \\ & -\mathcal{A} & \mathcal{E} & & \\ & & \ddots & \ddots & \\ & & & -\mathcal{A} & \mathcal{E} \\ & & & & -\mathcal{A} \quad \mathcal{E} \end{bmatrix}\right\} \; l \text{ block rows.} \tag{5.27}$$

Modulo row and column permutations, it is identical to

$$\operatorname{diag}\{S(0,l), S(1,l), \ldots, S(K-1,l)\}, \tag{5.28}$$

where the $S(i,l)$ refer to solvability matrices of the LPTV system (5.1) [97, 71]. This shows that (5.27) is of full rank iff (5.28) is. Since this holds for all $l > 0$, we conclude that (5.16) is solvable iff (5.1) is.

The argument for conditionability can be derived similarly. The conditionability matrix of (5.16) is the submatrix of (5.27) obtained by deleting the first and last block columns. Rearranging rows and columns as before, it is identical to

$$\operatorname{diag}\{C(0,l), C(1,l), \ldots, C(K-1,l)\}, \tag{5.29}$$

where the $C(i,l)$ refer to conditionability matrices of (5.1). This shows that (5.27) is of full rank iff (5.29) is. Since this holds for all $l > 0$, we conclude that (5.16) is conditionable iff (5.1) is. □

The solvability and conditionability of the cyclic lifted system (5.16) are also duel concepts. The cyclic lifted system (5.16) is solvable iff it is conditionable [71]. The reverse implication also holds.

5.2.2. Stability

Stability of the cyclic lifted system (5.16) is defined by the regularity of the cyclic matrix pencil $z\mathcal{E} - \mathcal{A}$, defined as

$$z\begin{bmatrix} E_0 & & & \\ & E_1 & & \\ & & \ddots & \\ & & & E_{K-1} \end{bmatrix} - \begin{bmatrix} & & & A_0 \\ A_1 & & & \\ & \ddots & & \\ & & A_{K-1} & \end{bmatrix}. \tag{5.30}$$

The cyclic matrix pencil $z\mathcal{E} - \mathcal{A}$ is said to be *regular* when $\det(z\mathcal{E} - \mathcal{A}) \neq 0$, for any $z \in \mathbb{C}$.

Definition 5.2.3:
The cyclic lifted system (5.16) is *asymptotically stable* iff $z\mathcal{E} - \mathcal{A}$ is regular and all its finite eigenvalues lie inside the unit circle. ◊

Stability of the original LPTV discrete-time descriptor system (5.1) is directly linked to the stability of the corresponding cyclic lifted system (5.16). Regularity of the periodic matrix pairs $\{(E_k, A_k)\}_{k=0}^{K-1}$ implies the regularity of the cyclic matrix pair $(\mathcal{E}, \mathcal{A})$ [59]. The reverse argument also holds true. With this concept, the periodic descriptor system (5.1) is said to be asymptotically stable iff the cyclic pencil (5.22) is regular and all its finite eigenvalues lie inside unit circle.

Remark 5.2:
The eigenvalues of $z\mathcal{E} - \mathcal{A}$ are identical to the eigenvalues of $\alpha\mathcal{E} - \beta\mathcal{A}$ and they are the K-th roots of the eigenvalues of the monodromy matrix (4.49) in Chapter 4, when it exists. This means that

$$\Lambda\Big(\{(E_k, A_k)\}_{k=0}^{K-1}\Big) = \{(\alpha^K, \beta^K) \mid \det(\alpha\mathcal{E} - \beta\mathcal{A}) = 0\}. \tag{5.31}$$

5.2.3. Reachability and Observability

Reachability and observability of the periodic descriptor system (5.1) can be redefined with the cyclic matrix pairs of system (5.16). For convenience, let us recall the forward-backward periodic subsystems of Chapter 4:

$$x_{k+1}^f = A_k^f x_k^f + B_k^f u_k, \quad y_k^f = C_k^f x_k^f, \tag{5.32}$$

$$E_k^b x_{k+1}^b = x_k^b + B_k^b u_k, \quad y_k^b = C_k^b x_k^b, \tag{5.33}$$

for $k = 0, 1, \ldots, K-1$. Using the periodic decomposition of the periodic matrix pairs as defined in (4.54), reachability and observability of the periodic descriptor system (5.1) can be redefined with the cyclic matrices of Equation (5.16) as described in the following two theorems.

Theorem 5.2.2:
[30] *(1) The forward subsystem (5.32) is completely reachable if for* $\prod_{i=0}^{K-1} \alpha_i \in \Lambda(\Phi_f(K,0))$ *the matrix*

$$\mathbf{C}^f(\alpha_0,\cdots,\alpha_{K-1}) := \left[\begin{array}{cccc|cccc} \alpha_0 I_{n_1^f} & & \cdots & 0 & -A_0^f & B_0^f & & & \\ -A_1^f & \alpha_1 I_{n_2^f} & & & 0 & & B_1^f & & \\ & \ddots & & & \vdots & & & \ddots & \\ 0 & & & -A_{K-1}^f & \alpha_{K-1} I_{n_0^f} & & & & B_{K-1}^f \end{array}\right]$$

has full row rank.

(2) The backward subsystem (5.33) is completely reachable if the pair $(\mathcal{E}^b, \mathcal{B}^b)$ *is reachable, where*

$$\mathcal{E}^b = \begin{bmatrix} 0 & E_0^b & & & \\ \vdots & \vdots & \ddots & & \\ 0 & 0 & & & E_{K-2}^b \\ E_{K-1}^b & 0 & \cdots & \cdots & 0 \end{bmatrix}, \quad \mathcal{B}^b = \begin{bmatrix} B_0^b & & & \\ & B_1^b & & \\ & & \ddots & \\ & & & B_{K-1}^b \end{bmatrix}. \tag{5.34}$$

◊

Proof. See [29, 65]. □

Similarly, forward and backward observability of the periodic descriptor system can be defined.

Theorem 5.2.3:

[30] *(1) The forward subsystem (5.32) is completely observable if for* $\prod_{i=0}^{K-1} \alpha_i \in \Lambda(\Phi_f(K,0))$ *the matrix*

$$\mathbf{O}^f(\alpha_0,\cdots,\alpha_{K-1}) := \left[\begin{array}{cccc} \alpha_0 I_{n_0^f} & \cdots & 0 & -A_{K-1}^f \\ -A_0^f & \alpha_1 I_{n_1^f} & & 0 \\ & \ddots & & \vdots \\ 0 & & -A_{K-2}^f & \alpha_{K-1} I_{n_{K-1}^f} \\ \hline C_0^f & & & \\ & C_1^f & & \\ & & \ddots & \\ & & & C_{K-1}^f \end{array}\right]$$

has full column rank.

(2) The backward subsystem (5.33) is completely observable if the pair $(\mathcal{E}^b, \mathcal{C}^b)$ *is observable, where*

$$\mathcal{E}^b = \begin{bmatrix} 0 & E_0^b & & \\ \vdots & \vdots & \ddots & \\ 0 & 0 & & E_{K-2}^b \\ E_{K-1}^b & 0 & \cdots & 0 \end{bmatrix}, \quad \mathcal{C}^b = \begin{bmatrix} C_0^b & & & \\ & C_1^b & & \\ & & \ddots & \\ & & & C_{K-1}^b \end{bmatrix}. \tag{5.35}$$

◊

Proof. See [29, 65]. □

Remark 5.3:

However, if the system (5.1) is *reachable* at time k, the cyclic lifted system (5.16) is not necessarily reachable. The appropriate statement is that system (5.1) is reachable (observable) at each time $k = 0, 1, \ldots, K-1$, if and only if system (5.16) is reachable (observable) [see [18] for details]. ◊

5.2.4. Gramians and Matrix Equations

The periodic reachability and observability Gramians of the periodic descriptor system (5.1) can be recovered from the block diagonal solutions of the reachability and observability type projected lifted discrete-time algebraic Lyapunov equations (PLDALEs) of system (5.16), respectively. It is shown in [57, 121] that the Gramians of standard

periodic systems satisfy the lifted form of the periodic Lyapunov equations and the solutions of these equations are diagonal matrices. The idea can be extended to the LPTV discrete-time descriptor system (5.1) and the corresponding cyclic lifted system (5.16). The periodic Gramians G_k^{cr}, G_k^{ncr}, G_k^{co} and G_k^{nco} of the periodic descriptor system (5.1) satisfy the projected lifted discrete-time algebraic Lyapunov equations (PLDALEs) of system (5.16).

The following theorem describes the block diagonal structures of the solutions of periodic Lyapunov equations in lifted form and their relations to the corresponding solutions of generalized PPDALEs in Theorem 4.3.5 of Chapter 4.

Theorem 5.2.4:

Consider the periodic discrete-time descriptor system (5.1) and its cyclic lifted representation (5.16), where the set of periodic matrix pairs $\{(E_k, A_k)\}_{k=0}^{K-1}$ is pd-stable. The causal and noncausal reachability Gramians $\mathcal{G}^{cr}$ and $\mathcal{G}^{ncr}$ of (5.16) satisfy the generalized PLDALEs

$$\begin{aligned} \mathcal{A}\mathcal{G}^{cr}\mathcal{A}^T - \mathcal{E}\mathcal{G}^{cr}\mathcal{E}^T &= -\mathcal{P}_l\mathcal{B}\mathcal{B}^T\mathcal{P}_l^T, \quad \mathcal{G}^{cr} = \mathcal{P}_r\mathcal{G}^{cr}\mathcal{P}_r^T, \qquad (5.36)\\ \mathcal{A}\mathcal{G}^{ncr}\mathcal{A}^T - \mathcal{E}\mathcal{G}^{ncr}\mathcal{E}^T &= \mathcal{Q}_l\mathcal{B}\mathcal{B}^T\mathcal{Q}_l^T, \quad \mathcal{G}^{ncr} = \mathcal{Q}_r\mathcal{G}^{ncr}\mathcal{Q}_r^T, \qquad (5.37) \end{aligned}$$

respectively, where $\mathcal{E}$, $\mathcal{A}$, $\mathcal{B}$ are as in (5.17) and

$$\begin{aligned} \mathcal{G}^{cr} &= \operatorname{diag}(G_1^{cr}, \ldots, G_{K-1}^{cr}, G_0^{cr}), \quad \mathcal{G}^{ncr} = \operatorname{diag}(G_1^{ncr}, \ldots, G_{K-1}^{ncr}, G_0^{ncr}),\\ \mathcal{P}_l &= \operatorname{diag}(P_l(0), P_l(1), \ldots, P_l(K-1)), \qquad \mathcal{Q}_l = I - \mathcal{P}_l, \qquad (5.38)\\ \mathcal{P}_r &= \operatorname{diag}(P_r(1), \ldots, P_r(K-1), P_r(0)), \qquad \mathcal{Q}_r = I - \mathcal{P}_r. \end{aligned}$$

◊

Proof. We will only give an outline of the proof. Let us consider a period-3 LPTV system ($k = 0, 1, 2$). We rewrite the first equation of (5.36) as its cyclic lifted structure:

$$\begin{aligned} &\begin{bmatrix} 0 & 0 & A_0 \\ A_1 & 0 & 0 \\ 0 & A_2 & 0 \end{bmatrix}\begin{bmatrix} G_1^{cr} & 0 & 0 \\ 0 & G_2^{cr} & 0 \\ 0 & 0 & G_0^{cr} \end{bmatrix}\begin{bmatrix} 0 & 0 & A_0 \\ A_1 & 0 & 0 \\ 0 & A_2 & 0 \end{bmatrix}^T - \begin{bmatrix} E_0 & 0 & 0 \\ 0 & E_1 & 0 \\ 0 & 0 & E_2 \end{bmatrix}\begin{bmatrix} G_1^{cr} & 0 & 0 \\ 0 & G_2^{cr} & 0 \\ 0 & 0 & G_0^{cr} \end{bmatrix}\begin{bmatrix} E_0 & 0 & 0 \\ 0 & E_1 & 0 \\ 0 & 0 & E_2 \end{bmatrix}^T \\ &= \begin{bmatrix} P_l(0)B_0 & 0 & 0 \\ 0 & P_l(1)B_1 & 0 \\ 0 & 0 & P_l(2)B_2 \end{bmatrix}\begin{bmatrix} P_l(0)B_0 & 0 & 0 \\ 0 & P_l(1)B_1 & 0 \\ 0 & 0 & P_l(2)B_2 \end{bmatrix}^T \end{aligned} \qquad (5.39)$$

By a straightforward computation and then equating the corresponding terms from both the sides, we obtain

$$\begin{aligned} A_0G_0^{cr}A_0^T - E_0G_1^{cr}E_0^T &= -P_l(0)B_0B_0^TP_l(0)^T,\\ A_1G_1^{cr}A_1^T - E_1G_2^{cr}E_1^T &= -P_l(1)B_1B_1^TP_l(1)^T, \qquad (5.40)\\ A_2G_2^{cr}A_2^T - E_2G_0^{cr}E_2^T &= -P_l(2)B_2B_2^TP_l(2)^T. \end{aligned}$$

Equation (5.40) is nothing but the periodic projected Lyapunov equations

$$A_k G_k^{cr} A_k^T - E_k G_{k+1}^{cr} E_k^T = -P_l(k) B_k B_k^T P_l(k)^T,$$

for $k = 0, 1, 2$ of Equation (4.69). The same holds true for any k, where $k = 0, 1, \ldots, K-1$. Since the periodic matrix pairs $\{(E_k, A_k)\}_{k=0}^{K-1}$ are pd-stable, the matrix pencil $z\mathcal{E} - \mathcal{A}$ associated with the cyclic lifted system (5.16) is regular and all its eigenvalues lie inside the unit circle. Then the Lyapunov equation (5.36) has a unique solution.

Using again the block structures of $\mathcal{G}^{cr}$ and $\mathcal{P}_r$, simple calculation shows that the second equation of (5.36) is equivalent to the unique symmetric property, i.e., $G_k^{cr} = P_r(k) G_k^{cr} P_r(k)^T$ for $k = 0, 1, \ldots, K-1$ of Equation (4.69). Therefore, the causal reachability Gramian $\mathcal{G}^{cr}$ is the unique symmetric positive semidefinite solution of the generalized PLDALEs (5.36). The proof for $\mathcal{G}^{ncr}$ can be treated similarly. □

For the observability Gramians, the situation becomes a bit more complex. In that case we take a backward time-shift of the original lifted system as done in [121, 119] for standard case ($E_k = I_{n_{k+1}}$). The reason is that we do not want to destroy the block diagonal structure of the lifted solutions and we would like to retrieve the periodic observability Gramians of the periodic descriptor system (5.1) from these lifted solutions.

The backward time-shift of the original lifted system is performed by taking the K-cyclic backward-shift of the cyclic matrices $\mathcal{M}_{\mu_k}$ and $\mathcal{N}_{n_k}$ in (5.11), and then using relation (5.15). We denote with $\sigma\mathcal{E}$ the K-cyclic shift of $\mathcal{E}$ in (5.16) and similarly the others. The simplified representation of these K-cyclic shift matrices are as follows:

$$\begin{aligned}
\sigma\mathcal{E} &= \begin{bmatrix} E_{K-1} & & & \\ & E_0 & & \\ & & \ddots & \\ & & & E_{K-2} \end{bmatrix}, \quad \sigma\mathcal{A} = \begin{bmatrix} 0 & \cdots & 0 & A_{K-1} \\ A_0 & & & 0 \\ & \ddots & & \vdots \\ 0 & & A_{K-2} & 0 \end{bmatrix}, \\
\sigma\mathcal{B} &= \begin{bmatrix} B_{K-1} & & & \\ & B_0 & & \\ & & \ddots & \\ & & & B_{K-2} \end{bmatrix}, \quad \sigma\mathcal{C} = \begin{bmatrix} 0 & \cdots & 0 & C_{K-1} \\ C_0 & & & 0 \\ & \ddots & & \vdots \\ 0 & & C_{K-2} & 0 \end{bmatrix}.
\end{aligned} \tag{5.41}$$

In that case the states, inputs and outputs of the original lifted system are also changed (due to K-cyclic backward-shift) by the relations described after Equation (5.11). Considering the periodic matrix pairs $\{(E_k, A_k)\}_{k=0}^{K-1}$ are pd-stable, we can show that the causal and noncausal observability Gramians $\mathcal{G}^{co}$ and $\mathcal{G}^{nco}$ of (5.16) satisfy the projected PLDALEs

$$\begin{aligned}
\sigma\mathcal{A}^T \mathcal{G}^{co} \sigma\mathcal{A} - \sigma\mathcal{E}^T \mathcal{G}^{co} \sigma\mathcal{E} &= -(\sigma\mathcal{P}_r)^T \sigma\mathcal{C}^T \sigma\mathcal{C} (\sigma\mathcal{P}_r), & \mathcal{G}^{co} &= (\sigma\mathcal{P}_l)^T \mathcal{G}^{co} (\sigma\mathcal{P}_l), \\
\sigma\mathcal{A}^T \mathcal{G}^{nco} \sigma\mathcal{A} - \sigma\mathcal{E}^T \mathcal{G}^{nco} \sigma\mathcal{E} &= (\sigma\mathcal{Q}_r)^T \sigma\mathcal{C}^T \sigma\mathcal{C} (\sigma\mathcal{Q}_r), & \mathcal{G}^{nco} &= (\sigma\mathcal{Q}_l)^T \mathcal{G}^{nco} (\sigma\mathcal{Q}_l),
\end{aligned}$$

respectively, where $\sigma\mathcal{E}$, $\sigma\mathcal{A}$, $\sigma\mathcal{C}$ are defined in (5.41), and the projectors $\sigma\mathcal{P}_l = \text{diag}(P_l(K-1), P_l(0), \ldots, P_l(K-2))$, $\sigma\mathcal{P}_r = \text{diag}(P_r(0), P_r(1), \ldots, P_r(K-1))$, $\sigma\mathcal{Q}_r = I - \sigma\mathcal{P}_r$, $\sigma\mathcal{Q}_l = I - \sigma\mathcal{P}_l$, and

$$\mathcal{G}^{co} = \text{diag}(G_0^{co}, \ldots, G_{K-1}^{co}), \quad \mathcal{G}^{nco} = \text{diag}(G_0^{nco}, \ldots, G_{K-1}^{nco}). \tag{5.42}$$

Note that the lifted solutions $\mathcal{G}^{co}$ and $\mathcal{G}^{nco}$ have also block diagonal structures, but now the diagonal blocks appear in different order.

Contrary to the backward time-shift of the original lifted system, we have observed that it is possible to recover the periodic observability Gramians of the periodic descriptor system (5.1) from the block diagonal solutions of the observability type PLDALEs of the original lifted system (5.16) by reformulating only the matrix $\mathcal{C}$ on the right-hand side. Our observation is summarized in the following theorem.

Theorem 5.2.5:

Consider the periodic discrete-time descriptor system (5.1) and its cyclic lifted representation (5.16), where the periodic matrix pairs $\{(E_k, A_k)\}_{k=0}^{K-1}$ are pd-stable. The causal and noncausal observability Gramians $\mathcal{G}^{co}$ and $\mathcal{G}^{nco}$ of (5.16) satisfy the generalized PLDALEs

$$\mathcal{A}^T\mathcal{G}^{co}\mathcal{A} - \mathcal{E}^T\mathcal{G}^{co}\mathcal{E} = -\mathcal{P}_r^T\hat{\mathcal{C}}^T\hat{\mathcal{C}}\mathcal{P}_r, \qquad \mathcal{G}^{co} = \mathcal{P}_l^T\mathcal{G}^{co}\mathcal{P}_l, \tag{5.43}$$

$$\mathcal{A}^T\mathcal{G}^{nco}\mathcal{A} - \mathcal{E}^T\mathcal{G}^{nco}\mathcal{E} = \mathcal{Q}_r^T\hat{\mathcal{C}}^T\hat{\mathcal{C}}\mathcal{Q}_r, \qquad \mathcal{G}^{nco} = \mathcal{Q}_l^T\mathcal{G}^{nco}\mathcal{Q}_l, \tag{5.44}$$

respectively, where $\mathcal{E}$ and $\mathcal{A}$ are as in (5.17), the projectors $\mathcal{P}_l$, $\mathcal{P}_r$, $\mathcal{Q}_l$ and $\mathcal{Q}_r$ are as in (5.38), $\hat{\mathcal{C}} = \text{diag}(C_1, \ldots, C_{K-1}, C_0)$ and

$$\mathcal{G}^{co} = \text{diag}(G_1^{co}, \ldots, G_{K-1}^{co}, G_0^{co}), \quad \mathcal{G}^{nco} = \text{diag}(G_1^{nco}, \ldots, G_{K-1}^{nco}, G_0^{nco}). \tag{5.45}$$

◊

Proof. The proof is analogous to the previous proof of Theorem 5.2.4. □

The periodic Gramians inside the block diagonal solutions in (5.45) appear in different order than in (5.42). The cyclic lifted representation (5.16) of the periodic descriptor system (5.1) can be considered as a generalized LTI system in descriptor form. Hence, analogous to the generalized descriptor case [103], the complete reachability Gramian of the cyclic lifted system (5.16) is defined as the sum of the causal and noncausal reachability Gramians, i.e.,

$$\mathcal{G}^c = \mathcal{G}^{cr} + \mathcal{G}^{ncr},$$

and the complete observability Gramian of the cyclic lifted system (5.16) is the sum of the causal and noncausal observability Gramians, i.e.,

$$\mathcal{G}^o = \mathcal{G}^{co} + \mathcal{G}^{nco}.$$

Remark 5.4:
The structural properties of the cyclic lifted system (5.16) are determined by the structural properties of the original periodic descriptor system (5.1) [16, 18, 79]. In particular, system (5.16) is completely reachable (observable) if and only if system (5.1) is completely reachable (observable) [79, 18].

5.2.5. Transfer Function

As we have already discussed in Section 5.1, the transfer function of the cyclic lifted system (5.16) can be described as

$$\mathcal{H}(z) = \mathcal{C}(z\mathcal{E} - \mathcal{A})^{-1}\mathcal{B}, \tag{5.46}$$

and the associated system pencil is defined as

$$\mathcal{W}^{\mathcal{C}}(z) = \begin{bmatrix} \mathcal{A} - z\mathcal{E} & \mathcal{B} \\ \mathcal{C} & 0 \end{bmatrix}. \tag{5.47}$$

It follows from Remark 5.4 and from [18] that if periodic descriptor system (5.1) is minimal (i.e., completely reachable and completely observable), then the lifted system (5.16) is minimal, too, and the converse is also true. The zeros and poles of the minimal periodic system (5.1) can be easily defined from the TFM corresponding to the associated cyclic lifted system (5.16) [125].

The $\mathbb{H}_\infty$-norm of the cyclic lifted system (5.16) is defined by

$$\|\mathcal{H}\|_{\mathbb{H}_\infty} = \max_{\omega\in[0,2\pi]} \sigma_{max}(\mathcal{H}(e^{i\omega})), \tag{5.48}$$

where $\sigma(.)$ denotes the singular values of the corresponding matrix. We can compute the $\mathbb{H}_\infty$-norm of the periodic descriptor system (5.1) by making use of the corresponding cyclic lifted system (5.16). The following lemma clarifies the connection.

Lemma 5.2.1:
The cyclic lifted system described by (5.16) has the same $\mathbb{H}_\infty$-norm as the periodic descriptor system (5.1). ◊

Proof. See Lemma 1 and Lemma 2 in [101]. □

The TFMs corresponding to various lifted systems and their relations with the associated periodic descriptor systems are briefly discussed in [125, 122]. Also, the TFM of a particular lifted system can be easily determined from the TFM of another lifted system [122].

5.3. Discussions Regarding the LPTV Descriptor System and Corresponding Cyclic Lifted System

Index of Periodic Matrix Pairs: We would like to point out that the indexes ν_j for the elements of regular periodic matrix pairs are not necessarily equal. Each individual pair of the set $\{(E_k, A_k)\}_{k=0}^{K-1}$ may have different index. For example, the matrix pairs $\{(E_k, A_k)\}_{k=0}^{1}$ with $A_k = I_2,\ k = 0, 1$ and

$$E_0 = \begin{bmatrix} 0 & 1 \\ 0 & 1 \end{bmatrix}, \quad E_1 = \begin{bmatrix} 0 & 1 \\ 0 & 0 \end{bmatrix},$$

have indexes $\nu_0 = 1$ and $\nu_1 = 2$.

As shown in Chapter 4 and in the preceding part of this chapter, the monodromy matrices

$$J_j = \prod_{k=j+K-1}^{j} A_k^f \quad \text{and} \quad N_j = \prod_{k=j}^{j+K-1} E_k^b, \quad j = 0, \ldots, K-1,$$

play an important role for defining the indexes for the regular set of periodic matrix pairs $\{(E_k, A_k)\}_{k=0}^{K-1}$ of system (5.1). Also note that the indexes of the cyclic forms as in (5.25) are not appropriate to define the indexes the periodic matrix pairs $\{(E_k, A_k)\}_{k=0}^{K-1}$. For example, consider the above periodic matrix pairs. Reconstructing the cyclic form (5.25) for these periodic matrix pairs, we get

$$\operatorname{ind}_\infty\left(\begin{bmatrix} E_0 & 0 \\ 0 & E_1 \end{bmatrix}, \begin{bmatrix} 0 & A_0 \\ A_1 & 0 \end{bmatrix}\right) = \operatorname{ind}_\infty\left(\begin{bmatrix} E_1 & 0 \\ 0 & E_0 \end{bmatrix}, \begin{bmatrix} 0 & A_1 \\ A_0 & 0 \end{bmatrix}\right) = 3,$$

which is neither equal to the nilpotency of E_0E_1 not to the nilpotency of E_1E_0. Note that nilpotency of E_0E_1 is 1 and nilpotency of E_1E_0 is 2. Appropriate method for defining the indexes of periodic matrix pairs using their corresponding cyclic form is discussed in [59] for discrete-time descriptor systems of constant dimensions. Developing such a representation (see Section 2 and Definition 2.1 in [59]) for discrete-time descriptor systems of time-varying dimensions is more computational task and we restrict our discussion to the time-varying case.

TFMs of Different Lifted Systems: Let us consider the TFM (5.3) and the associated system pencil (5.4) of the standard lifted system (5.2). Obviously, $\mathcal{H}_{k+K}^L(z) = \mathcal{H}_k^L(z)$ and we have the following relation for TFMs computed at two successive values of k [46, 125]:

$$\mathcal{H}_{k+1}^L(z) = \begin{bmatrix} 0 & I_J \\ zI_{q_k} & 0 \end{bmatrix} \mathcal{H}_k^L(z) \begin{bmatrix} 0 & z^{-1}I_{p_k} \\ I_R & 0 \end{bmatrix}, \tag{5.49}$$

where $J = \sum_{i=k+1}^{k+K-1} q_k$, and $R = \sum_{i=k+1}^{k+K-1} p_k$.

The TFMs of different lifted systems are directly linked to each other. It can be shown that the TFMs of the stacked and standard lifted systems are the same, i.e.,$\mathcal{H}_k^S(z) = \mathcal{H}_k^L(z)$. Similarly, the relationship between the TFMs of standard and cyclic lifted systems is given by

$$\mathcal{H}_k^C(z) = \triangle_{q_k}(z^{-1})\, \mathcal{H}_k^L(z^K)\, \triangle_{p_k}(z), \tag{5.50}$$

where $\triangle_{j_k}(x) = \text{diag}(I_{j_k}, xI_{j_{k+1}}, \ldots, x^{K-1}I_{j_{k+K-1}})$.

Thus, to avoid matrix multiplications in the computation of $\mathcal{H}_k^L(z^K)$ using (5.3), one can first compute the TFM $\mathcal{H}_k^C(z)$ of the cyclic lifted system, and then compute $\mathcal{H}_k^L(z^K)$ using relation (5.50) and finally replace z^K by z.

CHAPTER

SIX

MODEL REDUCTION

Contents

This chapter is intended to introduce the basic notations and the most common concepts of model order reduction (MOR) for LTI descriptor systems. The main idea behind this is that the theoretical and mathematical concepts in the LTI structures will help more precisely to understand their corresponding periodic interpretations in the subsequent chapters.

We first give a short introduction of MOR and present the available approaches for MOR. We introduce the two most competing projection based approaches for generating reduced-order models for LTI systems: the Krylov-subspace methods and the Balanced Truncation (BT) methods.

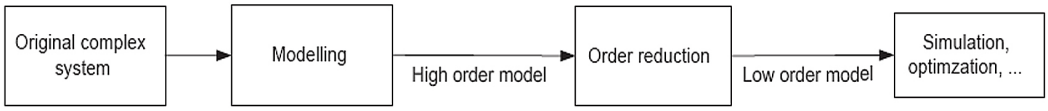

Figure 6.1. Order reduction for the purpose of simulation.

In Section 6.3 we first study the moment-matching approach via orthogonalized Krylov-subspace methods, which is one of the best choices for MOR of large scale systems. We will present the theoretical background and proofs to match the moments about different points. We also discuss the necessary numerical algorithms to calculate the projection matrices.

The BT approach for order reduction of LTI systems is briefly discussed in Section 6.4. In this section, we will represent the basic concepts of the BT approach and give the physical interpretations of the reachability and observability Gramians and Hankel singular values. We also represent the basic numerical algorithm for order reduction of singular systems using the BT approach, and discuss the stability and approximation error of the reduced systems.

In the last section we demonstrate the efficiencies and drawbacks of both the methods and compare them according to their fields of applications.

6.1. Introduction

Accurate modelling of an original system is a necessary part in many applications of modern engineering. Simulation and analysis of a high order model is difficult due to the lack of powerful computers, efficient algorithms, and the higher complexity induced in the model. In many cases simulation and analysis of such models are even impossible. A solution to simplify the preceding task in both fields of simulation and system analysis is to find a low order approximation of the original high order model. The procedure of order reduction is shown in Figure 6.1.

The main goal of the reduction is to replace the given mathematical model of a system or a process by a much smaller model which preserves certain crucial properties of the original system, such as stability or passivity, etc. Some other issues are also involved, such as the data structure of the original model, and the efficient and numerically stable computation of the model. Of course, the smallest possible approximation error in the reduced-order model compared to the original model is one of the main issues of MOR. The basic schematic view of MOR is shown in Figure 6.2.

Several methods have been proposed for reduction of LTI systems in different fields like control engineering, micro-systems and applied mathematics. We would like to mention the recent surveys [3, 48, 40, 41] and the references therein on that topic. The

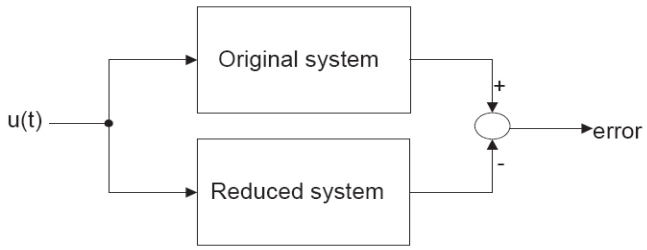

Figure 6.2. Order reduction by minimization the difference of the outputs.

order reduction procedures of LTI systems that have been discussed there fall into two major categories:

1. projection-based methods
2. non-projection based methods

The first category consists of such methods as Krylov-subspace (moment matching methods), BT method, Proper Orthogonal Decomposition (POD) methods, etc. The second category consists of Hankel optimal model reduction method, Singular perturbation method, and various optimization-based methods. The vast majority of model reduction methods are projection-based. In the next sections we will discuss briefly the two major competing projection based approaches: Krylov-subspace (moment-matching)-based methods and BT methods for order reduction of LTI descriptor systems.

6.2. Projection-Based Model Reduction Methods

Before proceeding with projection methods, the generalized state space form will be briefly described. This will help to create a more general framework for the projection techniques. Let us recall the LTI descriptor systems in the generalized state space form as defined in Equation (3.1) of Chapter 3. A continuous-time descriptor system of order n, with p inputs and q outputs, in generalized state space form is described by the equations,

$$\begin{aligned} E\dot{x}(t) &= Ax(t) + Bu(t), \quad x(0) = x_0, \\ y(t) &= Cx(t), \end{aligned} \tag{6.1}$$

and has the transfer function

$$H(s) = C(sE - A)^{-1}B. \tag{6.2}$$

A discrete-time descriptor system of order n, with p inputs and q outputs, in generalized

state space form is described by the equations,

$$\begin{aligned} Ex_{k+1} &= Ax_k + Bu_k, \quad x(0) = x_0, \\ y_k &= C_k x_k, \end{aligned} \tag{6.3}$$

and the transfer function is given by

$$H(z) = C(zE - A)^{-1}B. \tag{6.4}$$

If E is invertible, (6.1) and (6.3) can be easily converted to standard state space form. The reduced-order system of order r ($r < n$) for system (6.1) should have the form

$$\begin{aligned} \tilde{E}\dot{\tilde{x}}(t) &= \tilde{A}\tilde{x}(t) + \tilde{B}u(t), \\ \tilde{y}(t) &= \tilde{C}\tilde{x}(t), \end{aligned} \tag{6.5}$$

with the transfer function

$$\tilde{H}(s) = \tilde{C}(s\tilde{E} - \tilde{A})^{-1}\tilde{B}.$$

Similarly, the reduced-order system of order r ($r < n$) for system (6.3) should have the form

$$\begin{aligned} \tilde{E}\tilde{x}_{k+1} &= \tilde{A}\tilde{x}_k + \tilde{B}u_k, \\ \tilde{y}_k &= \tilde{C}\tilde{x}_k, \qquad k \in \mathbb{Z}, \end{aligned} \tag{6.6}$$

with the transfer function

$$\tilde{H}(z) = \tilde{C}(z\tilde{E} - \tilde{A})^{-1}\tilde{B}.$$

A projection method reduces (6.1) (also (6.3)) by choosing two r-dimensional projection spaces, $S_1, S_2 \subseteq \mathbb{R}^n$, so that the solution space is projected onto S_2, $\tilde{x} \in S_2$, and the residual of (6.1) is orthogonal to S_1. The projection can be considered as follows:

$$\begin{aligned} x &= U\tilde{x}, \\ U &\in \mathbb{R}^{n\times r},\ x \in \mathbb{R}^n,\ \tilde{x} \in \mathbb{R}^r. \end{aligned} \tag{6.7}$$

By applying this projection to system (6.1) (also (6.3)) and then pre-multiplying by V^T, a realization of the reduced-order system of order r satisfies the projection equations

$$\tilde{E} = V^T EU,\ \tilde{A} = V^T AU,\ \tilde{B} = V^T B,\ \tilde{C} = C\,U, \tag{6.8}$$

where the columns of V and U form bases for S_1 and S_2, respectively,

$$\text{colspan}(V) = S_1, \quad V \in \mathbb{R}^{n\times r}, \quad \text{colspan}(U) = S_2, \quad U \in \mathbb{R}^{n\times r}.$$

Note that for the SISO case, the matrices B and C change to vectors b and c^T, respectively. If $S_1 = S_2$, the projection is *orthogonal*, otherwise *oblique*. The matrices V and U are refered to as the left truncation matrix and the right truncation matrix, respectively. The following proposition shows that the choice of basis for S_1 and S_2 is not important.

Proposition 6.1:

If the columns of $\hat{V}$ also form a basis for S_1, and the columns of $\hat{U}$ also form a basis for S_2, then the reduced order system obtained by projection with $\hat{V}$ and $\hat{U}$ according to (6.8), is equivalent to (has the same transfer function as) the reduced order model obtained by projection with V and U. ◊

Proof. Let us consider two nonsingular $r \times r$ matrices, W and T, such that

$$V = \hat{V}W, \quad U = \hat{U}T.$$

Then the transfer function $\tilde{H}(s)$ can be represented as

$$\begin{aligned} \tilde{H}(s) &= CU(s\,V^TEU - V^TAU)^{-1}\,V^TB \\ &= C\hat{U}\,T(s\,W^T\hat{V}^TE\hat{U}\,T - W^T\hat{V}^TA\hat{U}\,T)^{-1}\,W^T\hat{V}^TB \\ &= C\hat{U}(s\,\hat{V}^TE\hat{U} - \hat{V}^TA\hat{U})^{-1}\,\hat{V}^TB \\ &= \hat{H}(s). \end{aligned}$$

This completes the proof. □

Hence, the input-output properties of the reduced system in (6.5) depend only on the column spans of V and U, that is, only on the choice of the projection subspaces S_1 and S_2. The projection matrices are enforced to be bi-orthogonal, i.e., $V^TU = I$.

6.3. Krylov-Subspace Based MOR

Nowadays, moment matching using Krylov subspaces is one of the best choices in order reduction of large scale systems and it was first proposed in [126]. In this approach, the lower order model is obtained by matching the *moments* (and/or *Markov parameters*) of the original and reduced-order systems where the moments are the coefficients of the Taylor series expansion of the transfer function about a suitable expansion point. When the expansion point tends to infinity, the coefficients are called Markov parameters. Well established algorithms, such as Arnoldi [40, 36], Lanczos [40, 5] or two-sided Arnoldi [91] can be used to compute a projection framework for the reduced-order system. A very recent release of the Krylov subspaces based order reduction technique is global Arnoldi [21], which approximates the large, sparse systems (specially MIMO systems) to significantly small order. In Figure (6.3), the steps of reduction for moment matching are shown.

6.3.1. Transfer Function Moments

Let us assume that system (6.1) is a MIMO system with transfer function as in (6.2). By assuming that A is nonsingular, the Taylor series expansion of the transfer matrix (6.2)

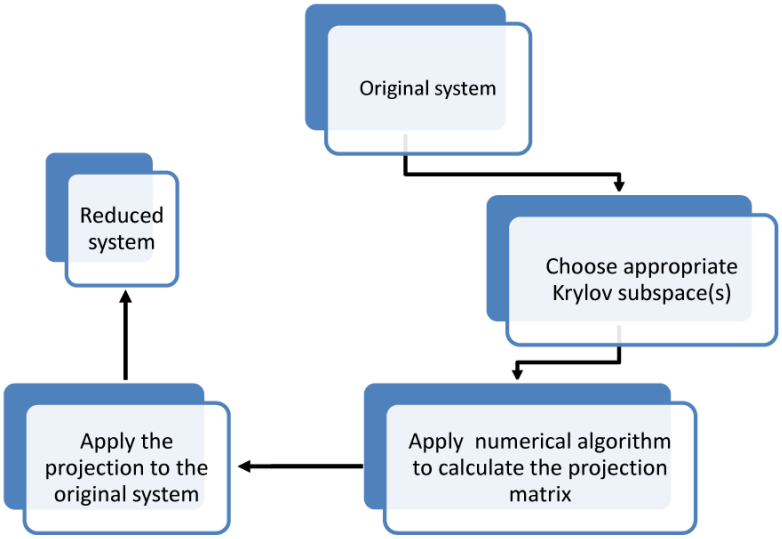

Figure 6.3. The main steps of Krylov subspace methods.

about zero is,

$$H(s) = -CA^{-1}B - C(A^{-1}E)A^{-1}B\,s - \cdots - C(A^{-1}E)^iA^{-1}B\,s^i - \cdots \tag{6.9}$$

The coefficients of this series, without negative sign, are called moments.

Definition 6.3.1:
In system (6.1), suppose that A is nonsingular, then the i-th moment (about zero) of this system is given by

$$m_i = C(A^{-1}E)^iA^{-1}B, \quad i = 0, 1, \ldots, \tag{6.10}$$

where m_i is a $q \times p$ matrix in the MIMO case and a scalar m_i, in the SISO case. ◊

Moments can be defined about different interpolation points $\sigma \neq 0$ by rewriting the transfer matrix with the shifted variable $s - \sigma$, i.e.,

$$H(s) = C[(s-\sigma)E - (A - \sigma E)]^{-1}B = \sum_{i=0}^{\infty}(s-\sigma)^i\,m_i, \tag{6.11}$$

where

$$m_i = C\{(A-\sigma E)^{-1}E\}^i\,(A-\sigma E)^{-1}B, \quad i = 0, 1, \ldots,$$

assuming that $A - \sigma E$ is nonsingular. These moments are called *shifted moments*. In fact, the moments of $H(s)$ about σ are the moments of $H(s + \sigma)$ about zero and σ should not be a generalized eigenvalue of the pair (E, A) [47].

When $\sigma \to \infty$, a different series results from (6.2). In that case, we set $s = 1/\xi$ in (6.2) and expanding the Taylor series about $\xi = 0$. The series is then

$$H(s) = CE^{-1}B\,s^{-1} + C(E^{-1}A)E^{-1}B\,s^{-2} + \cdots + C(E^{-1}A)^iE^{-1}B\,s^{-i} + \cdots,$$

and its coefficients are called *Markov parameters* if E is nonsingular.

Definition 6.3.2:
In system (6.1), suppose that E is nonsingular, then the i-th Markov parameter is defined as

$$M_i = C(E^{-1}A)^iE^{-1}B, \quad i = 0, 1, \ldots \tag{6.12}$$

In simple words, moments about zero reflect the behavior of a system at low frequencies, while the Markov parameters reflect the behavior of a system at higher frequencies.

6.3.2. Krylov Subspaces and Moment Matching

The reduced-order model is computed applying suitable projections to system (6.1). We will calculated these projections via Krylov subspaces, defined in the following:

Definition 6.3.3:
The order m Krylov subspace is the space defined as

$$\mathcal{K}_m(A, b) = span\{b, Ab, A^2b, ..., A^{m-1}b\}, \tag{6.13}$$

where $A \in \mathbb{R}^{n\times n}$ and $b \in \mathbb{R}^n$ is called the starting vector. The vectors $b, Ab, A^2b, ..., A^{m-1}b$ that construct the subspace, are called *basic vectors*. ◊

It is assumed that the basic vectors in a Krylov subspace are linearly independent, that means the i-th basic vector in the Krylov subspace (6.13) is a linear combination of the previous $i-1$ vectors. Those independent basic vectors form a basis of the Krylov subspace. But it is also possible that all the basic vectors in a Krylov subspace are not linearly independent. In that case the first independent basic vectors can be considered as a basis of the Krylov subspace.

Definition 6.3.4:
The block Krylov subspace of order m is the space defined as

$$\mathcal{K}_m(A, B) = span\{B, AB, A^2B, ..., A^{m-1}B\}, \tag{6.14}$$

where $A \in \mathbb{R}^{n\times n}$ and $B \in \mathbb{R}^{n\times p}$. The columns of B are the starting vectors. Note that $\text{rank}(\mathcal{K}_m(A, B)) \leq p \cdot m$. ◊

The block Krylov subspace with p starting vectors can be considered as a union of p Krylov subspaces defined for each starting vector.

The following theorems demonstrate how to choose the projection matrices to find the reduced-order system and explain details of matching the moments of the original and reduced-order systems.

Theorem 6.3.1:
If the columns of the matrix U used in (6.8) form a basis for the order r_a Krylov subspace $\mathcal{K}_{r_a}(A^{-1}E, A^{-1}B)$ and the matrix V is chosen such that $\tilde{A}$ is nonsingular, then the first r_a moments (about zero) of the original and reduced-order systems match. ◊

Proof. See the proof of Theorem 5 in [90]. □

The subspace $\mathcal{K}_{r_a}(A^{-1}E, A^{-1}B)$ is called *input Krylov subspace* and order reduction using a bases of this subspace for projection is called *one-sided Krylov subspace*, where V is chosen optionally so that $\tilde{A}$ is nonsingular.

Remark 6.2:
The order r of the reduced-order system is the dimension of the Krylov subspace which is at most $p \cdot r_a$ in the MIMO case. It can be less if there are dependent basic vectors in $\mathcal{K}_{r_a}(A^{-1}E, A^{-1}B)$ and then only r_a moments of the original and reduced-order systems match. ◊

It is possible to match even more than r_a moments by appropriate choice of V. For this, we introduce another type of Krylov subspace, known as *output Krylov subspace* and use it in the following theorem.

Theorem 6.3.2:
If the columns of the matrix V form a basis for the order r_b Krylov subspace $\mathcal{K}_{r_b}(A^{-T}E^T, A^{-T}C^T)$ and the matrix U is chosen such that $\tilde{A}$ is nonsingular, then the first r_b moments (about zero) of the original and reduced-order order systems match. ◊

Proof. See [90] for the proof. □

The subspace $\mathcal{K}_{r_b}(A^{-T}E^T, A^{-T}C^T)$ is called *output Krylov subspace*. Now combining Theorems 6.3.1 and 6.3.2, we summarize in the following theorem.

Theorem 6.3.3:
Assumed that A and $\tilde{A}$ are invertible. If the columns of the matrices U and V used in (6.8), form bases for $\mathcal{K}_{r_a}(A^{-1}E, A^{-1}B)$ and $\mathcal{K}_{r_b}(A^{-T}E^T, A^{-T}C^T)$, respectively, then the reduced-order transfer function $\tilde{H}(s) = \tilde{C}(s\tilde{E} - \tilde{A})^{-1}\tilde{B}$ matches the first $(r_a + r_b)$ moments of the original transfer function $H(s) = C(sE - A)^{-1}B$. ◊

Proof. See [90, 47] □

Order reduction by using both input and output Krylov subspaces for projection is called *two-sided Krylov subspace* method.

Remark 6.3:
In MIMO system with p inputs and q outputs, each moment is a matrix of $p \cdot q$ entries. Therefore, we have multiple moments matching in MIMO case, and the number of matching moments is $p \cdot q \cdot \frac{r}{p} = q \cdot r$ for Theorem 6.3.1 and $p \cdot q \cdot (\frac{r}{p} + \frac{r}{q}) = (q \cdot r + p \cdot r)$ for Theorem 6.3.3. Hence, choosing only the first r columns of U and V, one can find a reduced model of order r; because each column of U and V is responsible to match one more row or column of the moment matrices (for details see [90]). ◊

The idea of moments matching (about zero) using Theorem 6.3.3 can be easily extended to match the moments about different interpolation points $\sigma \neq 0$ by substituting A by $A - \sigma E$ in the definition of moments and Krylov subspaces. Before going into detail of this shifted moment matching, we would like to discuss two more important properties of Krylov subspaces.

6.3.3. Preconditioning and Shift-Invariance

Preconditioning is sometime essential to generate better projection subspaces (yield faster convergence) without drastically complicating the construction of the Krylov subspaces. In that case one solves the problem $FAx = Fb$, rather than solving the problem $Ax = b$, where $F \in \mathbb{R}^{n \times n}$ is the preconditioner. If F exactly equals A^{-1}, then the solution is $x = Fb$. In general, F is chosen such a way that the transformed system is hopefully easier to solve (iteratively) compare to the original system.

Let us consider the transformations with preconditioner F such that the preconditioned system is

$$\begin{aligned} FE\dot{x}(t) &= FAx(t) + FBu(t), \\ y(t) &= Cx(t). \end{aligned} \tag{6.15}$$

Note that (6.1) and (6.15) both describe the same system and the generalized eigenvalues of (FA, FE) and (A, E) are identical. Now consider the reduced-order model with this new description, which is given by

$$\begin{aligned} W^T FEU\dot{\tilde{x}}(t) &= W^T FAU\tilde{x}(t) + W^T FBu(t), \\ \tilde{y}(t) &= CU\tilde{x}(t), \end{aligned} \tag{6.16}$$

where the matrix $U \in \mathbb{R}^{n \times r}$ now satisfies

$$\text{colspan}\{U(s)\} = \mathcal{K}_r(F(A - sE), FB)$$

and the matrix $W \in \mathbb{R}^{n\times r}$ satisfies

$$\text{colspan}\{W(s)\} = \mathcal{K}_r((A - sE)^T F^T,\, C^T).$$

The reduced-order system described by (6.16) is different than (6.5), although (6.1) and (6.15) describe the same original system. This happens because of the presence of the preconditioned matrix F in (6.16) and the modifications of the projection matrices U and W. If we chose $V = F^T W$ rather than (6.8), then the new reduced-order model in (6.16) can be written in the desired form of (6.5) [47].

A special type of preconditioner, known as *exact preconditioner*, are generally used in the frequency dependent problems. This is the exact inverse of the matrix pencil, $F = (A - \sigma E)^{-1}$, at a fixed interpolating point σ (scalar). These exact preconditioners are very important if rational interpolation is to be used for the projection matrices [47, 84, 114]. An important property of exact preconditioning is presented in Lemma 6.3.1.

Lemma 6.3.1:
[47] *For any value of s and σ,*

$$(A - \sigma E)^{-1}(A - sE) = I + (\sigma - s)(A - \sigma E)^{-1} E.$$

◊

In other words, applying an exact preconditioner $F = (A - \sigma E)^{-1}$ to the pencil $(A - sE)$ leads to the simpler transformed pencil which consists of a scaled matrix FE shifted by the identity matrix. An important property of Krylov subspaces is its *shift-invariance* property which says that shifting the original matrix pencil by an identity matrix does not affect the original Krylov subspace.

Lemma 6.3.2 (Krylov subspace shift-invariance [47]):
For any matrix A, starting vectors B and nonzero scalar η,

$$\mathcal{K}_m(\eta A + I, B) = \mathcal{K}_m(A, B)$$

◊

Proof. The proof for the SISO case is given in the Appendix of [47]. The proof for the MIMO case is analogous to that. □

Now using Lemmas 6.3.1 and 6.3.2, we can summarize that

$$\mathcal{K}_m\left((A - \sigma E)^{-1}(A - sE),\, (A - \sigma E)^{-1} B\right) = \mathcal{K}_m\left((A - \sigma E)^{-1} E,\, (A - \sigma E)^{-1} B\right) \tag{6.17}$$

and

$$\mathcal{K}_m\left((A - \sigma E)^{-T}(A - sE)^T,\, (A - \sigma E)^{-T} C^T\right) = \mathcal{K}_m\left((A - \sigma E)^{-T} E^T,\, (A - \sigma E)^{-T} C^T\right). \tag{6.18}$$

Hence, the preconditioned projection subspaces on the left sides of (6.17) and (6.18) are equivalent to the frequency-independent subspace on the right sides of (6.17) and (6.18), respectively.

The frequency-independent subspaces in (6.17) and (6.18) can be used to match the shifted moments (about $\sigma \neq 0$) of the original and reduced-order systems. We proceed with two fundamental lemmas and later combine them in Theorem 6.3.5 to get our desire result. The proofs for Lemmas 6.3.3 and 6.3.4 can be found in the Appendix of [47].

Lemma 6.3.3:
If $\mathcal{K}_{r_a}\left((A-\sigma E)^{-1}E,\,(A-\sigma E)^{-1}B\right) \subseteq colspan\,\{U\}$, *then*

$$\{(A-\sigma E)^{-1}E\}^i\,(A-\sigma E)^{-1}B = U\,\{(\tilde{A}-\sigma\tilde{E})^{-1}\tilde{E}\}^i\,(\tilde{A}-\sigma\tilde{E})^{-1}\tilde{B}$$

for $i = 0, 1, \ldots, r_a - 1$. *Here* $\tilde{E}, \tilde{A}, \tilde{B}$ *are the matrices of the corresponding reduced-order system.* ◊

Lemma 6.3.4:
If $\mathcal{K}_{r_b}\left((A-\sigma E)^{-T}E^T,\,(A-\sigma E)^{-T}C^T\right) \subseteq colspan\,\{V\}$, *then*

$$C\,(A-\sigma E)^{-1}\{E\,(A-\sigma E)^{-1}\}^i = \tilde{C}(\tilde{A}-\sigma\tilde{E})^{-1}\{\tilde{E}\,(\tilde{A}-\sigma\tilde{E})^{-1}\}^i$$

for $i = 0, 1, \ldots, r_b - 1$. ◊

Combining Lemmas 6.3.3 and 6.3.4 leads to the following lemma. The proof can be found in [47].

Lemma 6.3.5:
If $\mathcal{K}_{r_a}\left((A-\sigma E)^{-1}E,\,(A-\sigma E)^{-1}B\right) \subseteq colspan\,\{U\}$, *and* $\mathcal{K}_{r_b}\left((A-\sigma E)^{-T}E^T,\,(A-\sigma E)^{-T}C^T\right) \subseteq colspan\,\{V\}$, *then the first* $(r_a + r_b)$ *moments (about* $\sigma \neq 0$*) of the original and reduced-order systems match.* ◊

Matching moments about multiple interpolation points requires multiple Krylov subspaces. Treating these points concurrently and constructing these multiple subspaces may give rise to complications, but these difficulties can be avoided through a proper computational approach. The following theorem connects projection via Krylov subspaces and the matching of moments at points $\sigma_1, \sigma_2, \ldots, \sigma_{\bar{k}} \neq \infty$.

Theorem 6.3.4:
[47] *If*

$$\bigcup_{k=1}^{\bar{k}} \mathcal{K}_{r_a^k}\left((A-\sigma_k E)^{-1}E,\,(A-\sigma_k E)^{-1}B\right) \subseteq colspan\,\{U\}, \tag{6.19}$$

and

$$\bigcup_{k=1}^{\bar{k}} \mathcal{K}_{r_b^k}\left((A-\sigma_k E)^{-T}E^T,\,(A-\sigma_k E)^{-T}C^T\right) \subseteq colspan\,\{V\}, \tag{6.20}$$

then the moments of the original and reduced-order models satisfy

$$C\{(A-\sigma_k E)^{-1}E\}^{i_k}(A-\sigma_k E)^{-1}B = \tilde{C}\{(\tilde{A}-\sigma_k \tilde{E})^{-1}\tilde{E}\}^{i_k}(\tilde{A}-\sigma_k \tilde{E})^{-1}\tilde{B}, \tag{6.21}$$

for $i_k = 0, 1, \ldots, (r_a^k + r_b^k) - 1$ *and* $k = 1, 2, \ldots, \bar{k}$. ◊

Proof. For the proof, see [47]. □

Remark 6.4:
One important point in MIMO problem it is not necessary that the same number of moments match for Krylov subspaces generated for different interpolation points σ_k in (6.21). ◊

6.3.4. Computational Aspects for Krylov Subspaces

In most application related models, choosing a suitable basis for the concerned Krylov subspace is the most crucial task, since it guarantees the better approximation of the reduced-order model. In one-sided methods, the most popular algorithm is the *Arnoldi algorithm* which finds an orthonormal basis for a Krylov subspace [5, 41, 92].

The classical Arnoldi method [5, 41] finds a set of orthonormal vectors that can be considered as a basis for a given Krylov subspace with one starting vector. The generalization of this method for more than one starting vector is known as *block Arnoldi method*. In the following, we briefly describe a version of the Arnoldi algorithm [92] for more than one starting vector $B = [b_1, \cdots, b_p]$, in which the resulting matrix of basis vectors is orthonormal.

Algorithm 6.1 Arnoldi algorithm with deflation using modified Gram-Schmidt [92]

Input: A, $B = [b_1, \cdots, b_p]$
Output: Orthonormal basis U, block Hessenberg matrix H

1: Delete all linearly dependent starting vectors to find p_1 independent starting vectors for the Krylov subspace.
2: Set

$$u_1 = \frac{b_1}{\sqrt{b_1^T b_1}},$$

where b_1 is the first starting vector after deleting the dependent starting vectors.
3: **for** $j = 2, 3, \ldots,$ **do**
4: **if** $j \leq p_1$ **then**
5: $r_j = b_j$
6: **else**
7: $r_j = A u_{j-p_1}$
8: **end if**
9: set $\hat{u}_j = r_j$
10: **for** $i = 1$ to $j - 1$ **do**
11: $h_{i,j-1} = \hat{u}_j^T u_i$
12: $\hat{u}_j = \hat{u}_j - h_{i,j-1} u_i$
13: **end for**
14: **if** $\hat{u}_j = 0$ **then**
15: set $p_1 \leftarrow p_1 - 1$
16: **if** $p_1 \neq 0$ **then**
17: go to step 3
18: **else**
19: break
20: **end if**
21: **else if** $\hat{u}_j \neq 0$ **then**
22: $h_{j,j-1} = \|\hat{u}_j\|_2$
23: $u_j = \frac{\hat{u}_j}{h_{j,j-1}}$
24: **end if**
25: increase j and go to step 3
26: **end for**

Consider the Krylov subspace $\mathcal{K}_r(A, B)$ with p starting vectors. The algorithm finds a set of vectors with length one that are orthogonal to each other, $U^T U = I$, where the columns of the matrix U are the basis for the given Krylov subspace. The specialization of Algorithm 6.1 is that it can be used for SISO systems as well as MIMO systems, too. More details about this algorithm and about the construction of orthonormal basis can be found in [92].

Remark 6.5:

In Algorithm 6.1, in each step one more vector orthogonal to all other previous vectors is constructed and then it is normalized to have length one. In a general case, when dimension r of $\mathcal{K}_r(A, B)$ is not small enough, it can happen that not all of the basic vectors are linearly independent. Then, linearly dependent vectors must be deleted during the iterations (=deflation). In Algorithm 6.1, Step 14 occurs in case of deflation. ◊

Other suitable methods for generating reduced-order models using Krylov subspaces are the *two-sided Arnoldi method* and the *Lanczos method*, where the methods find two bases for the input and output Krylov subspaces. The two-sided Arnoldi method [41, 47, 92] uses Algorithm 6.1 twice, first for the calculation of a basis U of the input Krylov subspace, then for the calculation of a basis V for the output Krylov subspace and then reduces the model using (6.8). Lanczos methods are also very popular when using two-sided methods for the reduced-order model [5, 41]. It finds two bases for input and output Krylov subspaces that are orthogonal to each other.

In the general case, specially for MIMO systems, when r is not small enough, it can happen that with repetitive multiplications by a fixed matrix, it is no longer possible in finite precision to introduce additional new information into the reduced-order model. This loss of information due to repetitive multiplications manifests itself through ill-conditioned Hankel matrices in the explicit moment matching equations. The same situation may arise in case of multipoint rational interpolations of $\mathcal{K}\left((A-\sigma_k E)^{-1}E, (A-\sigma_k E)^{-1}B\right)$ using Theorem 6.3.4 for $k = 0, 1, \ldots, \bar{k}$. For example, forming u_m by simply multiplying u_{m-1} by $(A-\sigma_k E)^{-1}E$ will quickly make the columns of U linear dependent in finite precision. In that case one may experience rank deficiency in the computed U or V. It is seen in [47] that one really has no need to form U of size n to find a minimal realization of system (6.1). In the context of the Lanczos method, a loss of rank in U or V is termed immediate breakdown [5]. There are multiple sources for rank-deficient U or V discussed in [47].

6.3.5. Stability and Passibity

Recall from the discussion in Chapter 3 that, for singular E, stability of the continuous-time descriptor system (6.1) can be characterized in terms of the finite eigenvalues of the matrix pencil $\lambda E - A$. More precisely we have the following theorem.

Theorem 6.3.5:

The continuous-time descriptor system (6.1) is stable if and only if, the following two conditions are satisfied:
(i) All finite eigenvalues λ of the pencil $\lambda E - A$ satisfy $Re(\lambda) \leq 0$.
(ii) All finite eigenvalues λ of $\lambda E - A$ with $Re(\lambda) = 0$ are simple. ◊

In view of Theorem 6.3.5, stability of system (6.1) is characterized by the finite eigenvalues of the pencil $\lambda E - A$, and the infinite eigenvalues of $\lambda E - A$ have no effect on stability. These infinite eigenvalues of $\lambda E - A$ result only in impulsive motions, which tend to zero when $t \to \infty$. In using Krylov Krylov methods to reduce the order of a stable models, there is no general guarantee to find a stable reduced-order model except under some special conditions [6, 7] .

An important property to be preserved in order reduction is *passivity* of the original system. In general speaking, a system is *passive* if it does not generate energy. For descriptor systems as in (6.1) with identical numbers of inputs and outputs (i.e., $p = q$), passivity is characterized by the positive realness of the transfer function $H(s)$.

Definition 6.3.5:

A square ($p = q$) transfer matrix $H(s) : \mathbb{C} \mapsto (\mathbb{C}^{p\times p} \cup \infty)$ is *positive real* if
(i) $H(s)$ has no poles in $\mathbb{C}^+$.
(ii) $H(s^*) = (H(s))^*$ for all $s \in \mathbb{C}$.
(iii) $Re(w^H H(s)w) \geq 0$ for all $s \in \mathbb{C}$ with $Re(s) > 0$ and $w \in \mathbb{C}^p$. ◊

The following theorem establishes that the descriptor system (6.1) can be stable and passive in some restricted cases.

Theorem 6.3.6:

[92] *In the system (6.1), if $A + A^T \preceq 0$ and $E = E^T \geq 0$, then the reduced-order system (6.5) using a one-sided method with the choice $V = U$, is stable and furthermore, the transfer matrix $\tilde{H}(s) = B^T U(sU^T EU - U^T AU)^{-1}U^T B$ is positive real.* ◊

Proof. See [40] for the proof. □

Hence we can conclude that for certain passive (stable) systems, one-sided Krylov subspace methods can be used to find passive (stable) reduced-order models.

6.4. Balanced Truncation MOR

A popular model reduction technique for linear state space system is the BT approach where the original state space system is transformed into a balanced form whose reachability and observability Gramians become diagonal and equal. The balanced truncation method truncates all those states of the balanced system that are both difficult to reach and to observe. An important property of this method is that asymptotic stability is preserved in the reduced order system and an a priori error bound can be computed. In the following subsections we will briefly review some important concepts of the balanced truncation model reduction technique which are applicable for linear discrete-time singular systems. A similar description can be found in [75, 106, 108] for linear

continuous-time descriptor systems.

6.4.1. Basics of Balanced Truncation

We consider again the linear discrete-time descriptor system of order n, with p inputs and q outputs, in generalized state space form (with nonsingular E) as described by Equation (6.3) and its transfer function described by Equation (6.4). We will assume that system (6.3) is d-stable.

Definition 6.4.1:
A transfer function $H(z)$ ad described in (6.4) *proper* if $\lim_{z\to\infty} H(z) < \infty$, and *improper*, otherwise. If $\lim_{z\to\infty} H(z) = 0$, then $H(z)$ is said to be *strictly proper*. ◊

The main idea of balanced truncation model reduction is to rewrite the system (6.4) using a system equivalence transformation T called *balancing transformation*. Such a balanced transformation is defined by the property that both the reachability and observability Gramians of system (6.4) are diagonal and equal. In this coordinate system one has

$$TG_cT^T = T^{-T}G_oT^{-1} = \Sigma = \text{diag}(\sigma_1, \sigma_2, \ldots, \sigma_n),$$

where $\sigma_1 \geq \sigma_2 \ldots \sigma_n > 0$, the σ_i are the Hankel singular values of (6.3) and G_c and G_o are the reachability and observability Gramians of (6.3), respectively. Note that these Gramians are given by the solutions of the two dual Stein equations

$$AG_cA^T - EG_cE^T = -BB^T, \quad A^TG_oA - E^TG_oE = -C^TC.$$

A natural question now arises: why are balanced state space representations so interesting? We will answer this question from [129] by assuming system (6.3) in its standard state space representation (i.e., assume $E = I$) in order to make the understanding more easier. Then the reachability and observability Gramians associated with the system $\mathbf{\Sigma}(A, B, C)$ can be represented as

$$G_c := \sum_{k=0}^{\infty} A^kBB^T(A^T)^k, \quad G_o := \sum_{k=0}^{\infty}(A^T)^kC^TC(A)^k,$$

respectively. Let us have a look at the interpretation of the reachability and observability Gramians. The system $\mathbf{\Sigma}(A, B, C)$ with input $u = 0$ and initial state $x(0) = x_0$ produces as its output the trajectory $y_k = CA^kx_0$ for $k \geq 0$. The $\mathbb{l}_2$ norm of this output is given by

$$\|y\|_2^2 := \sum_{k=0}^{\infty} x_0^T(A^T)^kC^TCA^kx_0 = x_0^TG_ox_0 \tag{6.22}$$

and it represents the *observation energy* of the state x_0. Hence, the observability Gramian measures the effect of initial states on the output of the system when the input $u = 0$. If

G_o is nearly singular, then there exist states which have low observation energy in the sense that $\|y\|_2$ will be small.

We can give an interpretation of the reachability Gramian by considering the *minimal energy control problem* given by

$$\mathbb{J}(u) := \sum_{k=-\infty}^{-1} u_k^T u_k, \tag{6.23}$$

where one needs to compute the minimum cost $\mathbb{J}$ subject to the constraint that the control u can steer the state x to x_0 at sampling time $k = 0$. Therefore, such a minimal energy control problem and the minimal cost relate only with state equation

$$x_{k+1} = Ax_k + Bu_k$$

at sampling times $k < 0$. The minimum norm solution to this problem is given by

$$u_k^{\text{opt}} = B^T (A^T)^{-1-k} G_c^{-1} x_0, \quad k < 0,$$

and the resulting cost

$$\mathbb{J}(u^{\text{opt}}) = x_0^T G_c^{-1} x_0. \tag{6.24}$$

Hence, we can see that the inverse reachability Gramian reflects the minimal cost to reach a state x_0 by applying suitable (past) input signals. If G_c is nearly singular then there exist states x_0 that are difficult to reach as the minimal control energy needed to reach these states may become large.

We now investigate both the issues for a balanced system. Now suppose that the system is balanced. In that case we have

$$G_c = G_o = \Sigma = \text{diag}(\sigma_1, \sigma_2, \ldots, \sigma_n)$$

with $\sigma_1 \geq \sigma_2 \ldots \geq \sigma_n > 0$. Then the minimal energy cost to reach the i-th state component

$$x_0 = e_i = [0 \ldots 1\ 0 \ldots 0]$$

(with the 1 at the i-th position) is given by the number

$$e_i^T G_c^{-1} e_i = e_i^T \Sigma^{-1} e_i = \sigma_i^{-1}. \tag{6.25}$$

The corresponding output energy for this i-th state is given by

$$\|y\|_2^2 = e_i^T G_o e_i = e_i^T \Sigma e_i = \sigma_i. \tag{6.26}$$

Since the Hankel singular values for a balanced system appear in descending order, we notice that state components with low indices (like e_1, e_2, etc.) are *easy to observe* (in the sense that the output energy is large) and at the same time *easy to reach* (in the sense

that the minimal energy to reach these states is small). Similarly, state components with high indices (like e_n, e_{n-1}, etc.) are *difficult to observe* (in the sense that the observation energy is small) and at the same time *difficult to reach* (in the sense that the minimal cost to reach these states is large).

Therefore, in a balanced state space representation the following relations are followed

$$\begin{aligned} &e_1^T G_c^{-1} e_1 \leq e_2^T G_c^{-1} e_2 \leq \ldots \leq e_n^T G_c^{-1} e_n, \\ &e_1^T G_o e_1 \geq e_2^T G_o e_2 \geq \ldots \geq e_n^T G_o e_n. \end{aligned} \tag{6.27}$$

In general speaking, in a balanced state space representation, the states that are easy to reach are also easy to observe, and states that are difficult to reach are also difficult to observe. In this sense reachability and observability properties are balanced in a balanced state space representation.

We would like to discuss one more interesting fact from [28] regarding the balanced realization and its balanced state truncation. Let us consider system (6.3) as in generalized descriptor form and assume that it is balanced, i.e., G_c and G_o are equal and diagonalized. Consider now the energy functions described by the Gramians G_c and G_o associated with system (6.3). As we know from previous considerations, the reachability and observability Gramians measure to what degree each state is excited by an input, and each state excites future outputs, respectively. For a given stable system (6.3), the energy functions for any state x can be described as [28]

$$\Delta_c(x) = (x^T G_c^{-1} x)^{\frac{1}{2}}, \quad \Delta_o(x) = (x^T G_o x)^{\frac{1}{2}}, \tag{6.28}$$

where $\Delta_c(x)$ is the smallest amount of energy needed to steer the system from 0 to x, and $\Delta_o(x)$ is the largest amount of energy obtained by observing the output of the free system with the initial condition x. If we define the energy storage efficiency at state x_0 (x_0 is the state at time $t = 0$) by

$$\Delta(x_0) = \frac{x_0^T G_o x_0}{x_0^T G_c^{-1} x_0}, \tag{6.29}$$

then the maximization of $\Delta(x_0)$ with respect to x_0 results the generalized eigenproblem

$$G_o x_0 = G_c^{-1} \Delta(x_0) x_0,$$

or, more simply,

$$G_c G_o x_0 = \Delta(x_0) x_0.$$

Hence, $\Delta(x_0)$ takes an extremum value for x_0 at an eigenvector of $G_c G_o$ (or, equivalently a generalized eigenvector of the pair (G_o, G_c^{-1})). Therefore, the extremum value of $\Delta(x_0)$ corresponds to the maximal eigenvalue of the product $G_c G_o$, and hence the square root of the largest Hankel singular value σ_1 of the considered system.

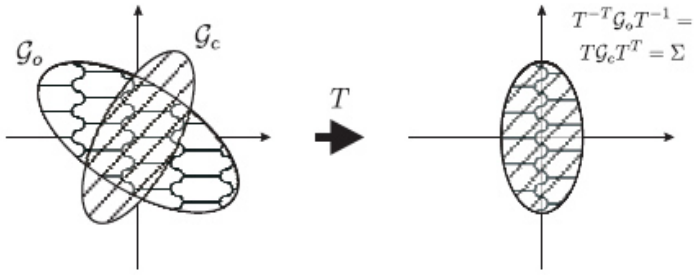

Figure 6.4. The effect of a balancing transformation T on the reachability and observability ellipsoids. image source:[28]

It is shown in [76] that for non-minimal systems the reachable subspace and the unobservable subspace are the image and the kernel of G_c and G_o, respectively. The balancing transformation T transforms the observability and reachability ellipsoids to an identical ellipsoid aligned with principal axes along the coordinate axes as shown in Figure 6.4.

After balancing the system, a reduced-order model is obtained by truncating the least reachable and observable states, corresponding to the smallest Hankel singular values and having little effect on the input/output behavior. Hence, for a reduced-order model the original state $x = (x_1, \ldots, x_n)^T$ is reduced to $\tilde{x} = (x_1, \ldots, x_r)^T$, where $r \ll n$.

We summarize the procedure of balanced truncation in Algorithm 6.2.

Remark 6.6:
Note that $\tilde{E} = I_r$ and needs not be computed. The balancing transformation matrices for the generalized discrete-time systems (6.3) are not unique [106, 111]. ◊

6.4.2. Balanced Truncation for Singular Systems

Balanced truncation model reduction for singular systems (i.e., E is singular in (6.3) are more involved than the order reduction approach explained in Algorithm 6.2. In that case we use the spectral decomposition technique which reduces the original system into two subsystems: the *forward subsystem* and the *backward subsystem*. Very basics of this spectral decomposition technique can be found in Chapter 3 of this thesis and also in [9, 107]. Computing the reduced-order system for the stable system (6.3) can be interpreted as performing a system equivalence transformation $(\hat{W}, \hat{T})$ such that

$$\left[\begin{array}{c|c} \hat{W}(zE - A)\hat{T} & \hat{W}B \\ \hline C\hat{T} & \end{array}\right] = \left[\begin{array}{cc|c} zE_f - A_f & 0 & B_f \\ 0 & zE_\infty - A_\infty & B_\infty \\ \hline C_f & C_\infty & \end{array}\right], \tag{6.30}$$

Algorithm 6.2 Balanced truncation for discrete-time system

Input: $\mathbf{\Sigma}(E, A, B, C)$ realization of the original system of order n such that $zE - A$ is stable and a reduced-order r.

Output: $\mathbf{\Sigma}(\tilde{E}, \tilde{A}, \tilde{B}, \tilde{C})$ reduced-order system realization.

1: Solve the Stein equations

$$AG_cA^T - EG_cE^T = -BB^T, \quad A^TG_oA - E^TG_oE = -C^TC.$$

for R and L, where $G_c = RR^T$ and $G_o = LL^T$ are full rank factorizations.

2: Compute the SVD

$$L^TER = U\Sigma V^T = [U_1, U_2]\begin{bmatrix}\Sigma_1 & 0\\ 0 & \Sigma_2\end{bmatrix}[V_1, V_2]^T,$$

where the matrices $[U_1, U_2]$ and $[V_1, V_2]$ have orthonormal columns,

$$\Sigma_1 = \operatorname{diag}(\sigma_1, \ldots, \sigma_r), \quad \Sigma_2 = \operatorname{diag}(\sigma_{r+1}, \ldots, \sigma_n).$$

3: Compute the projection matrices

$$W_L = LU_1\Sigma_1^{-\frac{1}{2}}, \quad T_R = RV_1\Sigma_1^{-\frac{1}{2}}.$$

4: Compute the reduced-order model

$$(\tilde{E}, \tilde{A}, \tilde{B}, \tilde{C}) = (W_L^TET_R,\ W_L^TAT_R,\ W_L^TB,\ CT_R).$$

where the pencil $zE_f - A_f$ contains only those eigenvalues of $zE - A$ which lie inside the unit circle, all eigenvalues of $zE_\infty - A_\infty$ are infinite, and the matrices $\hat{W}B$ and $C\hat{T}$ are partitioned in blocks conformally to the matrix pencil $zE - A$. Then we reduce the order of the *forward subsystem* $\mathbf{\Sigma}(E_f, A_f, B_f, C_f)$ and the *backward subsystem* $\mathbf{\Sigma}(E_\infty, A_\infty, B_\infty, C_\infty)$ separately. The Gramians that correspond to the forward subsystems are called *causal Gramians* and those that corresponds to the backward subsystem are called *noncausal Gramians*.

The decoupling of the system matrices described above is equivalent to the additive decomposition of the transfer function as $H(z) = H_{sp}(z) + P(z)$, where

$$H_{sp}(z) = C_f(zE_f - A_f)^{-1}B_f, \quad \text{and} \quad P(z) = C_\infty(zE_\infty - A_\infty)^{-1}B_\infty$$

are the strictly proper part and the polynomial part of $H(z)$, respectively. The Hankel singular values corresponding to the strictly proper part $H_{sp}(z)$ are called *causal Hankel singular values* and Hankel singular values that correspond to the improper part $P(z)$ are called *noncausal Hankel singular values* of system (6.3).

Then the transfer function of the reduced-order system (6.6) has the form $\tilde{H}(z) = \tilde{H}_{sp}(z) + \tilde{P}(z)$, where

$$\tilde{H}_{sp}(z) = \tilde{C}_f(z\tilde{E}_f - \tilde{A}_f)^{-1}\tilde{B}_f \quad \text{and} \quad \tilde{P}(z) = \tilde{C}_\infty(z\tilde{E}_\infty - \tilde{A}_\infty)^{-1}\tilde{B}_\infty.$$

A short overview of the order reduction procedure for singular systems can be represented as follows: we first balance both the forward and backward subsystems using similar type algorithm as Algorithm 6.2 and then truncate the balanced proper part to get the reduced-order forward subsystem. Unfortunately, we can not do the same for the backward subsystem. The equations associated with the noncausal Hankel singular values describe constraints of the system, i.e., they define a manifold in which the solution dynamics takes place. If we truncate the states that correspond to the small non-zero noncausal Hankel singular values, then the pencil for the reduced-order system may get finite eigenvalues outside the unit circle which will lead to additional errors in the system approximation. Hence, $\tilde{P}(z)$ is not the reduced part of $P(z)$ but balanced.

Last of all we combine the reduced forward subsystem with the unreduced but balanced backward subsystem. The order of the reduced system is the sum of the order of the forward reduced system and of the order of the balanced backward subsystem. Some suitable numerical algorithms for balanced truncation of singular systems using the above concept can be found in [15, 75, 109, 108] for the continuous-time case.

It is shown in [103, 107] that the causal and noncausal Gramians of the discrete-time descriptor system (6.3) satisfy some projected generalized discrete-time Lyapunov equations with special right-hand side.

Theorem 6.4.1:

[103] *Consider the discrete-time descriptor system (6.3), where the pencil $\lambda E - A$ is d-stable. (1) The causal and noncausal reachability Gramians G_{cr} and G_{ncr} are the unique symmetric, positive semidefinite solutions of the projected generalized discrete-time Lyapunov equations*

$$\begin{aligned} AG_{cr}A^T - EG_{cr}E^T &= -P_l B B^T P_l^T, \\ G_{cr} &= P_r G_{cr} P_r^T, \end{aligned} \tag{6.31}$$

and

$$\begin{aligned} AG_{ncr}A^T - EG_{ncr}E^T &= (I - P_l)BB^T(I - P_l)^T, \\ G_{ncr} &= (I - P_r)G_{ncr}(I - P_r)^T, \end{aligned} \tag{6.32}$$

respectively.
(2) The causal and noncausal observability Gramians G_{co} and G_{nco} are the unique symmetric, positive semidefinite solutions of the projected generalized discrete-time Lyapunov equations

$$\begin{aligned} A^T G_{co}A - E^T G_{co}E &= -P_r^T C^T C P_r, \\ G_{co} &= P_l^T G_{co} P_l, \end{aligned} \tag{6.33}$$

and

$$\begin{aligned} A^T G_{nco} A - E^T G_{nco} E &= (I - P_r)^T C^T C (I - P_r), \\ G_{nco} &= (I - P_l)^T G_{nco} (I - P_l), \end{aligned} \tag{6.34}$$

respectively. ◊

Proof. See [103, 105]. □

Remark 6.7:
Note that $G_c = G_{cr} + G_{ncr}$ and $G_o = G_{co} + G_{nco}$ for the complete reachability and observability Gramians. ◊

Solving these projected Lyapunov equations mentioned in Theorem 6.4.1 is also a challenging and tricky job. Two well known methods, the Bartels-Stewart method and Hammarling's method for solving these PGDLEs have been discussed in [103]. The causal and noncausal Gramians are now used to define Hankel singular values for the descriptor system (6.3) that are of great importance in model reduction via balanced truncation.

It has been shown in [107] that all the eigenvalues of the matrices $G_{cr}E^T G_{co}E$ and $G_{ncr}A^T G_{nco}A$ are real and non-negative. The square roots of the largest n_f eigenvalues of the matrix $G_{cr}E^T G_{co}E$, denoted by σ_j, are called *causal Hankel singular values* of the discrete-time descriptor system (6.3). The square roots of the largest n_∞ eigenvalues of the matrix $G_{ncr}A^T G_{nco}A$, denoted by θ_j, are called *noncausal Hankel singular values* of the discrete-time descriptor system (6.3).

For symmetric and positive semidefinite Gramians we also have the full rank *Cholesky factorizations*

$$\begin{aligned} G_{cr} &= R_c R_c^T, \quad G_{co} = L_c L_c^T, \\ G_{ncr} &= R_i R_i^T, \quad G_{nco} = L_i L_i^T, \end{aligned} \tag{6.35}$$

where the lower triangular matrices R_c, L_c, R_i, L_i are the Cholesky factors of the Gramians. In this case the causal Hankel singular values can be computed as the n_f largest singular values of the matrix $L_c^T E R_c$, and the noncausal Hankel singular values can be computed as the n_∞ largest singular values of the matrix $L_i^T A R_i$, see [107]. In that case, we define a balanced realization of the discrete-time descriptor system (6.3).

Definition 6.4.2:
A realization $\mathbf{\Sigma}(E, A, B, C)$ of the discrete-time descriptor system (6.3) is called *balanced* if

$$G_{cr} = G_{co} = \begin{bmatrix} \Sigma & 0 \\ 0 & 0 \end{bmatrix}, \quad G_{ncr} = G_{nco} = \begin{bmatrix} 0 & 0 \\ 0 & \Theta \end{bmatrix}$$

where $\Sigma = \mathrm{diag}(\sigma_1, \ldots, \sigma_{n_f})$ and $\Theta = \mathrm{diag}(\theta_1, \ldots, \theta_{n_\infty})$. ◊

For a minimal realization $\mathbf{\Sigma}(E, A, B, C)$ with d-stable pencil $zE - A$, we can find nonsingular W_L and TR such that the transformed realization $\mathbf{\Sigma}(W_L^T E T_R,\ W_L^T A T_R,\ W_L^T B,\ C T_R)$ is balanced. Note that we do not need to transform the descriptor system into a balanced form explicitly in order to perform order reduction. It is sufficient to determine the subspaces associated with the dominant causal and non-zero noncausal Hankel singular values and project the descriptor system onto these subspaces. We summarize the whole order reduction process in Algorithm 6.3.

Remark 6.8:

(i) The order of the reduced-order model computed using Algorithm 6.3 is $r = r_f + l_\infty$.

(ii) Since we do not truncate any non-zero noncausal Hankel singular value, the equality $P(z) = \tilde{P}(z)$ holds. The reduced-order system computed using Algorithm 6.3 is minimal and the pencil $z\tilde{E} - \tilde{A}$ is d-stable. ◊

6.4.3. Stability and Approximation Error

One advantageous characteristic of balanced truncation order reduction techniques as compared to the moment matching techniques is that it preserves the stability of the original model and an a-priori error bound for the reduced-order system can be easily chosen. One can easily show that the reduced-order system computed by this method is asymptotically stable, minimal and balanced [75, 108]. Moreover, several error norms for the reduced system can be defined [107, 118, 28].

The $\mathbb{H}_\infty$-norm of the transfer function $H(z) \in \mathbb{H}_\infty$ is defined by [107]

$$\|H\|_{\mathbb{H}_\infty} = \sup_{\omega \in [0,2\pi]} \sigma_{max}(H(e^{i\omega})) = \sup_{\omega \in [0,2\pi]} \|H(e^{i\omega})\|_2.$$

Then, the a-priori error bound can be given for the error between the original and the reduced-order system:

$$\|H - \tilde{H}\|_{\mathbb{H}_\infty} = \sup_{\omega \in [0,2\pi]} \|H(e^{i\omega}) - \tilde{H}(e^{i\omega})\|_2 \leq 2\,\mathrm{trace}(\Sigma_2), \tag{6.36}$$

where $\|.\|_2$ denotes the spectral norm of matrices and Σ_2 contains the truncated causal Hankel singular values. We can also define a computable upper bound of the error system by computing the $\mathbb{H}_2$ norm. For the $\mathbb{H}_2$ norm we use the following formula:

$$\|H\|_{\mathbb{H}_2}^2 = \mathrm{trace}(B^T G_o B) = \mathrm{trace}(C G_c C^T),$$

where G_c and G_o are respectively the reachability and observability Gramians of the system. To compute the $\mathbb{H}_2$ norm of the error system, one needs to solve again another Lyapunov equation for one Gramian of this error system which leads computational cost of order $(n + r)^3$. One suitable and efficient method which only needs the Gramian of the original method has been proposed in [1]. Several representations for the $\mathbb{H}_2$ norm of the error system using this proposed method are derived in [28].

Algorithm 6.3 Balanced truncation for discrete-time descriptor (singular) systems

Input: $\mathbf{\Sigma}(E, A, B, C)$ realization of the original system of order n such that $zE - A$ is d-stable and a reduced-order r.
Output: $\mathbf{\Sigma}(\tilde{E}, \tilde{A}, \tilde{B}, \tilde{C})$ reduced-order system realization.

1: Solve (6.31) and (6.32) for G_{cr} and G_{ncr}, respectively.
2: Solve (6.33) and (6.34) for G_{co} and G_{nco}, respectively.
3: Compute the Cholesky factors R_c and R_i for the reachability Gramians

$$G_{cr} = R_c R_c^T, \quad G_{ncr} = R_i R_i^T.$$

4: Compute the Cholesky factors L_c and L_i for the observability Gramians

$$G_{co} = L_c L_c^T, \quad G_{nco} = L_i L_i^T.$$

5: Compute the skinny SVD

$$L_c^T E R_c = U \Sigma V^T = [U_1, U_2] \begin{bmatrix} \Sigma_1 & 0 \\ 0 & \Sigma_2 \end{bmatrix} [V_1, V_2]^T,$$

where the matrices $[U_1, U_2]$ and $[V_1, V_2]$ have orthonormal columns,

$$\Sigma_1 = \operatorname{diag}(\sigma_1, \ldots, \sigma_{r_f}), \quad \Sigma_2 = \operatorname{diag}(\sigma_{r+1}, \ldots, \sigma_{n_f})$$

with $n_f = \operatorname{rank}(L_c^T E R_c)$.
6: Compute the skinny SVD

$$L_i^T A R_i = U_3 \Theta V_3^T$$

where U_3 and V_3 have orthonormal columns, $\Theta = \operatorname{diag}(\theta_1, \ldots, \theta_{l_\infty})$ with $l_\infty = \operatorname{rank}(L_i^T A R_i)$.
7: Compute the projection matrices

$$W_L = [L_c U_1 \Sigma_1^{-\frac{1}{2}}, \quad L_i U_3 \Theta^{-\frac{1}{2}}] \qquad T_R = [R_c V_1 \Sigma_1^{-\frac{1}{2}}, \quad R_i V_3 \Theta^{-\frac{1}{2}}].$$

8: Compute the reduced-order model

$$(\tilde{E}, \tilde{A}, \tilde{B}, \tilde{C}) = (W_L^T E T_R,\ W_L^T A T_R,\ W_L^T B,\ C T_R).$$

6.5. Discussion

Krylov subspace-based order reduction techniques are suitable for model reduction for large scale linear dynamical systems, especially those that arise in the simulation of electric circuits and of micro-electro-mechanical systems. Although Krylov subspace

methods seem to be superior to balanced truncation in numerical efficiency with cheaper computational costs, but the stability of the original system may be lost and there is no general error bound similar to balanced truncation except under some special conditions [6, 7].

On the other hand, the most prominent characteristics of balanced truncation approach are: first, for a reasonable small or medium order system (say a few hundred), it gives a satisfactory approximation; second, this approximation can be obtained at relatively reasonable computational cost; and thirdly, an a-priori upper bound for the error between the original and reduced-order systems exists for the $\mathbb{H}_\infty$-norm. Stability of the original system is preserved in the reduced system almost in all cases.

But the drawbacks of the BT approach are that it requires (in most cases) to solve the matrix equation (well known as Lyapunov equations or Stein equations) which seems to have computational complexity of huge order when the order of the system is very high, i.e., $n > \mathcal{O}(10^4)$. Also for singular systems, reduction to stable and unstable modes of the original system takes numerous efforts. But there are several iterative techniques available (See Chapter 9 of this thesis, and also in [67, 13, 70, 82, 49, 110, 10] for more details) which approximate the solutions of those matrix equations with a prescribed tolerance.

CHAPTER

SEVEN

MODEL REDUCTION VIA KRYLOV SUBSPACES

Contents

Krylov subspace projection method is one of the best choices for model reduction of time-varying systems in the field of signal analysis and electrical interconnections. *Balanced truncation* methods [76, 93] can also be applied, but there is some doubt about the effective implementation of these techniques. Therefore, a lot of work has been devoted to developing the techniques of model reduction using rational approximations and the projection formulations [88, 47, 41].

In this chapter we focus on the problems that result from the linearization of nonlinear circuit problems and the resulting models are periodically linear time-varying. Our implementations and application examples also focus on these systems. In Section 7.1, we discuss the LTV signal analysis for a small response and discuss the *frequency-domain matrix* formulation of the system which gives the concept for the model reduction procedure. In Section 7.2, we choose a projection framework using a finite discretization method, known as *time-domain matrix* formulation of the LPTV systems. This section

also discusses an approximation scheme using Krylov subspaces to approximate the appropriate subspaces and discuss how to compute them more efficiently. We also show that the model based on approximate multipoint Krylov subspace methods can be efficiently achieved from the approximated subspace. Then in Section 7.3, we discuss our proposed model order reduction procedure in detail. In the last section we give numerical examples of the proposed model reduction technique. We generalize the method from [84] to differential-algebraic equations.

7.1. Background

Let us recall the linear time-invariant MIMO system in differential-algebraic form

$$\begin{aligned} E(t)\dot{x}(t) &= A(t)x(t) + B(t)u(t), \\ y(t) &= C(t)x(t), \end{aligned} \tag{7.1}$$

where $x(t) \in \mathbb{R}^n$ contains the descriptor variables, $u(t) \in \mathbb{R}^p$ ($p \leq n$), is the system input, $y(t) \in \mathbb{R}^q$ is the system output, n is the system order, and p and q are the numbers of system inputs and outputs, respectively. $E(t)$, $A(t)$, $B(t)$, $C(t)$ are matrices of order compatible with $x(t)$, $u(t)$, and $y(t)$ and assumed to be continuous functions of time. All the above matrices are periodic with a period $T > 0$ and the matrices $E(t)$ are allowed to be singular. For SISO systems, p, q=1, the matrices B and C change to vectors b and c^T, respectively.

Simply speaking, we can consider obtaining a reduced-order system in similar form by applying a projection operation with matrices V and U just as in LTI case

$$\begin{aligned} \tilde{E}(t)\dot{\tilde{x}}(t) &= \tilde{A}(t)\tilde{x}(t) + \tilde{B}(t)u(t), \\ y(t) &= \tilde{C}(t)\tilde{x}(t), \end{aligned} \tag{7.2}$$

where

$$\begin{aligned} \tilde{E}(t) &= V^T(t)E(t)U(t),\ \tilde{A}(t) = V^T(t)A(t)U(t), \\ \tilde{B}(t) &= V^T(t)B(t),\ \tilde{C}(t) = C(t)\,U(t). \end{aligned} \tag{7.3}$$

Similar to the LTI case, the dimension r of the reduced-order system is smaller than the original system (7.1). Hence, the reduced-order system requires lower computation cost and suitable for higher level simulation.

In integrated circuit applications, the most common basis for generating reduced-order LPTV macromodels is mainly based on the concept of time-varying system (TVS) function [133, 78], denoted by $h(s, t)$. In circuit applications, $h(s, t)$ is time-varying and periodical in t, and hence classical steady-state approaches can be involved to compute the compact transient representation of the system. Two well known approaches based on frequency- and time-domain formulations are mainly used for such transformations; the frequency-domain approach uses the idea of the harmonic balance (HB) [58, 42, 87], and

the time-domain formulation uses a collocation-based finite-differences (FD) method [84, 87, 78]. A reduced-order LPTV macromodels is then carried out by a reduced-order approximation of $h(s,t)$ via appropriate Krylov-subspace approximation techniques.

We have already shown in Chapter 2 that in the field of integrated circuits, the model LPTV systems in the time-domain are typically carried out using the MNA approach which casts the linearized LTV systems into the familiar forms

$$\bar{G}(t)v + \frac{d}{dt}(\bar{C}(t)v) = Bu(t), \tag{7.4}$$

for a small signal v, where $u(t)$ represents the input signal, $\bar{G}(t)$ and $\bar{C}(t)$ are the time-varying conductance and capacitance matrices, respectively. The output, y(t), of the LPTV system can be an arbitrary node voltage and can be written as

$$y(t) = C(t)v(t), \tag{7.5}$$

where $C(t)$ contains the vectors that link the set of variables to the output nodes. To relate to the standard notation as in (7.1), we may make the identification $E(t) = \bar{C}(t)$, $A(t) = -(\bar{G}(t) + \dot{\bar{C}}(t))$.

Most of the work in model reduction for LPTV macromodels using LTI framework has been done on the basis of rational approximations of the time-varying transfer functions, which were introduced by L. Zadeh [133] to describe the response of LTV systems. According to Zadeh's formalism, the transfer path from the input $u(t)$ to the output $y(t)$ can be described by the TVS function $h(s,t)$ [133, 84], where the response of the system due to an input of the form

$$u(t) = e^{st}, \tag{7.6}$$

is given by

$$v(t) = e^{st}\, h(s,t). \tag{7.7}$$

Substituting (7.6) and (7.7) into (7.4), we get an equation for $h(s,t)$ as

$$\bar{G}(t)h(s,t) + \frac{d}{dt}(\bar{C}(t)h(s,t)) + s\bar{C}(t)h(s,t) = B(t). \tag{7.8}$$

Hence, the transfer path of the system from the input $u(t)$ to the output $y(t)$ can be represented by the time-varying transfer function $\Phi(s,t)$ where,

$$\Phi(s,t) = C(t)h(s,t). \tag{7.9}$$

It is clear from (7.9) that a full characterization of the system transfer functions can be obtained by solving (7.4) with substitution of s by $j2\pi f$, and solving the corresponding LPTV system. This process is repeated for all possible frequency values f of interest.

In the frequency-domain representation, all the time varying coefficient matrices in (7.8) are represented in Fourier series as

$$\begin{aligned} \bar{C}(t) &= \textstyle\sum_{i=-\infty}^{\infty} \bar{C}_i\, e^{ji\omega_0 t}, \\ \bar{G}(t) &= \textstyle\sum_{i=-\infty}^{\infty} \bar{G}_i\, e^{ji\omega_0 t}, \\ h(s,t) &= \textstyle\sum_{i=-\infty}^{\infty} H_i(s)\, e^{ji\omega_0 t}. \end{aligned} \tag{7.10}$$

Substituting (7.10) into (7.8) we get the following system of equations

$$[sC_{FD} + (G_{FD} + \Omega C_{FD})]H_{FD}(s) = B_{FD}, \tag{7.11}$$

where

$$\begin{aligned} C_{FD} &= \begin{bmatrix} \vdots & \vdots & \vdots & \vdots & \\ \cdots & \bar{C}_0 & \bar{C}_{-1} & \bar{C}_{-2} & \cdots \\ \cdots & \bar{C}_1 & \bar{C}_0 & \bar{C}_{-1} & \cdots \\ \cdots & \bar{C}_2 & \bar{C}_1 & \bar{C}_0 & \cdots \\ & \vdots & \vdots & \vdots & \end{bmatrix}, \quad G_{FD} = \begin{bmatrix} \vdots & \vdots & \vdots & \vdots & \\ \cdots & \bar{G}_0 & \bar{G}_{-1} & \bar{G}_{-2} & \cdots \\ \cdots & \bar{G}_1 & \bar{G}_0 & \bar{G}_{-1} & \cdots \\ \cdots & \bar{G}_2 & \bar{G}_1 & \bar{G}_0 & \cdots \\ & \vdots & \vdots & \vdots & \end{bmatrix}, \\ \Omega &= j\omega_0\, \mathrm{diag}[\cdots, -2I, -I, 0, I, 2I, \cdots], \quad H_{FD}(s) = [\cdots, H_{-1}(s), H_0(s), H_1(s), \cdots]^T, \\ B_{FD} &= [\cdots, 0, B^T, 0, \cdots]^T. \end{aligned} \tag{7.12}$$

Now defining

$$\mathbf{K}_{FD} = G_{FD} + \Omega C_{FD}, \tag{7.13}$$

Equation (7.11) can be written as

$$[sC_{FD} + \mathbf{K}_{FD}]H_{FD}(s) = B_{FD}, \tag{7.14}$$

where $\mathbf{K}_{FD}$ and C_{FD} both work as continuous operators. Representation (7.11), or equivalently (7.14) is known as the *frequency-domain matrix form* of the LTV transfer functions. However, it is also possible to get the above expression from the finite-difference formulations [85, 87] in the limit as the time step goes to zero.

Remark 7.1:

The time-varying transfer function $\Phi(s,t)$ can be represented in the Fourier expansion [87] as

$$\Phi(s,t) = \sum_{i=-\infty}^{\infty} H_i(s)\, e^{ji\omega_0 t}. \tag{7.15}$$

Equation (7.15) implies that any LPTV system can be decomposed into LTI systems followed by simple multiplications with $e^{ji\omega_0 t}$. The quantities $H_i(s)$ are called *baseband-referred transfer functions*. ◊

7.2. Model Reduction for LTV Systems

Model reduction of LPTV systems has been proposed in [84, 87, 77] by analyzing the transfer characteristics of such systems efficiently. The key task of generating small LTV macromodels is essentially that of constructing reduced-order approximation for $\Phi(s,t)$.

We assume that the time-varying transfer functions $\Phi(s,t)$ considered here are rational functions. Therefore, from (7.9) we can notice that $h(s,t)$ are also rational. Hence, the reduced-order model will be obtained from the same sorts of rational approximations that have been suitable for reduction of LTI systems. Therefore, we first find an equivalent LTI representation of the time-varying transfer functions in terms of finite-dimensional matrices.

7.2.1. Discretization of Transfer Function

The rational matrix function can be obtained by discretizing the operators $\mathbf{K}_{FD}$ and C_{FD}. Since, we focus our work to LPTV systems, we need to specify $C(t)$ and $B(t)$ over a fundamental period, T. We construct a time-domain version of the equation in (7.14) by collocating $h(s,t)$ over time samples $t \in [0,T]$ at M sample time points $t_1,\ldots,t_M$, with periodicity $t_M = T$.

Using linear multistep formula (e.g., backward Euler [114, 113]) and considering the periodicity of $h(s,t)$, i.e., $h(s,t) = h(s,t_M)$, we get the representation of (7.8) in terms of finite-dimensional matrices

$$(s\,E_{TD} - A_{TD})H(s) = B_{TD}, \tag{7.16}$$

with

$$A_{TD} = -(G_{TD} + \Delta E_{TD}), \tag{7.17}$$

$$G_{TD} = \begin{bmatrix} \bar{G}_1 & & & \\ & \bar{G}_2 & & \\ & & \ddots & \\ & & & \bar{G}_M \end{bmatrix}, \quad E_{TD} = \begin{bmatrix} \bar{C}_1 & & & \\ & \bar{C}_2 & & \\ & & \ddots & \\ & & & \bar{C}_M \end{bmatrix}, \tag{7.18}$$

$$\Delta = \begin{bmatrix} \frac{1}{\Delta_1}I & & & -\frac{1}{\Delta_1}I \\ -\frac{1}{\Delta_2}I & \frac{1}{\Delta_2}I & & \\ & \ddots & \ddots & \\ & & -\frac{1}{\Delta_M}I & \frac{1}{\Delta_M}I \end{bmatrix}, \tag{7.19}$$

$$H(s) = \left[h_1^T(s),\ h_2^T(s),\ \ldots\ , h_M^T(s)\right]^T, \tag{7.20}$$

$$B_{TD} = [B_1^T,\ B_2^T,\ \ldots\ , B_M^T]^T, \tag{7.21}$$

where $\bar{G}_j = \bar{G}(t_j)$, $\bar{C}_j = \bar{C}(t_j)$, $B_j = B(t_j)$, $h_j(s) = h(s, t_j)$, and $\triangle_j$ is the jth time step.

Setting additionally

$$C_{TD} = [C_1\, C_2 \ldots C_M]^T, \tag{7.22}$$

where $C_j = C(t_j)$, the matrix of baseband-referred transfer functions $H_{TD}(s)$ is given by

$$H_{TD}(s) = C_{TD}H(s) = C_{TD}(s\,E_{TD} - A_{TD})^{-1}B_{TD}. \tag{7.23}$$

Equation (7.23) is called *time-domain matrix form* of of the LTV transfer functions. The discretization procedure has converted the n dimensional time-varying system of (7.14) to an equivalent LTI system of dimension $N = nM$, which is larger by a factor equal to the number of time steps M in the discretization. Equation (7.23) can be used directly for reduced-order modelling. At that point algorithmic approaches that can be used for the model reduction of LTI systems, can be applied to matrices defined in (7.17)-(7.23).

7.2.2. Approximation by Krylov Subspace Methods

Following the work in [114], the transfer function for a small-signal steady-state response of the periodic time-varying system is obtained by solving the finite-difference equations

$$\begin{bmatrix} \frac{\bar{C}_1}{\triangle_1} + \bar{G}_1 & & & -\frac{\bar{C}_M}{\triangle_1} \cdot \alpha(s) \\ -\frac{\bar{C}_1}{\triangle_2} & \frac{\bar{C}_2}{\triangle_2} + \bar{G}_2 & & \\ \ddots & \ddots & & \\ & -\frac{\bar{C}_{M-1}}{\triangle_M} & \frac{\bar{C}_M}{\triangle_M} + \bar{G}_M & \end{bmatrix} \begin{bmatrix} \tilde{v}(t_1) \\ \tilde{v}(t_2) \\ \vdots \\ \tilde{v}(t_M) \end{bmatrix} = \begin{bmatrix} \tilde{B}(s, t_1) \\ \tilde{B}(s, t_2) \\ \vdots \\ \tilde{B}(s, t_M) \end{bmatrix}, \tag{7.24}$$

where $\alpha(s) \equiv e^{-sT}$, T is the fundamental period, and $\tilde{B}(s, t_k) = e^{st_k}B$. The transfer function $h(s, t)$ is then given by $h(s, t) = e^{-st}\tilde{v}(t)$.

Although (7.24) can be solved using sparse matrix techniques, but we look for a more efficient approach which exploits the fact that the matrix is mostly block lower triangular and is typically solved for the shift of frequencies. To describe this approach, we first find a suitable representation of (7.24) in the time-domain matrix form.

For this purpose, we decompose the coefficient matrix of (7.17) into two triangular parts, $A_{TD} = \mathrm{L} + \mathrm{U}$, where L be the nonsingular lower triangular portion and U is the upper triangular portion of A_{TD} in (7.17), i.e.,

$$\mathrm{L} = \begin{bmatrix} \frac{\bar{C}_1}{\triangle_1} + \bar{G}_1 & & & \\ -\frac{\bar{C}_1}{\triangle_2} & \frac{\bar{C}_2}{\triangle_2} + \bar{G}_2 & & \\ \ddots & \ddots & & \\ & -\frac{\bar{C}_{M-1}}{\triangle_M} & \frac{\bar{C}_M}{\triangle_M} + \bar{G}_M & \end{bmatrix}, \tag{7.25}$$

and

$$\mathrm{U} = \begin{bmatrix} 0 & \dots & 0 & -\frac{\bar{C}_M}{\triangle_1} \\ 0 & \ddots & 0 & 0 \\ \vdots & & \ddots & \vdots \\ 0 & \dots & 0 & 0 \end{bmatrix}. \tag{7.26}$$

Using the expressions for L and U, we can represent (7.24) in the time-domain matrix form

$$(\mathrm{L} + \alpha(s)\mathrm{U})\tilde{v} = \tilde{B}(s). \tag{7.27}$$

If we define a small-signal modulation operator $\psi(s)$,

$$\psi(s) = \begin{bmatrix} Ie^{st_1} & & & \\ 0 & Ie^{st_2} & & \\ & \ddots & \ddots & \\ & & 0 & Ie^{st_M} \end{bmatrix} \tag{7.28}$$

then we obtain an expression of the transfer function as follows,

$$H(s) = \psi^H(s)\tilde{v}(s) \tag{7.29}$$

and also

$$\tilde{B}(s) = \psi(s)B_{TD}.$$

Now we can obtain an approximation from the finite-difference discretization as

$$(s\,E_{TD} - A_{TD}) \approx \psi^H(s)[\mathrm{L} + \alpha(s)\mathrm{U}]\psi(s). \tag{7.30}$$

The difference between the two sides of (7.30) depends on the treatment of the small signal that has been applied to the test. The left hand side represents a spectral discretization, and the right hand side represents a finite-difference discretization.

It is briefly discussed in [85, 84] that the spectral form (7.16) that is ameanable to model reduction is less convenient to work with. If we even use the Krylov subspace scheme and use a lower-triangular preconditioner, at each different frequency point the preconditioner needs to be reconstructed. That means we need to re-factor the diagonal blocks, and the computational cost as well as the problem size increases (see [114]).

To resolve this dilemma assume the projection matrix V is not a basis for the Krylov subspace generated by $(s\,E_{TD} - A_{TD})^{-1}$, but instead for a nearby matrix. In that case, the reduced-order model would still be a projection of the original, having some small error in it. As long as the model is not evaluated in the neighborhood of a pole, it can be expected that the additional errors introduce into the model are small enough. Hence, instead of choosing the spectral form, the basis for the projector in the model reduction procedure can be obtained from the finite-difference equations.

7.2.3. Preconditioning and Recycling of Krylov Subspaces

Our interest is to see how the finite difference method approximates the appropriate basis V for the reduced-order system. Suppose we need to solve (7.27) for some different $\tilde{B}$. Again following [114], consider preconditioning with the matrix L. Then the preconditioned system can be written as

$$(I + \alpha(s)\mathrm{L}^{-1}\mathrm{U})\tilde{v} = \mathrm{L}^{-1}\tilde{B}(s) \tag{7.31}$$

As L is lower triangular, its inverse is easily applied by factoring the diagonal blocks and then back-solving. The structure of (7.31) suggests to explore the shift-invariance property of Krylov subspaces [see Chapter 6, Lemma 6.3.2 of this thesis]. It says that the Krylov subspace of a matrix A is invariant with respect to shifts of the form $A \to A + \alpha I$, for α being any nonzero scaler. This *recycled Krylov subspace method* also enables us to use the same Krylov subspace to solve (7.31) at multiple frequency points. In that context we would like to introduce the following corollary to clarify the fact.

Corollary 7.2.1:
[114] *The Krylov subspace spanned by the vectors*

$$\{p^0, (I + \alpha(s)\mathrm{L}^{-1}\mathrm{U})\, p^0, (I + \alpha(s)\mathrm{L}^{-1}\mathrm{U})^2\, p^0, \ldots, (I + \alpha(s)\mathrm{L}^{-1}\mathrm{U})^{m-1}\, p^0\} \tag{7.32}$$

is identical to the Krylov subspace spanned by the vectors

$$\{p^0, (\mathrm{L}^{-1}\mathrm{U})\, p^0, (\mathrm{L}^{-1}\mathrm{U})^2\, p^0, \ldots, (\mathrm{L}^{-1}\mathrm{U})^{m-1}\, p^0\} \tag{7.33}$$

independent of α, where p^0 is vector. ◊

Proof. The proof follows from the shift-invariance property of Krylov subspaces and can be found in [47]. □

Hence, the subspace spanned by $\mathrm{L}^{-1}\mathrm{U}$ is invariant to shifts of the form $\mathrm{L}^{-1}\mathrm{U} \to I + \alpha(s)\mathrm{L}^{-1}\mathrm{U}$, for $\alpha(s)$ being any nonzero scaler. The question now arises how we make use of the result in Theorem 7.2.1 to solve (7.31), where the matrix and the right hand side are functions of a variable (=swept) parameter. If we look inside the problem (7.31), we see that the matrix-vector products for different frequency changes in this problem are constrained, and so previous iterative solutions can be exploited. To see this, we look at the following representation for two different frequencies s and $\bar{s}$:

$$\beta(I + \alpha(s)\,\mathrm{L}^{-1}\mathrm{U})\, p^0 + \gamma p^0 = (I + \alpha(\bar{s})\,\mathrm{L}^{-1}\mathrm{U})\, p^0, \tag{7.34}$$

where $\beta = \alpha(\bar{s})/\alpha(s)$ and $\gamma = 1 - \beta$. This implies that a matrix-vector product computed using the matrix associated with frequency s can be converted into a matrix-vector product using the matrix associated with frequency $\bar{s}$ by a simple scalar multiplication. Therefore, we have no extra cost to obtain the projectors from the expansions about

multiple frequency-points (due to the reason of the recycling scheme) compared to single frequency-point expansions [54].

The above discussion suggests that the basis for the projector in the model reduction procedure can be obtained by using the finite-difference equations. All these lead us to the proposed model reduction algorithm, Algorithm 7.1.

7.3. Outline of the Proposed Algorithm

In order to simplify the presentation, only real-valued expansion points are used in Algorithm 7.1, and $B(t_j)$ is considered as a time-varying column vector for each time step. The overall algorithm can be described in two stages. In the first stage, the algorithm produces a matrix approximating the Krylov subspace for several s_i. Note that at each iteration $i \in [1, n_s]$, Algorithm 7.1 generates m columns of the projection matrix V, where m is the approximation-order of the Krylov subspace. Once the projection matrix V is computed for several s_k, it is used to construct the reduced-order model via the projection equations.

Suppose we start with a particular frequency s_1 form a set of different frequencies. At the beginning, Step 9 takes B_{TD} as its right side vector and generates the first column of V. For the second column, it takes now $E_{TD} \cdot v$ as its right side vector, where v is the previous orthonormal column generated for V. The process continues till m is reached for s_1. For the next frequency s_2, Step 9 computes the first column and then orthonormalizes it with respect to all the previously computed orthonormalized columns of V generated for s_1 (such an orthonormalization is efficient and fruitful because of the recycled Krylov scheme used for multiple expansion points). The total number of such orthonormalized columns is counted by k and it is initialized at the beginning of the algorithm.

As soon as the projection columns of V for a particular s_i are computed, the algorithm run for the next frequency point. The projection matrix V is the union of all these projections obtained for all s_i, where i runs form 1 to n_s. Therefore , the number of columns of the projection matrix V is $m \cdot n_s$. This can be expressed as

$$\text{range}(V) = \bigcup_{i=1}^{n_s} \mathcal{K}\left(L^{-1}U,\ \tilde{B}(s_i)\right) \tag{7.35}$$

Remark 7.2:

In Algorithm 7.1, Step 9 uses recycling technique to produce the projection columns of V. It is clear from the context that if a preconditioner L is not used to solve Step 9, each new vector in the model reduction is obtained by an inner Krylov iteration with the matrix A_{TD} . Also, each new right-hand-sides u_i is generated for each sweep of frequency s_i. Due to the shift-invariance property, since each new right-hand-side u_i in the model reduction procedure is drawn from a Krylov subspace of $\mathcal{K}_m(A_{TD}, B_{TD})$

Algorithm 7.1 Approximate Multipoint Krylov-Subspace Model Reduction

Input: $A_{TD}, E_{TD}, B_{TD}, C_{TD}, n_s, m$.
Output: $V, \tilde{A}_{TD}, \tilde{E}_{TD}, \tilde{B}_{TD}, \tilde{C}_{TD}$.

Set $k = 1$
for $i = 1$ to n_s **do**
  for $j = 1$ to m **do**
    if j=1 **then**
      $w = B_{TD}$
    else
      $w = E_{TD}\, v_{k-1}$
    end if
    $u = \psi^H(s_i)[L + \alpha(s_i)U]^{-1}\psi(s_i)w$
    for $l = 1$ to $k - 1$ **do**
      $u = u - v_l^T u$
    end for
    $v_k = u/\|u\|$
    $k = k + 1$
  end for
end for
$[V, R] = RRQR(V, \tau)$
$\tilde{A}_{TD} = -V^T A_{TD}\, V, \quad \tilde{E}_{TD} = V^T E_{TD}\, V,$
$\tilde{B}_{TD} = V^T B_{TD}, \quad \tilde{C}_{TD} = C_{TD}\, V.$

for some m, it is reasonable that the next term in the space of $\mathcal{K}_i(A_{TD}, B_{TD})$ is related to the $\mathcal{K}_m(A_{TD}, B_{TD})$, where i slightly exceeds m [84]. ◊

The net result of the algorithm is an $N \times mn_s$ projection matrix V with orthonormal columns. We use the rank revealing QR factorization (RRQR) [43] with prescribed tolerance τ for the formulation of the projected matrix V. Because, the matrix V, we have obtained from the direct use of the proposed algorithm, has linear dependent columns. The rank revealing QR factorization truncates those redundant constraints and produces an orthonormal basis of the projected matrix for the reduced-order system. Last of all the reduced-order system is generated through the projection with V.

7.4. Numerical Results

To test the time-varying model reduction procedure, the proposed algorithm has been implemented in a time-domain RF circuit simulator. The large-signal periodic steady state is calculated using a shooting method [113]. The LTV system is discretized using second-order backward-difference formulas. The data files for both the following model

problems have been provided by Michael Striebel [1], former postdoctoral researcher, NXP Semiconductors, High Tech Campus 37, NL-5656 AE Eindhoven, The Netherlands.

7.4.1. Simple RF Circuit

We consider here a simple example where the data is obtained from small RF circuit simulator. The circuit system consists of 5 nodes, and is excited by a local oscillator (LO) at 2 KHz driving the mixer, while the RF input is fed into the I-channel buffer. The time-varying system is obtained around a steady state of the circuit at the oscillatory frequency; a total of $M = 129$ timesteps are used to describe the steady-state waveform. For the model reduction procedure, the input function $B(t)$ is a constant column vector, corresponding to the continuous small-signal input. To analyze the circuit, we consider a period of $T = 1ms$ for the steady state analysis. The final discretized model is a real LTI system of order $N = 645$.

The assigned algorithm produces a very good approximation of the original model for multiple frequency points. Three different expansion points on the positive real axis at s = 2kHz, 4kHz, 6kHz are considered. The reduced-order model is generated by matching four moments of the Krylov subspace generated for every expansion point. We use the rank revealing QR factorization for the formulation of the projected matrix with tolerance, $tol = 10^{-5}$.

We obtain a reduced-order model of order $r = 3$. The computing time for the reduced model is very small and efficient compared to the original model. We plot the frequency response of the transfer functions for both the original and reduced-order systems and compare the relative error. Fig. 7.1 shows a very nice matching of the baseband transfer functions $H_{TD}(s)$ and $\tilde{H}_{TD}(s)$, and the relative error in Fig. 7.2 is very small. The Bode diagram and the step response in Fig. 7.3 and Fig. 7.4 show the better efficiency of the reduced-order model.

7.4.2. Mixer Circuit

In this example, we apply the proposed algorithm on a multi-tone mixer circuit, consisting of several functional component blocks. The circuit generates 43 equations in the circuir simulator. 201 timesteps are needed for time-domain analysis, so that the matrix A_{TD} has rank $N = 8643$.

The mixing elements shift the input from the RF frequency to the mixer LO frequency. For the model reduction procedure, the input function $B(t)$ is chosen to be a constant column vector, corresponding to the continuous small-signal input. To analyze the circuit, a periodic steady state analysis is run with a $T = 1ns$ period.

[1]Current address: Bergischen Universitt Wuppertal, Applied Mathematics / Numerical Analysis Gaustr. 20, 42119 Wuppertal; (*michael.striebel@math.uni-wuppertal.de*)

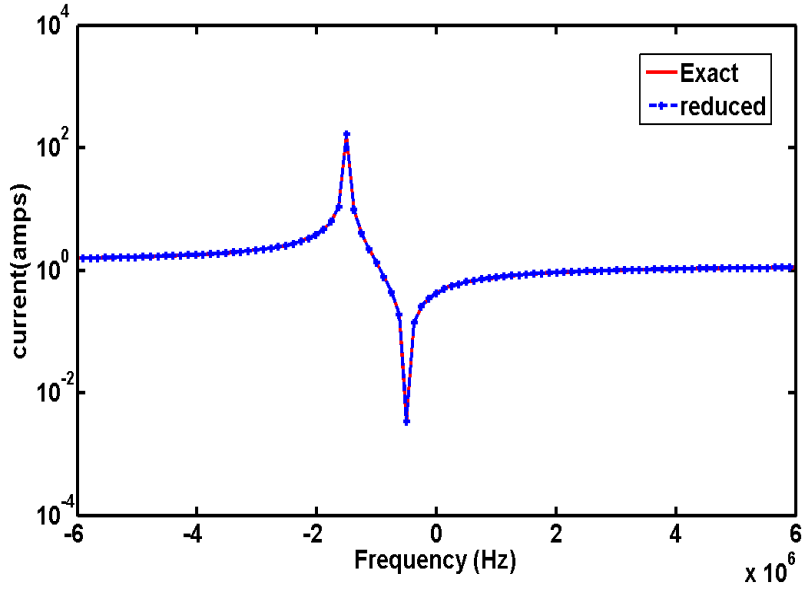

Figure 7.1. Frequency response of transfer function: exact system versus reduced-order system of order $r = 3$ (RF circuit).

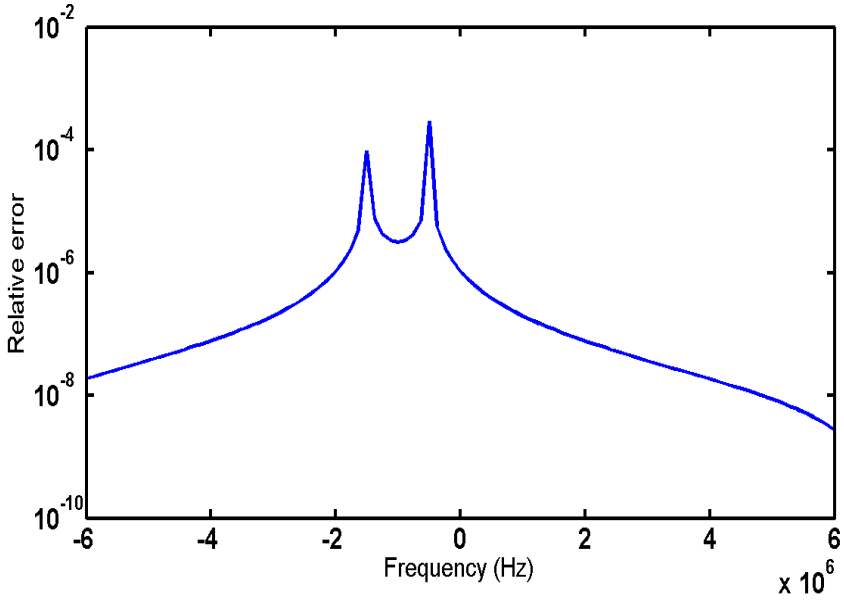

Figure 7.2. Error in the frequency response of transfer function of reduced-order system (RF circuit).

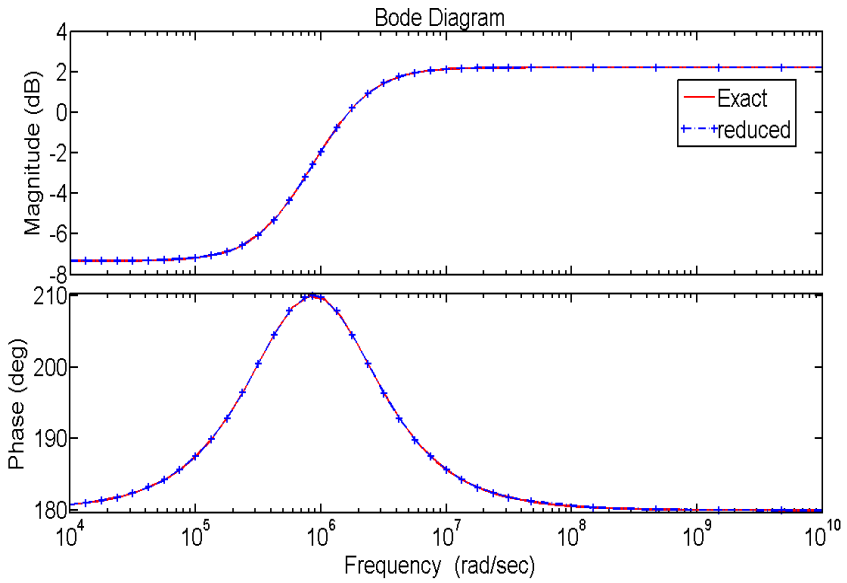

Figure 7.3. Bode plots for the exact system and the reduced-order system of order $r = 3$ (RF circuit).

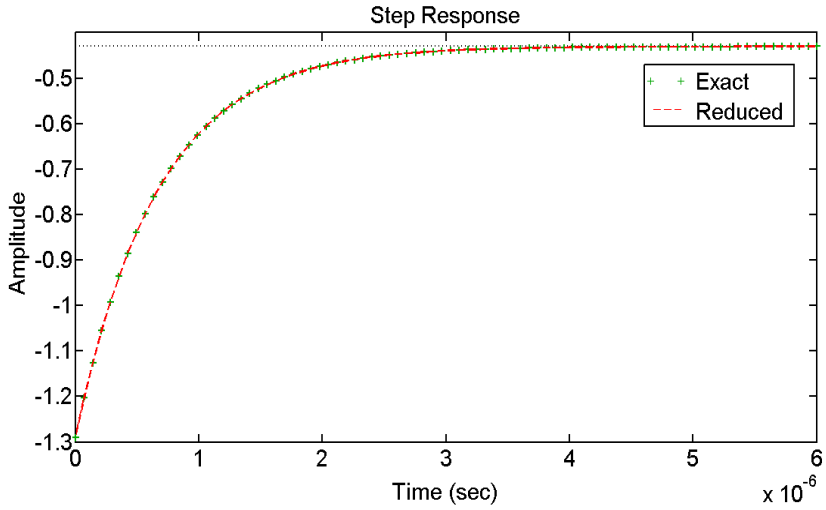

Figure 7.4. Step response for exact system and the reduced-order system of order $r = 3$ (RF circuit).

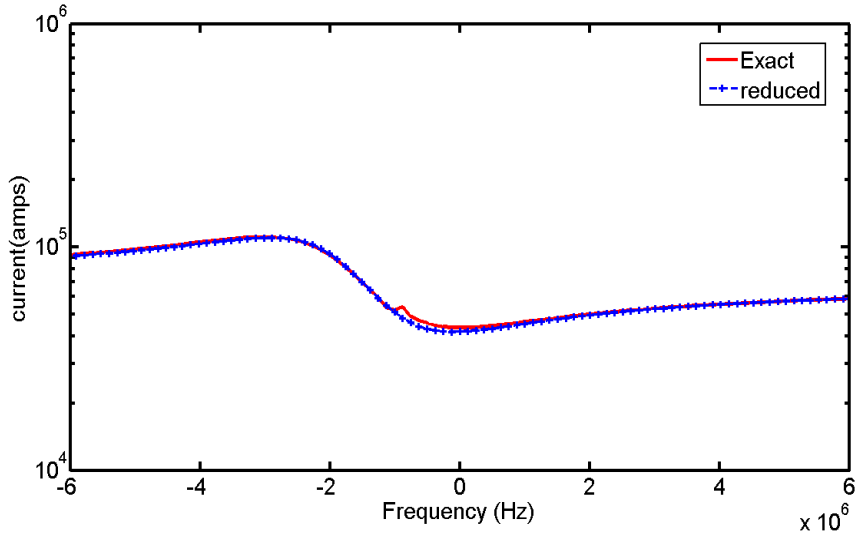

Figure 7.5. Transfer function: exact system versus reduced-order system of order $r = 4$ (Mixer circuit).

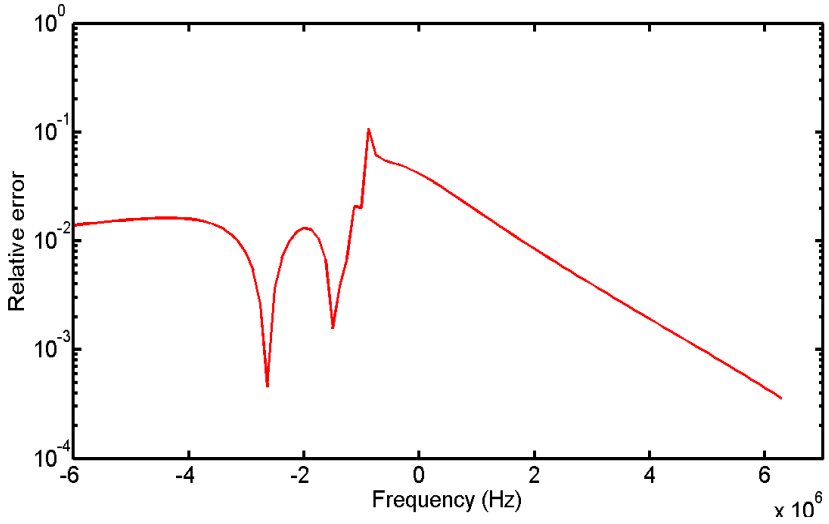

Figure 7.6. Error in the frequency response of transfer function of reduced-order system (Mixer circuit).

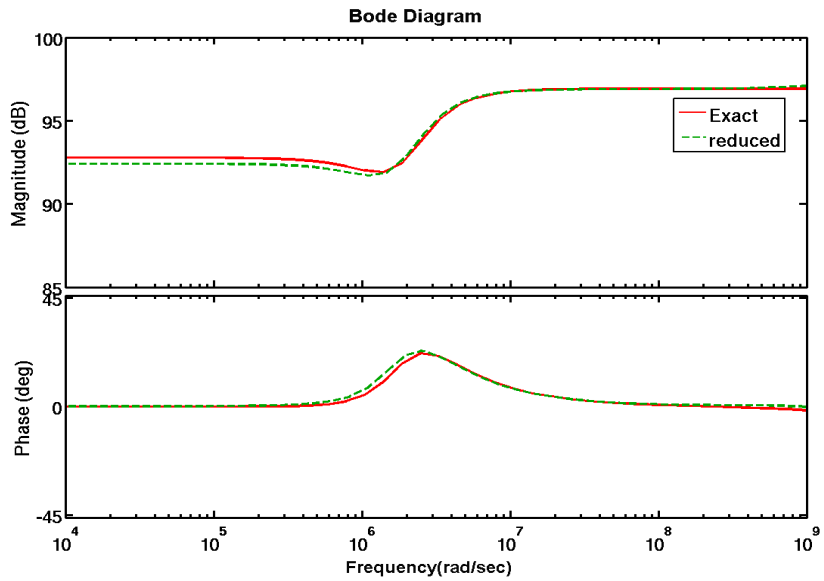

Figure 7.7. Bode plots for the exact system and the reduced-order system of order $r = 4$ (Mixer circuit).

The proposed algorithm produces a very good approximation of the original model for multiple frequency points. Five different expansion points on the positive real axis in the range from s=2MHz to 6MHz are used. The reduced-order model is generated by matching six moments of the Krylov subspace generated for every expansion point. We use the rank revealing QR factorization for the formulation of the projected matrix with tolerance $tol = 10^{-6}$.

We obtain a reduced-order model of order $r = 4$. The computing time for the reduced-order model is only 0.0037 CPU seconds, while the original model took almost 8×10^3 CPU seconds. We plot the transfer functions for both the original and reduced-order systems in Fig. 7.5 and depict their relative error in Fig. 7.6. Both the transfer functions match and the relative error is very small. In addition, the plotted Bode diagram and the step response in Fig. 7.7 and Fig. 7.8 show the better efficiency of the reduced-order model.

7.5. Discussion

The system model-design applied here is efficient for small-signal analysis and time parameters. Therefore the model is capable of representing very complicated physical dynamics in circuit problems. We observe that the proposed algorithm produces a very good approximation of the original model and the reduced-order model is very small and efficient compared to the original model.

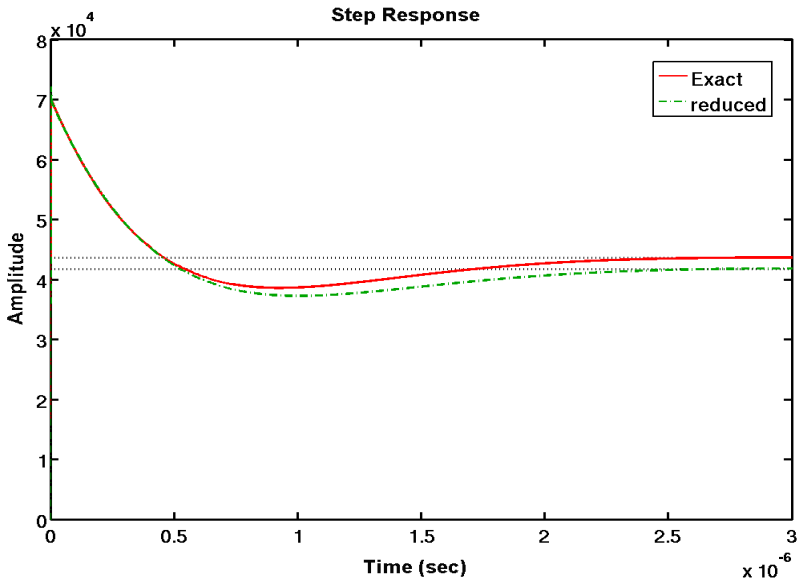

Figure 7.8. Step response for exact system and the reduced-order system of order $r = 4$ (Mixer circuit).

There are several scopes for the future extensions of the ideas of this section. The formalism and algorithms can be trivially extended to the case of quasi-periodic small signal analysis [131].

CHAPTER

EIGHT

MODEL REDUCTION OF LPTV DISCRETE-TIME SYSTEMS VIA BALANCED TRUNCATION

Contents

In this chapter, we consider LPTV discrete-time descriptor systems and review some basic concepts of LPTV discrete-time descriptor systems which link them to their corresponding cyclic lifted system. We also discuss a solution technique for PPDALEs in lifted form which arise in model reduction of periodic descriptor systems and propose a balanced truncation model reduction method for such systems. The behavior of the suggested model reduction technique is illustrated using numerical examples.

In Section 8.1, we recall some definitions and basic concepts of LPTV discrete-time descriptor systems and the corresponding cyclic lifted system representation from Chapter 4 and 5. Section 9.2 then reviews the PPDALEs and the corresponding PLDALEs

of these periodic Lyapunov equations along with their specific block diagonal solutions. We then discuss an efficient method to solve those lifted Lyapunov equations in Section 9.3. The periodic Hankel singular values and their relations with the periodic Gramians are presented in Section 9.4. A balanced truncation model reduction method for periodic descriptor systems is presented in Section 9.5. Section 9.6 contains numerical examples that illustrate the properties of the suggested model reduction technique. We give a short discussion in the last section.

8.1. Introduction

Let us recall the linear discrete-time periodic descriptor system with time-varying dimensions of the form

$$\begin{aligned} E_k x_{k+1} &= A_k x_k + B_k u_k, \\ y_k &= C_k x_k, \qquad k \in \mathbb{Z}, \end{aligned} \tag{8.1}$$

where $E_k \in \mathbb{R}^{\mu_{k+1} \times n_{k+1}}$, $A_k \in \mathbb{R}^{\mu_{k+1} \times n_k}$, $B_k \in \mathbb{R}^{\mu_{k+1} \times p_k}$, $C_k \in \mathbb{R}^{q_k \times n_k}$ are periodic with a period $K \geq 1$ and $\sum_{k=0}^{K-1} \mu_k = \sum_{k=0}^{K-1} n_k = n$, $\sum_{k=0}^{K-1} p_k = p$ and $\sum_{k=0}^{K-1} q_k = q$.

We already discussed in Chapter 4 that regularity and stability are two important properties to handle the dynamics of the discrete-time periodic descriptor system (8.1). Since the matrices E_k are allowed to be singular for all k, regularity and stability of the periodic descriptor system (8.1) can only be defined via the cyclic lifted structure of the periodic matrix pairs associated with system (8.1). In this context, we would like to introduce shortly the cyclic lifted system associated with the periodic descriptor system (8.1). The details of this lifting isomorphism of periodic descriptor systems can be found in Chapter 5.

The cyclic lifted representation of the periodic descriptor system (8.1) to be used here is given by

$$\begin{aligned} \mathcal{E}\mathcal{X}_{k+1} &= \mathcal{A}\mathcal{X}_k + \mathcal{B}\,\mathcal{U}_k, \\ \mathcal{Y}_k &= \mathcal{C}\mathcal{X}_k, \end{aligned} \tag{8.2}$$

where

$$\mathcal{E} = \operatorname{diag}(E_0, E_1, \ldots, E_{K-1}), \quad \mathcal{B} = \operatorname{diag}(B_0, B_1, \ldots, B_{K-1}),$$

$$\mathcal{A} = \begin{bmatrix} 0 & \cdots & 0 & A_0 \\ A_1 & & & 0 \\ & \ddots & & \vdots \\ 0 & & A_{K-1} & 0 \end{bmatrix}, \quad \mathcal{C} = \begin{bmatrix} 0 & \cdots & 0 & C_0 \\ C_1 & & & 0 \\ & \ddots & & \vdots \\ 0 & & C_{K-1} & 0 \end{bmatrix}. \tag{8.3}$$

The descriptor vector, system input and output of (8.2) are related to those of (8.1) via

$$\mathcal{X}_k = [x_1^T, \ldots, x_{K-1}^T, x_0^T]^T, \quad \mathcal{U}_k = [u_0^T, u_1^T, \ldots, u_{K-1}^T]^T, \quad \mathcal{Y}_k = [y_0^T, y_1^T, \ldots, y_{K-1}^T]^T,$$

respectively. We also define a transfer function of the lifted system (8.2) as $\mathcal{H}(z) = \mathcal{C}(z\mathcal{E} - \mathcal{A})^{-1}\mathcal{B}$.

Note that system (8.1) can be said to be regular if the set $(\mathbb{E}, \mathbb{A})$ of periodic matrix pairs $\{(E_k, A_k)\}_{k=0}^{K-1}$ is regular, which can be equivalently defined by the regularity of the cyclic matrix pencil $z\mathcal{E} - \mathcal{A}$, i.e., $\det(z\mathcal{E} - \mathcal{A}) \neq 0$, for some $z \in \mathbb{C}$ (see Section 4.2 in Chapter 4 for detail). The set of periodic matrix pairs $\{(E_k, A_k)\}_{k=0}^{K-1}$ is said to be pd-stable if $z\mathcal{E} - \mathcal{A}$ is regular and all its finite eigenvalues lie inside the unit circle. System (8.1) is asymptotically stable if the corresponding set of periodic matrix pairs $\{(E_k, A_k)\}_{k=0}^{K-1}$ is pd-stable.

It is shown in Chapter 4 that if the set of periodic matrix pairs $\{(E_k, A_k)\}_{k=0}^{K-1}$ is regular, then the periodic descriptor system (8.1) is equivalent to the canonical forward-backward form (see Subsection 4.2.2 of Chapter 4) given by

$$x_{k+1}^f = A_k^f x_k^f + B_k^f u_k, \quad y_k^f = C_k^f x_k^f, \tag{8.5}$$

$$E_k^b x_{k+1}^b = x_k^b + B_k^b u_k, \quad y_k^b = C_k^b x_k^b, \tag{8.6}$$

respectively, with

$$\begin{aligned} W_k E_k Z_{k+1} &= \begin{bmatrix} I_{n_{k+1}^f} & 0 \\ 0 & E_k^b \end{bmatrix}, \quad W_k A_k Z_k = \begin{bmatrix} A_k^f & 0 \\ 0 & I_{n_k^\infty} \end{bmatrix}, \\ W_k B_k &= \begin{bmatrix} B_k^f \\ B_k^b \end{bmatrix}, \quad C_k Z_k = \begin{bmatrix} C_k^f, & C_k^b \end{bmatrix}, \end{aligned} \tag{8.7}$$

where $W_k \in \mathbb{R}^{\mu_{k+1} \times \mu_{k+1}}$ and $Z_k \in \mathbb{R}^{n_k \times n_k}$ are two nonsingular matrices for each $k = 0, 1, \ldots, K-1$. Note that $y_k = y_k^f + y_k^b$, $n_k = n_k^f + n_k^\infty$ and $\mu_{k+1} = n_{k+1}^f + n_k^\infty$ for such a periodic decomposition . The index ν of the periodic descriptor system (8.1) is defined as $\nu = \max(\nu_0, \nu_1, \ldots, \nu_{K-1})$, where $(\nu_0, \nu_1, \ldots, \nu_{K-1})$ are the indices of the regular set of periodic matrix pairs $\{(E_k, A_k)\}_{k=0}^{K-1}$ (see Remark 4.6 of Chapter 4).

For such a canonical representation of the periodic matrix pairs, we also define, for $k = 0, 1, \ldots, K-1$, the spectral projectors

$$P_r(k) = Z_k \begin{bmatrix} I_{n_k^f} & 0 \\ 0 & 0 \end{bmatrix} Z_k^{-1}, \quad P_l(k) = W_k^{-1} \begin{bmatrix} I_{n_{k+1}^f} & 0 \\ 0 & 0 \end{bmatrix} W_k,$$

onto the k-th right and left deflating subspaces of the periodic matrix pairs $\{(E_k, A_k)\}_{k=0}^{K-1}$ corresponding to the finite eigenvalues, and $Q_r(k) = I - P_r(k)$ and $Q_l(k) = I - P_l(k)$ as complementary projectors.

Similar to discrete-time descriptor systems [24], the finite pole structure of the periodic system (8.1) is completely determined by the forward subsystems and the infinite pole structure is determined by the backward subsystems. Computing the zeros and poles of periodic descriptor systems are well studied in [125] using the lifted formulations associated with the periodic system. Note that the finite eigenvalues of $\{(E_k, A_k)\}_{k=0}^{K-1}$ coincide with the finite eigenvalues of the lifted pencil $z\mathcal{E} - \mathcal{A}$.

8.2. Periodic Projected Lyapunov Equations and their Lifted Forms

In Chapter 4, we have shown that the periodic reachability and observability Gramians for the periodic discrete-time descriptor system (8.1) satisfy some PPDALEs with special right-hand sides. Considering the periodic discrete-time descriptor system (8.1) and the set $(\mathbb{E}, \mathbb{A})$ of periodic matrix pairs $\{(E_k, A_k)\}_{k=0}^{K-1}$ to be pd-stable, we have shown that the causal reachability Gramians $\{G_k^{cr}\}_{k=0}^{K-1}$ are the unique symmetric, positive semidefinite solutions of the generalized PPDALEs

$$\begin{aligned} A_k G_k^{cr} A_k^T - E_k G_{k+1}^{cr} E_k^T &= -P_l(k) B_k B_k^T P_l(k)^T, \\ G_k^{cr} &= P_r(k) G_k^{cr} P_r(k)^T, \end{aligned} \tag{8.8}$$

for $k = 0, 1, \ldots, K-1$, where $G_K^{cr} = G_0^{cr}$, $E_{-1} = E_{K-1}$, and $P_l(-1) = P_l(K-1)$. The proof of (8.8) can be found in Subsection 4.3.3, Chapter 4.

The numerical solution of (8.8) has been considered in [30]. The method proposed there extends the periodic Schur method [19, 20, 123, 119] and the generalized Schur-Hammarling method [104] developed for periodic standard and projected generalized Lyapunov equations, respectively. This method is based on an initial reduction of the periodic matrix pairs $\{(E_k, A_k)\}_{k=0}^{K-1}$ to the generalized periodic Schur form [56, 123] and on solving the resulting generalized periodic Sylvester and Lyapunov equations of (quasi)-triangular structure using the recursive blocked algorithms [44]. Computing the Kronecker-like canonical forms of the periodic matrix pairs and solving the resulting periodic Sylvester equations are the most computationally expensive tasks in this algorithm (Algorithm 5.1 of [30]).

On the other hand, since we have constructed a relationship between the Gramians of the periodic systems and those of the cyclic lifted system as in Subsection 5.2.4 of Chapter 5, it is straightforward and also promising to solve the reachability and observability Gramians of the lifted system for the corresponding LPTV Gramians. So we focus on the lifted representation of the periodic projected Lyapunov equations that we have discussed in Subsection 5.2.4 of Chapter 5.

Considering the periodic discrete-time descriptor system (8.1) and its cyclic lifted representation (8.2), where the set of periodic matrix pairs $\{(E_k, A_k)\}_{k=0}^{K-1}$ is pd-stable, we have shown that the causal reachability Gramians $\mathcal{G}^{cr}$ of (8.2) satisfy the generalized PLDALEs

$$\mathcal{A}\mathcal{G}^{cr}\mathcal{A}^T - \mathcal{E}\mathcal{G}^{cr}\mathcal{E}^T = -\mathcal{P}_l \mathcal{B}\mathcal{B}^T \mathcal{P}_l^T, \quad \mathcal{G}^{cr} = \mathcal{P}_r \mathcal{G}^{cr} \mathcal{P}_r^T, \tag{8.9}$$

where $\mathcal{E}$, $\mathcal{A}$, $\mathcal{B}$ are as in (8.3) and

$$\begin{aligned} \mathcal{G}^{cr} &= \operatorname{diag}(G_1^{cr}, \ldots, G_{K-1}^{cr}, G_0^{cr}), \\ \mathcal{P}_l &= \operatorname{diag}(P_l(0), P_l(1), \ldots, P_l(K-1)), \qquad \mathcal{Q}_l = I - \mathcal{P}_l, \\ \mathcal{P}_r &= \operatorname{diag}(P_r(1), \ldots, P_r(K-1), P_r(0)), \qquad \mathcal{Q}_r = I - \mathcal{P}_r. \end{aligned} \tag{8.10}$$

Similarly, the noncausal reachability Gramians and the causal and noncausal observability Gramians of the periodic descriptor system (8.1) can be easily retrieved from the block diagonal solutions of the corresponding PLDALEs. We discussed these PLDALEs and their block diagonal solutions in Chapter 5 (see Theorem 5.2.4 and 5.2.5) with necessary proofs. Note that for the lifted system (8.2) the complete reachability Gramian $\mathcal{G}^r$ is defined as $\mathcal{G}^r = \mathcal{G}^{cr} + \mathcal{G}^{ncr}$, where $\mathcal{G}^{cr}$ is defined in (8.10) and $\mathcal{G}^{ncr}$ is the noncausal reachability Gramian of (8.2) defined in (5.38). The complete observability Gramian $\mathcal{G}^o$ of (8.2) is defined as $\mathcal{G}^o = \mathcal{G}^{co} + \mathcal{G}^{nco}$, where $\mathcal{G}^{co}$ and $\mathcal{G}^{nco}$ are the causal and noncausal observability Gramians of (8.2) defined in (5.45).

8.3. Solving for Reachability and Observability Gramians of LPTV Descriptor Systems

We generalizes the method from [103] to solve the generalized PLDALEs for periodic reachability and observability Gramians. Let us consider the generalized PLDALE (8.9) corresponding to the generalized PPDALEs (8.8) of the periodic descriptor system (8.1) given by

$$\mathcal{A}\mathcal{G}^{cr}\mathcal{A}^T - \mathcal{E}\mathcal{G}^{cr}\mathcal{E}^T = -\mathcal{P}_l\mathcal{B}\mathcal{B}^T\mathcal{P}_l^T, \quad \mathcal{G}^{cr} = \mathcal{P}_r\mathcal{G}^{cr}\mathcal{P}_r^T, \tag{8.11}$$

where $\mathcal{E}, \mathcal{A}, \mathcal{G} \in \mathbb{R}^{n\times n}$ (the complex case is similar). Let the pencil $\lambda\mathcal{E} - \mathcal{A}$ be in GUPTRI form (3.13) such that

$$\lambda\mathcal{E} - \mathcal{A} = \mathcal{V}\begin{bmatrix} \lambda\mathcal{E}_f - \mathcal{A}_f & \lambda\mathcal{E}_u - \mathcal{A}_u \\ 0 & \lambda\mathcal{E}_\infty - \mathcal{A}_\infty \end{bmatrix}\mathcal{U}^T, \tag{8.12}$$

where $\mathcal{U}, \mathcal{V}$ are orthogonal matrices. Note that the pencil $\lambda\mathcal{E} - \mathcal{A}$ is stable, and the pencil $\lambda\mathcal{E}_f - \mathcal{A}_f$ is quasi-triangular and has only finite eigenvalues, while the pencil $\lambda\mathcal{E}_\infty - \mathcal{A}_\infty$ is triangular and has infinite eigenvalues. Clearly, $\mathcal{E}_f, \mathcal{A}_f \in \mathbb{R}^{n_f\times n_f}$, $\mathcal{E}_\infty, \mathcal{A}_\infty \in \mathbb{R}^{n_\infty\times n_\infty}$, and $n = n_f + n_\infty$.

In order to compute the left and right deflating subspaces of $\lambda\mathcal{E} - \mathcal{A}$ corresponding to the finite eigenvalues we need to compute matrices $\mathbf{Z}, \mathbf{W} \in \mathbb{R}^{n_f\times n_\infty}$ such that

$$\begin{bmatrix} I & \mathbf{Z} \\ 0 & I \end{bmatrix}\begin{bmatrix} \lambda\mathcal{E}_f - \mathcal{A}_f & \lambda\mathcal{E}_u - \mathcal{A}_u \\ 0 & \lambda\mathcal{E}_\infty - \mathcal{A}_\infty \end{bmatrix}\begin{bmatrix} I & -\mathbf{W} \\ 0 & I \end{bmatrix} = \begin{bmatrix} \lambda\mathcal{E}_f - \mathcal{A}_f & 0 \\ 0 & \lambda\mathcal{E}_\infty - \mathcal{A}_\infty \end{bmatrix}, \tag{8.13}$$

and $(\mathbf{Z}, \mathbf{W})$ is the solution of the generalized Sylvester equation

$$\begin{aligned} \mathcal{E}_f\mathbf{W} - \mathbf{Z}\mathcal{E}_\infty &= \mathcal{E}_u, \\ \mathcal{A}_f\mathbf{W} - \mathbf{Z}\mathcal{A}_\infty &= \mathcal{A}_u. \end{aligned} \tag{8.14}$$

Since the pencils $\lambda\mathcal{E}_f - \mathcal{A}_f$ and $\lambda\mathcal{E}_\infty - \mathcal{A}_\infty$ have no common eigenvalues, the solution $(\mathbf{Z}, \mathbf{W})$ of the generalized Sylvester equation (8.14) is unique. Therefore the pencil $\lambda\mathcal{E} - \mathcal{A}$

can be transformed into the Kronecker-like form

$$\begin{aligned} \lambda\mathcal{E}-\mathcal{A} &= \mathcal{V}\begin{bmatrix} I & -\mathbf{Z} \\ 0 & I \end{bmatrix}\begin{bmatrix} \lambda\mathcal{E}_f-\mathcal{A}_f & 0 \\ 0 & \lambda\mathcal{E}_\infty-\mathcal{A}_\infty \end{bmatrix}\begin{bmatrix} I & \mathbf{W} \\ 0 & I \end{bmatrix}\mathcal{U}^T \\ &= \mathcal{M}\begin{bmatrix} \lambda\mathcal{E}_f-\mathcal{A}_f & 0 \\ 0 & \lambda\mathcal{E}_\infty-\mathcal{A}_\infty \end{bmatrix}\mathcal{N}, \end{aligned} \tag{8.15}$$

where the matrices

$$\mathcal{M}=\mathcal{V}\begin{bmatrix} I & -\mathbf{Z} \\ 0 & I \end{bmatrix} \quad \text{and} \quad \mathcal{N}=\begin{bmatrix} I & \mathbf{W} \\ 0 & I \end{bmatrix}\mathcal{U}^T \tag{8.16}$$

are nonsingular. We argue that the matrices $\mathcal{E}_f, \mathcal{A}_f$, $\mathcal{E}_\infty$, and $\mathcal{A}_\infty$ in (8.15) preserve the following cyclic lifted structures,

$$\mathcal{E}_f=\begin{bmatrix} E_0^f & & & \\ & E_1^f & & \\ & & \ddots & \\ & & & E_{K-1}^f \end{bmatrix}, \quad \mathcal{A}_f=\begin{bmatrix} 0 & & \cdots & 0 & A_0^f \\ A_1^f & 0 & & & 0 \\ & \ddots & & & \vdots \\ 0 & & & A_{K-1}^f & 0 \end{bmatrix}, \tag{8.17}$$

and

$$\mathcal{E}_\infty=\begin{bmatrix} 0 & E_0^\infty & & \\ & & \ddots & \\ 0 & & & E_{K-2}^\infty \\ E_{K-1}^\infty & 0 & & 0 \end{bmatrix}, \quad \mathcal{A}_\infty=\begin{bmatrix} A_0^\infty & & & \\ & A_1^\infty & & \\ & & \ddots & \\ & & & A_{K-1}^\infty \end{bmatrix}, \tag{8.18}$$

where the periodic matrix pairs $\{(E_k^f, A_k^f)\}_{k=0}^{K-1}$ contain only the finite eigenvalues of the periodic matrix pairs $\{(E_k, A_k)\}_{k=0}^{K-1}$ that lie inside the unit circle, and the periodic matrix pairs $\{(E_k^\infty, A_k^\infty)\}_{k=0}^{K-1}$ contain only infinite eigenvalues.

Now to check whether such structure-preserving $\mathcal{M}, \mathcal{N}$ exist, we consider the pd-stable set $\{(E_k, A_k)\}_{k=0}^{K-1}$ and the decompositions (8.7) (without orthogonalization) of the periodic

matrices. Therefore we have

$$
\begin{aligned}
\mathcal{E} &= \begin{bmatrix} W_0^{-1}\begin{bmatrix} E_0^f & 0 \\ 0 & E_0^\infty \end{bmatrix} Z_1^{-1} & & & \\ & W_1^{-1}\begin{bmatrix} E_1^f & 0 \\ 0 & E_1^\infty \end{bmatrix} Z_2^{-1} & & \\ & & \ddots & \\ & & & W_{K-1}^{-1}\begin{bmatrix} E_{K-1}^f & 0 \\ 0 & E_{K-1}^\infty \end{bmatrix} Z_0^{-1} \end{bmatrix} \\
&= \begin{bmatrix} W_0^{-1} & & & \\ & W_1^{-1} & & \\ & & \ddots & \\ & & & W_{K-1}^{-1} \end{bmatrix} \begin{bmatrix} \begin{bmatrix} E_0^f & 0 \\ 0 & E_0^\infty \end{bmatrix} & & & \\ & \begin{bmatrix} E_1^f & 0 \\ 0 & E_1^\infty \end{bmatrix} & & \\ & & \ddots & \\ & & & \begin{bmatrix} E_{K-1}^f & 0 \\ 0 & E_{K-1}^\infty \end{bmatrix} \end{bmatrix} \begin{bmatrix} Z_1^{-1} & & & \\ & Z_2^{-1} & & \\ & & \ddots & \\ & & & Z_0^{-1} \end{bmatrix} \\
&= \mathcal{W} \begin{bmatrix} \begin{bmatrix} E_0^f & 0 \\ 0 & E_0^\infty \end{bmatrix} & & & \\ & \begin{bmatrix} E_1^f & 0 \\ 0 & E_1^\infty \end{bmatrix} & & \\ & & \ddots & \\ & & & \begin{bmatrix} E_{K-1}^f & 0 \\ 0 & E_{K-1}^\infty \end{bmatrix} \end{bmatrix} \mathcal{Z},
\end{aligned}
\tag{8.19}
$$

where $\mathcal{W} = \text{diag}(W_0^{-1}, W_1^{-1}, \ldots, W_{K-1}^{-1})$ and $\mathcal{Z} = \text{diag}(Z_1^{-1}, Z_2^{-1}, \ldots, Z_0^{-1})$.
Similarly, we have the following representation for $\mathcal{A}$:

$$
\mathcal{A} = \mathcal{W} \begin{bmatrix} & & & \begin{bmatrix} A_0^f & 0 \\ 0 & A_0^\infty \end{bmatrix} \\ \begin{bmatrix} A_1^f & 0 \\ 0 & A_1^\infty \end{bmatrix} & & & \\ & \ddots & & \\ & & \begin{bmatrix} A_{K-1}^f & 0 \\ 0 & A_{K-1}^\infty \end{bmatrix} & \end{bmatrix} \mathcal{Z}. \tag{8.20}
$$

Hence using appropriate permutation matrices Π_1 and Π_2 we can reorder the blocks of

$\lambda\mathcal{E} - \mathcal{A}$ [123] such that

$$\lambda\mathcal{E} - \mathcal{A} = \lambda\mathcal{W}\Pi_1 \left[\begin{array}{ccc|ccc} E_0^f & & & & & \\ & E_1^f & & & & \\ & & \ddots & & & \\ & & E_{K-1}^f & 0 & E_0^\infty & \\ & & & & \ddots & \\ & & & 0 & & E_{K-2}^\infty \\ & & & E_{K-1}^\infty & 0 & 0 \end{array}\right] \Pi_2\mathcal{Z}$$
$$-\mathcal{W}\Pi_1 \left[\begin{array}{ccc|ccc} 0 & & A_0^f & & & \\ A_1^f & & & & & \\ & \ddots & & & & \\ 0 & A_{K-1}^f & 0 & & & \\ & & & A_0^\infty & & \\ & & & & A_1^\infty & \\ & & & & & \ddots \\ & & & & & A_{K-1}^\infty \end{array}\right] \Pi_2\mathcal{Z}. \tag{8.21}$$

Comparing (8.15) and (8.21), we can make the following identifications

$$\mathcal{M} = \mathcal{W}\Pi_1, \quad \mathcal{N} = \Pi_2\mathcal{Z}.$$

Therefore, the spectral projections $\mathcal{P}_l$ and $\mathcal{P}_r$ onto the left and right deflating subspaces of $\lambda\mathcal{E} - \mathcal{A}$ are given by

$$\mathcal{P}_l = \mathcal{M}\begin{bmatrix} I & 0 \\ 0 & 0 \end{bmatrix}\mathcal{M}^{-1}, \quad \mathcal{P}_r = \mathcal{N}^{-1}\begin{bmatrix} I & 0 \\ 0 & 0 \end{bmatrix}\mathcal{N}. \tag{8.22}$$

Now substituting $\mathcal{M}$ and $\mathcal{N}$ from (8.16) into (8.22), we get

$$\mathcal{P}_l = \mathcal{V}\begin{bmatrix} I & \mathbf{Z} \\ 0 & 0 \end{bmatrix}\mathcal{V}^T, \quad \mathcal{P}_r = \mathcal{U}\begin{bmatrix} I & \mathbf{W} \\ 0 & 0 \end{bmatrix}\mathcal{U}^T. \tag{8.23}$$

Hence, setting

$$\mathcal{U}^T\mathcal{G}^{cr}\mathcal{U} = \begin{bmatrix} \mathcal{G}_{11}^{cr} & \mathcal{G}_{12}^{cr} \\ \mathcal{G}_{21}^{cr} & \mathcal{G}_{22}^{cr} \end{bmatrix}, \quad \mathcal{V}^T\mathcal{B} = \begin{bmatrix} \mathcal{B}_{11} \\ \mathcal{B}_{12} \end{bmatrix},$$

we obtain from the PLDALE (8.9) the following system of matrix equations

$$\begin{aligned} \mathcal{A}_f\mathcal{G}_{11}^{cr}\mathcal{A}_f^T - \mathcal{E}_f\mathcal{G}_{11}^{cr}\mathcal{E}_f^T &= -(\mathcal{B}_{11} + \mathbf{Z}\mathcal{B}_{12})(\mathcal{B}_{11} + \mathbf{Z}\mathcal{B}_{12})^T + \mathcal{E}_f\mathcal{G}_{12}^{cr}\mathcal{E}_u^T + \mathcal{E}_u\mathcal{G}_{21}^{cr}\mathcal{E}_f^T + \mathcal{E}_u\mathcal{G}_{22}^{cr}\mathcal{E}_u^T \\ &\quad -\mathcal{A}_f\mathcal{G}_{12}^{cr}\mathcal{A}_u^T - \mathcal{A}_u\mathcal{G}_{21}^{cr}\mathcal{A}_f^T - \mathcal{A}_u\mathcal{G}_{22}^{cr}\mathcal{A}_u^T, \end{aligned} \tag{8.24}$$

$$\mathcal{A}_f\mathcal{G}_{12}^{cr}\mathcal{A}_\infty^T - \mathcal{E}_f\mathcal{G}_{12}^{cr}\mathcal{E}_\infty^T = \mathcal{A}_u\mathcal{G}_{22}^{cr}\mathcal{E}_\infty^T - \mathcal{A}_u\mathcal{G}_{22}^{cr}\mathcal{A}_\infty^T, \tag{8.25}$$

$$\mathcal{A}_\infty\mathcal{G}_{22}^{cr}\mathcal{A}_\infty^T - \mathcal{E}_\infty\mathcal{G}_{22}^{cr}\mathcal{E}_\infty^T = 0. \tag{8.26}$$

Since $\Lambda(\lambda\mathcal{E}_f - \mathcal{A}_f) \cap \Lambda(\lambda\mathcal{E}_\infty - \mathcal{A}_\infty) = \emptyset$, and $\Lambda(\lambda\mathcal{E}_\infty - \mathcal{A}_\infty)$ contains only infinite eigenvalues, we have from (8.26) that

$$\mathcal{G}_{22}^{cr} = 0. \tag{8.27}$$

Hence Equation (8.25) can be simplified to

$$\mathcal{A}_f \mathcal{G}_{12}^{cr} \mathcal{A}_\infty^T - \mathcal{E}_f \mathcal{G}_{12}^{cr} \mathcal{E}_\infty^T = 0. \tag{8.28}$$

It can be easily verified that $\mathcal{G}_{21}^{cr} = (\mathcal{G}_{12}^{cr})^T$ [104] and the solution of (8.28) is given by

$$\mathcal{G}_{12}^{cr} = 0. \tag{8.29}$$

Using (8.27) and (8.29), (8.24) can be simplified and rewritten as

$$\mathcal{A}_f \mathcal{G}_{11}^{cr} \mathcal{A}_f^T - \mathcal{E}_f \mathcal{G}_{11}^{cr} \mathcal{E}_f^T = -(\mathcal{B}_{11} + \mathbf{Z}\mathcal{B}_{12})\,(\mathcal{B}_{11} + \mathbf{Z}\mathcal{B}_{12})^T. \tag{8.30}$$

Therefore, the solution of the generalized PLDALE (8.9) is given by

$$\mathcal{G}^{cr} = \mathcal{U} \begin{bmatrix} \mathcal{G}_{11}^{cr} & \mathcal{G}_{12}^{cr} \\ \mathcal{G}_{21}^{cr} & \mathcal{G}_{22}^{cr} \end{bmatrix} \mathcal{U}^T = \mathcal{U} \begin{bmatrix} \mathcal{G}_{11}^{cr} & 0 \\ 0 & 0 \end{bmatrix} \mathcal{U}^T, \tag{8.31}$$

where $\mathcal{G}_{11}^{cr}$ is the unique symmetric positive semidefinite solution of the generalized periodic Lyapunov equation (8.30). It follows from (8.22) and (8.31) that the solution $\mathcal{G}^{cr}$ satisfies $\mathcal{G}^{cr} = \mathcal{P}_r \mathcal{G}^{cr} \mathcal{P}_r^T$.

Now suppose that $\mathcal{R}_{11}$ is the Cholesky factor of $\mathcal{G}_{11}^{cr}$, i.e., $\mathcal{G}_{11}^{cr} = \mathcal{R}_{11}\mathcal{R}_{11}^T$. If $\text{rank}(\mathcal{R}_{11}) = n_s$ and $n_s < n_f$, then we use *Householder* or *Givens transformations* [43] to compute the full column rank matrix $\mathcal{R}_1$ from the QR decomposition

$$\mathcal{R}_{11}^T = Q_{\mathcal{R}_1} \begin{bmatrix} \mathcal{R}_1^T \\ 0 \end{bmatrix},$$

where $Q_{\mathcal{R}_1} \in \mathbb{R}^{n_f \times n_f}$ and $\mathcal{R}_1 \in \mathbb{R}^{n_f \times n_s}$. Otherwise, $\mathcal{R}_1 = \mathcal{R}_{11}$. Then the full column rank factor $\mathcal{R}^{cr}$ is given by

$$\mathcal{R}^{cr} = \mathcal{U} \begin{bmatrix} \mathcal{R}_1 \\ 0 \end{bmatrix}. \tag{8.32}$$

We summarize the whole precess in Algorithm 8.1. The numerical solution of the generalized PLDALEs (5.37), (5.43), and (5.44) can be treated similarly and following the work in [104].

Remark 8.1 (about Algorithm 8.1):

(i) In Step 1, one may not directly get such a structure using only the GUPTRI algorithm [34, 35]. It requires to multiply the block matrix pencil by two permutation matrices from its right and left sides to get the the structure as in Step 1 (see (8.21)).

Algorithm 8.1 Generalized Schur-Hammarling method for the PLDALE (8.9) and PPDALEs (8.8).

Input: A real d-stable pencil $\lambda\mathcal{E} - \mathcal{A}$ and a real matrix $\mathcal{B}$ (complex case is similar).
Output: Full column rank Cholesky factors R_k^{cr} of the solution $G_k^{cr} = R_k^{cr}(R_k^{cr})^T$ $(k = 0, 1, \ldots, K-1)$.

1: Use the GUPTRI algorithm [34, 35] to compute (8.12), i.e.,

$$\lambda\mathcal{E} - \mathcal{A} = \mathcal{V}\begin{bmatrix} \lambda\mathcal{E}_f - \mathcal{A}_f & \lambda\mathcal{E}_u - \mathcal{A}_u \\ 0 & \lambda\mathcal{E}_\infty - \mathcal{A}_\infty \end{bmatrix}\mathcal{U}^T,$$

where $\mathcal{U}, \mathcal{V}$ are orthogonal matrices, $\mathcal{E}_f, \mathcal{A}_f \in \mathbb{R}^{n_f \times n_f}$, $\mathcal{E}_\infty, \mathcal{A}_\infty \in \mathbb{R}^{n_\infty \times n_\infty}$ as in (8.17) and (8.18), respectively.

2: Compute the generalized Sylvester equation

$$\begin{aligned} \mathcal{E}_f\mathbf{W} - \mathbf{Z}\mathcal{E}_\infty &= \mathcal{E}_u, \\ \mathcal{A}_f\mathbf{W} - \mathbf{Z}\mathcal{A}_\infty &= \mathcal{A}_u. \end{aligned}$$

3: Compute the matrix

$$\mathcal{V}^T\mathcal{B} = \begin{bmatrix} \mathcal{B}_{11} \\ \mathcal{B}_{12} \end{bmatrix}.$$

4: Use the generalized Hammarling method [50, 104] to compute the Cholesky factor $\mathcal{R}_{11}$ of the solution $\mathcal{G}_{11}^{cr} = \mathcal{R}_{11}(\mathcal{R}_{11})^T$ of the PLDALE (8.11)

$$\mathcal{A}_f\mathcal{G}_{11}^{cr}\mathcal{A}_f^T - \mathcal{E}_f\mathcal{G}_{11}^{cr}\mathcal{E}_f^T = -(\mathcal{B}_{11} + \mathbf{Z}\mathcal{B}_{12})\,(\mathcal{B}_{11} + \mathbf{Z}\mathcal{B}_{12})^T.$$

5: If rank$(\mathcal{R}_{11})$= $n_s < n_f$, then use the *Householder* or *Givens transformations* [43] to compute the full column rank matrix $\mathcal{R}_1$ from the QR decomposition

$$\mathcal{R}_{11}^T = Q_{\mathcal{R}_1}\begin{bmatrix} \mathcal{R}_1^T \\ 0 \end{bmatrix},$$

where $Q_{\mathcal{R}_1} \in \mathbb{R}^{n_f \times n_f}$ and $\mathcal{R}_1 \in \mathbb{R}^{n_f \times n_s}$. Otherwise, $\mathcal{R}_1 = \mathcal{R}_{11}$.

6: Compute the full column rank factor $\mathcal{R}^{cr}$ given by

$$\mathcal{R}^{cr} = \mathcal{U}\begin{bmatrix} \mathcal{R}_1 \\ 0 \end{bmatrix}.$$

7: Identify the full column rank periodic factors R_k^{cr} from $\mathcal{R}^{cr}$, where

$$\mathcal{R}^{cr} = \text{diag}(R_1^{cr}, \ldots, R_{K-1}^{cr}, R_0^{cr}),$$

and $G_k^{cr} = R_k^{cr}(R_k^{cr})^T$ for $k = 0, 1, \ldots, K-1$.

(ii) Step 6 needs to be computed more technical way such that the periodic factors $R_k^{cr} \in \mathbb{R}^{n_k \times n_k^f}$ receive full column rank and $G_k^{cr} = R_k^{cr}(R_k^{cr})^T \in \mathbb{R}^{n_k \times n_k}$ $(k = 0, 1, \ldots, K-1)$. One can also follow the explicit formulations (not in lifted form) of these periodic factors of Step 6 from [30] (see Steps 5 and 6, Algorithm 5.1 therein).

The full column rank Cholesky factors computed using Algorithm 8.1 preserve the block diagonal structure of their original lifted Gramians. For the computed Cholesky factor using Algorithm 8.1, we have

$$\mathcal{G}^{cr} = \mathcal{R}^{cr}(\mathcal{R}^{cr})^T = \operatorname{diag}(R_1^{cr}(R_1^{cr})^T, \ldots, R_{K-1}^{cr}(R_{K-1}^{cr})^T, R_0^{cr}(R_0^{cr})^T),$$

where $G_k^{cr} = R_k^{cr}(R_k^{cr})^T$ and R_k^{cr} are the full column rank Cholesky factors of the periodic Gramians G_k^{cr} for $k = 0, 1, \ldots, K-1$. The same holds true for the solutions of the generalized PLDALEs (5.37), (5.43), and (5.44).

Remark 8.2:

We generalize the Schur-Hammarling method from [50, 104] to our periodic discrete-time case in lifted form. A solution technique which deals directly with the periodic matrix equations (not in lifted form) has been proposed in [30]. Solving the periodic Sylvester equations and the periodic projected Lyapunov equations in that proposed algorithm are the most computational expensive tasks, especially when the system has periodic matrix pairs with time varying-dimensions, and the input and output are also time-varying (see, Algorithm 5.1 of [30]). On the other hand, our proposed method, which works with the lifted forms of the periodic matrix equations, can handle those time-varying periodic matrix pairs even if all E_k (or at least one E_k) are singular and also the time-varying input and output very easily during the solution process. ◊

8.4. Hankel Singular Values

Analogous to the standard periodic discrete-time systems [121] and continuous-time descriptor systems [106, 75], the reachability and observability Gramians of the periodic discrete-time descriptor system (8.1) can be used to define the periodic *Hankel singular values* of system (8.1). These Hankel singular values are then used find a reduced-order model of (8.1) using the balanced truncation method. Analogous to continuous-time descriptor systems [106, 75], the following result holds for system (8.1).

Theorem 8.4.1:

[30] *Let the periodic matrix pairs* $\{(E_k, A_k)\}_{k=0}^{K-1}$ *be pd-stable. Then the causal and noncausal matrices* $M_k^c = G_k^{cr} E_{k-1}^T G_k^{co} E_{k-1}$ *and* $M_k^{nc} = G_k^{ncr} A_k^T G_{k+1}^{nco} A_k$, $k = 0, 1, \ldots, K-1$, *have real and nonnegative eigenvalues.* ◊

Proof. We sketch the proof from [30] to show that the fundamental matrices defined for the forward and backward subsystems in (4.68) are directly linked to the Hankel singular values of the periodic discrete-time descriptor system (8.1). Let us consider the periodic Gramians defined in Chapter 4, Section 4.3.2. Using the definitions of G_k^{cr} and G_k^{co}, we can write

$$M_k^c = \sum_{j=-\infty}^{k-1} \Psi_{k,j} B_j B_j^T \Psi_{k,j}^T E_{k-1}^T \sum_{j=k}^{\infty} \Psi_{j,k-1}^T C_j^T C_j \Psi_{j,k-1} E_{k-1} \tag{8.33}$$

Now using the forward fundamental matrices defined in (4.68), we can represent (8.33) more simply as

$$M_k^c = Z_k \begin{bmatrix} \bar{G}_{1,k}^{cr} \bar{G}_{1,k}^{co} & 0 \\ 0 & 0 \end{bmatrix} Z_k^{-1}, \tag{8.34}$$

where

$$\begin{aligned} \bar{G}_{1,k}^{cr} &= \textstyle\sum_{i=-\infty}^{k-1} \Phi_f(k, i+1) B_i^f (B_i^f)^T \Phi_f(k, i+1)^T, \\ \bar{G}_{1,k}^{co} &= \textstyle\sum_{i=k}^{\infty} \Phi_f(i,k)^T (C_i^f)^T C_i^f \Phi_f(i,k). \end{aligned}$$

The matrices $\bar{G}_{1,k}^{cr}$ and $\bar{G}_{1,k}^{co}$ are symmetric positive semidefinite (see the proof of Theorem 4.3.6 in Chapter 4 for details), hence the matrices M_k^c for $k = 0, 1, \ldots, K-1$, have real nonnegative eigenvalues. Similarly, we can show that all M_k^{nc} have real and nonnegative eigenvalues. □

The real nonnegative eigenvalues of M_k^c and M_k^{nc} are used to define the causal and noncausal Hankel singular values of system (8.1).

Definition 8.4.1:

Let the set of periodic matrix pairs $\{(E_k, A_k)\}_{k=0}^{K-1}$ be pd-stable. For $k = 0, 1, \ldots, K-1$, the square roots of the largest n_k^f eigenvalues of the matrix M_k^c, denoted by $\sigma_{k,j}$, are called the *causal Hankel singular values* and the square roots of the largest n_k^∞ eigenvalues of M_k^{nc}, denoted by $\theta_{k,j}$, are called the *noncausal Hankel singular values* of the periodic descriptor system (8.1). ◊

Similar to continuous-time descriptor systems, the causal and noncausal Hankel singular values of the periodic descriptor system (8.1) are invariant under system equivalence transformation. For a completely reachable and completely observable periodic system (8.1), the ranks of the matrices G_k^{cr} and G_k^{co} equal n_k^f, which is also the rank of M_k^c. Also the ranks of G_k^{ncr} and G_k^{nco} equal n_k^∞, which is then also the rank of M_k^{nc}, for $k = 0, 1, \ldots, K-1$.

Since the causal and noncausal reachability and observability Gramians are symmetric and positive semidefinite, there exist the Cholesky factorizations

$$G_k^{cr} = R_k R_k^T, \quad G_k^{co} = L_k^T L_k, \quad G_k^{ncr} = \check{R}_k \check{R}_k^T, \quad G_k^{nco} = \check{L}_k^T \check{L}_k. \tag{8.35}$$

Simple calculations [30] show that

$$\begin{aligned} \sigma_{k,j} &= \sqrt{\lambda_j(G_k^{cr}E_{k-1}^T G_k^{co}E_{k-1})} = \zeta_j(L_k E_{k-1} R_k), \\ \theta_{k,j} &= \sqrt{\lambda_j(G_k^{ncr}A_k^T G_{k+1}^{nco}A_k)} = \zeta_j(\check{L}_{k+1} A_k \check{R}_k), \end{aligned} \tag{8.36}$$

where $\lambda_j(.)$ and $\zeta_j(.)$ denote the eigenvalues and singular values of the corresponding product matrix, and $\sigma_{k,j}$ and $\theta_{k,j}$ are the *causal and noncausal Hankel singular values* of the periodic descriptor system (8.1), respectively.

8.5. Balanced Truncation Model Reduction

Model order reduction (MOR) is an approach, where the original system is approximated by a reduced-order system that is in some measure close to the original model. For system (8.1), a reduced-order model of dimension r would be a system of the form

$$\begin{aligned} \tilde{E}_k \tilde{x}_{k+1} &= \tilde{A}_k \tilde{x}_k + \tilde{B}_k u_k, \\ \tilde{y}_k &= \tilde{C}_k \tilde{x}_k, \qquad k \in \mathbb{Z}, \end{aligned} \tag{8.37}$$

where $\tilde{E}_k \in \mathbb{R}^{\gamma_{k+1}\times r_{k+1}}$, $\tilde{A}_k \in \mathbb{R}^{\gamma_{k+1}\times r_k}$, $\tilde{B}_k \in \mathbb{R}^{\gamma_{k+1}\times p_k}$, $\tilde{C}_k \in \mathbb{R}^{q_k\times r_k}$ are K-periodic matrices, $\sum_{k=0}^{K-1}\gamma_k = \sum_{k=0}^{K-1} r_k = r$ and $r \ll n$. Apart from having a much smaller state-space dimension, it is also important that the reduced-order model preserves physical properties of the original system such as regularity and stability, and that the approximation error is small. In this section, we present a generalization of a balanced truncation model reduction method to periodic descriptor systems.

8.5.1. Balancing of Periodic Descriptor Systems

For a balanced system, the reachability and observability Gramians are both equal to a diagonal matrix [76, 108]. Balanced truncation for periodic standard discrete-time systems has been considered in [37, 121]. An extension of such important concepts as balanced realization and Hankel singular values to periodic descriptor systems has been presented in [30]. We will follow here the derivation in [30].

Definition 8.5.1:
A realization (E_k, A_k, B_k, C_k) of a periodic descriptor system (8.1) is called *balanced* if

$$G_k^{cr} = G_k^{co} = \begin{bmatrix} \Sigma_k & 0 \\ 0 & 0 \end{bmatrix}, \quad G_k^{ncr} = G_{k+1}^{nco} = \begin{bmatrix} 0 & 0 \\ 0 & \Theta_k \end{bmatrix},$$

where $\Sigma_k = \operatorname{diag}(\sigma_{k,1}, \ldots, \sigma_{k,n_k^f})$ and $\Theta_k = \operatorname{diag}(\theta_{k,1}, \ldots, \theta_{k,n_k^\infty})$, $k = 0, 1, \ldots, K-1$. ◊

Consider the Cholesky factorizations (8.35) of the reachability and observability Gramians [30] and let

$$L_k E_{k-1} R_k = U_k \Sigma_k V_k^T, \quad \check{L}_{k+1} A_k \check{R}_k = \check{U}_k \Theta_k \check{V}_k^T \tag{8.38}$$

be the singular value decompositions of the matrices $L_k E_{k-1} R_k$ and $\check{L}_{k+1} A_k \check{R}_k$ for $k = 0, 1, \ldots, K-1$. Here $U_k, V_k, \check{U}_k, \check{V}_k$ are orthogonal, and Σ_k and Θ_k are diagonal. Moreover, we can can easily show from Theorem 4.3.5 and Equation (4.64) that

$$\begin{aligned}
&G_k^{cr} = P_r(k) G_k^{cr} P_r(k)^T, \quad G_k^{co} = P_l(k-1)^T G_k^{co} P_l(k-1), \\
&P_r(k) G_k^{ncr} = 0, \quad G_k^{nco} P_l(k-1) = 0, \\
&E_{k-1} P_r(k) = P_l(k-1) E_{k-1}, \quad A_k P_r(k) = P_l(k) A_k.
\end{aligned}$$

Then using these relations, we have for $k = 0, 1, \ldots, K-1$, that

$$G_k^{nco} E_{k-1} G_k^{cr} = G_k^{co} E_{k-1} G_k^{ncr} = 0, \quad G_{k+1}^{nco} A_k G_k^{cr} = G_{k+1}^{co} A_k G_k^{ncr} = 0,$$

which also imply

$$\check{L}_k E_{k-1} R_k = 0, \quad L_k E_{k-1} \check{R}_k = 0, \quad \check{L}_{k+1} A_k R_k = 0, \quad L_{k+1} A_k \check{R}_k = 0,$$

for $k = 0, 1, \ldots, K-1$.

If a realization $\mathbf{\Sigma}(E_k, A_k, B_k, C_k)$ with pd-stable matrix pairs $\{(E_k, A_k)\}_{k=0}^{K-1}$ is minimal, i.e., Σ_k and Θ_k are nonsingular, then there exist nonsingular periodic matrices $S_k \in \mathbb{R}^{\mu_{k+1} \times \mu_{k+1}}$ and $T_k \in \mathbb{R}^{n_k \times n_k}$ defined as

$$S_k = [L_{k+1}^T U_{k+1} \Sigma_{k+1}^{-1/2}, \ \check{L}_{k+1}^T \check{U}_k \Theta_k^{-1/2}], \quad T_k = [R_k V_k \Sigma_k^{-1/2}, \ \check{R}_k \check{V}_k \Theta_k^{-1/2}], \tag{8.39}$$

such that the transformed realization

$$(S_k^T E_k T_{k+1}, S_k^T A_k T_k, S_k^T B_k, C_k T_k) \tag{8.40}$$

is balanced [30]. Note that as in the case of standard state space systems, the balancing transformation matrices for periodic discrete-time descriptor system (8.1) are not unique.

8.5.2. Model Reduction

Model reduction via balanced truncation is discussed very widely for standard discrete-time periodic systems [57, 121] and also for continuous-time descriptor systems [75, 108]. For a balanced system, truncation of states related to the small causal Hankel singular values does not change system properties essentially. Unfortunately, we can not do the same for the noncausal Hankel singular values. If we truncate the states that correspond to the small non-zero noncausal Hankel singular values, then the pencil for the reduced-order system may get finite eigenvalues outside the unit circle that will lead to additional errors in the system approximation. Therefore, we truncate only the

zero noncausal Hankel singular values and all the non-zero noncausal Hankel singular values are kept unaltered (without any truncation).

Assume that the periodic matrix pairs $\{(E_k, A_k)\}_{k=0}^{K-1}$ are pd-stable. Consider the Cholesky factorizations in (8.35). Let

$$L_k E_{k-1} R_k = [U_{k,1}, U_{k,2}] \begin{bmatrix} \Sigma_{k,1} & \\ & \Sigma_{k,2} \end{bmatrix} [V_{k,1}, V_{k,2}]^T, \quad \check{L}_{k+1} A_k \check{R}_k = \check{U}_k \Theta_k \check{V}_k^T, \tag{8.41}$$

be singular value decompositions of $L_k E_{k-1} R_k$ and $\check{L}_{k+1} A_k \check{R}_k$, where

$$\Sigma_{k,1} = \mathrm{diag}(\sigma_{k,1}, \ldots, \sigma_{k,r_k^f}), \quad \Sigma_{k,2} = \mathrm{diag}(\sigma_{k,r_{k+1}^f}, \ldots, \sigma_{n_k^f}),$$

with $\sigma_{k,1} \geq \cdots \geq \sigma_{k,r_k^f} > \sigma_{k,r_{k+1}^f} \geq \ldots \geq \sigma_{k,n_k^f} > 0$, and $\Theta_k = \mathrm{diag}(\theta_{k,1}, \ldots, \theta_{k,r_k^\infty})$ is nonsingular for $k = 0, 1, \ldots, K-1$. Note that for MOR, $\sigma_{k,n_k^f} = 0$ is possible and allowed, although for such a case balancing transformation does not exist.

Similar to continuous-time descriptor systems [108], the number of non-zero noncausal Hankel singular values of (8.1) for $k = 0, 1, \ldots, K-1$ is equal to

$$r_k^\infty = \mathrm{rank}(\hat{L}_{k+1} A_k \hat{R}_k) \leq \min(\nu_k p_k, \nu_k q_k, n_k^\infty), \tag{8.42}$$

where ν_k are the indices of the regular set of periodic matrix pairs $\{(E_k, A_k)\}_{k=0}^{K-1}$. This estimate shows that if for $k = 0, 1, \ldots, K-1$, the nilpotency index ν_k of a regular periodic matrix pair $\{(E_k, A_k)\}_{k=0}^{K-1}$ times the number p_k of inputs or the number q_k of the outputs is much smaller than the dimension n_k^∞ of its k-th periodic deflating subspace corresponding to the infinite eigenvalues, then the order of system (8.1) can be reduced significantly.

The reduced-order system can be computed as [30]

$$\tilde{E}_k = S_{k,r}^T E_k T_{k+1,r}, \quad \tilde{A}_k = S_{k,r}^T A_k T_{k,r}, \quad \tilde{B}_k = S_{k,r}^T B_k, \quad \tilde{C}_k = C_k T_{k,r}, \tag{8.43}$$

where

$$\begin{aligned} S_{k,r} &= [\, L_{k+1}^T U_{k+1,1} \Sigma_{k+1,1}^{-1/2}, \ \check{L}_{k+1}^T \check{U}_k \Theta_k^{-1/2} \,] \in \mathbb{R}^{\mu_{k+1}, r_{k+1}}, \\ T_{k,r} &= [\, R_k V_{k,1} \Sigma_{k,1}^{-1/2}, \quad \check{R}_k \check{V}_k \Theta_k^{-1/2} \,] \in \mathbb{R}^{n_k, r_k}, \end{aligned}$$

with $r_k = r_k^f + r_k^\infty$.

Let $\tilde{\mathcal{H}}(z)$ be the transfer function of the reduced-order lifted system formed from the reduced-order subsystems in (8.43). Since our model reduction approach does not truncate any nonzero state from the noncausal Hankel singular values, the error bound for the reduced system will be defined over the causal part of the original and reduced-order transfer functions. Also the reduced-order system computed by this method is stable and balanced. Hence the error bound can be obtained similarly to the standard

periodic state space case [61, 121, 60]. Then we have the following $\mathbb{H}_\infty$-norm error bound

$$\|\mathcal{H} - \tilde{\mathcal{H}}\|_{\mathbb{H}_\infty} = \sup_{\omega\in[0,2\pi]} \|\mathcal{H}(e^{i\omega}) - \tilde{\mathcal{H}}(e^{i\omega})\|_2 \leq 2\,\mathrm{trace}\,(\mathrm{diag}(\Sigma_{0,2}, \ldots, \Sigma_{K-1,2})), \tag{8.44}$$

where $\|.\|_2$ denotes the spectral matrix norm and $\Sigma_{k,2}$, $k = 0, 1, \ldots, K-1$, contains the truncated causal Hankel singular values.

8.6. Numerical Results

In this section we consider numerical examples to illustrate the reliability of the proposed model reduction method for periodic time-varying discrete-time descriptor systems. For such systems we solve the periodic projected Lyapunov equations (i.e., the PPDALEs in Theorem 4.3.5) using their corresponding lifted forms (i.e., the PLDALEs in Theorem 5.2.4 and 5.2.5) that we have discussed in Section 9.3. The solutions of these projected lifted Lyapunov equations have specific block diagonal structure and the diagonal blocks of these lifted solutions correspond to the solutions of the periodic projected Lyapunov equations (see, Theorems 5.2.4 and 5.2.5, and the proofs therein). We pick up the periodic Gramians, i.e., $G_k^{cr}, G_k^{ncr}, G_k^{co}$, and G_k^{nco}, $k = 0, 1, \ldots, K-1$, from the block diagonal solutions of these projected lifted Lyapunov equations, i.e., from $\mathcal{G}^{cr}, \mathcal{G}^{ncr}, \mathcal{G}^{co}$, and $\mathcal{G}^{nco}$, respectively. These periodic Gramians are used to find a balanced realization of the periodic time-varying discrete-time descriptor systems using the procedure described in [30]. Finally, a balancing based model reduction method is discussed and a reduced-order model is obtained by the algorithms that we have described in Section 9.5. Note that for MOR, it is not necessary to find a balanced realization of the periodic time-varying discrete-time descriptor systems explicitly. One can omit the explicit formulation of the balancing steps for MOR.

We consider here two artificial problems because real life problems were very difficult to collect from prescribed application fields. The first test example is a small dimensional problem taken from [30], and the second test problem is a self-generated artificial problem.

8.6.1. Model Problem 1

We consider a periodic discrete-time descriptor system with $\mu_k = n_k = 10$, $p_k = 2$, $q_k = 3$, and period $K = 3$ as presented in [30, Example 1]. The periodic matrix pairs $\{(E_k, A_k)\}_{k=0}^{K-1}$ are pd-stable with $n_k^f = 8$ and $n_k^\infty = 2$ for $k = 0, 1, 2$. The original lifted system has order $n = 30$. The sparsity patterns of $\mathcal{E}$ and $\mathcal{A}$ of the corresponding lifted system are plotted in Figure 8.1.

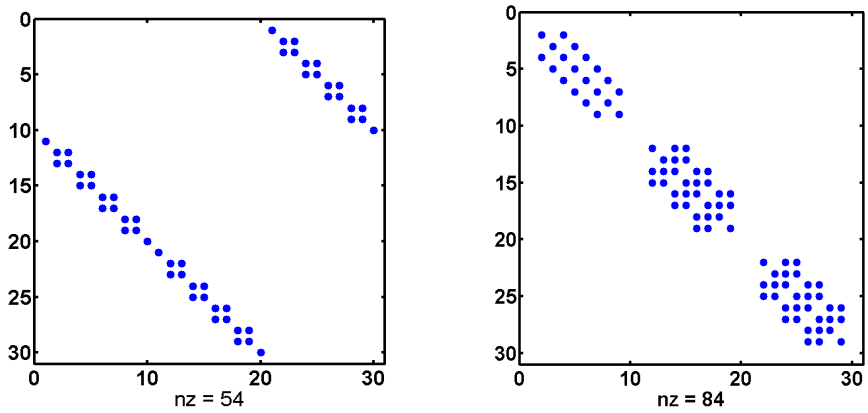

(a) (b)

Figure 8.1. (a) Sparsity pattern of $\mathcal{A}$, (b) sparsity pattern of $\mathcal{E}$ (Model problem 1).

The norms of the computed solutions of the periodic Lyapunov equations and the corresponding residuals, e.g.,

$$\rho_k^{cr} \quad = \quad \|A_k G_k^{cr} A_k^T - E_k G_{k+1}^{cr} E_k^T + P_l(k) B_k B_k^T P_l(k)^T\|_2, \tag{8.45}$$

are shown in Table 8.1 and Table 8.2.

Table 8.1. Norms and absolute residuals for the reachability Gramians (Model problem 1)

k	$\| G_k^{cr} \|_2$	ρ_k^{cr}	$\| G_k^{ncr} \|_2$	ρ_k^{ncr}
0	5.8182×10^2	6.1727×10^{-12}	1.3946×10^1	1.5444×10^{-14}
1	8.2981×10^4	8.2172×10^{-12}	1.3660×10^1	1.7508×10^{-14}
2	7.1107×10^3	3.0961×10^{-12}	1.4308×10^1	3.3847×10^{-14}

Table 8.2. Norms and absolute residuals for the observability Gramians (Model problem 1)

k	$\| G_k^{co} \|_2$	ρ_k^{co}	$\| G_k^{nco} \|_2$	ρ_k^{nco}
0	9.7353×10^1	2.7678×10^{-13}	1.6866×10^0	1.3372×10^{-15}
1	1.1373×10^3	7.7003×10^{-14}	1.7406×10^0	2.1113×10^{-15}
2	9.6984×10^0	1.7859×10^{-14}	1.6866×10^0	1.1626×10^{-15}

Figure 8.2 shows the causal Hankel singular values of the different subsystems for $k = 0, 1, 2$. We see that they decay gradually, and, hence the system (8.1) can be well approximated by a reduced-order model. We have 24 causal Hankel singular values

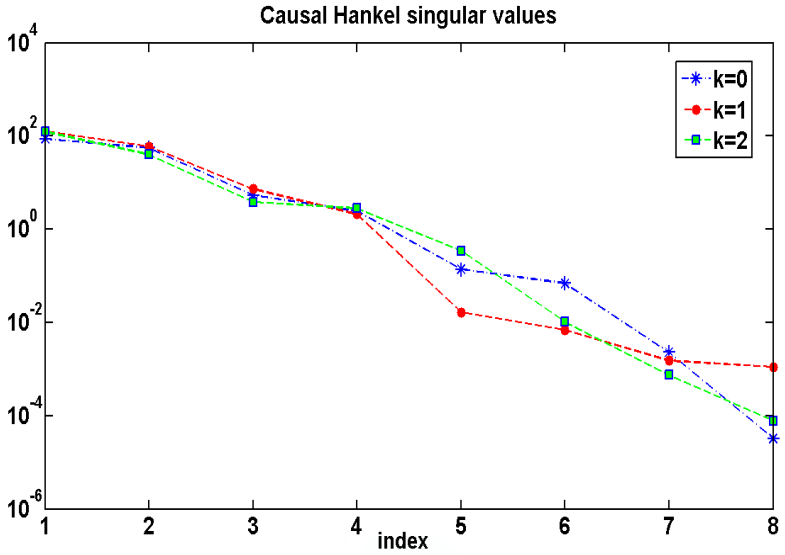

Figure 8.2. Causal Hankel singular values for different subsystems (Model problem 1).

for the original lifted system and the remaining 6 are noncausal Hankel singular values which are positive. We approximate system (8.1) to the tolerance 10^{-2} by truncating the states corresponding to the smallest 7 causal Hankel singular values.

The computed reduced-order model has subsystems of orders, $r = (7, 8, 8)$. Figure 8.3 shows the finite eigenvalues of the original and reduced-order lifted systems. We observe that stability is preserved for the reduced-order system.

In Figure 8.4, we present the norms of the frequency responses $\mathcal{H}(e^{i\omega})$ and $\tilde{\mathcal{H}}(e^{i\omega})$ of the original and reduced-order lifted systems for a frequency range $[0, 2\pi]$. We observe nice match of the system norms.

In Figure 8.5, we display the absolute error $\|\mathcal{H}(e^{i\omega}) - \tilde{\mathcal{H}}(e^{i\omega})\|_2$ and the error bound (8.44). One can see that the absolute error is smaller than the error bound. Note that the absolute error curve is flat in Figure 8.5. This is due to the reason that the absolute error $\|\mathcal{H}(e^{i\omega}) - \tilde{\mathcal{H}}(e^{i\omega})\|_2$ computed at different frequency points in the frequency range $[0, 2\pi]$ lies between 6.91×10^{-3} and 6.92×10^{-3}. These small absolutes errors produce almost a flat line in the frequency range $[0, 2\pi]$.

8.6.2. Model Problem 2

Model problem 2 is an artificial periodic discrete-time descriptor system with $\mu_k = n_k = 404$, $p_k = 10$, $q_k = 15$, and period $K = 10$. The periodic matrices E_k and A_k are dense matrices for each $k = 0, 1, \ldots, 9$. The matrix pairs $\{(E_k, A_k)\}_{k=0}^{K-1}$ are pd-stable with $n_k^f = 400$ and $n_k^\infty = 4$ for every $k = 0, 1, \ldots, 9$. The original lifted system has order $n = 4040$. The

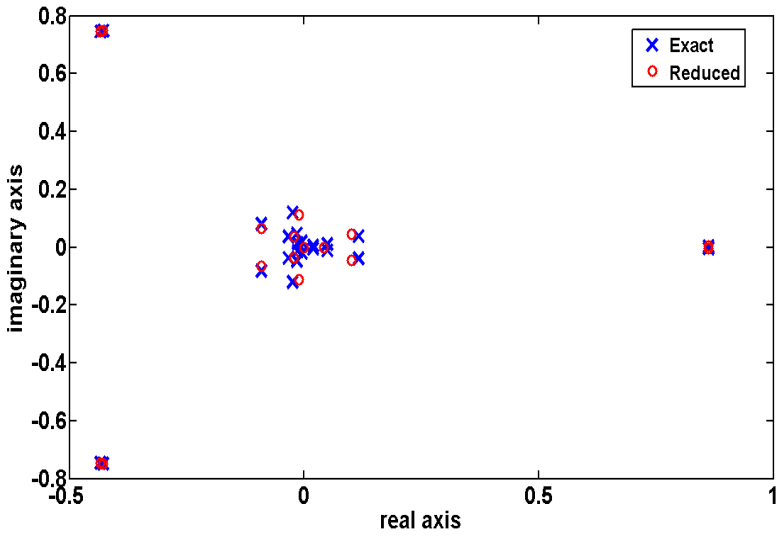

Figure 8.3. Finite eigenvalues of the original and the reduced-order lifted systems (Model problem 1).

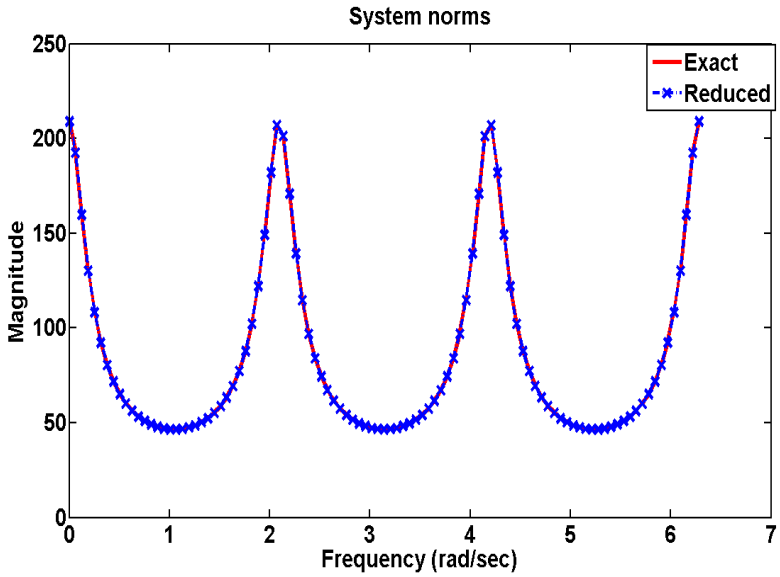

Figure 8.4. The frequency responses of the original and the reduced-order lifted systems (Model problem 1).

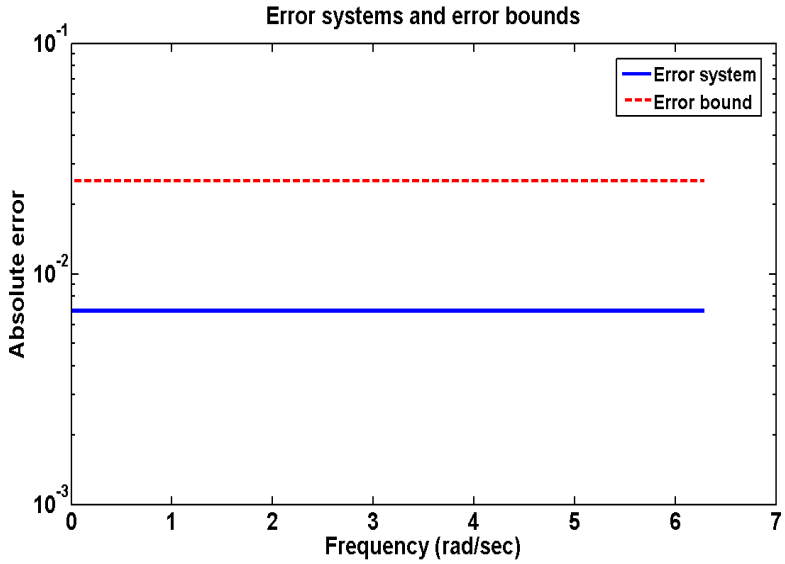

Figure 8.5. Absolute error and error bound (Model problem 1).

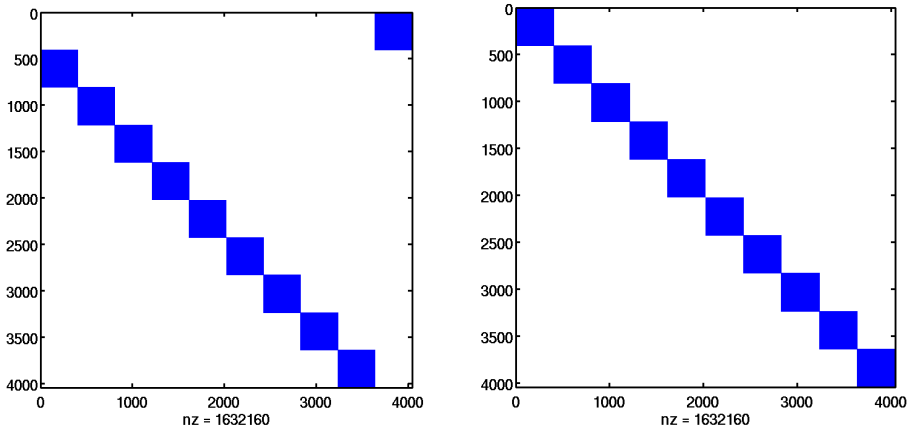

(a) (b)

Figure 8.6. (a) Sparsity pattern of $\mathcal{A}$, (b) sparsity pattern of $\mathcal{E}$ (Model problem 2).

sparsity patterns of $\mathcal{E}$ and $\mathcal{A}$ of the corresponding lifted system are plotted in Figure 8.6.

The norms of the computed solutions of the periodic Lyapunov equations and the corresponding residuals are shown in Table 8.3. Similar results also hold for the observability Gramians.

We compute the causal Hankel singular values of the original system in lifted form. These Hankel singular values are the combination of all the Hankel singular values given by different subsystems, for $k = 0, 1, \ldots, 9$. The Hankel singular values decay fast, and, hence the original system can be well approximated by a reduced-order model. We

Table 8.3. Norms and absolute residuals for the approximate Gramians (Model problem 2)

k	$\| G_k^{cr} \|_2$	ρ_k^{cr}	$\| G_k^{ncr} \|_2$	ρ_k^{ncr}
0	2.009×10^{0}	9.123×10^{-11}	1.094×10^{0}	9.103×10^{-12}
1	2.122×10^{1}	4.247×10^{-10}	2.655×10^{0}	1.563×10^{-12}
2	8.803×10^{0}	1.303×10^{-10}	2.701×10^{-1}	1.300×10^{-13}
3	2.337×10^{0}	1.518×10^{-11}	4.587×10^{-1}	3.289×10^{-13}
4	2.698×10^{0}	1.193×10^{-11}	1.390×10^{0}	2.726×10^{-12}
5	4.765×10^{0}	1.910×10^{-10}	4.856×10^{0}	2.084×10^{-11}
6	8.876×10^{1}	6.688×10^{-10}	1.137×10^{1}	2.887×10^{-12}
7	3.786×10^{1}	1.345×10^{-10}	6.047×10^{-1}	1.441×10^{-13}
8	1.146×10^{1}	1.267×10^{-11}	3.415×10^{-1}	2.074×10^{-13}
9	3.776×10^{0}	8.574×10^{-12}	3.464×10^{-1}	1.680×10^{-12}

have 4000 causal Hankel singular values for the original lifted system and the remaining 40 are noncausal Hankel singular values which are positive. We plot them in Figure 8.8.

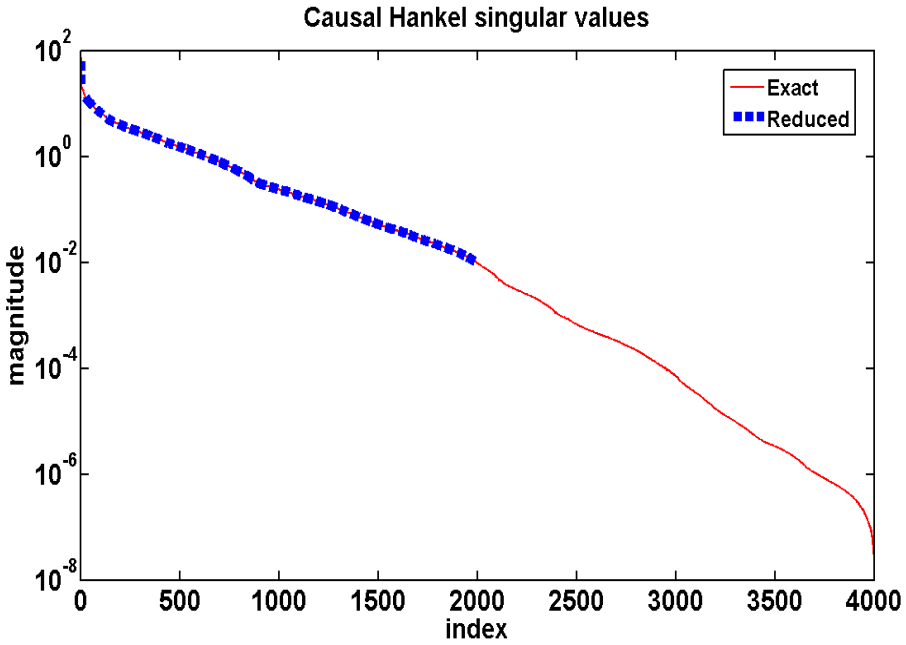

Figure 8.7. Causal Hankel singular values for original and reduced-order lifted systems (Model problem 2).

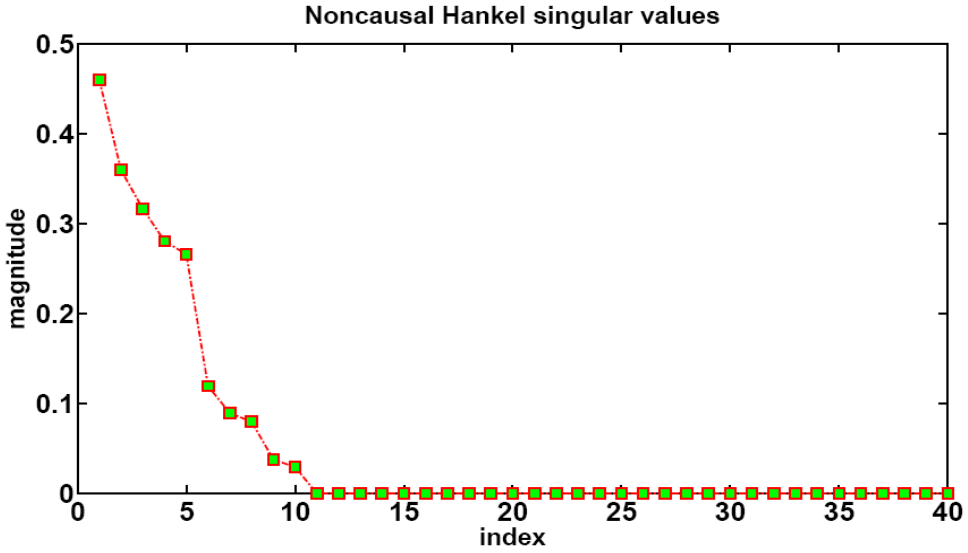

Figure 8.8. Noncausal Hankel singular values for original and reduced-order lifted systems (Model problem 2).

We approximate the original system to the tolerance 10^{-2} by truncating the states corresponding to the smallest 2007 causal Hankel singular values. For different subsystems, the numbers of the computed non-zero noncausal Hankel singular values are the same and $r_k^{\infty} = 4$ for $k = 0, 1, \ldots, 9$. The computed reduced-order model has subsystems of order, $r = (192, 197, 228, 232, 220, 192, 186, 194, 195, 197)$. The causal Hankel singular values for original and reduced-order lifted systems are plotted in Figure 8.7.

Figure 8.9 shows the finite eigenvalues of the original and reduced-order lifted systems. One can see that stability is preserved for the reduced-order system.

In Figure 8.10, we present the norms of the frequency responses $\mathcal{H}(e^{i\omega})$ and $\tilde{\mathcal{H}}(e^{i\omega})$ of the original and reduced-order lifted systems for a frequency range $[0, 2\pi]$. We observe a nice match of the system norms. In Figure 8.11, we display the absolute error $\|\mathcal{H}(e^{i\omega}) - \tilde{\mathcal{H}}(e^{i\omega})\|_2$ and the error bound (8.44). One can see that the absolute error is smaller than the error bound.

To investigate the efficiency of the reduced-order system, we plot the frequency responses and the deviation of the frequency responses for the individual component of the transfer function $\mathcal{H}(e^{i\omega})$ and $\tilde{\mathcal{H}}(e^{i\omega})$ in Figure 8.12. For example, Figure 8.12(a) shows the magnitudes of the frequency responses of original (full) and the reduced-order model for $\mathcal{H}_{10,1}(e^{i\omega})$ and $\tilde{\mathcal{H}}_{10,1}(e^{i\omega})$, and Figure 8.12(b) shows their deviation. Similarly, we plot the frequency responses for the other component of $\mathcal{H}(e^{i\omega})$ and $\tilde{\mathcal{H}}(e^{i\omega})$.

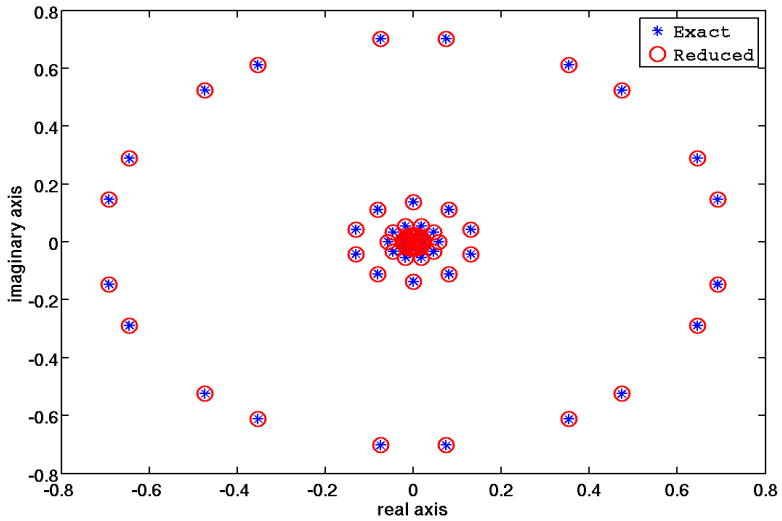

Figure 8.9. Finite eigenvalues of the original and the reduced-order lifted systems (Model problem 2).

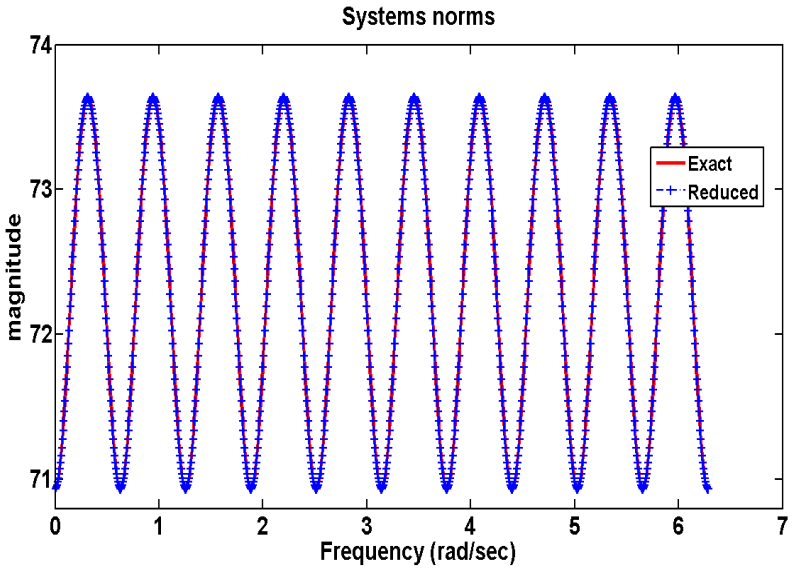

Figure 8.10. The frequency responses of the original and the reduced-order lifted systems (Model problem 2).

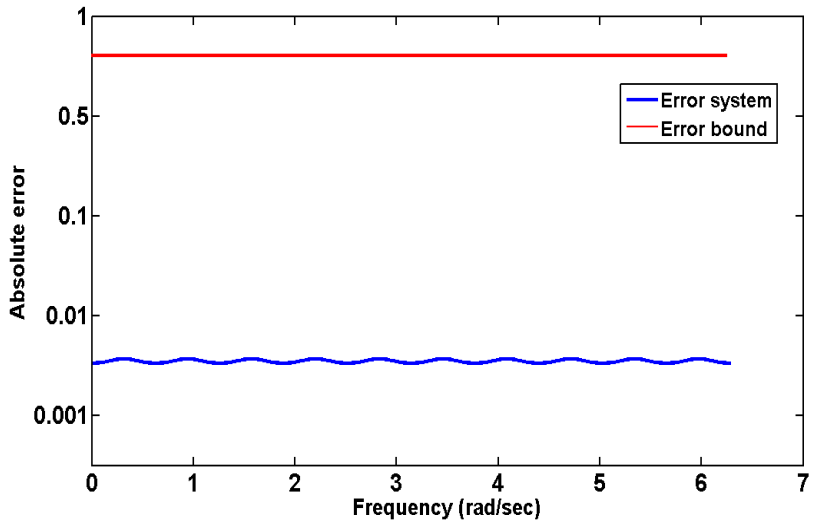

Figure 8.11. Absolute error and error bound (Model problem 2).

8.7. Discussion

In this chapter, we have considered the reachability and observability Gramians as well as Hankel singular values for periodic discrete-time descriptor systems. For such systems, a balanced truncation model reduction method has been presented. We solve the periodic projected Lyapunov equations via their corresponding lifted representations which can handle the time-varying periodic matrix pairs and the time-varying input and output very easily during the solution process. The solutions of these projected lifted Lyapunov equations have specific block diagonal structures and the diagonal blocks of these lifted solutions are the solutions of the periodic projected Lyapunov equations (i.e, the periodic Gramians). These periodic Gramians are then used to find a reduced-order model of the original system.

The proposed balanced truncation model reduction method delivers a reduced-order model that preserves the regularity and stability properties of the original system. A computable global error bound for the approximate system is also available.

The main drawback of this method is that one has to solve the large dimensional PLDALEs which has the computational complexity of $\mathcal{O}(K\bar{n}^3)$, where $\bar{n} = \max(\mu_k, n_k)$. Therefore, the proposed direct method (dense computation) is suitable for problems of small and medium size. For large dimensional problems, we will introduce an efficient iterative method to compute the approximate solutions of the resulting very large dimensional PLDALEs in Chapter 9.

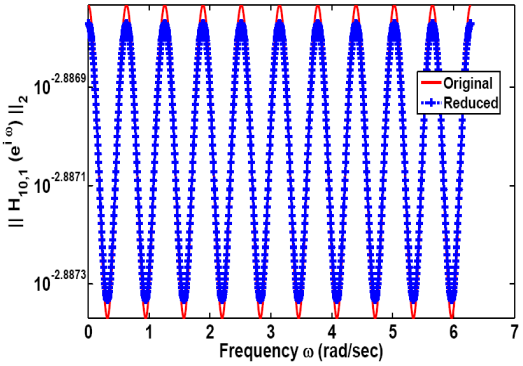

(a) Frequency responses for $\mathcal{H}_{10,1}(e^{i\omega})$

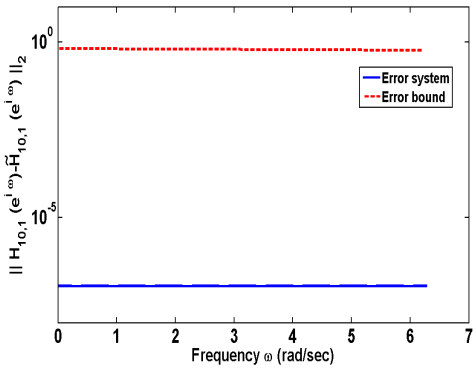

(b) Deviation of frequency responses for $\mathcal{H}_{10,1}(e^{i\omega})$

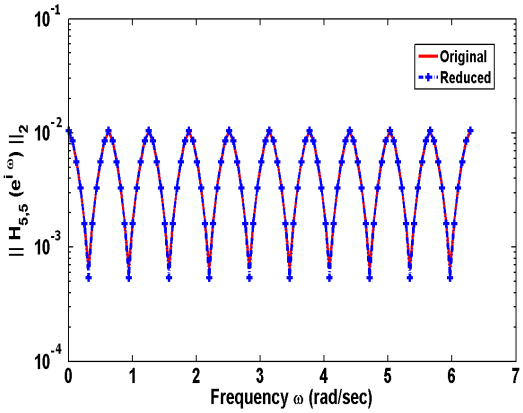

(c) Frequency responses for $\mathcal{H}_{5,5}(e^{i\omega})$

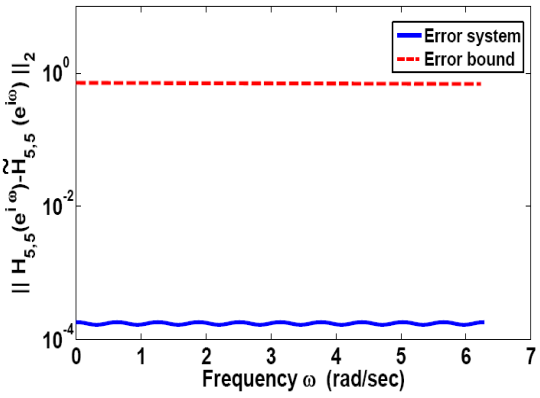

(d) Deviation of frequency responses for $\mathcal{H}_{5,5}(e^{i\omega})$

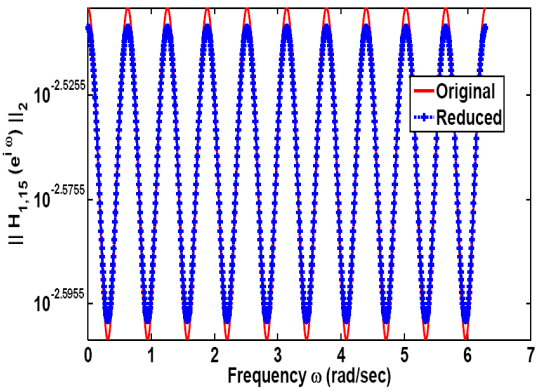

(e) Frequency responses for $\mathcal{H}_{1,15}(e^{i\omega})$

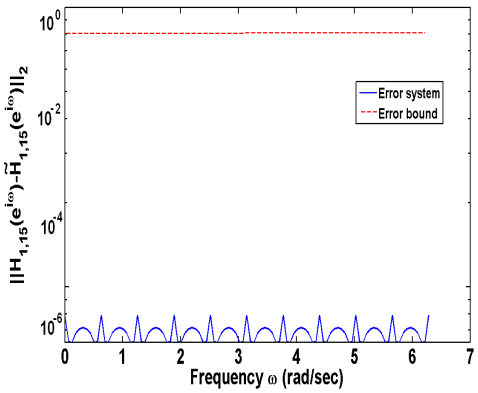

(f) Deviation of frequency responses for $\mathcal{H}_{1,15}(e^{i\omega})$

Figure 8.12. Frequency responses for original and reduced-order systems for individual components of $\mathcal{H}(e^{i\omega})$ and respective deviations (Model Problem 2).

CHAPTER

NINE

LOW-RANK SOLUTION OF LARGE SCALE PERIODIC MATRIX EQUATIONS

Contents

This chapter presents iterative methods for solving large sparse projected generalized discrete-time periodic Lyapunov equations in lifted form which arise in Chapter 8 in the context of model reduction of periodic descriptor systems. These iterative methods are based on the generalization of the alternating direction implicit method and the Smith method used for large-scale projected continuous-time Lyapunov equations in [110, 81].

We present a low-rank version of the alternating direction implicit method and the generalized Smith method to compute low-rank approximations to the solutions of projected generalized discrete-time periodic Lyapunov equations in lifted form with low-rank right-hand side. We also discuss the application of the solvers in balancing-based model reduction of discrete-time periodic descriptor systems. Numerical results are given to illustrate the efficiency and accuracy of the proposed methods.

The chapter outline is as follows. In Section 9.2, we briefly review the basic ADI iteration and its application to Lyapunov equations. In Sections 9.3 and 9.4, we discuss the numerical solution of the causal and noncausal lifted Lyapunov equations using the ADI method and the Smith method, respectively. Low-rank versions of these methods are also presented that can be used to compute low-rank approximations to the solutions of projected periodic Lyapunov equations in lifted form with low-rank right-hand side. A balanced truncation model reduction method for periodic descriptor systems is considered in Section 9.5. Section 9.6 contains numerical examples that illustrate the properties of the described iterative methods for lifted projected Lyapunov equations and their application to model reduction.

9.1. Motivation

In Chapter 8 we have discussed the numerical solutions of large-scale projected discrete-time periodic Lyapunov equations in lifted form which arise in model reduction of periodic descriptor systems. We have observed that the lifted forms of those large-scale projected Lyapunov equations have some sparsity patterns in their matrix coefficients. In practice, it is not very efficient to use direct methods to generate the numerical solutions of large-scale PLDALEs described in Theorem 5.2.4 and 5.2.5 of Chapter 5. One should avoid direct methods because the computational complexity for solving such a PLDALE using directs methods is of at least $\mathcal{O}(K\bar{n}^3)$, where $\bar{n} = \max(\mu_k, n_k)$, and they require extensive storage. Therefore, we will develop iterative methods for such equations, which can exploit the sparse structures of system matrices to generate well approximating solutions (with prescribed tolerance), and have low memory requirements and low computational cost.

Recently, increasing attention has been devoted to the numerical solution of large-scale sparse Lyapunov equations using the alternating directions implicit (ADI) method [67, 82], the Smith method [49, 82, 96], and Krylov subspace methods [55, 95]. For an overview and further references, see [13]. Many of these methods have also been generalized to projected Lyapunov equations [110, 112]. On the other hand, an extension of the Smith method and the Krylov subspace method based on a block Arnoldi algorithm to standard periodic Lyapunov equation has been presented in [57]. These methods cannot be directly applied to the projected periodic Lyapunov equations. Here, we consider the projected periodic Lyapunov equations in lifted form and propose a generalization of the ADI iteration and the Smith method for solving such equations.

9.2. Background

The basic version of the ADI method has been proposed in [80] to solve linear systems arising from the discretization of elliptic boundary value problems and then used in [67, 70, 82, 110] to solve standard continuous-time Lyapunov equations. For the discrete-time case, the ADI method is suggested in [64, 10]. In this section, we present a short discussion of the basic ADI iteration in case of standard continuous-time Lyapunov equations.

The ADI iteration is generally used to solve linear systems like

$$Ly = b,$$

where L is a symmetric positive definite matrix and can be split into the parts, i.e., $L = L_1 + L_2$, where L_1 and L_2 both are symmetric positive definite matrices for which the following iteration converges.

$$\begin{aligned} y_0 &= 0, \\ (L_1 + \tau_j I)\, y_{j-\frac{1}{2}} &= b - (L_2 - \tau_j I)\, y_{j-1}, \\ (L_2 + \eta_j I)\, y_j &= b - (L_1 - \eta_j I)\, y_{j-\frac{1}{2}}, \quad \text{for } j = 1, 2, \ldots, J. \end{aligned}$$

Here τ_j and η_j are suitably chosen shift parameters and they are determined from the spectral bounds of L_1 and L_2 to increase the convergence rate for the solutions y_j [49]. This is known as *ADI model problem* when the matrices L_1 and L_2 commute.

Now consider a Lyapunov equation of the form

$$FX + XF^T = -BB^T \tag{9.1}$$

with stable F, i.e., all eigenvalues of F have negative real part. One can consider (9.1) as a model ADI problem because it is a linear system involving the sum of two commutating operators acting on the unknown X, which is a matrix in this case. Therefore, the ADI iteration produces the approximation X_j to the Lyapunov solution X according to the two step iteration as follows:

$$\begin{aligned} (F + \tau_j I)X_{j-\frac{1}{2}} &= -BB^T - X_{j-1}(F^T - \tau_j I) \\ (F + \tau_j I)X_j &= -BB^T - X_{j-\frac{1}{2}}^T(F^T - \tau_j I), \end{aligned} \tag{9.2}$$

where $\tau_1, \tau_2, \ldots, \tau_j \in \mathbb{C}^-$ are called *ADI shift parameters*.

To keep the final ADI approximation $X_{j_{final}}$ real, it is assumed that each shift parameter is either real or comes as a part of a complex conjugate pair $\{\tau_j, \tau_{j+1}\}$ with $\tau_{j+1} = \bar{\tau}_j$, where $\bar{\tau}_j$ denotes the complex conjugate of τ_j. Note that the intermediate matrix $X_{j-\frac{1}{2}}$ in (9.2) may not be symmetric, but X_{j-1} and X_j are symmetric.

The main idea behind the low-rank version of an ADI iteration is to write the two step iteration (9.2) into a one step iteration

$$\begin{aligned} X_j &= -2\,Re(\tau_j)\,(F+\tau_j I)^{-1}BB^T(F+\bar{\tau}_j I)^{-T} \\ &\quad +(F+\tau_j I)^{-1}(F-\bar{\tau}_j I)Z_{j-1}Z_{j-1}^T(F-\tau_j I)^T(F+\bar{\tau}_j I)^{-T}, \end{aligned} \tag{9.3}$$

which is symmetric. Now assuming $X_j = Z_j Z_j^T$ and $X_0 = 0$, we can write (9.3) in terms of the factors Z_j as

$$\begin{aligned} Z_1 &= \sqrt{-2Re(\tau_1)}\,(F+\tau_1 I)^{-1}B, \\ Z_j &= [\sqrt{-2Re(\tau_j)}\,(F+\tau_j I)^{-1}B,\ (F+\tau_j I)^{-1}(F-\bar{\tau}_j I)Z_{j-1}]. \end{aligned}$$

Hence we work on the factors Z_j which have comparably low column rank instead of working with the square matrices X_j. One can also show that only the new columns need to be processed in every iteration step [82]. The convergence of the ADI iteration is determined by the spectral radius $\rho_{adi} = \rho(\Pi_{j=1}^{i}(F+\tau_j I)^{-1}(F-\bar{\tau}_j I))$ where i is the number of shifts used [49], and depends strongly on the choice of ADI parameters. The minimization of ρ_{adi} with respect to shift parameters τ_j leads to the ADI minimax problem:

$$\{\tau_1,\tau_2,\ldots,\tau_i\} = \arg \min_{\tau_1,\tau_2,\ldots,\tau_i\in\mathbb{C}^-} \max_{\lambda\in\Lambda(F)} \left|\prod_{j=1}^{i}\frac{(\lambda-\bar{\tau}_j)}{(\lambda+\tau_j)}\right|.$$

The details about the solution of the ADI minimax problem will be given in the next section and contributions to the solution of the ADI minimax problem can also be found in [127, 70, 82]. For a diagonalizable F, it can be shown that the i-th iterate satisfies the following convergence relation [67]

$$\|X - X_i\|_F \leq \|M\|^2\,\|M^{-1}\|^2\,\rho_{adi}^2\,\|X\|_F,$$

where M is the matrix of eigenvectors of F. A good stopping criterion of the ADI iteration can be determined by the evaluation of the residual norm

$$\frac{\|FZ_jZ_j^T + Z_jZ_j^TF^T + BB^T\|_F}{\|BB^T\|_F} < \epsilon,$$

for a given tolerance ϵ or a stagnation of the normalized residual norms is observed. If the number of shift parameters is smaller than the number of iterations required to achieve accuracy upto a certain tolerance, then these shift parameters are reused again in a cyclic manner. In the following section we generalize the ADI method to the PLDALEs with large and sparse matrix coefficients.

9.3. ADI Method for Causal Lifted Lyapunov Equations

Let us consider the PLDALE

$$\mathcal{A}\mathcal{G}^{cr}\mathcal{A}^T - \mathcal{E}\mathcal{G}^{cr}\mathcal{E}^T = -\mathcal{P}_l\mathcal{B}\mathcal{B}^T\mathcal{P}_l^T, \quad \mathcal{G}^{cr} = \mathcal{P}_r\mathcal{G}^{cr}\mathcal{P}_r^T, \tag{9.4}$$

in (8.9), where all the finite eigenvalues of the pencil $\lambda\mathcal{E} - \mathcal{A}$ lie inside the unit circle. If $\mathcal{E}$ is nonsingular, then the PLDALE (9.4) can be transformed to the standard discrete-time Lyapunov equation by the multiplication from the left and right with $\mathcal{E}^{-1}$ and $(\mathcal{E}^{-1})^T$. This equation can be solved by the ADI method [10, 26] or the Smith method [49, 82, 96]. However, for the descriptor system (8.1), the matrix $\mathcal{E} = \operatorname{diag}(E_0, \ldots, E_{K-1})$ is singular. If the pencil $\lambda\mathcal{E} - \mathcal{A}$ has no zero eigenvalues, then $\mathcal{A}$ is nonsingular and (9.4) can be transformed to a standard discrete-time Lyapunov equation by the multiplication from the left and right with $\mathcal{A}^{-1}$ and $(\mathcal{A}^{-1})^T$. Note that $\lambda\mathcal{E} - \mathcal{A}$ is stable since all its finite eigenvalues lie inside unit circle. Then the Smith iteration [110]

$$\mathcal{G}_{i+1}^{cr} = \mathcal{A}^{-1}(-\mathcal{P}_l\mathcal{B}\mathcal{B}^T\mathcal{P}_l^T + \mathcal{E}\mathcal{G}_i^{cr}\mathcal{E}^T)\mathcal{A}^{-T}, \quad \mathcal{G}_0^{cr} = \mathcal{P}_r\mathcal{B}\mathcal{B}^T\mathcal{P}_r^T \tag{9.5}$$

can be used to compute the approximate solution of (9.4) provided $\mathcal{A}$ is invertible. But the negative semidefinite term inside the bracket of (9.4) may lead to indefinite intermediate approximations. Also in this case both the ADI and Smith iterations fail to converge for the resulting Lyapunov equation, because $\mathcal{A}^{-1}\mathcal{E}$ has eigenvalues outside the unit circle. This problem can be circumvented by considering the generalized Cayley transformation of the lifted system. In the sequel, we will introduce the generalized Cayley transformation and some of its important properties that we will exploit in our ADI model problem reformulation.

9.3.1. Cayley Transformation

Let us consider a standard discrete-time system with realization $\mathbf{\Sigma}_d = (A_d, B_d, C_d)$. Using the bilinear transformation

$$s = \frac{z-1}{z+1},$$

we get its continuous-time counterpart as

$$\mathbf{\Sigma}_c = \Big(A_c = (A_d + I)^{-1}(A_d - I),\ B_c = \sqrt{2}(A_d + I)^{-1}B_d,\ C_c = \sqrt{2}C_d(A_d + I)^{-1}\Big). \tag{9.6}$$

The bilinear transformation above is known as Cayley transformation, see, e.g., [52, 1]. The concept can be extended to generalized systems. Let $\lambda_d E_d - A_d$ be a matrix pencil of a generalized discrete-time system. Then by generalized Cayley transformation $\mathfrak{C}(E_d, A_d)$, we get its continuous-time counterpart as

$$\mathfrak{C}(E_d, A_d) := \lambda_c E_c - A_c = \lambda_d(A_d - E_d) - (E_d + A_d), \tag{9.7}$$

which connects the generalized Lyapunov equations in the continuous-time and discrete-time cases [74, 103]. It can be proved that analogous to the standard case, the Cayley transformation preserves Gramians in the generalized case too, i.e. the Gramians X_c of a generalized continuous-time Lyapunov equation equals to its discrete-time counterpart X_d, obtained by using transformation (9.7). So analysis of the Gramians and the eigenstructure of a generalized discrete-time LTI system can be studied with its generalized continuous-time counterpart.

Note that the generalized Cayley transformation only changes the eigenvalues but not the eigenvectors (it even does not change the deflating subspaces when the pencil is singular, if the deflating subspaces exist in singular case) [74]. Thus the generalized eigenvector matrices of $\lambda_d E_d - A_d$ and $\lambda_c E_c - A_c$ are the same, while the generalized eigenvalues of $\lambda_c E_c - A_c$ are

$$\lambda_c = \frac{\lambda_d + 1}{\lambda_d - 1}.$$

Hence, we introduce the following proposition to summarize the relations between the eigenvalues of the pencil $\lambda E_c - A_c$ and $\lambda E_d - A_d$.

Proposition 9.1:

[103] *Consider the generalized Cayley transformation (9.7) for the pencil $\lambda_d E_d - A_d$ of a generalized discrete-time LTI system. Then*

1. *the finite eigenvalues of $\lambda_d E_d - A_d$ inside and outside the unit circle are mapped to eigenvalues of $\lambda_c E_c - A_c$ with negative real part and positive real part, respectively;*
2. *the finite eigenvalues of $\lambda_d E_d - A_d$ on the unit circle except $\lambda_d = 1$ are mapped to eigenvalues of $\lambda_c E_c - A_c$ on the imaginary axis and the eigenvalue $\lambda_d = 1$ is mapped to ∞;*
3. *the infinite eigenvalues of $\lambda_d E_d - A_d$ are mapped to eigenvalues at 1 of $\lambda_c E_c - A_c$.* ◊

In the next subsection, we will use the generalized Cayley transformation for the cyclic lifted pencil $\lambda\mathcal{E} - \mathcal{A}$ and generate an approximate solution of (9.4) using the continuous-time counterpart of (9.4).

9.3.2. Derivation of the ADI Method for Cayley Transformed Systems

We just have observed that the generalized Cayley transformation given by

$$\mathfrak{C}(\mathcal{E}, \mathcal{A}) = \lambda(\mathcal{A} - \mathcal{E}) - (\mathcal{A} + \mathcal{E}), \tag{9.8}$$

transfers the projected discrete-time Lyapunov equation to a projected continuous-time Lyapunov equation. Indeed, $\mathcal{G}^{cr}$ is the solution of the PLDALE (9.4) if and only if it satisfies the projected continuous-time Lyapunov equation (PCALE)

$$\mathbf{E}\mathcal{G}^{cr}\mathbf{A}^T + \mathbf{A}\mathcal{G}^{cr}\mathbf{E}^T = -2\mathcal{P}_l\mathcal{B}\mathcal{B}^T\mathcal{P}_l^T, \quad \mathcal{G}^{cr} = \mathcal{P}_r\mathcal{G}^{cr}\mathcal{P}_r^T, \tag{9.9}$$

where $\lambda\mathbf{E} - \mathbf{A} = \lambda(\mathcal{A} - \mathcal{E}) - (\mathcal{A} + \mathcal{E})$ is the Cayley-transformed pencil. Now, the finite eigenvalues of $\lambda\mathcal{E} - \mathcal{A}$ lying inside the unit circle are mapped to eigenvalues of $\lambda\mathbf{E} - \mathbf{A}$ in the open left half-plane, and the eigenvalues of $\lambda\mathcal{E} - \mathcal{A}$ at infinity are mapped to $\lambda = 1$. Moreover, the spectral projectors $\mathcal{P}_l$ and $\mathcal{P}_r$ are preserved by the Cayley transformation and now are the projectors onto the left and right deflating subspaces of $\lambda\mathbf{E} - \mathbf{A}$ corresponding to the finite eigenvalues with negative real part.

If $\lambda\mathcal{E}-\mathcal{A}$ is pd-stable, the matrices $\mathbf{E}$ and $\mathbf{A}$ are both nonsingular (see [74], and references therein). Using the relation $P_l E = E P_r$, we can transform the PCALE (9.9) to the projected standard Lyapunov equation

$$(\mathbf{E}^{-1}\mathbf{A})\mathcal{G}^{cr} + \mathcal{G}^{cr}(\mathbf{E}^{-1}\mathbf{A})^T = -2\mathcal{P}_r\mathbf{E}^{-1}\mathcal{B}(\mathbf{E}^{-1}\mathcal{B})^T\mathcal{P}_r^T, \quad \mathcal{G}^{cr} = \mathcal{P}_r\mathcal{G}^{cr}\mathcal{P}_r^T. \tag{9.10}$$

In this case, the solutions of (9.9) and (9.10) are identical and an approximate solution of (9.9) can be computed by the ADI method applied to (9.10). The ADI iteration for (9.10) is given by

$$\begin{aligned}\mathcal{G}_i^{cr} = {} & (\mathbf{E}^{-1}\mathbf{A}+\tau_i I)^{-1}(\mathbf{E}^{-1}\mathbf{A}-\bar{\tau}_i I)\mathcal{G}_{i-1}^{cr}(\mathbf{E}^{-1}\mathbf{A}-\tau_i I)^T(\mathbf{E}^{-1}\mathbf{A}+\bar{\tau}_i I)^{-T} \\ & -4Re(\tau_i)(\mathbf{E}^{-1}\mathbf{A}+\tau_i I)^{-1}\mathcal{P}_r\mathbf{E}^{-1}\mathcal{B}(\mathbf{E}^{-1}\mathcal{B})^T\mathcal{P}_r^T(\mathbf{E}^{-1}\mathbf{A}+\bar{\tau}_i I)^{-T},\end{aligned} \tag{9.11}$$

with an initial matrix $\mathcal{G}_0^{cr} = 0$ and the shift parameters $\tau_1, \tau_2, \ldots, \tau_i \in \mathbb{C}^-$. It follows from

$$\begin{aligned}\mathcal{P}_r(\mathbf{E}^{-1}\mathbf{A}-\bar{\tau}_i I) &= (\mathbf{E}^{-1}\mathbf{A}-\bar{\tau}_i I)\mathcal{P}_r, \\ \mathcal{P}_r(\mathbf{E}^{-1}\mathbf{A}+\tau_i I)^{-1} &= (\mathbf{E}^{-1}\mathbf{A}+\tau_i I)^{-1}\mathcal{P}_r,\end{aligned}$$

that $\mathcal{G}_i^{cr} = \mathcal{P}_r\mathcal{G}_i^{cr}\mathcal{P}_r^T$, i.e., the second equation in (9.9) is satisfied. Iteration (9.11) can be written as

$$\begin{aligned}\mathcal{G}_i^{cr} = {} & (\mathbf{A}+\tau_i\mathbf{E})^{-1}(\mathbf{A}-\bar{\tau}_i\mathbf{E})\mathcal{G}_{i-1}^{cr}(\mathbf{A}-\tau_i\mathbf{E})^T(\mathbf{A}+\bar{\tau}_i\mathbf{E})^{-T} \\ & -4Re(\tau_i)(\mathbf{A}+\tau_i\mathbf{E})^{-1}\mathcal{P}_l\mathcal{B}\mathcal{B}^T\mathcal{P}_l^T(\mathbf{A}+\bar{\tau}_i\mathbf{E})^{-T}.\end{aligned} \tag{9.12}$$

Similarly to [110], we can establish the convergence of the ADI iteration (9.12).

Proposition 9.2:

Consider the periodic discrete-time descriptor system (8.1) and its cyclic lifted representation (8.2), where the set of periodic matrix pairs $\{E_k, A_k\}_{k=0}^{K-1}$ is pd-stable. If $\tau_1, \tau_2, \ldots, \tau_i \in \mathbb{C}^-$, then the ADI iteration (9.12) converges to the solution $\mathcal{G}^{cr}$ of the projected PCALE (9.9). ◊

Proof. Let $\mathcal{G}^{cr}$ be the solution of the projected PCALE (9.9). After the i-th iteration, the error $\mathcal{G}_i^{cr} - \mathcal{G}^{cr}$ can be computed from (9.12) recursively as

$$\mathcal{G}_i^{cr} - \mathcal{G}^{cr} = \mathbf{R}_i\mathcal{G}^{cr}\mathbf{R}_i^*, \tag{9.13}$$

with

$$\mathbf{R}_i = \mathcal{P}_r(\mathbf{A}+\tau_i\mathbf{E})^{-1}(\mathbf{A}-\bar{\tau}_i\mathbf{E})\cdots(\mathbf{A}+\tau_1\mathbf{E})^{-1}(\mathbf{A}-\bar{\tau}_1\mathbf{E}). \tag{9.14}$$

Since the periodic descriptor system (8.1) is asymptotically stable, the Cayley transformed pencil $\lambda\mathbf{E}-\mathbf{A}$ has only eigenvalues with negative real part plus the eigenvalue $\lambda = 1$ (due to Proposition 9.1). Thus, it can be transformed into Weierstrass canonical form

$$\mathbf{E} = \mathbf{W}\begin{bmatrix} I_f & 0 \\ 0 & I \end{bmatrix}\mathbf{Z}, \quad \mathbf{A} = \mathbf{W}\begin{bmatrix} J & 0 \\ 0 & J_1 \end{bmatrix}\mathbf{Z}, \tag{9.15}$$

where the matrices $\mathbf{W}$ and $\mathbf{Z}$ are nonsingular, J has eigenvalues with negative real part and J_1 has the eigenvalue $\lambda = 1$ only. In that case the projectors $\mathcal{P}_l$ and $\mathcal{P}_r$ can be represented as

$$\mathcal{P}_l = \mathbf{W}\begin{bmatrix} I & 0 \\ 0 & 0 \end{bmatrix}\mathbf{W}^{-1}, \quad \mathcal{P}_r = \mathbf{Z}^{-1}\begin{bmatrix} I & 0 \\ 0 & 0 \end{bmatrix}\mathbf{Z}. \tag{9.16}$$

Substituting (9.15) and (9.16) in (9.14), we obtain that

$$\mathbf{R}_i = \mathbf{Z}^{-1}\begin{bmatrix} \mathbf{J}_i & 0 \\ 0 & 0 \end{bmatrix}\mathbf{Z}, \tag{9.17}$$

with

$$\mathbf{J}_i = (I + \tau_i J)^{-1}(I - \bar{\tau}_i J) \cdot \ldots \cdot (I + \tau_1 J)^{-1}(I - \bar{\tau}_1 J). \tag{9.18}$$

Since all eigenvalues of J have negative real part, then all eigenvalues of $(I+\tau_l J)^{-1}(I-\bar{\tau}_l J)$, $l = 1, \ldots, i$, lie inside the unit circle. Therefore,

$$\lim_{i\to\infty} \mathbf{R}_i = 0,$$

and, hence, the right-hand side of equation (9.13) tends to zero. In other words, $\mathcal{G}_i^{cr}$ converges to the solution $\mathcal{G}^{cr}$. □

Proposition 9.3:

Consider the PCALE (9.9). Assume that the pencil $\lambda\mathbf{E} - \mathbf{A}$ is in Weierstrass canonical form (9.15), where J is diagonal. Then the i-th iterate $\mathcal{G}_i^{cr}$ of the ADI method (9.12) satisfies the estimate

$$\|\mathcal{G}_i^{cr} - \mathcal{G}^{cr}\|_2 \le \kappa^2(Z)\rho^2(\mathbf{R}_i)\|\mathcal{G}^{cr}\|_2, \tag{9.19}$$

where $\kappa(Z) = \|Z\|_2\|Z^{-1}\|_2$ is the spectral condition number of the right transformation matrix Z in (9.15) and $\rho(\mathbf{R}_i)$ is the spectral radius of the matrix $\mathbf{R}_i$ in (9.14). ◊

Proof. From (9.13), we have

$$\|\mathcal{G}_i^{cr} - \mathcal{G}^{cr}\|_2 := \|\mathbf{R}_i\mathcal{G}^{cr}\mathbf{R}_i^*\|_2 \le \|\mathbf{R}_i\|_2\,\|\mathcal{G}^{cr}\|_2\,\|\mathbf{R}_i^*\|_2. \tag{9.20}$$

Now using (9.17), we can show that

$$\begin{aligned} \|\mathbf{R}_i\|_2\,\|\mathcal{G}^{cr}\|_2\,\|\mathbf{R}_i^*\|_2 &\le \|Z\begin{bmatrix} J_i & 0 \\ 0 & 0 \end{bmatrix}Z^{-1}\|_2\,\|\mathcal{G}^{cr}\|_2\,\|Z^{-*}\begin{bmatrix} J_i & 0 \\ 0 & 0 \end{bmatrix}^* Z^*\|_2 \\ &\le \|Z\|_2\,\rho(\mathbf{R}_i)\,\|Z^{-1}\|_2\,\|\mathcal{G}^{cr}\|_2\,\|Z^{-1}\|_2\,\rho(\mathbf{R}_i)\,\|Z\|_2 \\ &\le \|Z\|_2^2\,\rho^2(\mathbf{R}_i)\,\|Z^{-1}\|_2^2\,\|\mathcal{G}^{cr}\|_2 \\ &= \kappa^2(Z)\rho^2(\mathbf{R}_i)\|\mathcal{G}^{cr}\|_2. \end{aligned}$$

Hence, estimate (9.19) is established. □

Remark 9.4:

The solutions of PLDALE (9.4) and PCALE (9.9) are identical and have block diagonal structure. Hence, an approximation of the solution of (9.9) also means that this is an approximation of the solution of the projected lifted Lyapunov equation (9.4). ◊

9.3.3. Computing Shift Parameters

The convergence rate of the ADI iteration (9.12) is determined by the spectral radius of the matrix $\mathbf{R}_i$ and depends strongly on the choice of ADI parameters. The minimization of this spectral radius with respect to the shift parameters $\tau_1, \tau_2, \ldots, \tau_i \in \mathbb{C}^-$ leads to the generalized minimax problem

$$\{\tau_1, \tau_2, \ldots, \tau_i\} = \underset{\tau_1,\tau_2,\ldots,\tau_i\in\mathbb{C}^-}{\arg\min} \quad \max_{t\in \mathrm{Sp}_s(\mathbf{E},\mathbf{A})} \quad \prod_{j=1}^{i} \frac{\left|(t-\bar{\tau}_j)\right|}{\left|(t+\tau_j)\right|}, \tag{9.22}$$

where $\mathrm{Sp}_s(\mathbf{E}, \mathbf{A})$ denotes the set of stable eigenvalues of the pencil $\lambda\mathbf{E} - \mathbf{A}$, i.e., the finite eigenvalues with negative real part. The bounds needed to compute the optimal shift parameters are too expensive to compute exactly in case of large-scale systems because they need to compute the whole spectrum of the pencil $\lambda\mathbf{E} - \mathbf{A}$. An alternative approach based on heuristics, which does not explicitly compute the eigenspectrum, has been proposed in [82] for standard problems with $\mathbf{E} = I$. It is based on replacing the eigenspectrum by a set of largest and smallest in modulus Ritz values that approximate the eigenvalues of $\mathbf{A}$. The Ritz values can be computed by an Arnoldi process applied to the matrices $\mathbf{A}$ and $\mathbf{A}^{-1}$. This approach can also be extended to the generalized problem (9.22).

Since the pencil $\lambda\mathbf{E}-\mathbf{A}$ has finite eigenvalues with negative real part (stable eigenvalues) and also an eigenvalue $\lambda = 1$, an equivalent expression for (9.22) can be written as

$$\{\tau_1, \tau_2, \ldots, \tau_i\} = \underset{\tau_1,\tau_2,\ldots,\tau_i\in\mathbb{C}^-}{\arg\min} \quad \max_{t\in\, \Lambda(\mathbf{E}^{-1}\mathbf{A})\setminus\{1\}} \quad \prod_{j=1}^{i} \frac{\left|(t-\bar{\tau}_j)\right|}{\left|(t+\tau_j)\right|}, \tag{9.23}$$

Thus, the suboptimal ADI shift parameters $\tau_1, \tau_2, \ldots, \tau_i$ can be computed by the heuristic procedure [82] from the set of largest approximate stable eigenvalues of $\mathbf{E}^{-1}\mathbf{A}$ and $\mathbf{A}^{-1}\mathbf{E}$.

9.3.4. Low-Rank ADI Method

Low-rank version of the ADI method has been proposed in [67, 82] to compute a low-rank approximation to the solution of standard Lyapunov equations with large-scale matrix coefficients. It is known as the *low-rank alternating direction implicit* (LR-ADI) method. This method was extended to projected Lyapunov equations in [110].

It is observed in [110] that analogous to standard state space case [2, 83], the eigenvalues of the symmetric solutions of projected Lyapunov equations with low-rank right-hand sides often decay very rapidly, and such solutions can be well approximated by low-rank matrices. That means that one can find a matrix Z with a small number of columns such that ZZ^T is an approximation to the solution $\mathcal{G}^{cr}$ of PCALE (9.9). This matrix Z is referred to as a *low-rank Cholesky factor* of the solution of (9.9).

Since the matrices $\mathcal{G}_i^{cr}$ in the ADI iteration (9.12) are Hermitian and positive semidefinite, a factor Z_i of $\mathcal{G}_i^{cr} = Z_i Z_i^*$ can be represented as

$$Z_i = \Big[2\sqrt{-Re(\tau_i)}(\mathbf{A}+\tau_i\mathbf{E})^{-1}\mathcal{P}_l\mathcal{B}, \quad (\mathbf{A}+\tau_i\mathbf{E})^{-1}(\mathbf{A}-\bar{\tau}_i\mathbf{E})Z_{i-1}\Big], \tag{9.24}$$

and $Z_0 = 0$. Introducing the matrices $\Phi_j = (\mathbf{A}-\bar{\tau}_j\mathbf{E})$ and $\Psi_j = (\mathbf{A}+\tau_j\mathbf{E})^{-1}$, we can express the i-th iteration as

$$Z_i = 2[\sqrt{-Re(\tau_i)}\Psi_i\mathcal{P}_l\mathcal{B}, \sqrt{-Re(\tau_{i-1})}\Psi_i(\Phi_i\Psi_{i-1})\mathcal{P}_l\mathcal{B}, \ldots, \sqrt{-Re(\tau_1)}\Psi_i\Phi_i\cdots\Psi_2(\Phi_2\Psi_1)\mathcal{P}_l\mathcal{B}].$$

Since Ψ_j and Φ_j commute, we can reorder these matrices and rewrite Z_i in the form

$$Z_i = [\, G,\ F_{i-1}G,\ F_{i-2}F_{i-1}G,\ \ldots,\ F_1F_2\cdots F_{i-1}G\,],$$

where

$$G = 2\sqrt{-Re(\tau_i)}(\mathbf{A}+\tau_i\mathbf{E})^{-1}\mathcal{P}_l\mathcal{B}$$

and

$$F_j = \sqrt{\frac{Re(\tau_j)}{Re(\tau_{j+1})}}\Psi_j\Phi_{j+1} = \sqrt{\frac{Re(\tau_j)}{Re(\tau_{j+1})}}\Big(I-(\tau_j+\bar{\tau}_{j+1})(\mathbf{A}+\tau_j\mathbf{E})^{-1}\mathbf{E}\Big).$$

Reenumerating the shift parameters in reverse order, we obtain Algorithm 9.1 for computing the low-rank Cholesky factor of the solution of (9.9), which is also the solution of the PLDALE (9.4).

Note that if the complex shift parameters appear in complex conjugate pairs $\{\tau_i, \tau_{i+1} = \bar{\tau}_i\}$, then performing a double step as described in [13, 110] we can keep the low-rank Cholesky factor Z_i to be real.

Algorithm 9.1 Low-rank ADI iteration (LR-ADI) for causal PLDALE.

Input: $\mathbf{A}, \mathbf{E}, \mathcal{B}, \mathcal{P}_l$ and shift parameters $\tau_1, \tau_2, \ldots, \tau_i$.
Output: a low-rank Cholesky factor Z_i such that $\mathcal{G}^{cr} \approx Z_i Z_i^*$.

1: $V_1 = 2\sqrt{-Re(\tau_1))}(\mathbf{A}+\tau_1\mathbf{E})^{-1}\mathcal{P}_l\mathcal{B}$
2: $Z_1 = V_1$
3: **for** $i = 2, 3, \ldots,$ **do**
4: $\quad V_i = \sqrt{\frac{Re(\tau_i)}{Re(\tau_{i-1})}}(I-(\tau_i+\bar{\tau}_{i-1})(\mathbf{A}+\tau_i\mathbf{E})^{-1}\mathbf{E})V_{i-1}$
5: $\quad Z_i = [Z_{i-1},\ V_i]$
6: **end for**

The ADI iteration can be stopped as soon as the *normalized residual norm* given by

$$\eta(Z_i) = \frac{\|\mathbf{A}Z_iZ_i^T\mathbf{E}^T + \mathbf{E}Z_iZ_i^T\mathbf{A}^T + 2\mathcal{P}_l\mathcal{B}\mathcal{B}^T\mathcal{P}_l^T\|_F}{\|2\mathcal{P}_l\mathcal{B}\mathcal{B}^T\mathcal{P}_l^T\|_F} \tag{9.25}$$

satisfies the condition $\eta(Z_i) < tol$ with a user-defined tolerance tol or a stagnation of normalized residual norms is observed. If the number of shift parameters is smaller than the number of iterations required to attain a prescribed tolerance, then we reuse these parameters in a cyclic manner.

If $\mathcal{G}_i^{cr} = Z_i Z_i^*$ converges to the solution of (9.9), then

$$\lim_{i\to\infty} Z_i Z_i^* = \lim_{i\to\infty} (\mathcal{G}_i^{cr} - \mathcal{G}_{i-1}^{cr}) = 0.$$

Therefore, the stopping criterion in Algorithm 9.1 can also be defined by the condition $\|V_i\|_F \leq tol$ or $\|V_i\|_F / \|Z_i\|_F \leq tol$ with some tolerance tol.

Note that we do not need to compute the matrices $\mathbf{E}$ and $\mathbf{A}$ explicitly in Algorithm 9.1. Instead, we can rewrite the iteration for the original matrices $\mathcal{E}$ and $\mathcal{A}$. Using $\mathbf{E} = \mathcal{A} - \mathcal{E}$ and $\mathbf{A} = \mathcal{A} + \mathcal{E}$, we have

$$(\mathbf{A} + \tau_i \mathbf{E})^{-1}\mathbf{E} = \Big((1+\tau_i)\mathcal{A} + (1-\tau_i)\mathcal{E}\Big)^{-1}(\mathcal{A} - \mathcal{E}).$$

Then Steps 1 and 4 in Algorithm 9.1 can be reformulated as

$$\begin{aligned} V_1 &= 2\sqrt{-Re(\tau_1)}\Big((1+\tau_1)\mathcal{A} + (1-\tau_1)\mathcal{E}\Big)^{-1}\mathcal{P}_l\,\mathcal{B}, \\ V_i &= \sqrt{\frac{Re(\tau_i)}{Re(\tau_{i-1})}}\Big(V_{i-1} - (\tau_i + \bar{\tau}_{i-1})\Big((1+\tau_i)\mathcal{A} + (1-\tau_i)\mathcal{E}\Big)^{-1}(\mathcal{A} - \mathcal{E})V_{i-1}\Big). \end{aligned}$$

The minimax problem (9.23) for the ADI parameters can be reformulated accordingly.

Remark 9.5:

In exact arithmetic, the matrices Z_i satisfy $Z_i = \mathcal{P}_r Z_i$ and, hence, the second equation in (9.9) is fulfilled for the low-rank approximation $Z_i Z_i^T$. However, in finite precision arithmetic, a drift-off effect may occur. In this case, we need to project V_i onto the image of $\mathcal{P}_r$ by pre-multiplication with $\mathcal{P}_r$. In order to limit the additional computation cost, we can do this, for example, at every second or third iteration step. ◊

We observe that the ADI iteration does not preserve the block diagonal structure at every iteration step in Algorithm 9.1. This is due to the specific structure of the matrices $\mathbf{E}$ and $\mathbf{A}$. But we can show that after the successful i-th iteration step, the approximate Gramian $\mathcal{G}_i^{cr} = Z_i Z_i^T$ has almost block diagonal structure analogous to the solution of the PLDALE (9.4) given by $\mathcal{G}_i^{cr} = \mathrm{diag}(G_1^{cr}, \ldots, G_{K-1}^{cr}, G_0^{cr})$, where G_k^{cr} are the periodic solutions of the PPDALE (4.69) for $k = 0, 1, \ldots, K-1$. Since $\mathcal{G}_i^{cr}$ is almost block diagonal after the i-th iteration and $\mathcal{G}_i^{cr} = Z_i Z_i^T$, we let

$$Z_i = [R_{i,1}^T, \ldots, R_{i,K-1}^T, R_{i,0}^T]^T, \tag{9.26}$$

with $R_{i,k} \in \mathbb{R}^{n_k \times r_c}$. For simplicity, we leave the scripts i and write (9.26) more simply as

$$Z_i = [R_1^T, \ldots, R_{K-1}^T, R_0^T]^T,$$

with $R_k \in \mathbb{R}^{n_k \times r_c}$. Then $R_k R_k^T$ is an approximation to the causal reachability Gramian G_k^{cr}, $k = 0, 1, \ldots, K-1$.

Remark 9.6:
We have claimed that after the successful iteration steps in Algorithm 9.1, the approximate Gramian has almost block diagonal structure analogous to the solution of the PLDALE (9.4). Now suppose that after successful i-th iteration steps, we have the Cholesky factor Z_i given by Equation (9.26). Clearly, the periodic Cholesky factors $R_{i,k}$, for $k = 0, \ldots, K-1$, have off-diagonal columns. Consider now $\bar{R}_{i,k}$ contains all the off-diagonal columns of $R_{i,k}$ for each k, where $k = 0, \ldots, K-1$. Then it must be the case that

$$\lim_{i \to \infty} \| \bar{R}_{i,k} \, \bar{R}_{i,l}^T \|_2 = 0, \tag{9.27}$$

for some pairs (k, l), $k \neq l$, and $k = 0, \ldots, K-1$, $l = 0, \ldots, K-1$. The same holds true for observability type LR-ADI computation. ◊

9.3.5. Column Compression for the LR-ADI Method

For a fast convergence of the ADI iteration, it is very important to choose a set of good shift parameters. Since we are working with suboptimal parameters, the desired convergence in the LR-ADI iteration may not be achieved in few iteration steps and, as a result, the number of columns of the approximate Cholesky factor may grow. In order to keep the low-rank structure in Z_i, we truncate those columns that do not carry any additional information in the subsequent iteration steps. This truncation approach saves memory space and lowers the computational cost, because residual computations required in the stopping criteria will also incorporate these redundant columns.

Assume that $Z_i \in \mathbb{R}^{n \times r_c}$ has the numerical rank $\operatorname{rank}(Z_i, \tau) = r_n < r_c$ with a prescribed tolerance τ. Then we compute the rank-revealing QR decomposition (RRQR)

$$Z_i^T = Q_i \mathcal{R}_i \Pi_i^T, \qquad \mathcal{R}_i = \begin{bmatrix} \mathcal{R}_{i,11} & \mathcal{R}_{i,12} \\ 0 & \mathcal{R}_{i,22} \end{bmatrix},$$

where Q_i is orthogonal, Π_i is a permutation matrix, $\mathcal{R}_{i,11} \in \mathbb{R}^{r_n \times r_n}$ is upper triangular and $\|\mathcal{R}_{i,22}\|_F \leq \tau$. Setting $\mathcal{R}_{i,22} \approx 0$ and $\tilde{Z}_i^T = [\mathcal{R}_{i,11} \; \mathcal{R}_{i,12}] \Pi_i^T$, we find that $\tilde{Z}_i \tilde{Z}_i^T \approx \mathcal{G}^{cr}$. Note that we do not need to compute Q_i, since this matrix cancels out in the product $\tilde{Z}_i \tilde{Z}_i^T$ due to its orthogonality property. In practice, the rank determination has to be performed on the basis of the truncation tolerance τ in the RRQR. In [15], it is shown that a tolerance $\tau = \sqrt{\epsilon}$, where ϵ is the machine precision, is sufficient to achieve an error of the machine precision magnitude for the solution $\mathcal{G}^{cr}$ of the PLDALE (9.4). We summarize the resulting ADI iteration in Algorithm 9.2.

Algorithm 9.2 Low-rank Cholesky factor ADI (LRCF-ADI) iteration for causal PLDALE.

Input: $\mathcal{A}, \mathcal{E}, \mathcal{B}, \mathcal{P}_l$ and shift parameters $\tau_1, \tau_2, \ldots, \tau_i$.
Output: A low-rank Cholesky factor Z_i such that $\mathcal{G}^{cr} \approx Z_i Z_i^T$.

1: $V_1 = 2\sqrt{-Re(\tau_1)}\Big((1+\tau_1)\mathcal{A} + (1-\tau_1)\mathcal{E}\Big)^{-1}\mathcal{P}_l\mathcal{B}$
2: $Z_1 = V_1$
3: **for** $i = 2, 3, \ldots,$ **do**
4: $\quad V_i = \sqrt{\dfrac{Re(\tau_i)}{Re(\tau_{i-1})}}\Big(V_{i-1} - (\tau_i + \bar{\tau}_{i-1})\Big((1+\tau_i)\mathcal{A} + (1-\tau_i)\mathcal{E}\Big)^{-1}(\mathcal{A} - \mathcal{E})V_{i-1}\Big)$
5: $\quad Z_i = [\, Z_{i-1},\ V_i \,]$
6: $\quad [\mathcal{R}_i, \Pi_i, r_n] = \mathrm{RRQR}(Z_i^T,\ \sqrt{\epsilon})$
7: $\quad$ Update $Z_i = \Pi_i \mathcal{R}_i^T [\, I_{r_n},\ 0 \,]^T$
8: **end for**

9.4. Smith Method for Solving Noncausal Lifted Lyapunov Equations

Consider now the PLDALE

$$\mathcal{A}\mathcal{G}^{ncr}\mathcal{A}^T - \mathcal{E}\mathcal{G}^{ncr}\mathcal{E}^T = \mathcal{Q}_l\mathcal{B}\mathcal{B}^T\mathcal{Q}_l^T, \quad \mathcal{G}^{ncr} = \mathcal{Q}_r\mathcal{G}^{ncr}\mathcal{Q}_r^T. \tag{9.28}$$

For nonsingular $\mathcal{A}$, this equation is equivalent to the PLDALE

$$\mathcal{G}^{ncr} - (\mathcal{A}^{-1}\mathcal{E})\mathcal{G}^{ncr}(\mathcal{A}^{-1}\mathcal{E})^T = \mathcal{Q}_r\mathcal{A}^{-1}\mathcal{B}\mathcal{B}^T\mathcal{A}^{-T}\mathcal{Q}_r^T, \quad \mathcal{G}^{ncr} = \mathcal{Q}_r\mathcal{G}^{ncr}\mathcal{Q}_r^T. \tag{9.29}$$

In this case the relation $\mathcal{Q}_r\mathcal{A}^{-1}\mathcal{E} = \mathcal{A}^{-1}\mathcal{E}\mathcal{Q}_r$ holds [110] and such an equation can be solved by the Smith method [96] given by

$$\begin{aligned} \mathcal{G}_1^{ncr} &= \mathcal{Q}_r\mathcal{A}^{-1}\mathcal{B}\mathcal{B}^T\mathcal{A}^{-T}\mathcal{Q}_r^T, \\ \mathcal{G}_i^{ncr} &= \mathcal{Q}_r\mathcal{A}^{-1}\mathcal{B}\mathcal{B}^T\mathcal{A}^{-T}\mathcal{Q}_r^T + (\mathcal{A}^{-1}\mathcal{E})\mathcal{G}_{i-1}^{ncr}(\mathcal{A}^{-1}\mathcal{E})^T. \end{aligned}$$

Note that $\mathcal{Q}_r$ is the spectral projector onto the invariant subspace of the matrix $\mathcal{A}^{-1}\mathcal{E}$ corresponding to the zero eigenvalues. Then $\mathcal{Q}_r\mathcal{A}^{-1}\mathcal{E} = \mathcal{A}^{-1}\mathcal{E}\mathcal{Q}_r$ is nilpotent with the nilpotency index ν, where ν is the index of the periodic descriptor system (8.1). In this case, after ν iterations we obtain

$$\mathcal{G}_\nu^{ncr} = \sum_{k=0}^{\nu-1}(\mathcal{A}^{-1}\mathcal{E})^k\mathcal{Q}_r\mathcal{A}^{-1}\mathcal{B}\mathcal{B}^T\mathcal{A}^{-T}\mathcal{Q}_r^T((\mathcal{A}^{-1}\mathcal{E})^T)^k = \mathcal{G}^{ncr}.$$

Therefore, the Cholesky factor X of the solution $\mathcal{G}^{ncr} = XX^T$ of (9.29) and also of the PLDALE (9.28) takes the form

$$X = [\, \mathcal{Q}_r\mathcal{A}^{-1}\mathcal{B},\ \mathcal{A}^{-1}\mathcal{E}\mathcal{Q}_r\mathcal{A}^{-1}\mathcal{B},\ \ldots,\ (\mathcal{A}^{-1}\mathcal{E})^{\nu-1}\mathcal{Q}_r\mathcal{A}^{-1}\mathcal{B} \,]. \tag{9.30}$$

The computation of this factor is presented in Algorithm 9.3.

Algorithm 9.3 Generalized Smith method for noncausal PLDALE.

Input: $\mathcal{A}, \mathcal{E}, \mathcal{B}$, spectral projector $\mathcal{Q}_r$.
Output: A low-rank Cholesky factor X_ν such that $\mathcal{G}^{ncr} = X_\nu X_\nu^T$.

1: $W_1 = \mathcal{Q}_r \mathcal{A}^{-1}\mathcal{B}$
2: $X_1 = W_1$
3: **for** $i = 2, 3, \ldots, \nu$ **do**
4: $\quad W_i = \mathcal{A}^{-1}\mathcal{E}W_{i-1}$
5: $\quad X_i = [X_{i-1},\ W_i]$
6: **end for**

We note that the iteration only continues up to the index ν of the descriptor system (8.1). If the index ν is unknown, then Algorithm (9.3) can be stopped as soon as $\|W_i\|_F \leq tol$ or $\|W_i\|_F / \|X_i\|_F \leq tol$ with a user-defined tolerance tol. In practice, most of the systems we handle are index-1 or index-2 problems. For an index-1 problem, the algorithm only needs to compute the first block column of X in (9.30), and for an index-2 problem, it computes only the first two block columns of X. In that sense, the solution can be obtained with few computations.

Remark 9.7:
In order to guarantee that the second equation in (9.29) and also in (9.28) is satisfied in finite precision arithmetic, we have to project W_i onto the image of $\mathcal{Q}_r$ by pre-multiplication with $\mathcal{Q}_r$. ◊

Note that the generalized Smith iteration does not preserve the block diagonal structure at every iteration step in Algorithm 9.3, but the approximate Gramian $\mathcal{G}_i^{ncr} = X_i X_i^T$ has block diagonal structure at each iteration step, $i = 1, 2, \ldots, \nu$. After ν iterations we obtain $\mathcal{G}_\nu^{ncr} = \mathcal{G}^{ncr}$ and $\mathcal{G}^{ncr} = X_\nu X_\nu^T$ has block diagonal structure analogous to the solution of the PLDALE (9.28) given by $\mathcal{G}^{ncr} = \operatorname{diag}(G_1^{ncr}, \ldots, G_{K-1}^{ncr}, G_0^{ncr})$, where G_k^{ncr} are the periodic solutions of the PPDALE (4.70) for $k = 0, 1, \ldots, K-1$. Since $\mathcal{G}^{ncr} = X_\nu X_\nu^T$ has block diagonal structure, we can partition the factor X_ν as

$$X_\nu = [\, \tilde{X}_1^T,\ \ldots,\ \tilde{X}_{K-1}^T,\ \tilde{X}_0^T \,]^T$$

with $\tilde{X}_k \in \mathbb{R}^{n_k, \nu m}$. Then the noncausal reachability Gramians of system (8.1) can be computed in factored form $G_k^{ncr} = \tilde{X}_k \tilde{X}_k^T$.

Remark 9.8:
We have claimed that after each iteration step in Algorithm 9.3, the approximate Gramian has block diagonal structure and after ν iterations we obtain $\mathcal{G}_\nu^{ncr} = \mathcal{G}^{ncr}$ and $\mathcal{G}^{ncr} = X_\nu X_\nu^T$ has block diagonal structure analogous to the solution of the

PLDALE (9.28). Hence we must observe the similar case as in the LR-ADI computation (see Remark 9.6) that the norms of the product of off-diagonal matrices as in (9.27) will be zero at each iteration step i, where $i = 1, \ldots, \nu$. The same holds true for observability type Smith iteration. ◊

In the case of singular $\mathcal{A}$, we can again use the generalized Cayley transformation (9.7) and compute the Cholesky factor of the PLDALE (9.28) via the ADI iteration as in the causal case.

Remark 9.9:

The causal and noncausal observabiliy Gramians of the periodic descriptor system (8.1) can also be determined from the corresponding PLDALEs that are dual to the PLDALE (9.4) and (9.28), see [12] for details. Applying Algorithm 9.2 and Algorithm 9.3 to these equations, we find, respectively, the low-rank Cholesky factors L_k of the causal observability Gramians $G_k^{co} \approx L_k L_k^T$ and the Cholesky factor $\tilde{Y}_k$ of the noncausal observability Gramians $G_k^{nco} = \tilde{Y}_k \tilde{Y}_k^T$. ◊

9.5. Application to Model Order Reduction

Consider now the low-rank Cholesky factors of the causal and noncausal Gramians of the periodic descriptor system (8.1) obtained by using Algorithms 9.2 and 9.3, respectively.

Assume that the set of periodic matrix pairs $\{(E_k, A_k)\}_{k=0}^{K-1}$ is pd-stable. Consider the Cholesky factorizations of the causal and noncausal Gramians

$$\begin{aligned} G_k^{cr} &= R_k R_k^T, \quad & G_k^{co} &= L_k L_k^T, \\ G_k^{ncr} &= \tilde{X}_k \tilde{X}_k^T, \quad & G_k^{ncr} &= \tilde{Y}_k \tilde{Y}_k^T. \end{aligned}$$

Then the *causal* and *noncausal Hankel singular values* of the periodic descriptor system (8.1) are defined as

$$\begin{aligned} \sigma_{k,j} &= \sqrt{\lambda_j(G_k^{cr} E_{k-1}^T G_k^{co} E_{k-1})} = \zeta_j(L_k^T E_{k-1} R_k), \\ \theta_{k,j} &= \sqrt{\lambda_j(G_k^{ncr} A_k^T G_{k+1}^{nco} A_k)} = \zeta_j(\tilde{Y}_{k+1} A_k \tilde{X}_k), \end{aligned}$$

respectively. Let

$$\begin{aligned} L_k^T E_{k-1} R_k &= [U_{k,1}, U_{k,2}] \begin{bmatrix} \Sigma_{k,1} & \\ & \Sigma_{k,2} \end{bmatrix} [V_{k,1}, V_{k,2}]^T, \\ \tilde{Y}_{k+1}^T A_k \tilde{X}_k &= U_{k,3} \Theta_k V_{k,3}^T, \end{aligned} \tag{9.31}$$

be singular value decompositions, where $[U_{k,1}, U_{k,2}]$, $[V_{k,1}, V_{k,2}]$, $U_{k,3}$ and $V_{k,3}$ are orthogonal,

$$\Sigma_{k,1} = \operatorname{diag}(\sigma_{k,1}, \ldots, \sigma_{k,r_k^f}), \quad \Sigma_{k,2} = \operatorname{diag}(\sigma_{k,r_{k+1}^f}, \ldots, \sigma_{n_k^f}),$$

with $\sigma_{k,1} \geq \cdots \geq \sigma_{k,r_k^f} > \sigma_{k,r_{k+1}^f} \geq \ldots \geq \sigma_{k,n_k^f} > 0$, and $\Theta_k = \mathrm{diag}(\theta_{k,1}, \ldots, \theta_{k,r_k^\infty})$ is nonsingular for $k = 0, 1, \ldots, K-1$. Note that the number of non-zero noncausal Hankel singular values of (8.1) is estimated by the relation (8.42) [11].

We compute the reduced-order system of (8.1) as

$$\tilde{E}_k = S_{k,r}^T E_k T_{k+1,r}, \quad \tilde{A}_k = S_{k,r}^T A_k T_{k,r}, \quad \tilde{B}_k = S_{k,r}^T B_k, \quad \tilde{C}_k = C_k T_{k,r}, \tag{9.32}$$

where the projection matrices have the form

$$\begin{aligned} S_{k,r} &= [\, L_{k+1} U_{k+1,1} \Sigma_{k+1,1}^{-1/2}, \;\; \tilde{Y}_{k+1} U_{k,3} \Theta_k^{-1/2} \,] \in \mathbb{R}^{\mu_{k+1}, r_{k+1}}, \\ T_{k,r} &= [\, R_k V_{k,1} \Sigma_{k,1}^{-1/2}, \;\; \tilde{X}_k V_{k,3} \Theta_k^{-1/2} \,] \in \mathbb{R}^{n_k, r_k}, \end{aligned}$$

with $r_k = r_k^f + r_k^\infty$. Similarly, we can define the $\mathbb{H}_\infty$-norm error bound [11] for the reduced-order system by relation

$$\|\mathcal{H} - \tilde{\mathcal{H}}\|_{\mathbb{H}_\infty} = \sup_{\omega \in [0, 2\pi]} \|\mathcal{H}(e^{i\omega}) - \tilde{\mathcal{H}}(e^{i\omega})\|_2 \leq 2 \sum_{k=0}^{K-1} \mathrm{trace}(\Sigma_{k,2}), \tag{9.33}$$

where $\|.\|_2$ denotes the matrix spectral norm and $\Sigma_{k,2}$ contains the truncated causal Hankel singular values.

Remark 9.10:

(i) For balanced truncation model order reduction, we use a tolerance to truncate the Hankel singular values for having a reduced system with smaller dimension. To achieve a good approximation, the Gramians, i.e., the Cholesky factors should be computed as accurately as possible. Note that the tolerance $\tau = \sqrt{\epsilon}$, is a good choice to compute the low-rank Cholesky factors using Algorithms 9.2, because in that case the Gramian, i.e., the solution $\mathcal{G}^{cr}$ of the PLDALE (9.4) has error of machine precision ϵ. For MOR application this is not a good choice, since we use the Cholesky factors there, not the Garmians. So the Cholesky factors have to be computed more accurately. If the reduced-order model is computed with less accuracy, then this does not matter.

(ii) The error bound of the reduced-order system depends on the accuracy of the computed Cholesky factors and also on the accuracy we have considered for the reduced-order model. Therefore, we can only approximate the error bound. ◊

9.5.1. Numerical Results and Comparisons

In this subsection we consider numerical examples to illustrate the reliability of the proposed iterative methods for model order reduction of periodic time-varying discrete-time descriptor systems. The first test example is taken from [30], it is a small dimensional problem that has already been considered in Chapter 8. The second test problem

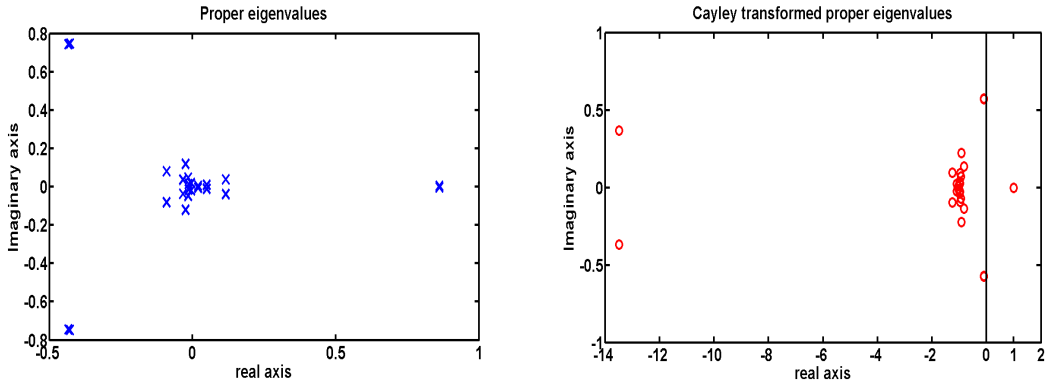

(a) (b)

Figure 9.1. (a) Finite eigenvalues of lifted system, (b) finite eigenvalues of Cayley transformed system (Model problem 1).

is an artificial problem of medium size (n=4040), and the third problem is a very large sparse problem (n=10^5) obtained from the discretization of a heat equation at different sampling time.

9.5.2. Model Problem 1

We consider here the model problem 1 of Chapter 8. We compare the results of dense computations with the results of LRCF-ADI iterative computations. The sparsity patterns of $\mathcal{E}$ and $\mathcal{A}$ have been shown in Figure 8.1.

The eigenspectrum of the lifted system and the corresponding Cayley transformed system are shown in Figure 9.1. We draw a line on the imaginary axis to show the nice shifts of the eigenvalues of the lifted pencil into the Cayley transformed pencil. We observe all the finite stable eigenvalues of the lifted pencil are shifted into the negative half of the complex plane, and infinite eigenvalues of the lifted pencil are mapped to 1 as expected.

We solve the causal lifted Lyapunov equations using the LRCF-ADI iteration as in Algorithm 9.2. The shift parameters are computed using the heuristic process discussed in Section 9.3.3 and shown in Figure 9.2.

We have computed the normalized residual at each step of the ADI-iteration. The iteration is stopped as soon as the normalized Lyapunov residual, computed by using Equation (9.25), exceeds $tol = 10^{-8}$.

We plot the norms of the products of off-diagonal matrices given by (9.27) to show that the approximate Gramian has block diagonal structure analogous to its exact solution. In Figure 9.4 we plot the norms of these off-diagonal matrices (i.e., norms of $\bar{R}_{i,k}\,\bar{R}_{i,l}^T$ for $k \neq l$ given by (9.27) for $k \neq l$, and $k, l = 0, 1, 2$), along the Y-axis and the index of

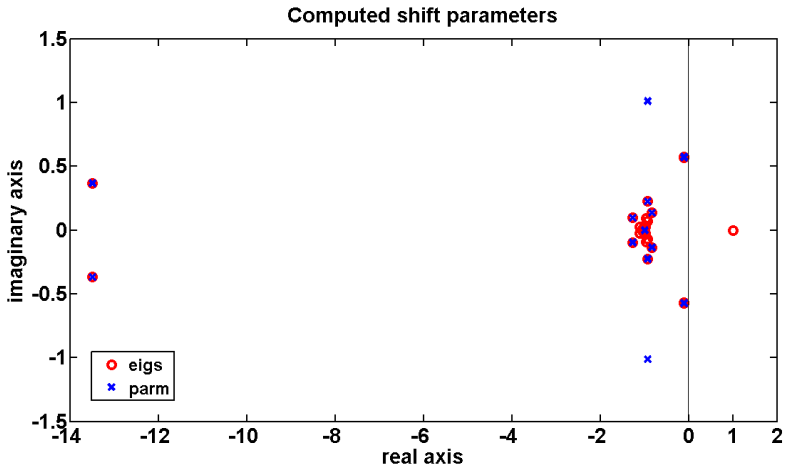

Figure 9.2. Computed shift parameters (Model problem 1); (eigs = eigenvalues, parm = parameters).

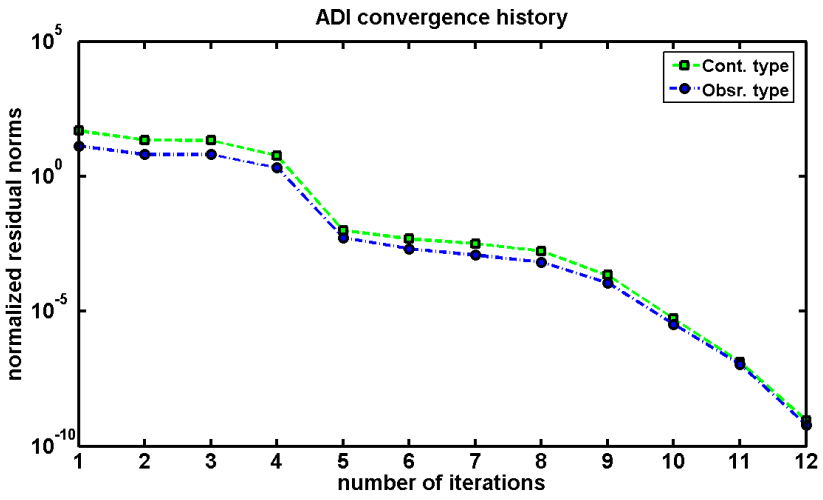

Figure 9.3. Normalized residual norms for Lyapunov equations (Model problem 1); (Cont. type = Reachability type, Obsr. type = Observability type).

iterations along the X-axis (for reachability type LR-ADI computation). In each case we notice that the norms tend to zero when the iteration steps increase. The same results hold true for the observability type LR-ADI computation which are shown in Figure 9.5.

Since our model problem is an index-1 problem, we only need one iteration in Algorithm 9.3. We then compute the norms of the products of the off-diagonal matrices and we observe that the norms are zero for the noncausal case.

Figure 9.14 shows the causal Hankel singular values of the original system in lifted form. These Hankel singular values are the combination of all the causal Hankel singular values $\sigma_{k,j}$ of the periodic descriptor system (8.1) given by its different subsystems for $k = 0, 1, 2$. We observe that the Hankel singular values decay fast, and, hence system (8.1) can be well approximated by a reduced-order model. We have 24 causal Hankel singular values for the original lifted system and the remaining 6 are the noncausal Hankel singular values which are computed using Algorithm 9.3. These noncausal Hankel singular values are positive.

We approximate system (8.1) to the tolerance 10^{-2} by truncating the states corresponding to the smallest 7 causal Hankel singular values. For different subsystems, the numbers of the computed non-zero noncausal Hankel singular values are identical and $r_k^\infty = 2$ for $k = 0, 1, 2$. The computed reduced-order model has subsystems of orders $r = (7, 8, 8)$. We observe that the reduced order system preserves the stability of the original system. In Figure 9.7 we present the norms of the frequency responses $\mathcal{H}(e^{i\omega})$ and $\tilde{\mathcal{H}}(e^{i\omega})$ of the original and reduced-order lifted systems for a frequency range $[0, 2\pi]$. To compare the results obtained by using the LRCF-ADI model reduction technique, in Figure 9.7 we also plot the norm of $\tilde{\mathcal{H}}(e^{i\omega})$ that we obtained by dense computations (see Chapter 8). We observe a nice match of the system norms.

In Figure 9.8, we display the absolute error $\|\mathcal{H}(e^{i\omega}) - \tilde{\mathcal{H}}(e^{i\omega})\|_2$ and the error bound given in (9.33). One can see that the absolute error is smaller than the error bound. We compare the absolute errors obtained using dense computation and LRCF-ADI iterative computation. Although the absolute error in the LRCF-ADI iterative computation is slightly higher than the absolute error of the dense computation, it is still bounded by the error tolerance.

9.5.3. Model Problem 2

We consider an artificial periodic discrete-time descriptor system with $\mu_k = n_k = 404$, $p_k = 2$, $q_k = 3$, and period $K = 10$. The periodic matrix pairs $\{(E_k, A_k)\}_{k=0}^{K-1}$ are periodic stable with $n_k^f = 400$ and $n_k^\infty = 4$ for every $k = 0, 1, \ldots, 9$. The sparsity patterns of the periodic matrix pair (E_0, A_0) are shown in Figure 9.9. The periodic matrices E_k and A_k vary for different values of k, $k = 0, 1, \ldots, K-1$, and the periodic matrix pairs $\{(E_k, A_k)\}_{k=1}^{K-1}$, for different values of k, have almost the same sparsity patterns as shown in Figure 9.9.

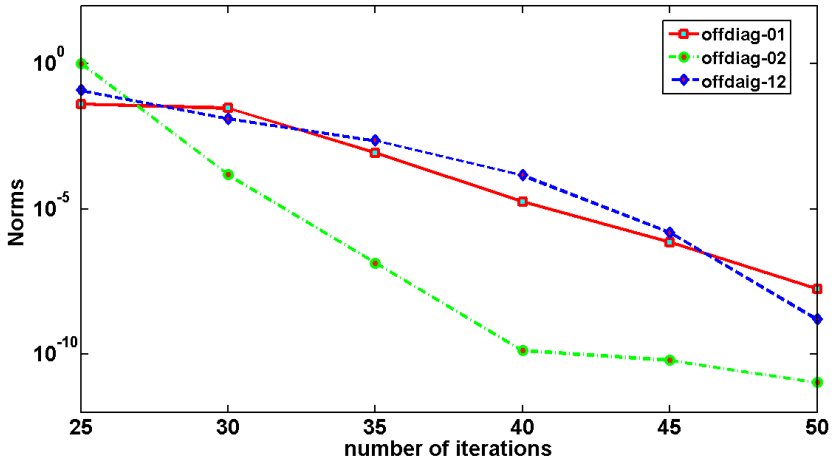

Figure 9.4. Norms of off-diagonal matrices: reachability type (Model problem 1); offdiag-01= norm of $(\bar{R}_{i,0}\ \bar{R}_{i,1}^{T})$, and i is number of iterations.

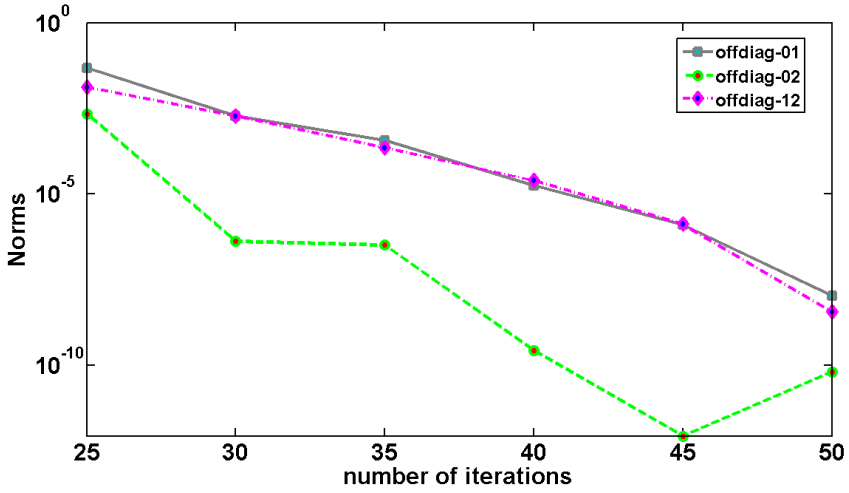

Figure 9.5. Norms of off-diagonal matrices: observability type (Model problem 1) offdiag-01= norm of $(\bar{R}_{i,0}\ \bar{R}_{i,1}^{T})$, and i is number of iterations.

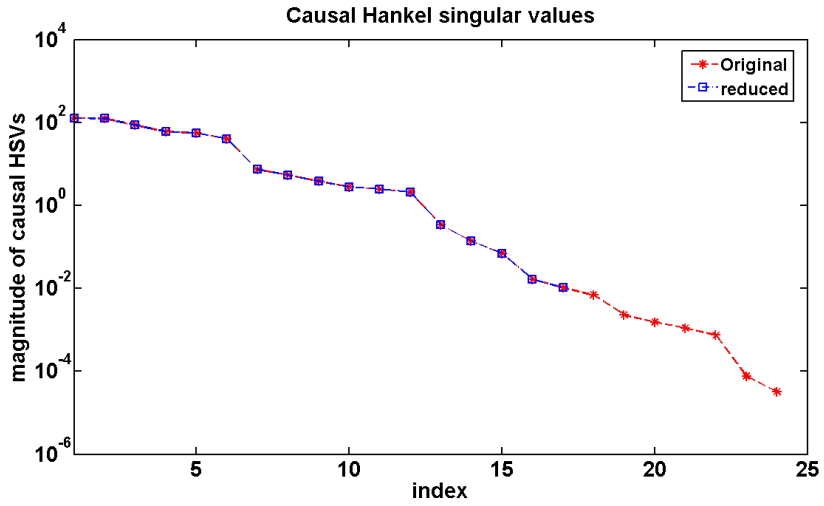

Figure 9.6. Causal Hankel singular values for original system in lifted form (Model problem 1).

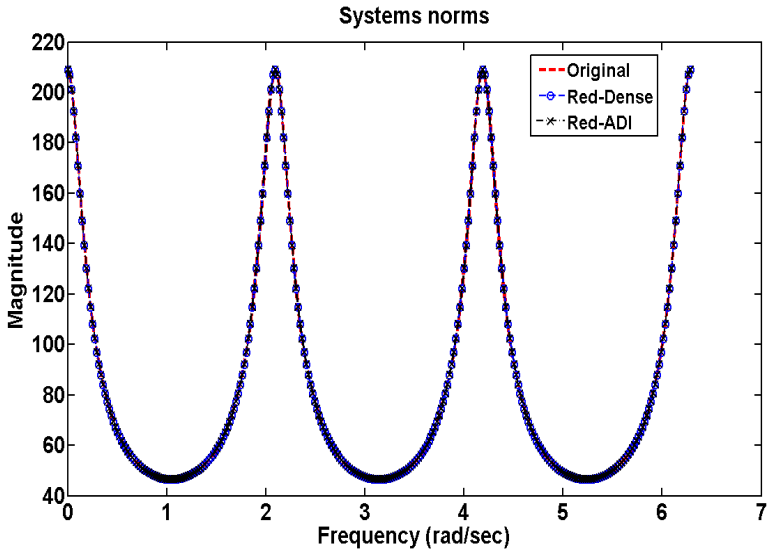

Figure 9.7. The frequency responses of the original and the reduced-order lifted systems (Model problem 1); (Red-Dense = Reduced system using dense computation, Red-ADI = Reduced system using LRCF-ADI computation)

.

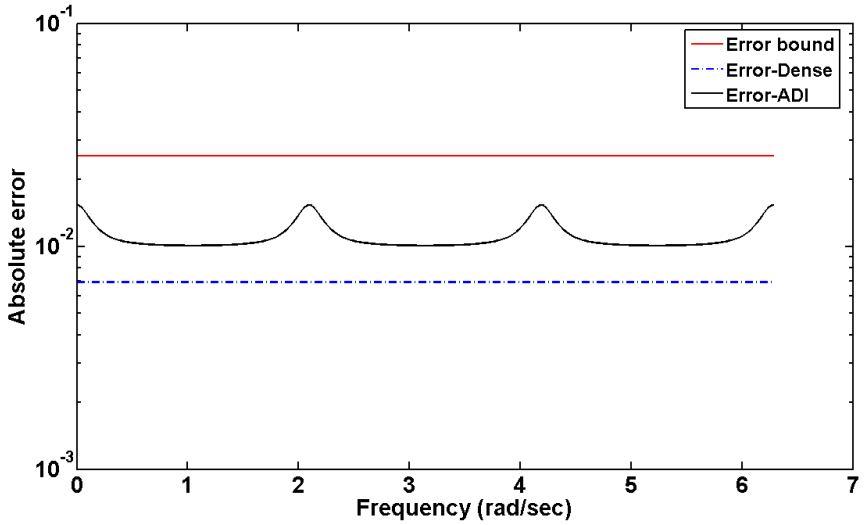

Figure 9.8. Absolute error and error bound (Model problem 1);
(Error-Dense = Error system using dense computation
Error-ADI = Error system using LRCF-ADI computation).

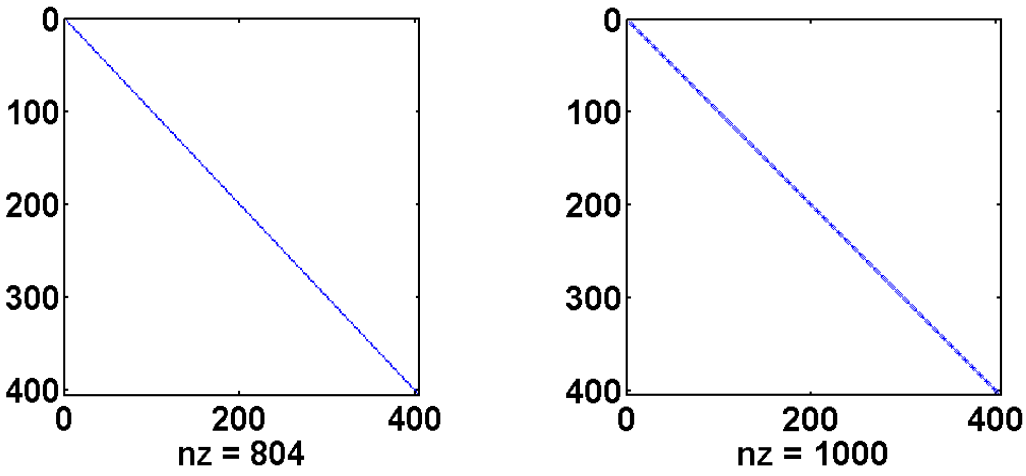

(a) (b)

Figure 9.9. (a) Sparsity pattern of A_0, (b) sparsity pattern of E_0 (Model problem 2).

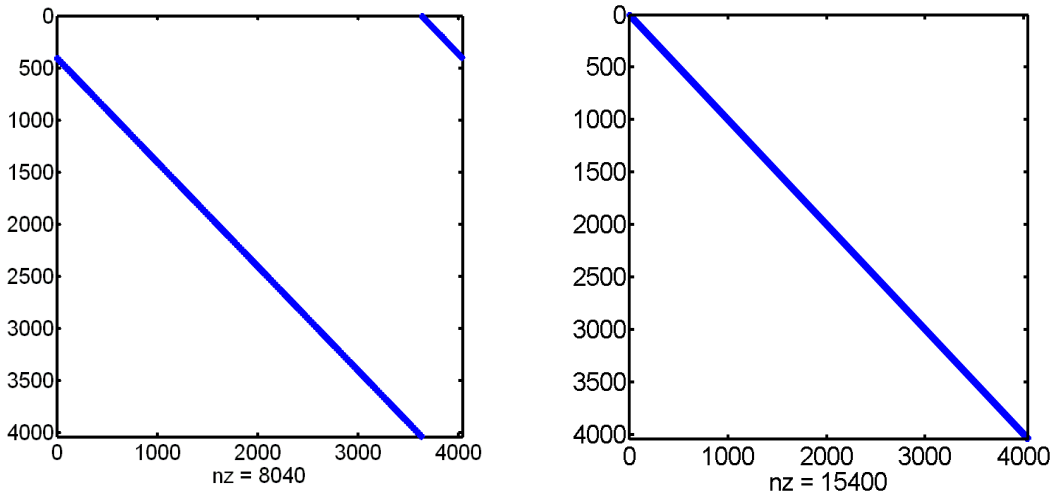

Figure 9.10. (a) Sparsity pattern of $\mathcal{A}$, (b) sparsity pattern of $\mathcal{E}$ (Model problem 2).

The original lifted system has order $n = 4040$. The sparsity patterns of $\mathcal{E}$ and $\mathcal{A}$ of the corresponding lifted system are plotted in Figure 9.10.

The eigenspectrum of the lifted system and the corresponding Cayley transformed system are shown in Figure 9.11. The shift parameters that are computed using the heuristic process are shown in Figure 9.12.

The normalized Lyapunov residuals are computed at each step of the ADI-iteration by using equation (9.25). The iteration is stopped as soon as the normalized Lyapunov residual exceeds $tol = 10^{-8}$.

Figures 9.13(a) and 9.13(b) show the decays of the normalized residual norms computed at each step of the ADI-iteration for reachability and observability type causal lifted Lyapunov equations. One can see that the solution of the PLDALE (8.9) (and also its dual, the observability type PLDALE) can be approximated by a matrix of rank 25.

Figure 9.14 shows the causal Hankel singular values of the original lifted system (8.2). These 4000 causal Hankel singular values are the combination of all the causal Hankel singular values $\sigma_{k,j}$ of the periodic descriptor system (8.1) given by its different subsystems for $k = 0, 1, \ldots, 9$. In Figure 9.15, we present the largest 300 causal Hankel singular values computed by solving the PLDALE (9.4) and its dual equation (5.43) using the direct method (by dense computation) that we have discussed in Chapter 8. One can see the Hankel singular values decay fast, and, hence system (8.1) can be well approximated by a reduced-order model. In Figure 9.15, we also present the 157 approximate largest causal Hankel singular values computed from the singular value decompositions of the matrices $L_k^T E_{k-1} R_k$ with the low-rank Cholesky factors R_k and L_k of the causal reachability and observability Gramians determined by Algorithm 9.2.

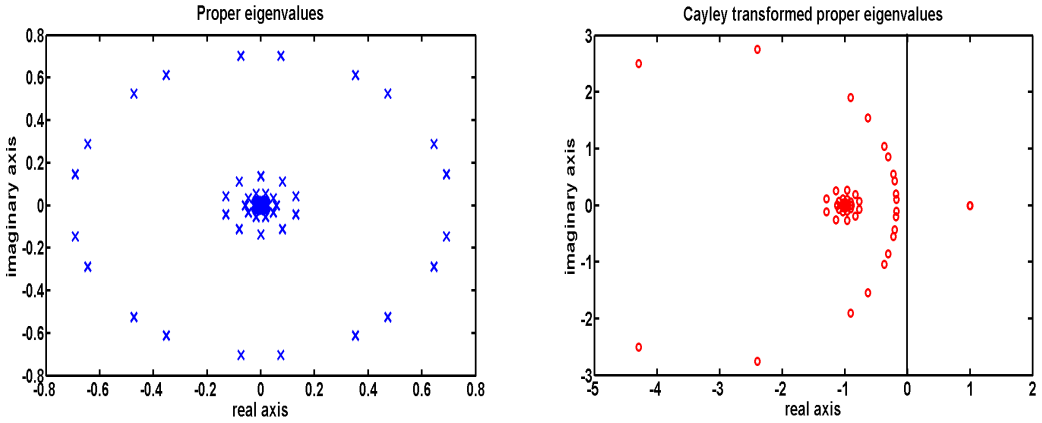

(a) (b)

Figure 9.11. (a) Finite eigenvalues of lifted system, (b) finite eigenvalues of Cayley transformed system (Model problem 2).

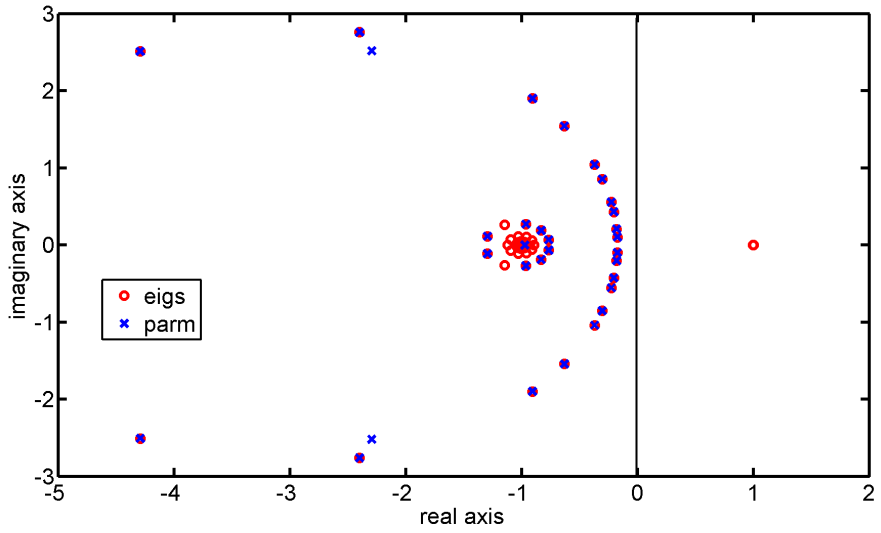

Figure 9.12. Computed shift parameters (Model problem 2); (eigs = eigenvalues, parm = parameters).

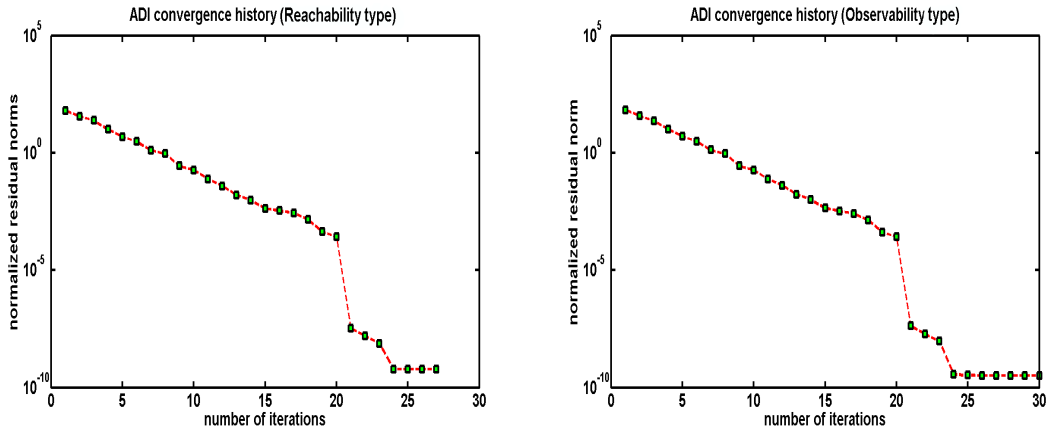

(a) (b)

Figure 9.13. (a) Normalized residual norms for reachability Lyapunov equation, (b) normalized residual norms for observability Lyapunov equation (Model problem 2).

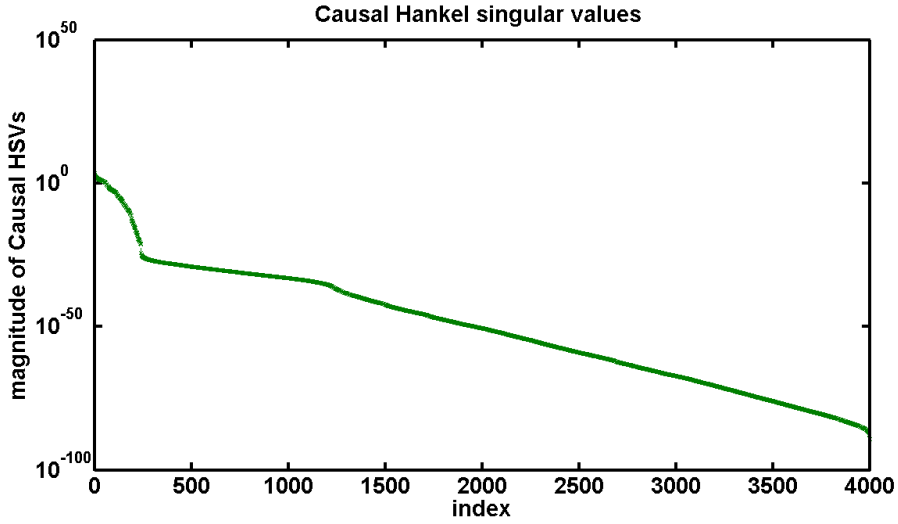

Figure 9.14. Causal Hankel singular values for original system in lifted form (Model problem 2).

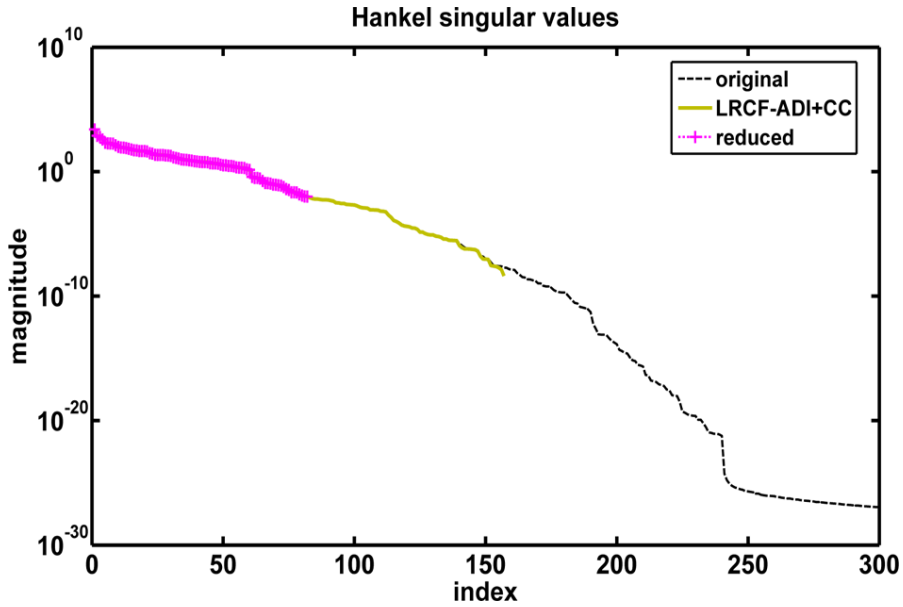

Figure 9.15. Causal Hankel singular values for original, computed (with column compression, CC) and reduced-order lifted systems (Model problem 2).

The number of non-zero noncausal Hankel singular values computed by Algorithm 9.3 is 20. These non-zero noncausal Hankel singular values are plotted in Figure 9.16. For different subsystems, the numbers of the computed non-zero noncausal Hankel singular values are identical and given by $r_k^\infty = 2$ for $k = 0, 1, \ldots, 9$.

We approximate system (8.1) to the tolerance 10^{-2} by truncating the states corresponding to the smallest 75 causal Hankel singular values. The computed reduced-order model has subsystems of orders $(9, 10, 10, 11, 10, 9, 10, 11, 11, 11)$. Note that stability is preserved in the reduced-order system. Figure 9.17 shows the norms of the frequency responses $\mathcal{H}(e^{i\omega})$ and $\tilde{\mathcal{H}}(e^{i\omega})$ of the original and reduced-order lifted systems for a frequency range $[0, 2\pi]$. We observe a good match of the system norms. Finally, in Figure 9.18, we display the absolute error $\|\mathcal{H}(e^{i\omega}) - \tilde{\mathcal{H}}(e^{i\omega})\|_2$ and the error bound given in (9.33). One can see that the error bound is tight in this example.

9.5.4. Semi-Discretized Heat Equation

As a model problem we consider here the heat diffusion equation for the one-dimensional (1D) PDE taken from the SLICOT[1] benchmark collection for model reduction (problem 2.8 of [27]). The dimension of the original semi-discretized continuous-time system is extended to a dimension of $N_c = 10^4$. That means, in our case the continuous-time model has $A \in \mathbb{R}^{N_c \times N_c}$, $B = (\delta_{i,N_c/3})_i \in \mathbb{R}^{N_c}$, and $C = (\delta_{i,2N_c/3})_i \in \mathbb{R}^{N_c}$, where $\delta_{i,j}$ means that

[1] http://www.slicot.org

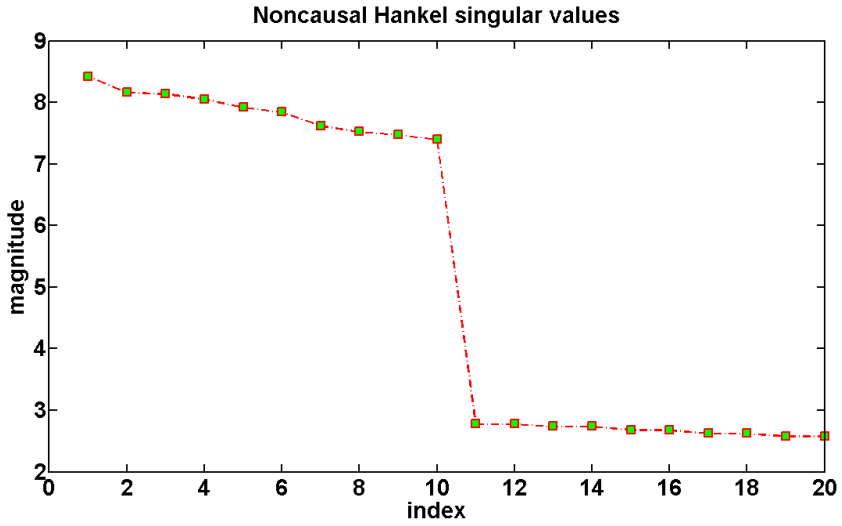

Figure 9.16. Non-zero noncausal Hankel singular values for original system in lifted form (Model problem 2).

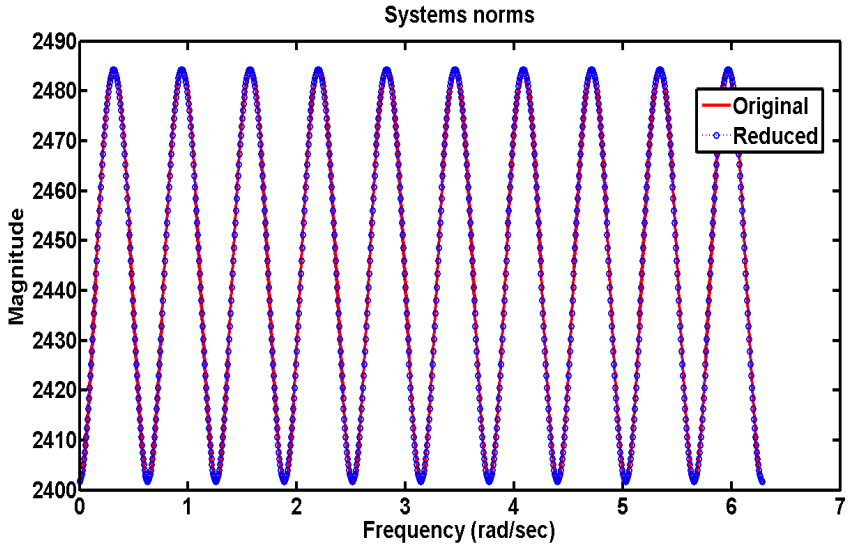

Figure 9.17. The frequency responses of the original and the reduced-order lifted systems (Model problem 2).

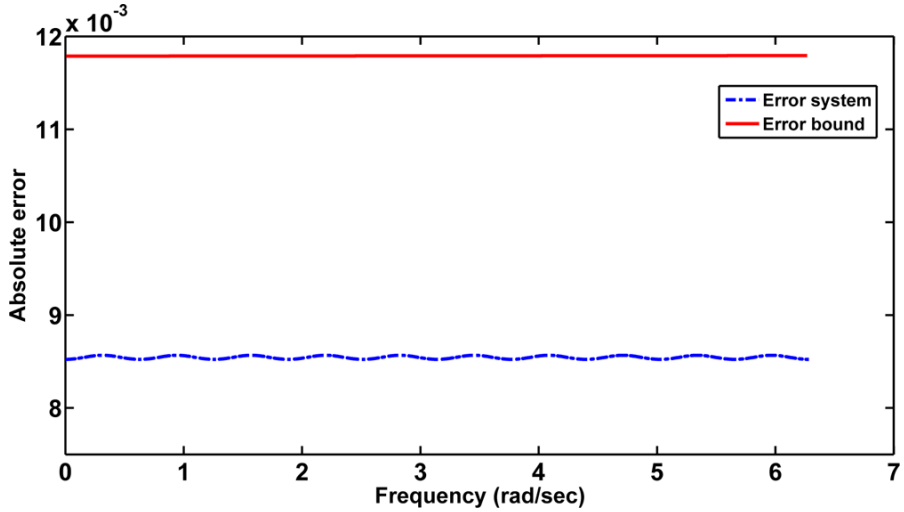

Figure 9.18. Absolute error and error bound (Model problem 2).

the corresponding vector has nonzero element (which is 1 in that case) only at the place where $i = j$, and all other entries are zeros for $i \neq j$. The semi-discretized continuous-time system is then completely discretized using the Crank-Nicholson method and we obtain a generalized discrete-time sparse system at every discretized sample time k, where k is chosen arbitrarily from the time interval $(0, 1)$. For each k, we have the periodic matrices (E_k, A_k, B_k, C_k). In this periodic formulation, we consider $k = 0, 1 \ldots, 9$, and period $K = 10$. More details about the benchmark example can be found in [27]. All the results for this test problem have been carried out in MATLAB 7.12.0 (R2011a) on an Intel Xeon Dual-Core CPU with a 3.0GHz clock and 64 GB of RAM.

For the periodic system, the periodic matrix pairs $\{(E_k, A_k)\}_{k=0}^{K-1}$ are pd-stable but have no infinite eigenvalues. The reason of considering such an example is that we want to test how our algorithms work and behave with very large sparse problem, and we like to check the efficiency of these algorithms. It is clear form the discussion of Section 9.3 that the crucial part of our proposed algorithms lies in the computations of the low rank Cholesky factors for the causal Gramians. We consider $\mu_k = n_k = 10^4$, $p_k = 1$, $q_k = 1$ for $k = 0, 1, \ldots, 9$. The sparsity patterns of the periodic matrix pair (E_0, A_0) are shown in Figure 9.19. All other periodic matrix pairs have the same sparsity patterns.

The original lifted system has order $n = 10^5$. The sparsity patterns of $\mathcal{E}$ and $\mathcal{A}$ of the corresponding lifted system are plotted in Figure 9.20.

We have solved the causal lifted Lyapunov equations using the LRCF-ADI iteration as in Algorithm 9.2. The shift parameters are computed using the heuristic process discussed in Section 9.3.3. We consider 50 shifts and these shifts are chosen from 100 Ritz values obtained from the Arnoldi process applied to $\mathbf{E}^{-1}\mathbf{A}$ and 60 for its inverse. In addition, to show the efficiency of Algorithm 9.2, we compute the low rank Cholesky factors of the reachability Gramians for models of different dimensions, and compare the execution

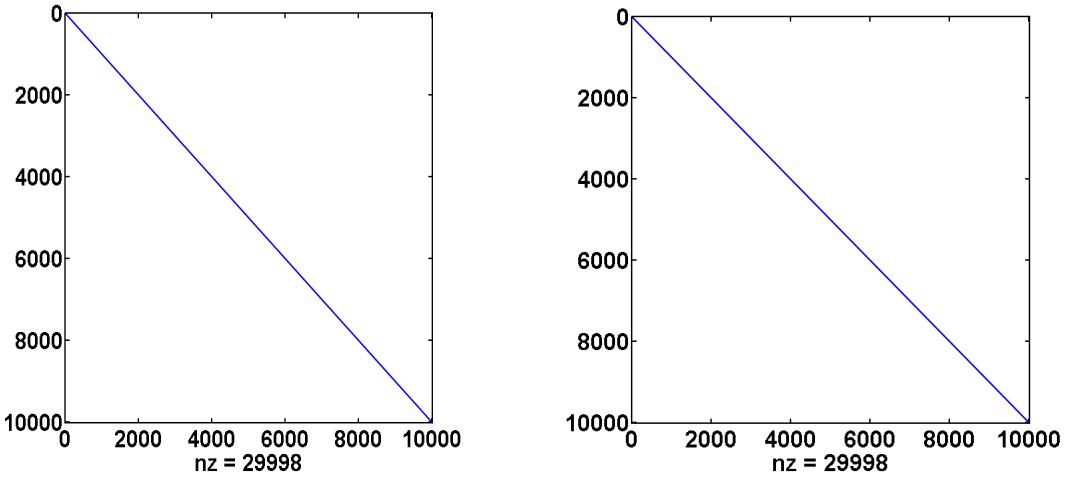

(a) (b)

Figure 9.19. (a) Sparsity pattern of A_0, (b) sparsity pattern of E_0 (heat equation).

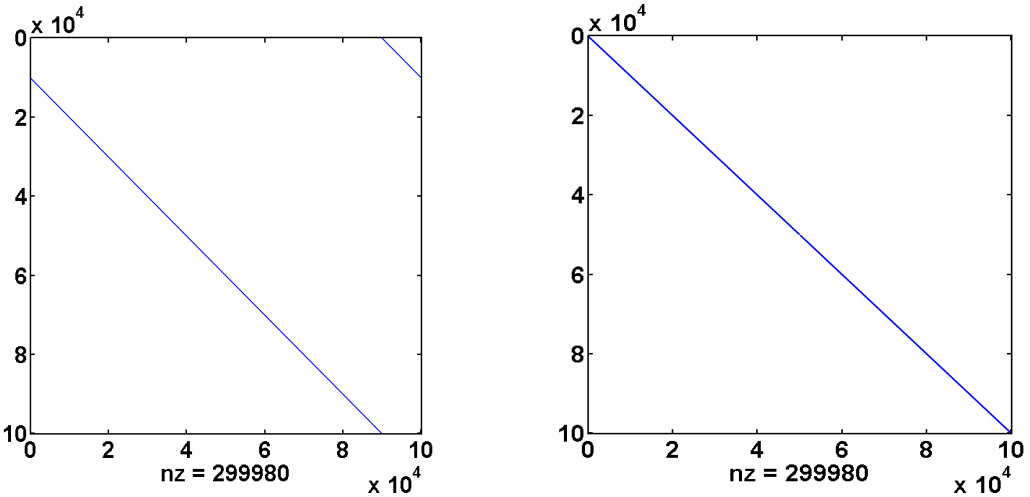

(a) (b)

Figure 9.20. (a) Sparsity pattern of $\mathcal{A}$, (b) sparsity pattern of $\mathcal{E}$ (heat equation).

dimension (n)	direct solver (sec)	LRCF-ADI (sec)
1000	22.59	10.64
2000	188.73	54.21
5000	1.937×10^3	93.37
10000	$> 2.16 \times 10^4$	1.80×10^2
100000	–	1.082×10^3

Table 9.1. Computational times for the Cholesky factors of reachability Gramians for different dimensional systems using direct solver and LRCF-ADI (Heat equation).

times with the times needed to solve those using direct solvers. We represent them in Table 9.1. In each case we notice the efficiency of our proposed algorithm. For a model of dimension $n = 10^5$, we wait several days to solve the low-rank Cholesky factor of the reachability Gramian but the computer still runs to generate solution, while using Algorithm 9.2 we can solve this in 1.082×10^3 sec ($\approx$ 18 mins).

For large-scale sparse problems, it is suggested in [13] that it is sufficient to terminate the LRCF-ADI iteration when the relative change criterion

$$\frac{\|Z_i - Z_{i-1}\|_F}{\|Z_i\|_F} \leq \varepsilon, \tag{9.34}$$

is satisfied for a tiny, positive constant ε. For the LRCF-ADI variants we observe that it can be evaluated cheaply as well. The difference between the two consecutive factors Z_i and Z_{i+1} in Algorithm 9.2 is the new column block V_i. Hence the numerator in (9.34) is just $\|V_i\|_F$. To do this we need not to compute $\|Z_i\|_F$ in each iteration step. Instead, $\|Z_i\|_F$ can be accumulated in the course of iteration as $\|Z_i\|_F^2 = \|Z_{i-1}\|_F^2 + \|V_i\|_F^2$, which ensures that at each step only $\|V_i\|_F$ needs to be computed where V_i contains only very few columns.

Figure 9.21 shows the relative changes that we have obtained for the results presented in Table 9.1, i.e., from the computation of low-rank Cholesky factors of reachability Gramians for systems of different dimensions using relation (9.34).

Remark 9.11:

While computing the low-rank Cholesky factors for models of different dimensions, we have noticed that the relative change in the low-rank factor decays very slowly. This is fast for model of small and medium dimensions ($n \leq 10^3$), but this rate is very very slow when the dimension of the system becomes higher, i.e, $n \geq 10^4$. We can hardly achieve a relative change of order $\mathcal{O}(10^{-3})$ for the model of dimension $n = 10^5$ with 400 LRCF-ADI iteration steps using Algorithm 9.2. For large-scale sparse problems, a Galerkin type projection method has been proposed in [89] in

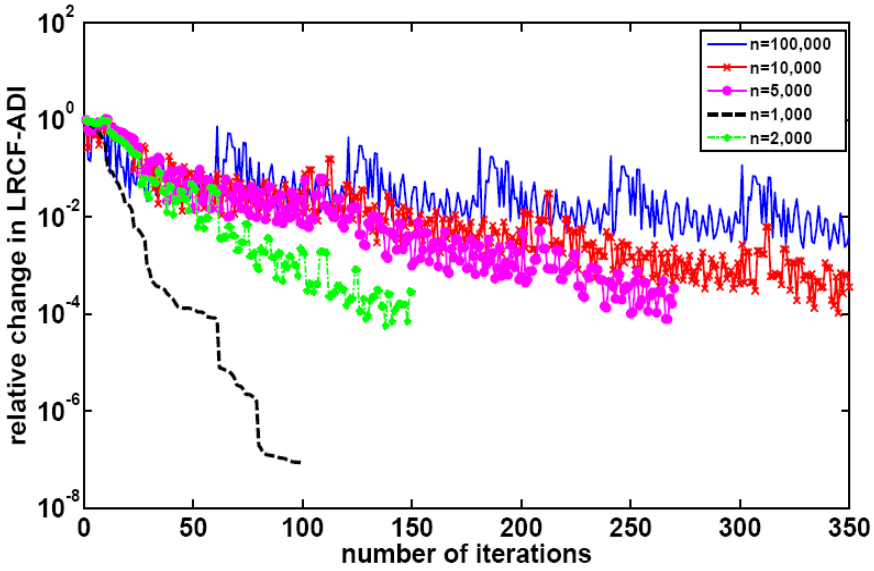

Figure 9.21. Relative change in low-rank factors of reachability Gramians (heat equation).

the computation of this low rank factors and to accelerate the convergence of the normalized residuals (also the relative changes) up to a satisfactory prescribed tolerance. But in each inner iteration loop of this proposed Galerkin type projection technique requires to solve a Lyapunov equation for the reformulated Cholesky factor, which also requires that the reformulated system matrices of this Lyapunov equation should have stable eigenvalues, i.e., the reformulated matrix pencil have all eigenvalues with negative real part (details can be found in Subsection 4.4.2 of [89]). This Galerkin type projection method is under our investigation. ◊

An important observation we want to state that in the MOR applications the convergence speed (or relative change rate) in the LRCF-ADI iteration is not a major issue to concern. In fact slower convergence may insure us to increase the accuracy of the MOR due to adding more subspace information in the factors. Similar result have been observed in [89] during the computations of low rank Cholesky factors of Gramians for large dimensional sparse system.

In Figure 9.22, we present the 360 approximate largest causal Hankel singular values computed from the singular value decompositions of the matrices $L_k^T E_{k-1} R_k$ with the low-rank Cholesky factors R_k and L_k of the causal reachability and observability Gramians determined by Algorithm 9.2. We approximate system (8.1) to the tolerance 10^{-6} by truncating the states corresponding to the smallest 320 causal Hankel singular values. The computed reduced-order model has subsystems of orders $(4, 4, 3, 4, 4, 5, 4, 4, 4, 4)$. We observe that stability is preserved in the reduced-order system.

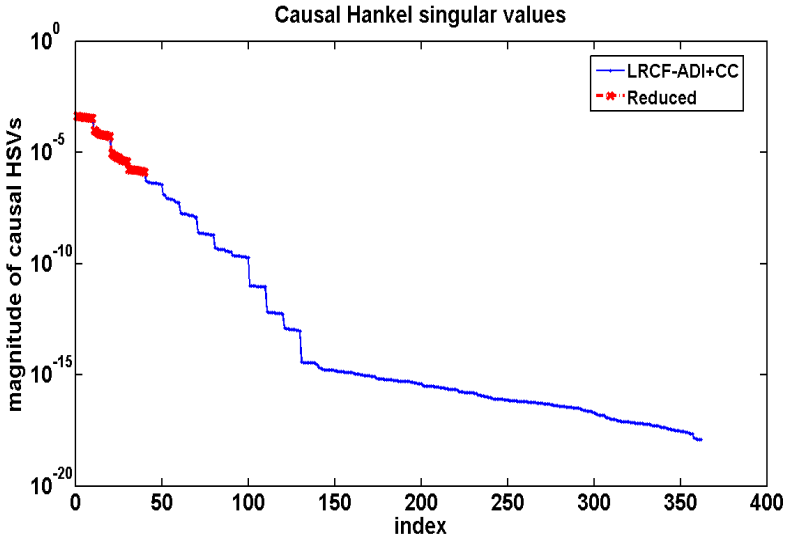

Figure 9.22. Causal Hankel singular values for computed (with column compression, CC) and reduced-order lifted systems (heat equation).

Figure 9.23 shows the norms of the frequency responses $\mathcal{H}(e^{i\omega})$ and $\tilde{\mathcal{H}}(e^{i\omega})$ of the original and reduced-order lifted systems for a frequency range $[0, 2\pi]$. The absolute error $\|\mathcal{H}(e^{i\omega}) - \tilde{\mathcal{H}}(e^{i\omega})\|_2$ and the error bound are displayed in Figure 9.24. We observe that the error bound is tight in this example.

To investigate the efficiency of the reduced-order system, we plot the frequency responses and the deviation of the frequency responses for the individual components of the transfer functions $\mathcal{H}(e^{i\omega})$ and $\tilde{\mathcal{H}}(e^{i\omega})$ in Figure 9.25. For example, Figure 9.25(a) shows the magnitudes of the frequency responses of the original (full) and the reduced-order lifted systems for $\mathcal{H}_{1,1}(e^{i\omega})$ and $\tilde{\mathcal{H}}_{1,1}(e^{i\omega})$, and Figure 9.25(b) shows their deviation. Similarly, we plot the frequency responses for the other components of $\mathcal{H}(e^{i\omega})$ and $\tilde{\mathcal{H}}(e^{i\omega})$. Note that $\mathcal{H}(e^{i\omega})$ and $\tilde{\mathcal{H}}(e^{i\omega})$ are the transfer functions of the original and reduced-order lifted systems.

We approximate the original system of dimension $n = 10^5$ to the tolerances of different scales and compute the reduced-order models with subsystems of different orders and show them in Table 9.2.

Original system (n)	MOR tolerence	reduced-order (r)	error bounds
10^5	10^{-5}	(3, 2, 2, 3, 2, 2, 4, 2, 2, 3)	1.5196×10^{-4}
10^5	10^{-6}	(4, 4, 3, 4, 4, 5, 4, 4, 4, 4)	1.0528×10^{-5}
10^5	10^{-7}	(5, 6, 6, 5, 5, 5, 5, 5, 5, 5)	1.4927×10^{-6}

Table 9.2. Reduced-order models for the system of dimension $n = 10^5$ with different approximation tolerances (heat equation).

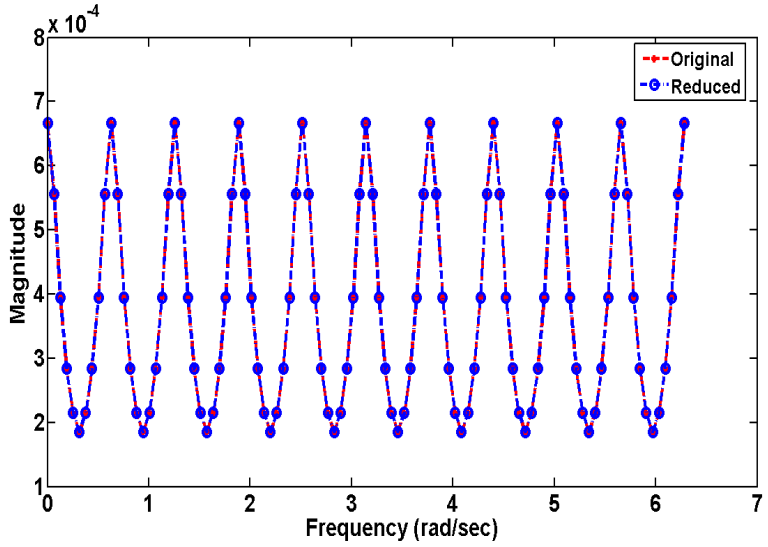

Figure 9.23. The frequency responses of the original and the reduced-order lifted systems (heat equation).

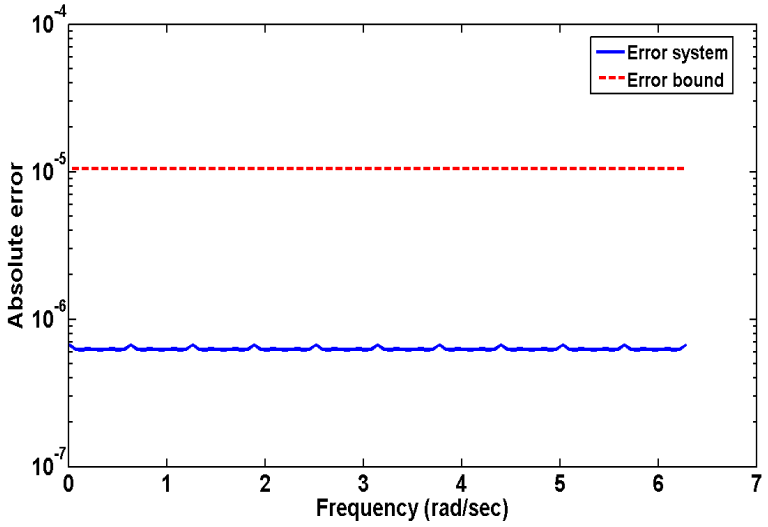

Figure 9.24. Absolute error and error bound (heat equation).

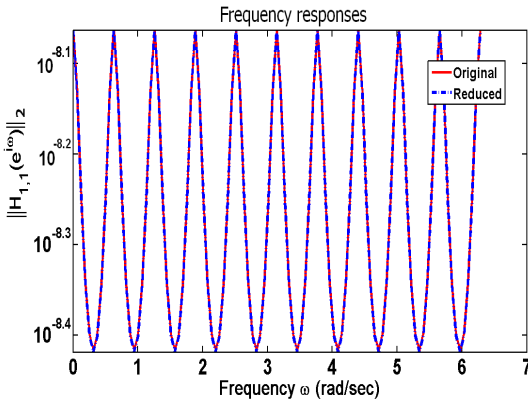

(a) Frequency responses for $\mathcal{H}_{1,1}(e^{i\omega})$

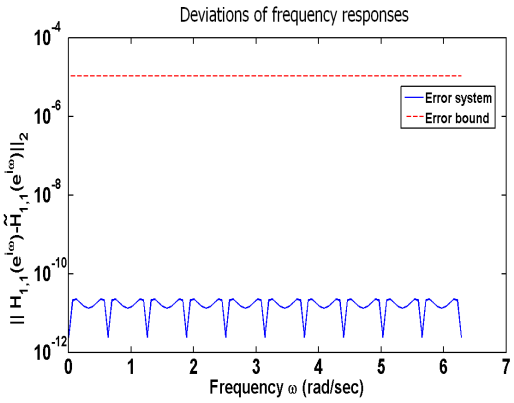

(b) Deviation of frequency responses for $\mathcal{H}_{1,1}(e^{i\omega})$

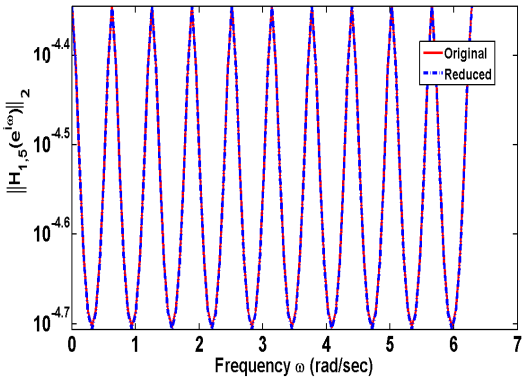

(c) Frequency responses for $\mathcal{H}_{1,5}(e^{i\omega})$

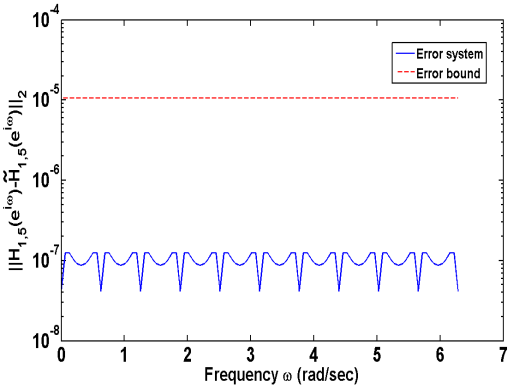

(d) Deviation of frequency responses for $\mathcal{H}_{1,5}(e^{i\omega})$

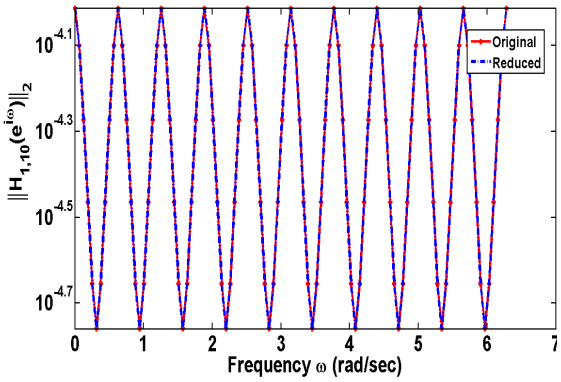

(e) Frequency responses for $\mathcal{H}_{1,10}(e^{i\omega})$

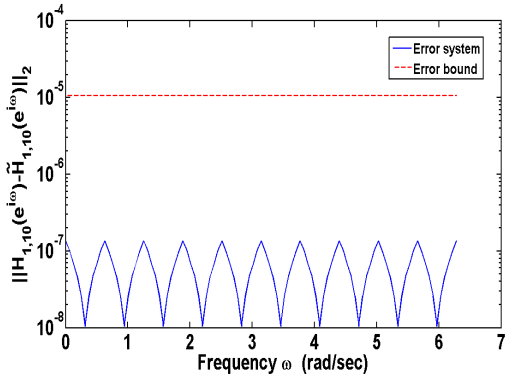

(f) Deviation of frequency responses for $\mathcal{H}_{1,10}(e^{i\omega})$

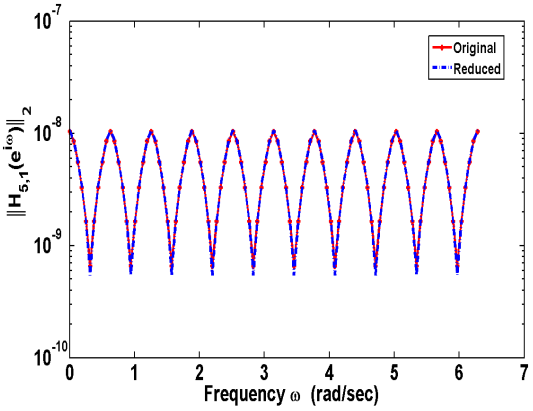

(g) Frequency responses for $\mathcal{H}_{5,1}(e^{i\omega})$

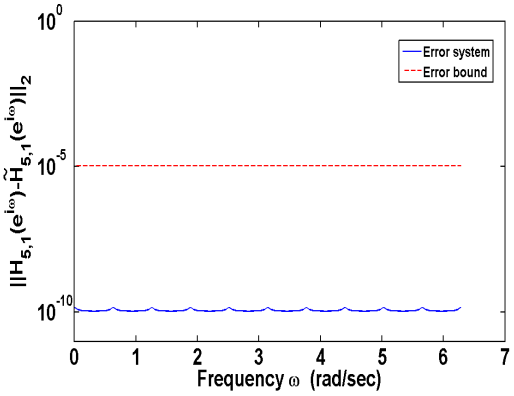

(h) Deviation of frequency responses for $\mathcal{H}_{5,1}(e^{i\omega})$

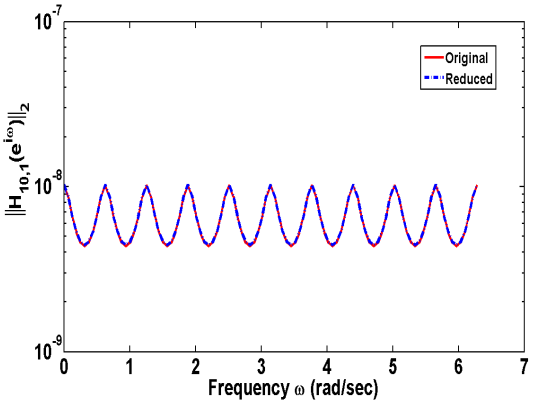

(i) Frequency responses for $\mathcal{H}_{10,1}(e^{i\omega})$

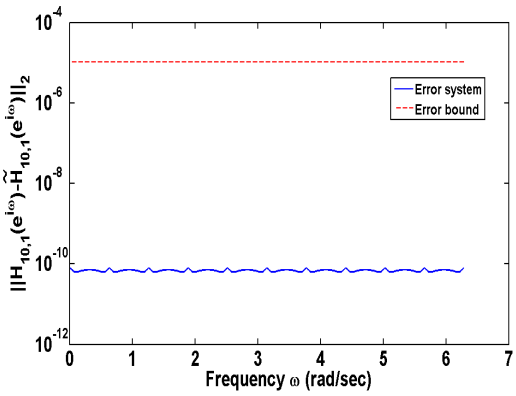

(j) Deviation of frequency responses for $\mathcal{H}_{10,1}(e^{i\omega})$

Figure 9.25. Frequency responses for original and reduced-order systems for individual components of $\mathcal{H}(e^{i\omega})$ and respective deviations (heat equation).

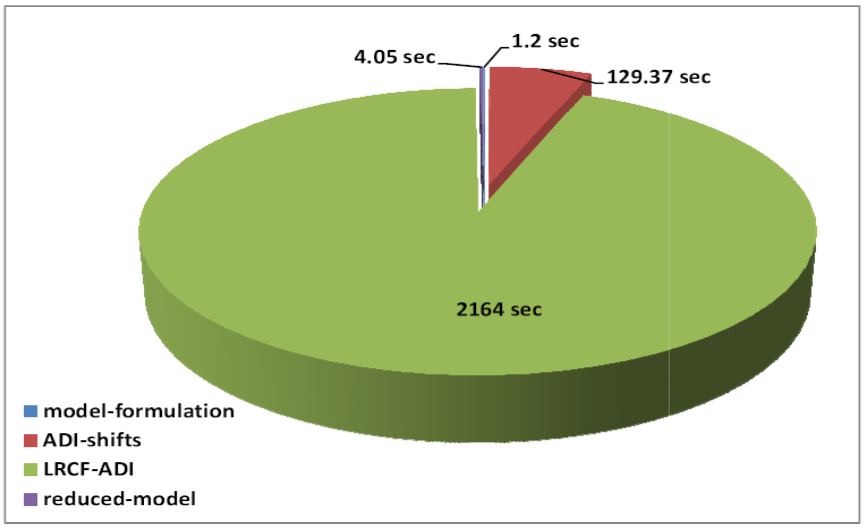

Figure 9.26. Computational time for different parts of the model reduction procedure (heat equation).

We draw a pie chart showing the computational time for different parts of the model reduction procedure (for the reduced-order model with MOR tolerance 10^{-6} in Table 9.2) in Figure 9.26, which shows that almost 94% of the overall computational time is consumed to compute the low-rank approximation of the Cholesky factors of the controllability and observability Gramians, 5% of the overall computational time is needed for the ADI shift parameters computation, and only 1% of the overall computational time is needed to generate the lifted reformulation of the original periodic system and to generate a reduced-order model after computing the low-rank Cholesky factors.

9.6. Discussion

Numerical iterative methods for computation of periodic reachability and observability Gramians as well as Hankel singular values for periodic discrete-time descriptor systems have been considered in this chapter. We have suggested iterative low-rank algorithms based on the ADI and Smith iterations for computing the low-rank factors of the Gramians. These factors have been used in a balanced truncation model reduction approach to find a reduced-order model for the periodic discrete-time descriptor system. The proposed model reduction method delivers a reduced-order model that preserves the regularity and stability properties of the original system. A computable global error bound for the approximate system is also available.

Though several colleagues working in the field of periodic systems have been contracted, so far it turned out to be impossible to collect large-scale sparse real-world

problems of periodic discrete-time descriptor systems from the application field. It remains therefore a task for further work to test the algorithms for real-world problems.

CHAPTER

TEN

CONCLUSIONS AND FUTURE WORK

Contents

10.1. Summary and Conclusions

In this thesis we have presented two important approaches for model reduction of periodic time-varying descriptor systems. The Krylov subspace based projection technique and the balancing based projection technique for model reduction of time-varying periodic descriptor systems have been considered. We first introduced the continuous-time periodic descriptor system with time-varying dimensions and discussed their root models from where (through linearization) the LPTV model problems are obtained. We then discussed the dynamics of such a periodic descriptor system in terms of the DAEs associated with the system. The stability analysis for the continuous-time periodic descriptor system has been considered after an extension of the Floquet theory to LPTV continuous-time systems of DAEs. We also showed that stability of such systems can be characterized by the Floquet exponents of the periodic DAEs that describe the original periodic system.

In Chapter 7 we focused on nonlinear circuit problems and analyse these problem so that they can be easily fit to our model reduction framework. We have analysed the models in the time-domain frame and discussed an approximation scheme based on Krylov subspace methods to approximate the appropriate subspaces for model reduction and discussed how to compute them more efficiently. We have also shown that the model based on approximate multipoint Krylov subspace can be efficiently achieved from the

approximated subspace. We have implemented a recycling technique to produce the columns of the projection matrix. Each new vector in the model reduction was obtained by an inner Krylov iteration. We have also shown that due to the shift-invariance property, the Krylov subspace generated at a particular frequency point can be used to generate the subspace at another frequency point. Hence, the approximation scheme for multiple frequency points becomes much simpler and faster.

On the other hand, the balancing based projection technique for model reduction of time-varying periodic descriptor systems has been considered for discrete-time case. Such systems have received a lot of attention in the last 30 years. Control-theoretic concepts including controllability and observability, Gramians, Hankel singular values and efficient numerical methods for computing poles and zeros, $\mathbb{L}_\infty$-norm, minimal and balanced realizations have been developed for such systems in [30, 124, 125]. But all these methods are based on the reduction of the periodic pairs $\{(E_k, A_k)\}_{k=0}^{K}$ to a periodic Kronecker-like form using the algorithm of [123], they are restricted to problems of small or medium size. Also solving the resulting generalized periodic Sylvester and the periodic projected Lyapunov equations of (quasi)-triangular structure using the recursive blocked algorithms [44] are the most computational and complex tasks in those proposed algorithms.

In Chapter 5 we have introduced the time-invariant reformulation of the LPTV discrete-time descriptor systems called *lifted system*. We have considered the *cyclic lifted system* in this thesis and showed that the dynamics and characteristics, such as solvability, conditionability, regularity and stability of the original periodic system can be described with its cyclic lifted reformulation. We have also discussed an analogous representation of the periodic Gramians and the periodic projected matrix equations with the cyclic lifted structure. We have proved that solving the periodic matrix equations using their cyclic lifted structures (we call them *lifted Lyapunov equations*) can handle the period descriptor systems very easily even if all E_k (or at least one E_k) are singular. We have shown that the solutions of those lifted Lyapunov equations have a specific block diagonal structure so that we could easily pick up the periodic Gramians of the original periodic projected Lyapunov equations for different values of k.

In Chapter 8 we have proposed a balanced truncation model reduction method for periodic discrete-time descriptor systems. Instead of solving the periodic projected Lyapunov equations, we have solved the corresponding projected lifted Lyapunov equations to obtain the periodic Gramians. The solutions of these projected lifted Lyapunov equations have a specific block diagonal structure and the diagonal blocks of these lifted solutions are the solutions of the periodic projected Lyapunov equations (i.e, the periodic Gramians). A solution technique which deals directly with the periodic matrix equations (not in lifted form) has been proposed in [30]. Solving the periodic Sylvester equations and the periodic projected Lyapunov equations in that proposed algorithm produces more complexity, especially when the system has periodic matrix pairs with time varying-dimensions, and the input and output are also time-varying (see Algorithm 5.1 of [30]). On the other hand, our proposed method, which works

with the lifted forms of the periodic matrix equations, can handle those time-varying periodic matrix pairs and the time-varying input and output very easily during the solution process.

We have used these periodic Gramians to find a reduced-order model of the original system. For a balanced system, we truncated the states related to the small causal Hankel singular values because those states require a large amount of input energy to reach but they generate very small output energy. Unfortunately, we can not do the same for the noncausal Hankel singular values. Truncation of the states that correspond to the small non-zero noncausal Hankel singular values can lead to additional errors in the system approximation. We have shown some numerical results to illustrate the efficiency and accuracy of the proposed methods. We have observed that the reduced-order model preserves the regularity and stability properties of the original system. A computable global error bound for the approximate system is also available.

We have observed that the computational complexity of the approach described in Chapter 8 to determine a minimal realization is $\mathcal{O}(K\bar{n}^3)$, where $\bar{n} = \max(\mu_k, n_k)$, and it requires extensive storage. Therefore, the proposed method we describe in Chapter 8 is suitable for small and medium size problems and that it produces a very efficient approximation of the original systems by reduced systems with very small orders. But one should always avoid that type of computation for very large systems. The most time-consuming operation in that process is the solution of the two periodic lifted Lyapunov equations satisfied by the periodic Gramians. Therefore, we have developed iterative methods for such equations, which exploit the sparse structures of system matrices to generate well approximating solutions (with prescribed tolerance) very efficiently.

In Chapter 9, we have presented iterative methods for solving these large-scale sparse projected discrete-time periodic Lyapunov equations in lifted form. These iterative methods are based on the generalization of the ADI method and the Smith method used for large-scale projected continuous-time Lyapunov equations in [110, 81]. These methods can not be directly applied to our projected periodic Lyapunov equations because the direct use contradicted the positive definiteness of the causal solutions. We have considered the Cayley transformation of our lifted system to resolve this problem and then solved the transformed continuous-time lifted Lyapunov equation for the causal solutions. For the noncausal solutions, we have considered the Smith method and simplified the iterative computation exploiting the index of the system.

Low-rank versions of these methods have been also presented in Chapter 9. These low-rank methods have been used to compute the low-rank approximations to the solutions of projected periodic Lyapunov equations in lifted form with low-rank right-hand side. A balanced truncation model reduction method for periodic descriptor systems has been considered. We have numerical examples to illustrate the properties of the described iterative methods for lifted projected Lyapunov equations and model reduction technique. The proposed model reduction method delivers a reduced-order model that preserves the regularity and stability properties of the original system. We have compared the results of the dense computations (from Chapter 8) to the results

of iterative computations of Chapter 9. We have observed that the iterative methods produce a very good approximation of the original system by a reduced-order system. A computable global error bound is also available for the approximate system.

10.2. Future Research Prospectives

There is room for future research both in the area of Krylov based model reduction method and in low-rank approximation of Lyapunov equations with application to balancing based model reduction of periodic descriptor systems.

In the case of Krylov based approximation schemes, a newly released global Arnoldi method proposed in [21] for MIMO systems can be considered to approximate the subspaces at multiple frequency points. Other iterative techniques suitable for solving linear systems with multiple right-hand sides can be tested to construct the projection matrix. But the acceptance of all these proposed methods depends on the efficient computational cost and suitable reduced order with better accuracy as well as other essential characteristics of the reduced-order model.

For balancing based model reduction, large-scale real-world problems are to be computed to test the algorithms derived in this thesis. We have observed that for the semi-discretized heat equation, the relative change in the low-rank factors is very slow. This results very slow convergence of the LRCF-ADI computation to the exact solution. A bad choice of the optimal shift parameters can be a reason for that slow convergency. Other ADI parameter choice rules (see Section 4.3 of [89] for a summary and also the references therein for details) need to be investigated further.

For the low-rank solution of projected lifted Lyapunov equations, the modified SVD based low-rank Smith method proposed in [49] can be considered. But the key problem is how to implement the iteration while preserving the cyclic structure of the system matrices. Also, very recently a Krylov subspace based iterative method has been proposed in [112] to solve projected Lyapunov equations. But the fact of preserving the cyclic structure of system matrices in the iteration is again the key issue that should be investigated.

APPENDIX

A

THESES

1. The thesis presents two important approaches for model reduction of periodic time-varying descriptor systems. The Krylov subspace based projection technique has been used for model reduction of time-varying continuous-time descriptor systems and the balancing based projection technique has been used for model reduction of time-varying discrete-time descriptor systems.
2. The modeling of nonlinear circuit models is described in detail where we linearize the nonlinear model around some equilibrium trajectory and use discretization in the time domain to get a LPTV continuous-time descriptor system. We then discuss the dynamics of such a periodic descriptor system in terms of the DAEs associated with the system. The stability analysis for the continuous-time periodic descriptor system has been considered after an extension of the Floquet theory to LPTV continuous-time systems of DAEs.
3. On the basis of the work of J. Phillips in [84], we have analysed the LPTV model in the time-domain frame and discussed an approximation scheme based on Krylov subspace methods to approximate the appropriate subspaces for model reduction and discussed how to compute them more efficiently. We have implemented a recycling technique to produce the columns of the projection matrix. We have also shown that due to the shift-invariance property, the Krylov subspace generated at a particular frequency point can be used to generate subspaces at another frequency point. Hence, the approximation scheme for multiple frequency points becomes much simpler and faster.
4. The balancing based projection technique has been considered for model reduction of time-varying periodic descriptor systems in the discrete-time case. Control-theoretic concepts including reachability and observability, Gramians, Hankel singular values and efficient numerical methods for computing poles and zeros,

$\mathbb{L}_\infty$-norm, minimal and balanced realizations have been developed for such systems in [30, 124, 125]. But all these methods are based on the reduction of the periodic pairs $\{(E_k, A_k)\}_{k=0}^{K}$ to a periodic Kronecker-like form using the algorithm of [123]. Hence, they are restricted to problems of small or medium size. Also solving the resulting generalized periodic Sylvester and the periodic projected Lyapunov equations of (quasi)-triangular structure using the recursive blocked algorithms [44] are the most computational and complex tasks in those proposed algorithms.

For easier computations, we have introduced the time-invariant reformulation of the LPTV discrete-time descriptor systems called *lifted system* in Chapter 5. We have considered the *cyclic lifted system* in this thesis and shown that the dynamics and characteristics, such as solvability, conditionability, regularity and stability of the original periodic system can be described with its cyclic lifted reformulation. We have also discussed an analogous representation of the periodic Gramians and the periodic projected matrix equations with the cyclic lifted structure. We have proved that solving the periodic matrix equations using their cyclic lifted structures (we call them *lifted Lyapunov equations*) can handle the periodic descriptor systems very easily even if all E_k (or at least one E_k) are singular. We have shown that the solutions of those lifted Lyapunov equations have a specific block diagonal structure so that we can easily pick up the periodic Gramians of the original periodic projected Lyapunov equations for different values of k.

5. We have proposed a balanced truncation model reduction method for periodic discrete-time descriptor systems. We have solved the lifted Lyapunov equations and used the periodic Gramians to find a reduced model of the original system. We have shown some numerical results to illustrate the efficiency and accuracy of the proposed methods. We have observed that the reduced-order model preserves the regularity and stability properties of the original system. A computable global error bound for the approximate system is also available.

6. We have observed that the computational complexity of the approach described in Chapter 8 to determine a minimal realization is $\mathcal{O}(K\bar{n}^3)$, where $\bar{n} = \max(\mu_k, n_k)$, and it requires extensive storage. The most time-consuming operation in that process is the solution of the two periodic lifted Lyapunov equations satisfied by the periodic Gramians. Therefore, we have developed iterative methods for such equations, which exploit the sparse structures of system matrices to generate well approximating solutions (with prescribed tolerance), and have low memory requirements and low computational cost.

7. The iterative methods used to approximate the Gramians are based on the generalization of the ADI method and the Smith method used for large-scale projected continuous-time Lyapunov equations in [110, 81]. These methods can not be directly applied to our projected periodic Lyapunov equations because the direct use contradicts the positive definiteness of the causal solutions. We have considered the Cayley transformation of our lifted system to resolve this problem and then

solved the transformed continuous-time lifted Lyapunov equation for the causal solutions. For the noncausal solutions, we have considered the Smith method and simplified the iterative computation exploiting the index of the system. Low-rank versions of these methods have also been presented. These low-rank methods have been used to compute the low-rank approximations to the solutions of projected periodic Lyapunov equations in lifted form with low-rank right-hand side.

8. Numerical examples have been presented to illustrate the properties of the described iterative methods for lifted projected Lyapunov equations and model reduction. The proposed model reduction method delivers a reduced-order model that preserves the regularity and stability properties of the original system. We have compared the results of the dense computations (from Chapter 8) to the results of iterative computations of Chapter 9. We have observed that the iterative methods produces a very good approximation of the original system by a reduced-order system. A computable global error bound is also available for the approximate system.

BIBLIOGRAPHY

[1] A. Antoulas, *Approximation of Large-Scale Dynamical Systems*, SIAM, Philadelphia, PA, 2005. 101, 151

[2] A. Antoulas, D. Sorensen, and Y. Zhou, *On the decay rate of the Hankel singular values and related issues*, Systems Control Lett., 46 (2002), pp. 323–342. 155

[3] A. C. Antoulas, D. C. Sorensen, and S. Gugercin, *A survey of model reduction methods for large-scale systems*, Contemporary Mathematics, 280 (2001), pp. 193–219. 80

[4] M. Araki and K. Yamamoto, *Multivariable multitrate sampled-data systems: State-space description, transfer characteristic , and nyquist criterion*, IEEE Trans. Automat. Control, AC-31 (February,1986), pp. 145–154. 11, 25, 42

[5] Z. Bai, *Krylov subspace techniques for reduced-order modeling for large-scale dynamical system*, App. Numer. Math, 43(1-2) (2002), pp. 9–44. 83, 90, 92

[6] Z. Bai, P. Feldmann, and R. W. Freund, *Stable and passive reduced-order models based on partial pad approximation via the lanczos process*, in Numerical Analysis Manuscript No. 97–3–10, Bell Laboratories, Murray Hill, 1997. 93, 103

[7] Z. Bai, R. D. Slone, W. T. Smith, and Q. Ye, *Error bound for reduced system model by Padé approximation via the Lanczos process*, IEEE Trans. on CAD of Integrated Circuits and Systems, 18 (1999), pp. 133–141. 93, 103

[8] D. Bender, *Lyapunov-like equations and reachability/observability Gramians for descriptor systems*, IEEE Trans. Automat. Control, 32 (1987), pp. 343–348. 50, 52, 53

[9] P. Benner, *Model reduction algorithm using spectral projection methods*, Householder symposium XV, Peebles, Schottland, 12 (June 17-21, 2002). 97

[10] P. Benner and H. Fassbender, *On the numerical solution of large-scale sparse discrete-time Riccati equations*, Adv. Comput. Math., (to appear). 103, 149, 151

[11] P. Benner, M.-S. Hossain, and T. Stykel, *Low- rank iterative methods of periodic projected Lyapunov equations and their application in model reduction of periodic descriptor*

systems, Chemnitz Scientific Computing Preprints 11–01, 2011. Available from `http://www.tu-chemnitz.de/mathematik/csc/2011/csc11-01.pdf`. 162

[12] ——, *Model reduction of periodic descriptor systems using balanced truncation*, in Model Reduction in Circuit Simulation, P. Benner, M. Hinze, and J. ter Maten, eds., vol. 74 of Lecture Notes in Electrical Engineering, Berlin, Heidelberg, 2011, Springer-Verlag, pp. 193–206. 66, 161

[13] P. Benner, J.-R. Li, and T. Penzl, *Numerical solution of large Lyapunov equations, Riccati equations, and linear-quadratic control problems*, Numer. Linear Algebra Appl., 15 (2008), pp. 755–777. 103, 148, 156, 176

[14] P. Benner, V. Mehrmann, and H. Xu, *Perturbation analysis for the eigenvalue problem of a formal product of matrices*, 42 (2002), pp. 1–43. 43

[15] P. Benner and E. Quintana-Ortí, *Model reduction based on spectral projection methods*, in Dimension Reduction of Large-Scale Systems, P. Benner, V. Mehrmann, and D. Sorensen, eds., vol. 45 of Lecture Notes in Computational Science and Engineering, Springer-Verlag, Berlin/Heidelberg, Germany, 2005, pp. 5–45. 99, 158

[16] S. Bittanti and P. Bolzern, *On the structure theory of discrete time linear systems*, Int. J. Systems Sci., 17 (1986), pp. 33–47. 76

[17] S. Bittanti and P. Colaneri, *Periodic control*, in Wiley Encyclopedia of Electrical and Electronic Engineering, J. Webster, ed., vol. 16, John Wiley & Sons, Inc., New York, Chichester, 1999, pp. 59–74. 16, 42, 63

[18] S. Bittanti and P. Colaneri, *Invariant representations of discrete-time periodic systems*, Automatica, 36 (2000), pp. 1777–1793. 62, 63, 72, 76

[19] A. Bojanczyk, G. Golub, and P. Van Dooren, *The periodic Schur decomposition. Algorithms and applications*, in Proceedings of SPIE Conference, San Diego, vol. 1770, 1992, pp. 31–42. 25, 43, 45, 124

[20] P. Bolzern and P. Colaneri, *Existence and uniqueness conditions for the periodic solutions of the discrete-time periodic Lyapunov equation*, in Proc. 25th IEEE Conference on Decision and Control, Athens, Greece, 1986, pp. 1439–1443. 62, 124

[21] T. Bonin, H. Fassbender, A. Soppa, and M. Zaeh, *A global Arnoldi method for the model reduction of second-order structural dynamical systems*, preprint, 2010. 83, 188

[22] H. G. Brachtendorf, *Theorie und Analyse von autonomen und quasiperiodisch angeregten elektrischen Netzwerken. Eine algorithmisch orientierte Betrachtung*. Universität Bremen, 2001. Habilitationsschrift. 33, 34, 35, 37, 38, 39

[23] K. Brenan, S. Campbell, and L. Petzold, *Numerical solution of initial-value problems in differential-algebraic equations*, SIAM, Philadelphia, 1996. 39

[24] R. Bru, C. Coll, and N. Thome, *Compensating periodic descriptor systems*, Systems

Control Lett., 43 (2001), pp. 133–139. 123

[25] J. C. Butcher, *Numerical Methods for Ordinary Differential Equations*, John Wiley and Sons, 2nd ed., 2003. 33

[26] D. Calvetti, N. Levenberg, and L. Reichel, *Iterative methods for X-AXB=C*, J. Comput. Appl. Math., 86 (1997), pp. 73–101. 151

[27] Y. Chahlaoui and P. Van Dooren, *A collection of benchmark examples for model reduction of linear time invariant dynamical systems*, SLICOT Working Note 2002–2, Feb. 2002. Available from `http://www.win.tue.nl/niconet/NIC2/reports.html`. 172, 174

[28] Y. Chahlauri, *A posteriori error bounds for discrete balanced truncation*, MIMS eprint, The University of Manchester, UK, 2009. Available from `http://www.manchester.ac.uk/mims/eprints`. 96, 97, 101

[29] E.-W. Chu, H.-Y. Fan, and W.-W. Lin, *Reachability and observability of periodic descriptor systems*, preprint NCTS, National Tsing Hua University, Hsinchu, Taiwan, 2005. 49, 50, 71, 72

[30] ——, *Projected generalized discrete-time periodic Lyapunov equations and balanced realization of periodic descriptor systems*, SIAM J. Matrix Anal. Appl., 29 (2007), pp. 982–1006. 45, 48, 49, 50, 51, 52, 53, 55, 56, 58, 67, 71, 72, 124, 131, 132, 133, 134, 135, 136, 162, 186, 190

[31] J. J. DaCunha and J. M. Davis, *A unified Floquet theory for discrete, continuous, and hybrid periodic linear systems*, (January 2009). Available from `http://arxiv.org/abs/0901.3841`. 33, 34

[32] A. Demir, *Phase noise in oscillators: DAEs and colored noise sources*, in Proceedings of the 1998 IEEE/ACM international conference on Computer-aided design, San Jose, California, United States, 1998, ACM, pp. 170–177. 36, 41

[33] ——, *Floquet theory and non-linear perturbation analysis for oscillators with differential-algebraic equations*, Internat. Journal of Circuit Theory and Applications, 28 (2000), pp. 163–185. 33, 34, 35

[34] J. Demmel and B. Kågström, *The generalized Schur decomposition of an arbitrary pencil $A - \lambda B$: Robust software with error bounds and applications. Part I: Theory and algorithms*, ACM Trans. Math. Software, 19 (1993), pp. 160–174. 27, 129, 130

[35] ——, *The generalized Schur decomposition of an arbitrary pencil $A - \lambda B$: Robust software with error bounds and applications. Part II: Software and applications*, ACM Trans. Math. Software, 19 (1993), pp. 175–201. 27, 129, 130

[36] I. Elfadel and D. D. Ling, *A block Arnoldi algorithm for multipoint passive model-order reduction of multiport RLC networks*, IEEE Transactions on circuits and systems, (1997), pp. 291–299. 2, 7, 83

[37] M. Farhood, C. Beck, and G. Dullerud, *Model reduction of periodic systems: a lifting approach*, Automatica,, 41 (2005), pp. 1085–1090. 133

[38] D. S. Flamm, *A new shift-invariant representation for periodic linear systems*, Systems Control Lett., 17 (1991), pp. 9–14. 4

[39] N. J. Fliege, *Multirate Digital Signal Processing: Multirate Systems - Filter Banks - Wavelets*, John Wiley and Sons, New York, NY, USA, first ed., 1994. 11, 12, 42

[40] R. Freund, *Reduced-order modeling techniques based on Krylov subspaces and their use in circuit simulation*, in Applied and Computational Control, Signals, and Circuits, B. Datta, ed., vol. 1, Boston, MA, 1999, ch. 9, pp. 435–498. 80, 83, 93

[41] ——, *Model reduction methods based on Krylov subspaces*, Acta Numerica, 12 (2003), pp. 267–319. 80, 90, 92, 105

[42] R. J. Gilmore and M. B. Steer, *Nonlinear circuit analysis using the method of harmonic balance A review of the art. Part I. Introductory concepts*, International Journal of Microwave and Millimeter-Wave Computer-Aided Engineering, 1 (1991), pp. 22–37. 32, 106

[43] G. Golub and C. Van Loan, *Matrix Computations*, Johns Hopkins University Press, Baltimore, third ed., 1996. 25, 114, 129, 130

[44] R. Granat, I. Jonsson, and B. Kågström, *Recursive blocked algorithms for solving periodic triangular Sylvester-type matrix equations*, in Applied Parallel Computing. State of the Art in Scientific Computing, B. Kågström, E. Elmroth, J. Dongarra, and J. Waśniewski, eds., vol. 4699 of Lecture Notes in Computer Science, Springer-Verlag, 2007, pp. 531–539. 124, 186, 190

[45] R. Granat, B. Kågström, and D. Kressner, *Computing periodic deflating subspaces associated with a specific set of eigenvalues*, BIT Num. Math., 43 (2003), pp. 1–18. 43, 44, 45

[46] O. M. Grasselli and S. Longhi, *Finite zero structure of linear periodic discrete-time systems*, Internat. J. Systems Sci., 22 (1991), pp. 1785–1806. 62, 64, 77

[47] E. J. Grimme, *Kryloy projection methods for model reduction*, PhD thesis, University of Illinois at Urbana, Champaign, 1997. 84, 86, 88, 89, 90, 92, 105, 112

[48] S. Gugercin and A. Antoulas, *A survey of model reduction by balanced truncation and some new results*, Internat. J. Control, 77 (2004), pp. 748–766. 80

[49] S. Gugercin, D. Sorensen, and A. Antoulas, *A modified low-rank Smith method for large-scale Lyapunov equations*, Numer. Algorithms, 32 (2003), pp. 27–55. 103, 148, 149, 150, 151, 188

[50] S. Hammarling, *Numerical solution of the stable non-negative definite Lyapunov equation*, IMA J. Numer. Anal., 2 (1982), pp. 303–323. 130, 131

[51] D. W. Hancock III, G. S. Hayne, R. L. Brooks, J. E. Lee, and D. W. Lockwood,

TOPEX radar altimeter engineering assessment report. Update: Launch to January 1, 1998, Raython ITSS,, (1998). NASA/TM-2003-21223611/Vol. 11. 18

[52] T. Haynes, *Stable matrics, the Cayley transform, and convergent matrices*, Internat. J. Math. and Math. Sci., 14 (1991), pp. 77–82. 151

[53] C.-W. Ho, A. E. Ruehli, and P. A. Brennan, *The modified nodal approach to network analysis*, IEEE Trans. Circuits and Systems, 22(6) (June 1975), pp. 504–509. 8

[54] M.-S. Hossain and P. Benner, *Projection-based model reduction for time-varying descriptor systems using recycled Krylov subspaces*, in Proceedings in Appllied Mathematics and Mechanics, vol. 8, 2008, pp. 10081–10084. 113

[55] K. Jbilou and A. Riquet, *Projection methods for large Lyapunov matrix equations*, Linear Algebra Appl., 415 (2006), pp. 344 – 358. 148

[56] D. Kressner, *An efficient and reliable implementation of the periodic QZ algorithm*, in Periodic Control Systems 2001. A Proceedings volume of the IFAC Workshop, Cernobbio-Como, Italy, 27–28 August 2001, S. Bittanti and P. Colaneri, eds., Elsevier Science, Oxford, UK, 2001. 43, 124

[57] ——, *Large periodic Lyapunov equations: Algorithms and applications*, in Proc. of ECC03, Cambridge, UK, 2003. 72, 134, 148

[58] K. S. Kundert and A. Sangiovanni-Vincentelli, *Simulation of nonlinear circuits in the frequency domain*, IEEE Transactions on Computer-Aided Design of Integrated Circuits and Systems, 5 (1986), pp. 521–535. 32, 106

[59] Y.-C. Kuo, W.-W. Lin, and S.-F. Xu, *Regularization of linear discrete-time periodic descriptor systems by derivative and proportional state feedback*, SIAM J. Matrix Anal. Appl., 25 (2004), pp. 1046–1073. 70, 77

[60] S. Lall and C. Beck, *Error-bounds for balanced model-reduction of linear time-varying systems*, IEEE Trans. Automat. Control, 48 (2003), pp. 946–956. 136

[61] S. Lall, C. Beck, and G. Dullerud, *Guaranteed error bounds for model reduction of linear time-varying systems*, in Proceedings of the American Control Conference, 1998, vol. 1, Philadelphia, PA , USA, 1998, pp. 634–638. 136

[62] R. Lamour, R. März, and R. Winkler, *How Floquet theory applies to index 1 differential algebraic equations*, J. Math. Anal. Appl., 217 (1998), pp. 372–394. 33, 37, 38

[63] S.-H. Lee, Y.-H. Kim, and C. C. Chung, *Multirate digital control system design*, in Proc. of the Ame. Con. Conf., Anchorage, AK, May 8-10, 2002, pp. 1861–1866. 2, 7, 25

[64] N. Levenberg and L. Reichel, *A generalized ADI iterative method*, Numer. Math., 66 (1993), pp. 215–233. 149

[65] F. Lewis, *Fundamental, reachability, and observability matrices for discrete descriptor*

systems, IEEE Trans. Automat. Control, AC-30 (1985), pp. 502–505. 50, 52, 53, 71, 72

[66] J.-R. Li and J. White, *Reduction of large circuit models via low rank approximate gramians*, Int. J. Appl. Math. Comp. Sci., 11 (2001), pp. 1151–1171. 2, 7, 42

[67] ——, *Low rank solution of Lyapunov equations*, SIAM J. Matrix Anal. Appl., 24 (2002), pp. 260–280. 103, 148, 149, 150, 155

[68] M. Lovera and A. Astolfi, *Spacecrafts attitude control using magnetic actuators*, Automatica, 40 (2004), pp. 1405–1414. 2, 7, 16, 42

[69] M. Lovera, E. De Marchi, and S. Bittanti, *Periodic attitude control techniques for small satellites with actuators*, IEEE Transactions on Control System Technology, 10 (2002), pp. 90–95. 16, 17, 42

[70] A. Lu and E. Wachspress, *Solution of Lyapunov equations by alternating direction implicit iteration*, Comput. Math. Appl., 21 (1991), pp. 43–58. 103, 149, 150

[71] D. G. Luenberger, *Dynamic equations in descriptor form*, IEEE Trans. Automat. Control, AC–22 (1977), pp. 312–321. 68, 69

[72] R. März, *On linear differential-algebraic equations and linearizations*, Applied Numerical Mathematics, 18 (1995), pp. 267–292. 38

[73] R. A. Mayer and C. S. Burrus, *Unified analysis of multirate and periodically time-varying digital filters*, IEEE Trans. Circuits and Systems, CAS-22 (March, 1975), pp. 162–168. 2, 7, 8, 11, 25, 42, 62

[74] V. Mehrmann, *A step toward a unified treatment of continuous and discrete time control problems*, Linear Algebra Appl., 241-243 (1996), pp. 749–779. 151, 152, 153

[75] V. Mehrmann and T. Stykel, *Balanced truncation model reduction for large-scale systems in descriptor form*, in Dimension Reduction of Large-Scale Systems, P. Benner, V. Mehrmann, and D. Sorensen, eds., vol. 45 of Lecture Notes in Computational Science and Engineering, Springer-Verlag, Berlin/Heidelberg, 2005, pp. 83–115. 93, 99, 101, 131, 134

[76] B. Moore, *Principal component analysis in linear systems: controllability, observability, and model reduction*, IEEE Trans. Automat. Control, AC-26 (1981), pp. 17–32. 53, 97, 105, 133

[77] M. Nakhla and E. Gad, *Efficient model reduction of linear time-varying systems via compressed transient system function*, in Proceedings of the conference on Design, automation and test in Europe, Paris, France, 2002, pp. 916–922. 109

[78] ——, *Efficient model reduction of linear periodically time-varying systems via compressed transient system function*, IEEE Transactions on Circuit and Systems, 52 (2005), pp. 1188–1204. 8, 32, 42, 106, 107

[79] B. Park and E. Verriest, *Canonical forms of discrete linear periodically time-varying*

systems and a control application, in Proc. of the 28th Conference on Decision and Control, Tampa, FL, Dec 1989, pp. 1220–1225. 4, 62, 64, 76

[80] D. Peaceman and H. Rachford, *The numerical solution of elliptic and parabolic differential equations*, J. Soc. Indust. Appl. Math., 3 (1955), pp. 28–41. 149

[81] T. Penzl, *A cyclic low rank Smith method for large, sparse Lyapunov equations with applications in model reduction and optimal control*, Tech. Rep. SFB393/98-6, Fakultät für Mathematik, TU Chemnitz, 09107 Chemnitz, FRG, 1998. Available from `http://www.tu-chemnitz.de/sfb393/sfb98pr.html`. 147, 187, 190

[82] ——, *A cyclic low rank Smith method for large sparse Lyapunov equations*, SIAM J. Sci. Comput., 21 (2000), pp. 1401–1418. 103, 148, 149, 150, 151, 155

[83] ——, *Eigenvalue decay bounds for solutions of Lyapunov equations: the symmetric case*, Systems Control Lett., 40 (2000), pp. 139–144. 155

[84] J. Phillips, *Model reduction of time-varying linear systems using multipoint Krylov-subspace projectors*, In Proc. ICCAD, (1998), pp. 96–102. 8, 10, 32, 88, 106, 107, 109, 111, 114, 189

[85] ——, *Projection-based approaches for model reduction of weakly nonlinear time-varying systems*, IEEE Trans. Computer-Aided Design, 22 (2003), pp. 171–187. 108, 111

[86] J. Roychowdhury, *Reduced-order modelling of linear time-varying systems*, Design Automation Conference, 1999.Proceedings of the ASP-DAC '99. Asia and South Pacific, 1 (18-21 Jan.1999), pp. 53–56. 8, 42

[87] ——, *Reduced-order modeling of time-varying systems*, IEEE Control Systems Magazine, 46 (1999), pp. 1273 – 1288. 10, 42, 106, 107, 108, 109

[88] Y. Saad, *Overview of Krylov subspace methods with applications to control*, in Proceedings of the International Symposium MTNS-89 on Signal Processing, Scattering and Operator Theory, and Numerical Methods, vol. 3, 1990. 10, 105

[89] J. Saak, *Efficient Numerical Solution of Large Scale Algebraic Matrix Equations in PDE Control and Model Order Reduction*, Ph.D. thesis, Fakultät für Mathematik, Technische Universität Chemnitz, Chemnitz, Germany, 2009. Available from `http://www.mpi-magdeburg.mpg.de/mpcsc/mitarbeiter/saak/Data/Diss-web.pdf`. 176, 177, 188

[90] B. Salimbahrami and B. Lohmann, *Krylov subspace methods in linear model order reduction: Introduction and invariance properties*, tech. rep., Institut of Automation, University of Bremen, Germany, 2002. Available at `http://www.rt.mw.tum.de/salimbahrami/Invariance.pdf`. 86, 87

[91] B. Salimbahrami, B. Lohmann, T. Bechtold, and J. Korvink, *Two-sided Arnoldi algorithm and its application in order reduction of MEMS*, in Proceedings of the Fourth International Conference on Mathematical Modelling, Vienna, 2003, pp. 1021–1028. 83

[92] S. B. Salimbahrami, *Structure Preserving Order Reduction of Large Scale Second Order Models*, Ph.D. thesis, Technische Universität München, Fakultät für Maschinenwesen, Germany, 2005. xix, 90, 91, 92, 93

[93] S. Shokoohi, L. Silverman, and P. Van Dooren, *Linear time-variable systems: Balancing and model reduction*, IEEE Trans. Automat. Control, AC-28 (1983), pp. 810–822. 42, 105

[94] E. Silani and M. Lovera, *Magnetic spacecraft attitude control: a survey and some new results*, Control Engineering Practice, 13 (2005), pp. 357–371. 2, 7, 16, 17, 42

[95] V. Simoncini, *A new iterative method for solving large-scale Lyapunov matrix equations*, SIAM J. Sci. Comput., 29 (2007), pp. 1268–1288. 148

[96] R. Smith, *Matrix equation $XA+BX = C$*, SIAM J. Appl. Math., 16 (1968), pp. 198–201. 148, 151, 159

[97] J. Sreedhar and P. V. Dooren, *Periodic descriptor systems: Solvability and conditionability*, IEEE Trans. Automat. Control, 44 (1999), pp. 310–313. 68, 69

[98] J. Sreedhar and P. Van Dooren, *Pole placement via the periodic Schur decomposition*, in In Proceedings Amer. Contr. Conf., 1993, pp. 1563–1567. 25

[99] ——, *Periodic Schur form and some matrix equations*, in Systems and Networks: Mathematical Theory and Applications, Proc. Intl. Symposium MTNS '93 held in Regensburg, Germany, August 2–6, 1993, U. Helmke, R. Mennicken, and J. Saurer, eds., Akademie Verlag, Berlin, FRG, 1994, pp. 339–362. 43

[100] ——, *Forward/backward decomposition of periodic descriptor systems*, in Proc. of European Control Conf., Brussels, Belgium, 1997. 48

[101] J. Sreedhar, P. Van Dooren, and B. Bamieh, *Computing the H_∞ norm of discrete-time periodic systems: A quadratically convergent algorithm*, in Proceedings of the 4th European Control Conference, Brussels, Belgium, 1997. 62, 65, 76

[102] G. Stewart, *On the sensitivity of the eigenvalue problem $Ax = \lambda Bx$*, SIAM J. Numer. Anal., 9 (1972), pp. 669–686. 26

[103] T. Stykel, *Analysis and Numerical Solution of Generalized Lyapunov Equations*, Ph.D. thesis, Institut für Mathematik, Technische Universität Berlin, Berlin, Germany, 2002. Available from `http://www.math.tu-berlin.de/~stykel/Publications/disser.ps`. 29, 45, 55, 75, 99, 100, 125, 151, 152

[104] ——, *Numerical solution and perturbation theory for generalized Lyapunov equations*, Linear Algebra Appl., 349 (2002), pp. 155–185. 124, 129, 130, 131

[105] ——, *Stability and inertia theorems for generalized Lyapunov equations*, Linear Algebra Appl., 355 (2002), pp. 297–314. 100

[106] ——, *Balanced truncation model reduction for descriptor systems*, Proceedings in Applied Mathematics and Mechanics (GAMM 2003, Abano Terme - Padua, Italy,

March 24-28, 2003), 3 (2003), pp. 5–8. 93, 97, 131

[107] ——, *Input-output invariants for descriptor systems*, preprint PIMS-03-1, The Pacific Institute for the Mathematical Sciences, Canada, 2003. Available from `http://www.math.tu-berlin.de/~stykel/Publications/PIMS-03-1.pdf`. 50, 55, 97, 99, 100, 101

[108] ——, *Gramian-based model reduction for descriptor systems*, Math. Control Signals Systems, 16 (2004), pp. 297–319. 52, 53, 93, 99, 101, 133, 134, 135

[109] ——, *Balancing-related model reduction of descriptor systems*, in Proceedings of the 6th International Conference on Scientific Computing in Electrical Engineering (SCEE 2006, Sinaia, Romania, September 17-22, 2006), Printech, 2006, pp. 17–18. 99

[110] ——, *Low-rank iterative methods for projected generalized Lyapunov equations*, Electron. Trans. Numer. Anal., 30 (2008), pp. 187–202. 103, 147, 148, 149, 151, 153, 155, 156, 159, 187, 190

[111] ——, *Model reduction of descriptor systems*, technical Report 720-2001, Institut für Mathematik, Technische Universität Berlin, D-10263 Berlin, Germany, December 2001. Available from `http://www.math.tu-berlin.de/~stykel/Publications/pr_720_01.ps`. 97

[112] T. Stykel and V. Simoncini, *Krylov subspace methods for projected Lyapunov equations*, Preprint 735, DFG Research Center Matheon, Technische Universität Berlin, 2010. Submitted for publication. 148, 188

[113] R. Telichevesky, J. White, and K. Kundert, *Efficient steady-state analysis based on matrix-free Krylov-subspace methods*, In Proceedings of 32rd Design Automation Conference, (1995). 10, 109, 114

[114] ——, *Efficient AC and noise analysis of two-tone RF circuits*, in Proceedings of the 33rd annual Design Automation Conference, DAC '96, NY, USA, 1996, ACM Press, pp. 292–297. 32, 88, 109, 110, 111, 112

[115] A. A. Vaidyanathan, *Multirate digital filters, filters banks, polyphase networks, and applications: A tutorial*, in Proc. of IEEE, vol. 78, 1990, pp. 56–93. 2, 7, 11, 14, 15, 25, 42

[116] P. Van Dooren, *Gramian based model reduction of large-scale dynamical systems*, in Numerical Analysis 1999, Chapman & Hall/CRC Research Notes in Mathematics, 420, Boca Raton, FL, 2000, Chapman & Hall/CRC, pp. 231–247. 53

[117] P. Van Dooren and J. Sreedhar, *When is a periodic discrete-time system equivalent to a time-invariant one?*, Linear Algebra Appl., 212-213 (1994), pp. 131–151. 62

[118] A. Varga, *On stabilization methods of descriptor systems*, Systems Control Lett., 24 (1995), pp. 133–138. 101

[119] ——, *Periodic Lyapunov equations: some applications and new algorithms*, Internat. J. Control, 67 (1997), pp. 69–87. 74, 124

[120] ——, *Balancing related methods for minimal realization of periodic systems*, Syst. Contr. Lett., 36 (1999), pp. 339–349. 54

[121] ——, *Balanced truncation model reduction of periodic systems*, in Proc. CDC'2000, Sydney, Australia, vol. 3, 2000, pp. 2379–2384. 53, 54, 72, 74, 131, 133, 134, 136

[122] ——, *Comutation of transfer function matrices of periodic systems*, Internat. J. Control, 76 (2003), pp. 1712–1723. 61, 62, 63, 76

[123] ——, *Computation of Kronecker-like forms of periodic matrix pairs*, in Proc. of Mathematical Theory of Networks and Systems (MTNS 2004), Leuven, Belgium, July 5-9, 2004), 2004. 44, 124, 128, 186, 190

[124] ——, *A PERIODIC SYSTEMS Toolbox for MATLAB*, in Proc. of IFAC'05 World Congress, Prague, Czech Republik, July 3-8, 2005. 61, 62, 186, 190

[125] A. Varga and P. Van Dooren, *Computing the zeros of periodic descriptor systems*, Systems Control Lett., 50 (2003), pp. 371–381. 62, 63, 76, 77, 123, 186, 190

[126] C. D. Villemagne and R. E. Skelton, *Model reductions using a projection formulation*, Internat. J. Control, 46 (1987), pp. 2141–2169. 83

[127] E. Wachspress, *Iterative solution of the Lyapunov matrix equation*, Appl. Math. Letters, 107 (1988), pp. 87–90. 150

[128] Y. Wan and J. Roychowdhury, *Operator-based model-order reduction of linear periodically time-varying systems*, in Proceedings of the 42nd annual Design Automation Conference, NY, USA, 13-17 Jun 2005, ACM Press, pp. 391–396. 8

[129] S. Weiland, *Balancing and Hankel norm approximation of dynamical systems*, handout, Technische Universiteit Eindhoven, The Netherlands, 2009. Available at `http://w3.tue.nl/fileadmin/ele/MBS/CS/Files/Courses/Model_Reduction/modred2.pdf`. 94

[130] J. R. Wertz, *Spacecraft attitude determination and control*, Kluwer Academin Publishers, Dordrecht, Boston, London, 1978. 16, 17

[131] B. Yang and D. Feng, *Efficient finite-difference method for quasi-periodic steady-state and small signal analyses*, in Proceedings of the 2000 IEEE/ACM International Conference on Computer-Aided Design, Piscataway, NJ, USA, 2000, IEEE Press, pp. 272–276. 120

[132] X. Yang, M. Kawamata, and T. Higuchi, *Balanced realisations and model reduction of periodically time-varying state-space digital filters*, in IEE Proc. Vision, Image & Singal Proc., vol. 143, 1996, pp. 370–376. 42

[133] L. Zadeh, *Frequency analysis of variable networks*, IEEE Transactions on Circuits and Systems, (March 1950), pp. 291–299. 106, 107